Fatigue analysis in recreational active runners & development of a real-time fatigue prediction model

Muhammad Jafar Ali

2018

Muhammad Jafar Ali. (2018). Fatigue analysis in recreational active runners & development of a real-time fatigue prediction model. Doctoral thesis, Nanyang Technological University, Singapore.

http://hdl.handle.net/10356/73344

https://doi.org/10.32657/10356/73344

NANYANG TECHNOLOGICAL UNIVERSITY
SINGAPORE

Doctoral Thesis

FATIGUE ANALYSIS IN RECREATIONAL ACTIVE RUNNERS & DEVELOPMENT OF A REAL-TIME FATIGUE PREDICTION MODEL

Author:

Muhammad Jafar Ali

Supervisors:

Assoc. Prof. Hoon Kay Hiang (PaCE – NTU)

Assoc. Prof. Seet Gim Lee Gerald (MAE – NTU)

A thesis submitted in partial fulfillment of the requirements for the degree of

Doctor of Philosophy

In the

School of Mechanical & Aerospace Engineering

Nanyang Technological University, Singapore

2018

Abstract

Millions of recreational active runners participate in endurance events to have better fitness, cardiovascular health, and longevity. These endurance events lead to fatigue in the individual. Fatigue is a sensation of tiredness and deterioration of the physical performance. It is a critical factor that has the potential to disrupt the running performance of the individuals by stressing the physiological as well as the biomechanical system. Fatigue due to endurance running can lead to wide-ranging effects, such as cardiovascular stress, metabolic derangements, and musculoskeletal injuries. To achieve positive outcomes of endurance training and reduce the risks of injury, it is important to monitor the running intensity and examine the implications of fatigue on physiological, neuromuscular and kinematic systems. This can be achieved by determining the physiological and biomechanical predictors of fatigue. Considering the classes of athletes, different demographics of runners have different fatigue thresholds. This study focused on male recreational endurance runners. This group was selected for several reasons. Firstly, there is a dearth of literature related to this group. Secondly, this group is much larger as compared to amateur and professional competitive runners. Lastly, there is no real-time metabolic estimation and fatigue prediction model for this group to help them monitor their running intensity and fatigue in real time.

This thesis analyzed endurance performance and evaluated fatigue during two scenarios. In the first scenario, the data was gathered during non-continuous running in which participants ran for 4 minutes followed by rest for 1 minute until exhaustion. In the second scenario, participants ran continuously and data was gathered until exhaustion. A total of 17 healthy male recreational active runners (age 22.94±1.48 years, BMI 22.16±1.92, $\dot{V}O_{2max}$ 57.63±5.46 $ml.kg^{-1}.min^{-1}$, HR_{max} 190.47±7.89 $beats.min^{-1}$, % body fat 13.01±3.31) were recruited. The physiological data included oxygen consumption ($\dot{V}O_2$), Heart Rate (HR), Respiratory Rate (RR), Respiratory Exchange Ratio (RER), Maximum HR (HRmax) and maximal aerobic capacity ($\dot{V}O_{2max}$). Kinematic data included hip angle, knee angle, ankle angle, pronation angle, landing impact on the tibia (I_T), landing impact on the hip (I_H) and hip push-off acceleration (ACC_H). The neuromuscular data included Integrated EMG (iEMG) and Time Dependent Median Power Frequency (TDMdPF). Perceived exertion data for the chest (RPE_C), leg muscles (RPE_M) and overall body feel (RPE_O) were recorded to determine fatigue. Non-continuous running test was administered to determine blood lactate (BLa) response. Both scenarios were evaluated at the

Critical Speed (CS), determined at Blood Lactate (BLa) of 4.0 $mmol.l^{-1}$.

Cardio-respiratory data was obtained using the 'Parvo Medics TrueOne 2400' with a POLAR chest strap heart rate sensor. To evaluate kinematics and neuromuscular activation in the lower extremity, the dominant leg was selected through the three manipulative tasks (back push-off test, stepping on the chair and kicking a soccer ball). Kinematic data were obtained using 2D video analysis system to track dominant leg joint angles. Two Trigno wireless IMU sensors were placed on the tibia of both legs to determine I_T in the lower extremity. One Trigno wireless accelerometer was placed on the sacrum to determine I_H and ACC_H. Neuromuscular data from the dominant leg was obtained using seven 'Trigno Wireless EMG sensors', attached to the belly of Rectus Femoris (RF), Vastus Lateralis (VL), Bicep Femoris (BF), Semitendinosus (ST), Gastro-medial (GM), Gastro-lateral (GL) and Tibialis Anterior (TA) muscles in the dominant leg. A combinatorial data analysis approach for both tests was devised to study the kinematic changes in the lower extremity, neuromuscular fatigue (power 'Pi' and fatigue index 'Fi'), cardiorespiratory stress, metabolic stress, time to exhaustion and perceived exertion. As the 1-min rest during the non-continuous test may change response to fatigue development in comparison to the continuous test, its effects on TTE, BLa and physiological markers of fatigue were investigated. The continuous test data is used to develop the real-time fatigue model as continuous running is most common among recreational active runners.

The results of the study showed that the time to exhaustion (TTE) during non-continuous run was almost 1.6 times of the continuous run. It also showed a decrease in RER and lower $\dot{V}O_2$, lower BLa and lower RPE_O at termination (End) during non-continuous run in comparison to the continuous run. Critical speed was found to be associated with Maximum Lactate Steady State (MLSS) during non-continuous running. However, continuous running showed a significant increase in BLa above MLSS. The influence of several physiological and kinematic fatigue predictors was examined using multilinear regression analysis. The analysis showed significant influence of oxygen cost ($\dot{V}O_2$) ($p=0.0002$), respiratory rate (RR) ($p=0.0002$), HR Recovery (HRR) ($p<0.00001$), HR Intensity ($\%HR_{max}$) ($p<0.0001$), ankle angle ($p<0.0001$), Non-dominant Tibia Impact (I_{NDT}) ($p=0.004$) and I_H ($p=0.001$) and ACC_H ($p=0.0004$) on RPE_O during non-continuous run. During continuous run, analysis showed significant influence of $\%HR_{max}$ ($p<0.0001$), RER ($p<0.0001$), knee angle ($p=0.036$), pronation angle ($p<0.0001$), I_{NDT} ($p=0.045$), I_H ($p=0.019$) and ACC_H ($p=0.003$) on RPE_O. To determine the physiological and endurance difference between both tests, paired sample t-test with 95% confidence interval was

used. Paired test between 'End' stage of continuous run in comparison with the non-continuous run showed a significant mean increase in '$\dot{V}O_2$' of 1.315 $ml.kg^{-1}.min^{-1}$ (p=0.012), 'RER' of 0.0316 (p=0.002) and 'BLa' of 1.285 $mmol.l^{-1}$ (p=0.001), and mean decrease in 'TTE' of 13.94 mins (p=0.00005). The neuromuscular fatigue indicated that 'Pi' of the GM (tb=-0.124, p=0.006), GL (tb=-0.206, p<0.0001), and TA (tb=-0.144, p=0.001) muscle and 'Fi' of RF (tb=-0.237, p<0.0001), VL (tb=0.160, p<0.0001), BF (tb=0.136, p=0.004), GM (tb=0.191, p<0.0001), GL (tb=0.096, p=0.028) and TA (tb=0.105, p=0.017) muscles were significantly linked with RPE_M during the continuous run. Whereas during the non-continuous run, 'Pi' of the RF (tb=-0.359, p<0.0001), VL (tb=-0.116, p=0.013), BF (tb=0.379, p<0.0001), ST (tb=0.133, p=0.002), GM (tb=-0.09, p=0.039), GL (tb=-0.103, p=0.011), and TA (tb=-0.183, p<0.0001) muscles and 'Fi' of BF (tb=-0.113, p=0.028), ST (tb= 0.169, p<0.0001), GM (tb=0.245, p<0.0001), GL (tb= 0.155, p=0.005), and TA (tb=-0.143, p=0.001) muscles were significantly correlated with RPE_M. Metabolic stress (BLa) showed significant correlation with RPE_O (tb=0.583, p=0.0001) and $\%HR_{max}$ (tb=0.581, p=0.0001). The significant fatigue predictors ($\%HR_{max}$, knee angle, pronation angle, I_{NDT}, I_H, ACC_H) from the continuous test were used to build real-time fatigue prediction model using multilinear regression. The model showed 88.26% variance (p<0.0001) in the observed subjective fatigue (RPE_O). Whereas the normalized fatigue model showed 87.7% variance (p<0.0001) by using normalized significant fatigue predictors ($\%HR_{max}$, pronation angle, ACC_H).

This research concluded that continuous and non-continuous tests showed a difference in fatigue manifestations on the biomechanical and physiological system. Neuromuscular activation (iEMG) levels were different in response to fatigue development during both tests. The observed 'Pi' of BF & GL and 'Fi' of BF were similar during both tests whereas other muscles showed a different response in relation with fatigue development. Time to Exhaustion (TTE) was higher during the non-continuous test and participants experienced lower metabolic and cardiorespiratory stress. $\%HR_{max}$ has been observed to predict metabolic stress during continuous running and could be used as a proxy for RPE_O and BLa. The proposed real-time statistical model for predicting fatigue has shown the potential to estimate subjective indicator of fatigue (RPE_O) for the selected participants under the laboratory controlled conditions. Further studies are needed to develop a robust model with larger population size, varied fitness levels and both genders under recreational, environmental factors and realistic endurance conditions.

Acknowledgement

I would like to express my deepest gratitude to my supervisor Associate Professor Hoon Kay Hiang and co-supervisor Associate Professor Seet Gim Lee Gerald for their inspiration, knowledge, encouragement, dedication, and patience. Accomplishments done so far would not have been possible without their guidance and sound knowledge. The uncountable meetings and brainstorming sessions have been the core contributor in my progress and highlights of my academic experience. Big thanks to Associate Professor Govindasamy Balasekaran, Associate Professor Domenico Campolo, and Associate Professor Swarup Mukherjee for their unconditional support, guidance, brainstorming thoughts and help in giving directions and in learning key essential principles for proceeding with this project.

I owe thanks to many members of the Exercise Physiology Laboratory and Biomechanics Laboratory, especially to Associate Professor Govindasamy Balasakaran and Associate Professor Kong Pui Wah, Veni for their support and permission to access their laboratory resources. I extend my appreciation to the laboratory staff, especially Tong Zhi Yi, Stuart and Ng Yew, Cheo for helping me in learning the use of equipment. I do thank the participants, recruited in this research, for their commitment and positive attitude to participate in this study. I also owe thanks to final year students to be the part of this research and help during experimentation and data collection.

To all my friends for their love, support, and fun-loving discussions throughout these years. Nevertheless, some of them deserve to be mentioned, due to their love, true friendship, and comfort: Dr. Ayesha Saleem, Dr. Syed Zeeshan Asghar, Dr. Nguyen Thanh Luan, and Yasir Mahmood Cheema.

To my beloved parents, beloved wife, brothers and sisters, thank you for your trust, support, strength, and prayers. I will do my best to make you proud.

Contents

List of Figures

Chapter 2: Literature Review

Chapter 3: Experimental Design, Methodology & Procedures

Chapter 4: Fatigue Manifestations During a Non-Continuous Endurance Training Protocol

Chapter 5: Fatigue Manifestations During a Continuous Endurance Training Protocol

Chapter 6: Physiological Differences Between a Non-Continuous & a Continuous Endurance Training Protocol

Chapter 7: Real-time Fatigue Prediction Model

List of Tables

Chapter 2: Literature Review

Chapter 3: Experimental Design, Methodology & Procedures

Chapter 4: Fatigue Manifestations During a Non-Continuous Endurance Training Protocol

Chapter 5: Fatigue Manifestations During a Continuous Endurance Training Protocol

Chapter 6: Physiological Differences Between a Non-Continuous & a Continuous Endurance Training Protocol

Chapter 7: Real-time Fatigue Prediction Model

Abbreviations

ACC_H: Hip Push-off Acceleration
ADP: Adenosine Diphosphate
AP: Action Potential
ASIS: Anterior Superior Iliac Spine
AT: Anaerobic Threshold
ATP: Adenosine Triphosphate
A-$\dot{V}O2$: Volume of Oxygen extracted from blood by tissues
BMI: Body Mass Index
BPMF: Biomarkers of Peripheral Muscle Fatigue
BW: Body Weight
BLa: Blood Lactate (Metabolic Stress)
CaO_2: Arterial Oxygen Content
CBF: Cerebral Blood Flow
CNS: Central Nervous System
CO_2: Carbon Dioxide
COM: Centre of Mass
CV: Conduction Velocity
DOF: Degree of Freedom
ECC: Excitation-Contraction Coupling
EMG: Electromyography
Fi: Fatigue Index
GRF: Ground Reaction Force
H^+: Hydrogen Ion
HR: Heart Rate
HRM: Heart Rate Monitor
HRR: Heart Rate Recovery
I_{DT}: Dominant Tibia Impact
iEMG: Integrated EMG
I_H: Hip Impact
IRB: Institutional Review Board
I_{NDT}: Non-dominant Tibia Impact
I_T: Tibia Impact
KPH: Kilometer per Hour
MdPF: Median Power Frequency
MFCV: Muscle Fiber Conduction Velocity
MHC: Myosin Heavy Chain
MLSS: Maximum Lactate Steady State
MMG: Mechanomyography
MN: Moto-neurons
MnPF: Mean Power Frequency
MS: Mid-stance
MVC: Maximal Voluntary Contraction
NAD^+: Oxidized Nicotinamide Adenine Dinucleotide
NADH: Reduced Nicotinamide Adenine Dinucleotide
O_2: Oxygen
One Way ANOVA: One Way Analysis of Variance
PCr: Creatine Phosphate
PETCO2: Partial Pressure of End-Tidal Carbon Dioxide
P: Inorganic Phosphate
Pi: Power Index
R-ankle: Right Ankle

R-knee: Right Knee
R-toe: Right Toe
RER: Respiratory Exchange Ratio
RM ANOVA: Repeated Measure of Analysis of Variance
ROS: Reactive Oxygen Species
RPE: Relative Perceived Exertion
RR: Respiratory Rate
RyR: Ryanodine Receptor (intracellular calcium channel)
sEMG: Surface Electromyography
SPF: Spectral Power Frequency
SR: Sarcoplasmic Reticulum
STR: Stride Rate
SV: Stroke Volume
TDMdPF: Time-Dependent Median Power Frequency
TMG: Tensiomyography
TMS: Transcranial Magnetic Simulation
TO: Toe-Off
VCO_2: Volume of Carbon Dioxide Exhaled
V_E: Ventilatory Minute Volume
CS: Critical Speed (AT Speed)
$\dot{V}O2$: Volume of Oxygen Uptake
$\dot{V}O2$ max: Maximum Oxygen Uptake

CHAPTER 1. INTRODUCTION

1.1 Background Knowledge and Motivation

Prolonged running is the most common form of exercise and is gaining popularity due to increased awareness on benefits of aerobic training. Several medical journals have reported the effectiveness of endurance training for prevention & treatment of chronic diseases and improvement in cardiovascular health [1, 2]. An observational study of 15-year on 52,000 adult runners reported 19% lower risk of all-cause mortality, compared to non-runners [1, 3]. The study also recommended that running distances of 1 to 20 miles/week with speed of 6 to 7 miles per hour, and frequencies of 2 to 5 days per week were associated with lower all-cause mortality. Whereas higher mileage, faster paces, and more frequent runs were not associated with better survival [3]. One more study on 416,000 participants (recorded for about 8 years) reported 40% reduced death risk with 40-50 minutes of vigorous exercise [4]. The exercise duration of 45 minutes was found to be demeaning, as afterward longer vigorous exercise efforts did not appear to reduce death risk. Light to moderate exercise intensity was reported to reduce death rates with an average of 110 minutes daily physical activity [4]. Considering the adverse effects of vigorous endurance exercise on myocardial activity, a study on 40 trained aerobic athletes reported elevation in biomarkers of myocardial injury, structural and electrical cardiac remodeling [5]. Published literature on running biomechanics has majorly reported that approximately 90% runners while doing marathon training and 56% recreational runners sustained lower extremity injuries each year. The most probable site of the lower extremity injuries has been the knee (7.2 - 50.0%), followed by the lower leg (9.0 - 32.2%), the foot (5.7 - 39.3%), and the upper leg (3.4 - 38.1%) [6]. The major reported injury development factors in lower extremity were individual's running biomechanics with fatigue progression, training frequency, flexibility, distance, pace, shoe type, history of injuries and coordinated imbalance in the lower extremity muscles [6-10].

The reported endurance intensity related injuries in the cardiovascular and biomechanical system have raised the importance of controlling running intensity for not only physiological benefits but also to reduce the occurrence of biomechanical injuries. One strong factor during endurance training that leads towards better management of running stress and to develop control over running intensity is fatigue. Fatigue has many definitions in the literature. According to bio-mechanist, fatigue is a decrement in the force output of a muscle [11], psychologist considers it as a sensation of tiredness [12] and physiologist views it as a failure of the specific physiological system [13]. This research considers all the above-stated aspects

of fatigue, which include the sensation of tiredness and the decrement in performance of a physiological and a biomechanical system from its optimal response [14].

Exercise is terminated at the point of exhaustion, not the fatigue [14]. Therefore, it is important to examine the undergoing changes in runners' body during endurance running to evaluate endurance performance. The mechanisms which contribute to the decline in performance are cardiovascular, energy depletion, neuromuscular, cortical drive, biochemical or psychological system [14]. The central governor (a governor located somewhere inside the Central Nervous System (CNS)) continuously manipulate the working physiological systems without pushing any single peripheral system beyond hemostasis and keeps the exercise for the longer duration [14]. Lambert et al. [15] and Noakes et al. [16] have proposed that fatigue is the result of multiple peripheral physiological systems and CNS. Many researchers have also reported the relationship between skeletal muscle performance and cardiac output [17, 18]. Hence, it is reasonable to conclude that fatigue is the outcome of the central and peripheral factors. In endurance performance, fatigue can be quantified as a decline in performance, examined through the physiological, neuromuscular and biomechanical response of the runner [14].

Development of fatigue in runners depends upon the running intensity, exposed running time and resting intervals. Performance is largely limited by the insufficient oxygen delivery of the cardiovascular system to the working muscles during the maximal aerobic intensity. Whereas, during submaximal aerobic activity, performance is limited by neurological alterations, energy depletion, the fatiguing status of active muscle or muscle trauma. Therefore, it is important for fatigue evaluation to consider nature of task (endurance running), force-fatigability relationship of working muscles (running intensity vs. exposure time), muscle wisdom (muscle composition and metabolic accumulations), sense of effort (to determine role of perceived effort in performance impairments) and recovery (to determine the effect of recovery on physiological and biomechanical system) [19]. Some other controlling factors that have potential to exacerbate the fatiguing conditions during submaximal exercise are hypoxia [20-22] and environment conditions [23] (thermal regulations, humidity). Hence, it is important to consider all these factors to simulate and reduce its effects on endurance performance in recreational active runners.

Blood Lactate (BLa) accumulation along with other intracellular changes (Na^+ and K^+ imbalance, increase in Pi and H^+ [24]) in skeletal muscles during exercise have reported its implication on the impairment of muscle Excitation and Contraction (E-C) cycle properties [19, 25, 26]. These intracellular metabolic accumulations, discussed in detail in Chapter 2, alter the contractile properties of the muscle, Muscle Fiber Conduction Velocity (MFCV), and

spectral factors in Electromyography (EMG) signal. These changes help in determining the peripheral and central fatigue [27, 28].

Peripheral fatigue is defined as the impairments at or distal to the neuromuscular junction which decrease muscle performance. Whereas, central fatigue is defined as the progressive reduction in voluntary activation of the working muscle and impairments above the neuromuscular junction of the motor unit [29]. Both sources of impairments cause the change in the spectral content of the EMG signal which can be computed in the time domain (integrated EMG = iEMG) and frequency domain (Mean Power Frequency (MnPF) and Median Power Frequency (MdPF)). The 'MnPF' and 'MdPF' represent the gold standard measure of neuromuscular fatigue [30]. Whereas 'BLa' concentration represents the active metabolic conditions in relation with fatigue development during running.

Neuromuscular fatigue during endurance performance can be quantified by measuring the spectral content of the neuromuscular activity. Several studies in the literature have reported the methodology to examine neuromuscular fatigue and its interaction with running mechanics and endurance performance for trained endurance runners and elite runners. Neuromuscular fatigue in lower extremity muscles against fatigue and progressive speed running is well reported. These existing studies [28, 31, 32] either include the intervened or maximal exertion or continuous running fatigue protocol to report fatigue significant effect on runner's joint mechanics. The published literature has also reported the interaction of neuromuscular fatigue with joint mechanics and running economy while studying group of muscles groups [33, 34] and/or individual muscle [35, 36]. However, literature has limited studies on examining skeletal muscle fatigue in relation to endurance time for the recreational class of runners. There is need to have a more detailed understanding of primary skeletal muscles, causing locomotion and are susceptible to earlier fatigue (e.g., biarticular muscles fatigue earlier than mono-articular muscles [33]). Therefore, this research aimed to quantify the neuromuscular fatigue in major lower extremity muscles which include Rectus Femoris (RF), Vastus Lateralis (VL), Bicep Femoris (BF), Semitendinosus (ST), Gastro-medial (GM), Gastro-lateralis (GL), and Tibialis Anterior (TA). There are also limited studies on the interaction of neuromuscular fatigue with running mechanics during continuous and non-continuous endurance fatiguing protocols in recreational active runners.

Fatigue is also known to affect running kinematics and gait parameters. The most known parameters which have proven the relationship with fatigue are stride parameters (Stride Length (SL), Stride Rate (STR), contact time) [37, 38] , knee flexion [39], hip flexion/extension [39, 40], Tibia Impact (I_T) acceleration [41] and Ground Reaction Force (GRF) [42]. Therefore,

it is important to observe the changes in these parameters during fatiguing contractions under selected fatiguing protocols to evaluate biomechanical fatigue in recreational active runners.

This study, in conjunction to all the above-stated fatigue manifestations on the neuromuscular, kinematic and physiological system, examined endurance fatigue in recreational active runners. The physiological measures under study include oxygen consumption ($\dot{V}O_2$), Heart Rate (HR), Respiratory Rate (RR), Respiratory Exchange Ratio (RER), Maximum HR (HR_{max}) and maximal aerobic capacity ($\dot{V}O_{2max}$). The neuromuscular parameters being measured include Integrated EMG (iEMG) and Time-Dependent Median Power Frequency (TDMdPF). Neuromuscular fatigue was evaluated using power index 'Pi' and fatigue index 'Fi' of selected RF, VL, BF, ST, GM, GL, TA muscles. Kinematic measures include hip angle, knee angle, ankle angle, pronation angle, landing impact on the dominant (I_{DT}) and non-dominant tibia (I_{NDT}), landing impact on the hip (I_H) and hip push-off acceleration (ACC_H). Rating of perceived exertion data for the chest (RPE_C), leg muscles (RPE_M) and overall body feel (RPE_O) were recorded to determine perceptual fatigue.

The findings of this thesis will help to understand how recreational active runners are different from the trained runners. This research also passionately aimed to lay out the framework of developing a real-time fatigue prediction model for recreational active runners. The model is aimed to predict metabolic stress and fatigue in real-time to have optimal benefits of endurance training as advised by the trainer.

1.2 Objectives and Hypotheses

The purpose of this thesis is to understand and analyze the physiological and biomechanical aspects of endurance performance during the non-continuous and continuous training scenarios. Furthermore, this research aimed to propose a methodology for modeling subjective fatigue response into a 'real-time fatigue prediction model' using the continuous test data. The proposed listed objectives are structured to successfully achieve the purpose of this research.

Objective 1: Determine the major locomotory and stability muscles susceptible to earlier fatigue in the lower extremity while running at Critical Speed (CS) till exhaustion during the non-continuous and continuous fatigue protocol.

Hypothesis 1.1: This research hypothesized that neuromuscular fatigue in the lower extremity muscles will result in increased neuromuscular activation levels (iEMG) and decreased Time-Dependent Median Power Frequency (TDMdPF) of the working muscles.

Hypothesis 1.2: This research hypothesized that the selected working muscles in the lower extremity will experience fatigue in a different fashion during both studied protocols (continuous vs. non-continuous).

Objective 2: Identify the physiological differences in endurance performance during the non-continuous and continuous fatigue protocol.

Hypothesis 2.1: This research hypothesized that 1-min rest intervals during the non-continuous protocol will change the fatiguing development response in recreational active runners. This 1-min rest will result in the difference in BLa accumulation and cardio-respiratory stress during non-continuous running as compared to continuous endurance protocol.

Hypothesis 2.2: This research hypothesized that 1-min rest during the non-continuous protocol will change TTE as compared to the continuous test.

Objective 3: Devise a non-invasive physiological marker to estimate metabolic stress (BLa) in recreational active runners.

Hypothesis 3.1: RPE has been found to show greater variation among runners against BLa buildup. This research hypothesized that there may be a physiological marker to estimate 'anaerobic threshold (AT)' with less prediction error than RPE.

Objective 4: Identification of most significantly correlated biomechanical and physiological variables to determine fatigue in relation to BLa and RPE.

Hypothesis 4.1: Currently, RPE and an invasive procedure of blood sampling are required to measure fatigue and BLa respectively. This research hypothesized that there may exist a significant correlation of non-invasive cardio-respiratory variables (HR, RR, $\%HR_{max}$, $\dot{V}O_2$, RER) and biomechanical variables (hip angle, knee angle, ankle angle, foot pronation, STR, I_{DT}, I_{NDT}, ACC_H, I_H) with RPE and BLa.

Objective 5: Development of a real-time fatigue prediction regression model to determine fatigue levels during continuous endurance running.

Hypothesis 5.1: Determining fatigue in real time is a complex phenomenon as it is dependent on several interconnected fatigue models (cardiovascular/anaerobic model, energy depletion model, neuromuscular fatigue, biomechanical model, psychological model and central governor model). However, the cumulative effect of all these interconnected fatigue development models results in changing the cardio-respiratory and biomechanical response. This research hypothesized that developing a regression model with all significant fatigue prediction factors will help in estimating fatigue in more accurate fashion as compared to single factor with compromised accuracy.

1.3 Scope and Significance of the Thesis

Extensive studies on endurance-trained runners exist to elucidate fatigue manifestations on running biomechanics and runner's physiology [43-45]. However, the findings from the trained runners cannot be simply implied to recreational runner due to the reported difference in

physiological response [46]. There is dire need to evaluate the body response of recreational active runners, considering their increasing participation count in endurance events. This will help recreational active runners by improving the quality of training with better awareness of endurance training protocols, metabolic stress levels and fatigue assessment in real time. Therefore, this research personally motivated me to study this topic and propose a solution which can improve the quality of training by revealing certain findings.

For achieving research objectives, two endurance fatigue protocols (continuous vs. non-continuous) were conducted. Fatigue was examined in the physiological, neuromuscular and kinematic system. Critical speed (CS) (determined at BLa of 4.0 mmol.l^{-1}) was selected due to its significant metabolic relationship with endurance conditions [47, 48]. Only one study, Penteado et. al. [49], has tested the response of different fatiguing protocol (continuous vs. non-continuous) on endurance performance. The findings of this study were limited to trained runners and triathletes and no physiological evidence for the difference in time to exhaustion (TTE) between both tests was provided. The study was also conducted on synthetic track and neuromuscular fatigue along with kinematic changes were not evaluated in the lower extremity. This research focuses on male recreational active runners as there is a dearth of reported literature on running biomechanics, exercise physiology, and neuromuscular fatigue. The physiological analysis was conducted by "True One 2400" analyzer. Whereas for neuromuscular activity, Trigno Wireless EMG system was used to monitor EMG signal from the selected muscles (RF, VL, BF, ST, GM, GL, TA). For kinematic analysis, 2D video camera system was used to track joint angles for the hip, knee, ankle and foot pronation. Inertial sensors (Trigno Wireless IM units) were used to measure tibia and hip impacts and hip acceleration. RPEO-OMNI scale was used to determine perceptual fatigue for the chest (RPE_C), legs (RPE_M) and overall body (RPE_O). The study successfully examined the effects of various physiological, neuromuscular and kinematic variables on TTE, metabolic stress and perceptual responses during both selected endurance protocols. The effect of 1-min rest during the non-continuous test was also examined to understand its impact on TTE, BLa and physiological markers of fatigue. Protocol dependent changes in neuromuscular fatigue of the lower extremity muscles were also successfully examined. The study also investigated the effect of neuromuscular fatigue in running mechanics. This study also explores the potential use of HR parameter to determine metabolic stress (BLa), as contradictory evidence exists on the rise of BLa and RPE during intermittent exercise [50]. Fatigue implications on the continuous run study were examined to identify physiological and biomechanical predictors of fatigue. Also, a real-time fatigue prediction model was built to estimate subjective perceived exertion by using the

continuous test data. The study provided the framework for future studies to examine the manifestation of fatigue in endurance runners on outdoor terrain or track in an integrated fashion. Future studies should also include larger population size and both gender to develop a robust fatigue prediction model.

1.4 Delimitations of the Research Study

This thesis covers only those male recreational active runners whose $\dot{V}O_{2max}$ is greater than 50 ml. $kg^{-1}.min^{-1}$ and were performing normal training routines for at least last three months. All the participants were students in NTU/ NIE and were active in running along with other different recreational sports (soccer, badminton, cycling, swimming, etc.). The study does not cover the female recreational active runners, due to the physiological difference in performance between male and female distance runners [51, 52]. The study also does not cover the aspect of participant's motivation, regular diet & running attire [53]. The study also does not cover the effect of lactate variance among individuals and its effect on onset of fatigue determination. The lactate tolerance among studied participants is another factor which delimits the finding of this study to the studied group of population. The other delimitations of the study include the use of treadmill [54], controlled laboratory conditions [53], personalized differences in body response at CS [53], and constant CS during endurance evaluation. All these factors contribute towards delimiting the research implications to the studied population with simulated testing conditions. The research conclusions are applicable to only studied group of recreational active runners with all the controlled conditions (laboratory setup, laboratory environment, treadmill, running surface) and will serve the purpose of understanding.

This thesis presented integrative analysis methodology to determine the fatigue predictors in the physiological and biomechanical system with limited sample size. Selected sample size delimits the inclusion of other non-explored biomechanical and physiological parameters. Future study should include higher sample size, both genders, non-explored biomechanical and physiological variables and different demographics of the participants across age and fitness level may surpass the delimitations.

1.5 Structure of the Thesis

A brief literature review has been stated in chapter 2, explaining about intracellular fatigue mechanisms and associated biochemical, cortical, neuromuscular, physiological and kinematic changes. Few biochemical, biomechanical and physiological parameters were selected based on the observed findings and practicality of fatigue measurands. A literature review has been conducted thoroughly to determine research gaps, key findings in the literature, and approach of this research. The experimental design, procedures, and data processing methodology of

this thesis has been generalized in chapter 3. The studied protocols in chapter 3 have been reviewed critically and have been cross-checked with other fellow researcher's protocols [49]. The research findings of two different endurance protocols (non-continuous and continuous, discussed in chapter 3) have been stated thoroughly in chapter 4 and 5 respectively. The research considered the limitation of BLa measurement during continuous running. A non-continuous protocol was administered to study the metabolic stress development. The non-continuous protocol also analyzed how 1-minute rest changes the fatigue response of the physiological and biomechanical system in endurance recreational active runners. A comparative analysis approach has been adopted to understand the physiological differences between two selected protocols in chapter 6. Metabolic stress estimation model has been proposed to determine the metabolic relationship with endurance running and to determine Anaerobic Threshold (AT), using a non-invasive $\%HR_{max}$ variable, in chapter 6.

Real-time fatigue prediction model has been proposed in chapter 7. The model fitting results have been presented for the observed data along with its prediction accuracy. The conclusion, summary of findings, limitations of the research study and future work have been explained in chapter 8. A wearable system "KETS" has been proposed in appendix section, to deploy the practical use of the developed model in the real-world applications.

1.6 Definition of Key Terms

Exhaustion: A state of extreme physical or mental tiredness

Termination: The action of terminating exercise due to maximal perceived exertion.

Rating of Perceived Exertion (RPE): Perceived exertion is how tired you feel while your body is working [55].

Endurance: Capacity to sustain a given speed for the longest possible time, also known as a time to exhaustion [56].

Endurance Pace: Speed which is maintained on average during endurance event [56].

Critical Speed (CS): Speed at anaerobic threshold of lactate 4.0 $mmol.l^{-1}$ [57].

Fatigue: Fatigue is defined as an exercise-induced decrease in maximal voluntary force produced by a muscle [58].

Peripheral Fatigue: Impairment at or distal to the neuromuscular junction is called neuromuscular fatigue [58].

Central Fatigue: Central fatigue is a progressive decline in voluntary activation of muscle during exercise [58].

Oxygen Cost ($\dot{V}O_2$): The amount of oxygen, consumed at certain speed.

Maximum Aerobic Capacity ($\dot{V}O_{2max}$): $\dot{V}O_{2max}$ is the maximum aerobic capacity of the athlete.

Respiratory Exchange Ratio (RER): RER is defined as the ratio of $\dot{V}O_2/VCO_2$.

Running Gait Cycle: Running gait is described as a series of movements of lower extremity between initial foot contact with the surface followed by re-contact of the same foot with the surface [59].

Tibia Impact (I_T): Impact, experience on tibia from the ground during the landing phase of running gait cycle.

Dominant Tibia Impact (I_{DT}): Impact on the dominant leg of the lower extremity.

Non-dominant Tibia Impact (I_{NDT}): Impact on the non-dominant leg of the lower extremity.

Hip Impact (I_H): Average impact on the hip segment from the lower extremity.

Hip Acceleration (ACC_H): Hip push-off acceleration during the toe-off phase of running gait cycle.

Stride Rate (STR): Number of strides per minute.

CHAPTER 2. LITERATURE REVIEW

Running is a critical locomotory skill for almost all sporting activities as it builds strength, stamina, improves the cardiovascular system, running mechanics and overall health. However, there are potential factors in runner's biomechanical and physiological system that can lead to injury development. The factors, leading to injury development, are intracellular accumulations and their effect on muscle performance, overstress, lacking control on running form, coordinated muscle imbalance, and inappropriate landing mechanics. The basic reason behind such potential changes during running is fatigue. The fatigue can be driven peripherally or from the central region of the brain.

This literature review is focused on explaining every perspective of fatigue (peripheral or central). The literature highlighted the fatigue manifestations on neuromuscular, physiological and biomechanical systems during endurance running. It will also provide an in-depth understanding of fatigue development process. It demonstrated the relation with running intensity/duration and associated metabolic, neuromuscular, physiological and running mechanics changes pertaining to fatigue. Section 2.1 will define fatigue and outline the primary factors entangled in peripheral and central fatigue. Fatigue measurement methods for detecting peripheral and central fatigue will be discussed along with its limitations in this section. Biological indicators of central and peripheral fatigue will be discussed in detail and most authenticated variables will be shortlisted in correlation with fatigue. Perceived exertion as a subjective measure of fatigue will also be discussed in this section. Section 2.2 will discuss cardiovascular and respiratory response in relation with running intensity and perceived exertion. Section 2.3 will demonstrate running biomechanics, neuromuscular fatigue in the lower extremity and will list down the most fatigue influenced biomechanical parameters. Section 2.4 will present the existing non-invasive fatigue measurement technologies along with instrumentation to access muscle fatigue. Section 2.5 will highlight the key findings in the literature, research gaps and approaches of this research to address those gaps.

2.1 Fatigue

Fatigue has many definitions in literature as it involves several different phenomena. Each phenomenon involves different physiological mechanisms [60], specific to the task being performed. This research aims to quantify fatigue for recreational active runners, engaged in a prolonged repetitive activity like endurance running. Fatigue, in this context, is "an acute impairment in exercise performance resulting in the increased perceived effort and decreased muscle ability to produce required force/power" [13, 61, 62]. The decline in muscle force,

known as muscle fatigue, can be most likely due to metabolites accumulation within working muscle [25] and/or reduced cortical drive [62].

Muscle is considered as a motor drive unit. The behavior of the muscle is dependent upon the intrinsic properties, cortical drive and the afferent feedback system [29, 62]. According to the modern muscle physiology review, the afferent feedback system may operate within the muscle cell, at the level of spinal motoneuron or at a supra-spinal level [29]. This can reduce the ability of a muscle to generate force or power at any stage of the motor system. Figure 2-1 explains about the descending drive from motor cortex through spinal motoneurons to activate muscle fiber and influence of afferent feedback over different sites. During repetitive contractions, neuromuscular fatigue may arise at any stage of the motor system including conscious psychomotor components, such as perceived exertion and motivation. Considering the sight of impairment along the motor path, fatigue produced at or distal to the neuromuscular junction is called peripheral fatigue. Whereas impairment above the neuromuscular junction or reduction in the cortical drive is called central fatigue. [29]

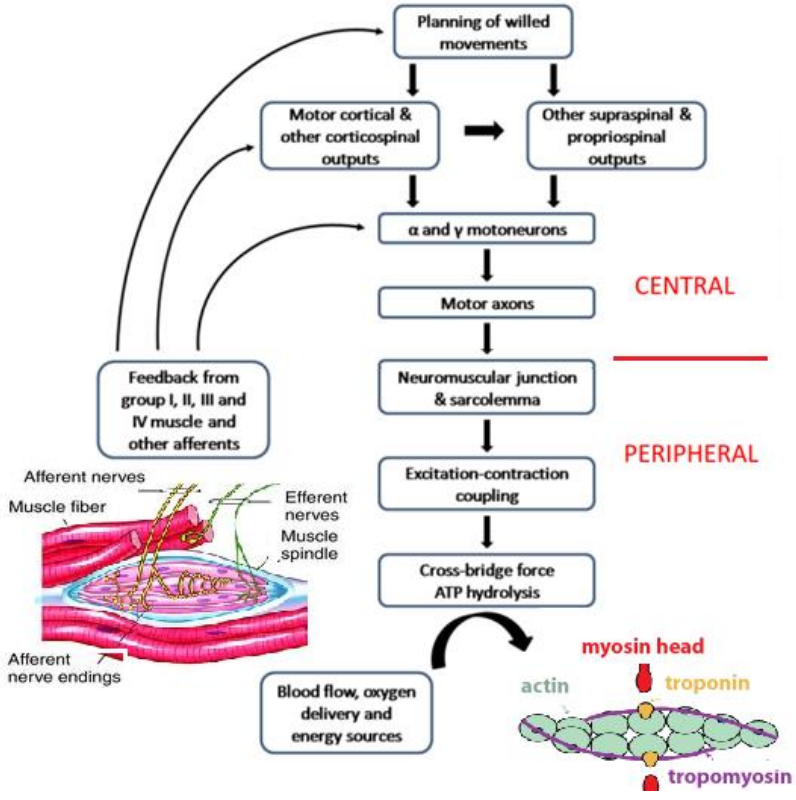

Figure 2-1: Structural diagram explaining about chain involved in voluntary activation of muscle and role of muscle afferent feedback over the central nervous system at three different level [29].

2.1.1 Peripheral Fatigue

Fatigue produced at or distal to the neuromuscular junction is referred to as peripheral fatigue [29] and ensures a progressive decline in performance (force/power, contraction velocity and relaxation time). Major reasons for peripheral fatigue (discussed below) are the failure of excitation-contraction coupling of muscle fiber or contractile proteins, intracellular and extracellular metabolites, reduction in the muscle fiber conduction velocity and/or delayed recovery [25]. In this research, the decline in performance is not immediate under submaximal activity like endurance running. Fatigue manifests itself as a failure to continue activity at the stated running intensity [63] and is considered reversible by rest.

2.1.1.1 Excitation-Contraction (EC) Coupling of Contractile Proteins

Various mechanisms are involved in excitation-contraction (EC) coupling in skeletal muscle. The action potential travels from the brain through several electrical and chemical events (through the spinal cord, motor nerve, and neuromuscular junction) and reaches to the muscle fiber [64]. It activates the cross-bridge cycle through the relative sliding of actin and myosin by the cyclic interaction of side pieces from the myosin filament [65], shown in Figure 2-2.

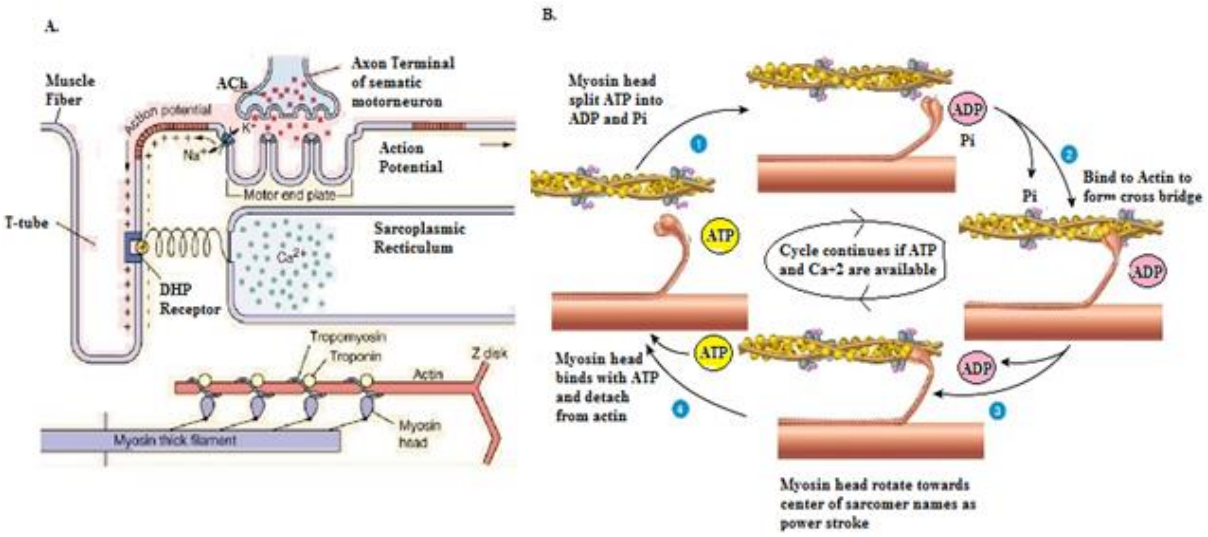

Figure 2-2: Cross-bridge cycle representing the whole chain of reaction from action potential to actin/myosin binding shown in A) and Sliding Filament Theory showed in B)

The neuromuscular junction provides 1:1 action potential transmission under normal physiological conditions [29] following an efflux of Na^+ followed by an influx of K^+ and travels to the transverse tubules into the interior of the muscle. Voltage sensor in t-tubules is in close contact with SR Ca^{2+} release channel. Once Ca^{2+} release from SR, it binds to troponin C and let the myosin be attached with actin to perform contraction and hence force production [66] using ATP. This chain of events has potential to limit performance and cause fatigue. Under fatigue condition, normal functionality of the contracting mechanism impairs [67] due to

inhibition of AP, increased extracellular concentration of K^+ over the sarcolemma and possible blockage on its propagation to t-tubules [68]. Change in electrochemical gradient of K^+ is associated with repeated activations, inhibition of excitation and muscle force reduction [25, 68]. Fatigue or muscle force reduction can also be associated with decreased availability of Ca^{2+} from SR or faster reuptake of Ca^{2+} by the calcium pump [25, 66, 69].

2.1.1.2 Metabolic pathways and neuromuscular component

Adenosine triphosphate (ATP) is the chief biochemical fuel utilized by cross-bridge contractile mechanism and to maintain the ionic balance within it [70, 71]. ATP is also required for energy-dependent cellular processes that have a fundamental role in EC coupling such as Na^+/K^+ exchange across sarcolemma and t-tubules and Ca^{2+} release and reuptake by SR [71]. Oxidative phosphorylation, glycolysis, and phosphocreatine are major ATP generation pathways and their contribution in generating ATP, shown in Figure 2-3, are completely based on exercise type, intensity [71] and the type of muscle fiber recruitment [25].

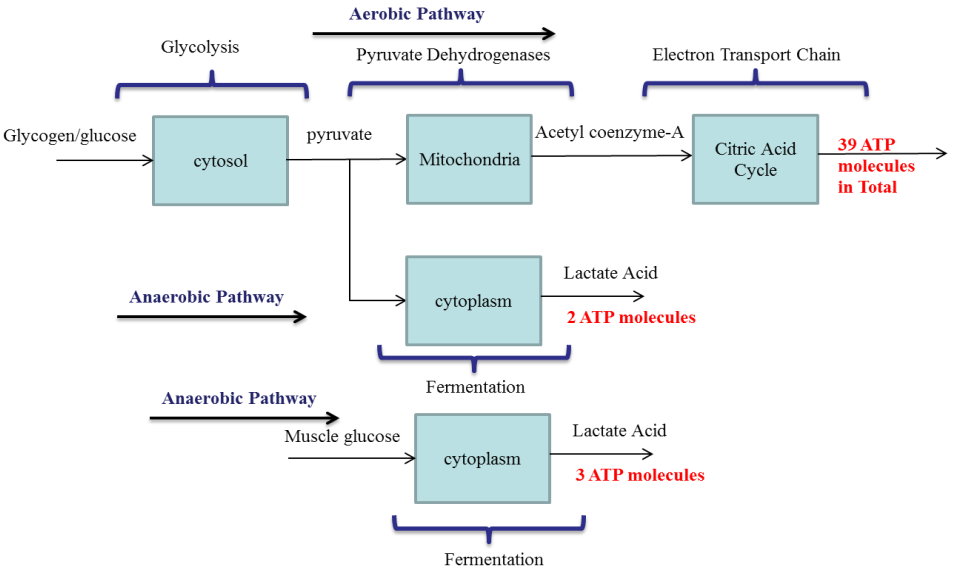

Figure 2-3: ATP energy production sources and their efficiency in generating biochemical fuel to contractile machinery

Muscle fibers are divided into these categories: slow-twitch oxidative type I, fast-twitch oxidative type IIA, fast-twitch glycolytic type IIB fibers and hybrid I-II A and IIA-IIB fibers, based on metabolic requirement and MHC isoform [72]. There are inherent differences in these fiber types. Type II fibers can generate higher force [73] and has faster shortening velocity [72] than type I fiber where type I fibers are fatigue resistant because of higher succinate dehydrogenase in mitochondria, and have greater oxidative capacity in comparison with type II fiber containing lactate dehydrogenase as a marker of anaerobic capacity [30]. This indicates

that type I fiber has the higher oxidative capacity and metabolic efficiency than type II fiber [25] and are considered best in a repetitive task with low power output while type IIA with intermediate duration are considered for intermediate force output and type IIB for high power output with short duration.

During endurance exercise, oxidative phosphorylation is the most efficient source of ATP supply. Activated fatty acid molecules along with pyruvate, NADH, protons (H^+) and products of ATP hydrolysis are used by mitochondria as a substrate for mitochondrial respiration. It keeps the intracellular pH at a neutral level as shown in Figure 2-4 (A). With increasing intensity of exercise and high ADP demand, non-mitochondrial ATP production occurs through fermentation which gives rise to Pi and H^+ concentrations that have been implicated in fatigue at multiple levels [74]. It is also argued in the literature that H^+ accumulation inhibits the rise in signal activation of oxidative phosphorylation and may limit the oxidative capacity to supply ATP [74]. Under oxidative stress (high-intensity activity), ATP hydrolysis is not fully supported by mitochondrial respiration. In this condition, cellular ADP generates ATP through glycolysis that results in cytoplasmic pyruvate, NADH, and H^+ accumulation, shown in Figure 2-4 (B). Following lactate dehydrogenase reaction, lactate and NAD^+ are produced to maintain the intracellular acidosis because of H^+ and continued ATP production [75]. Lactate formation consumes one H^+ to maintain the cellular acidosis and transports out of the cell to maintain pH [75]. As the intensity increases, the buffering mechanism reaches its limit in transporting lactate acid from the muscle and hence intracellular lactate and H^+ accumulation [75, 76]. This results in muscle acidosis and the onset of fatigue following termination of exercise. Energy metabolism mechanism during exercise and production of lactate and H+ are also dependent on the richness of mitochondrial capacity in reducing the oxidative stress and exercise intensity.

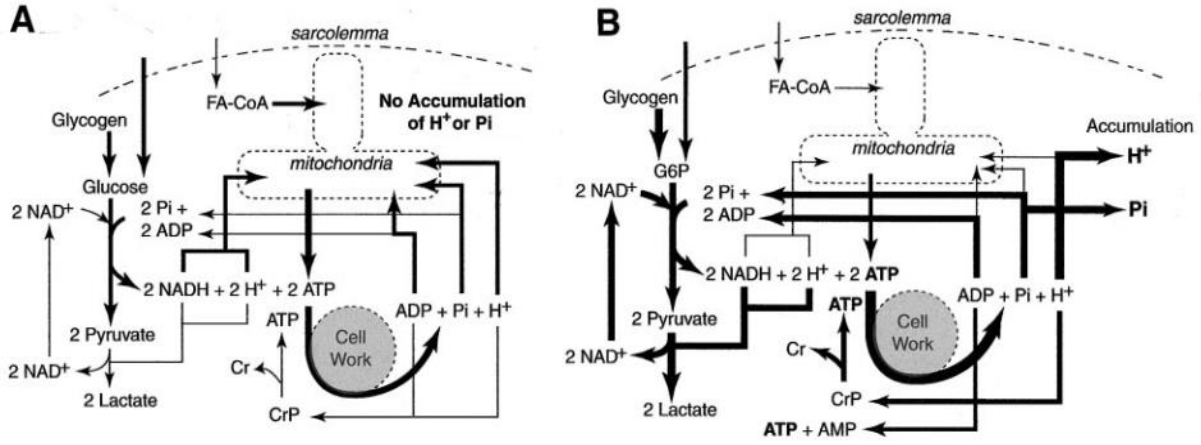

Figure 2-4: Energy metabolism during A) submaximal exercise, B) maximal exercise [25]

2.1.1.3 Summary of Intracellular and extracellular changes

Fatigue has many causes depending upon the physical activity and mechanism involved. Three major mechanisms of fatigue can be categorized into low-intensity exercise for a prolonged duration, intermediate intensity (submaximal exercise) with prolonged duration and high intensity with short duration. Fatigue development in each of these mechanisms has different causes. Following Figure 2-5 explains explicitly about the cellular changes that can contribute to muscle fatigue in any case. Each box represents the subcellular function and subsequent list of cellular changes that may change the cellular function during fatigue.

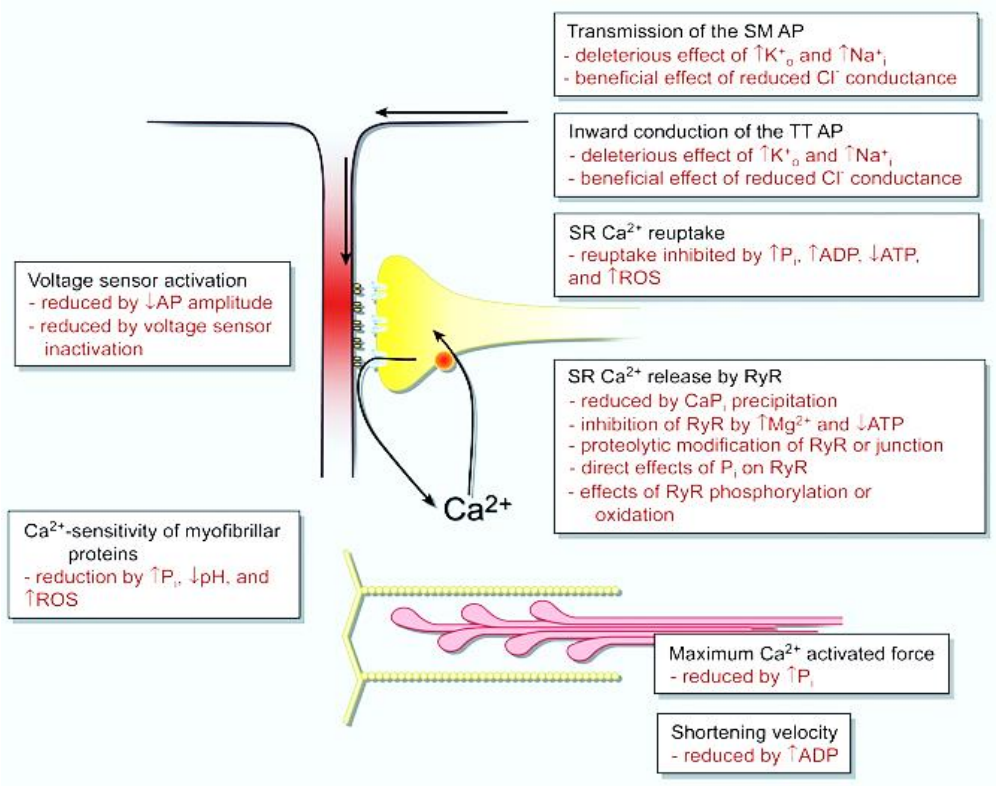

Figure 2-5: Mechanisms contributing to muscle fatigue [25]

2.1.2 Central Fatigue

Central fatigue is a progressive decline in voluntary activation of muscle during exercise [29, 77]. It may arise not only because of peripheral changes within or at the level of muscle but also because of spinal and supra-spinal factors, subject motivation, the perception of effort and perceived exertion and the afferents feedback system [29, 78]. Muscle wisdom hypothesis [19, 29] also state that motoneuron firing rate does decline to match the contractile speed of muscle to produce optimal maximal force during fatiguing contractions. If it does not do so, a neural dilemma occurs. If motor neuron rate declines too much, then voluntary activation will not be sufficient to produce maximal force and thus central fatigue appears [29].

Therefore, the role of the motor unit is critical because of regulation of firing rate and contractile machinery of muscle. Each motor unit needs its firing rate to be adjusted in a customized fashion to meet its contractile and force development capability. The contractile machinery is dependent on muscle fiber composition, fiber length, temperature, metabolic conditions and conditions of the exercising muscle, so customized motoneurons control is highly improbable. Under repetitive firing, suboptimal properties of recruitment of motor units reduce muscle force [79], known as spinal fatigue. Supra-spinal fatigue, a subcomponent of central fatigue, is defined as an exercise-induced decline in force by the suboptimal output from the motor cortex [77]. However, the mechanisms have not been clearly understood. One probable factor to supra-spinal fatigue is the firing of fatigue-sensitive muscle afferents that may act to impair voluntary descending drive [62, 77, 78]. It is also well-studied fact that central fatigue occurs in almost all kinds of exercises and test results have been reported using transcranial magnetic stimulation (TMS). Research studies on TMS revealed that motor cortex does produce suboptimal descending drive during human muscle fatigue [62, 80, 81].

To evaluate central and peripheral fatigue, exercise intensity is an important factor as it changes the contribution of peripheral and central factors towards fatigue development. According to the published studies [20, 81, 82], endurance exercise performance is determined to a significant extent by the feedback afferents of peripherals (working muscles) to the central drive. Furthermore, it was reported that arterial oxygen alterations caused significant changes in central motor drive whereas peripheral quadriceps fatigue at exercise termination remained constant [82]. One more study [81] cross-checked these findings by pre-fatiguing the locomotory muscle to varying degrees prior to performance trial. This study concluded that development of peripheral fatigue is confined to a certain level and further degradation in performance was mainly because of decline in the motor drive unit.

Central fatigue has also been considered as a safety mechanism for active organs to maintain the balance and overall homeostasis during exercise. In accordance with central governor model, exercise terminates before catastrophic failure of homeostasis in exercising muscle [83]. Continuous interaction between feedforward and feedback control mechanisms in the brain and peripheral physiological systems produces a robust self-sustaining mechanism. This maintains homeostasis by ensuring that no system is ever overwhelmed or used to absolute maximal capacity [16]. It also suggests that rising perception of discomfort or effort during prolonged activity progressively reduces the conscious desire to over-ride this control mechanism. Thus, an increase in perceived exertion serves to assure that damage does not rise to endangering level. Central nervous system (CNS) is the ultimate obvious factor to appear during exercise,

the notion of the ‘central governor’ to protect the integrity of organism remained hypothetical [12].

2.1.3 Fatigue Measurement

Identifying the site of impairment on the motor path is quite complex due to the chain of events that result in the muscle E-C cycle impairment. Several measurement technologies have been developed to quantify central and peripheral fatigue. These technologies include nerve stimulation, twitch interpolation, Mechanomyography (MMG), Tensiomyography (TMG), transcranial magnetic stimulation (TMS) and invasive electromyography and non-invasive or surface electromyography (sEMG). Every technique had its own limitations for detecting the site of impairment for fatigue. This review only focuses on sEMG for detecting peripheral and central mechanism of fatigue as it provides a practically viable solution to measure peripheral and central fatigue under dynamic exercising conditions.

Tensiomyography (TMG) [84], twitch interpolation [85], transcranial magnetic stimulation (TMS) [77, 86] are the good lab tested and well-proven techniques. These techniques measure the existence of peripheral, spinal and supra-spinal factors causing fatigue. The limitations of these techniques are that they require the participant to be properly seated with controlled posture for accurate results and cannot be used under dynamic exercising scenarios like running. Therefore, these techniques will not be discussed further in this dissertation.

2.1.3.1 Surface Electromyography (sEMG)

Electromyography (EMG) measures electrical activity through the summation of the motor unit action potential (MUAP), shown in Figure 2-6. The muscle is controlled by the action potential, electrode placement on the surface of muscle to pick up these signals is critical. Electrodes placed on the surface of the skin, collect signals from different motor units (MU). While traveling through EMG detector, these electrodes may generate crosstalk of different myoelectric signals from the neighboring tissues [87] and noise [88]. Apart from its sensitivity to signal noise, this method is widely used in biomechanics research due to its non-invasive nature and ability to measures change in EMG activity which is used as a metric to quantify fatigue of a muscle [87].

Captured sEMG signals provide valuable information about the changes in excitation level and recruitment of the muscle fibers [89]. Muscle fatigue is determined through the time domain and frequency domain analysis of the sEMG signal. Initial filtering by using bandwidth filter ranging 10-1000 Hz is required to clean noise from the meaningful data. Selection of this bandwidth depends on the type of sEMG capturing system and muscle type under study. In this

research, bandwidth filter of 35-500Hz was selected by analyzing the power spectral density of the sEMG signal. This was targeted to remove the motion artifacts, dc content, and noise.

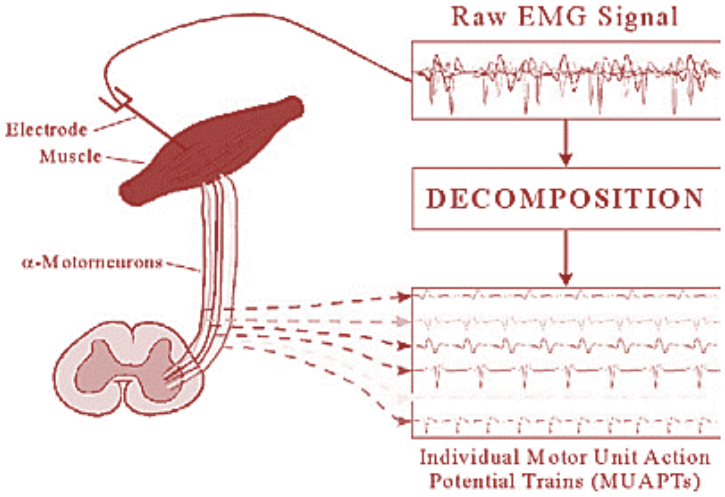

Figure 2-6: EMG raw signal and decomposition into MUAPs [*88*]

Time Domain Analysis

Time domain analysis helps to estimate the sEMG amplitude, known as muscle effort. Currently, two variables, mean absolute value (MAV) and root-mean-square (RMS) value, are used to estimate the muscle effort [87]. These two variables are defined by the following equations.

$$MAV = \frac{1}{N}\sum_{i=1}^{N}\left|X_i\right| \qquad \ldots\ldots\ldots \qquad (2\text{-}1)$$

$$RMS = \sqrt{\frac{1}{N}\sum_{i=1}^{N}X_i^{\,2}} \qquad \ldots\ldots\ldots \qquad (2\text{-}2)$$

In both equations, X_i represents the *i*th sample of the signal and N represents the number of samples or the averaging window size.

The other available techniques in the time domain analysis are the 'Zero-Crossing-Rate (ZCR)' and spike analysis of the signal. Due to the high sensitivity of signal-to-noise ratio of sEMG signal, use of ZCR is questionable [87]. Similarly, the use of spike analysis is not presented here due to contradictory results on the reliability of spike parameters [87].

Frequency Domain Analysis

Frequency domain analysis helps in assessing muscle fatigue by observing motor unit recruitment pattern [90] within working muscle. The shift in frequency towards lower or higher end depends on the type of load, contraction and exposed contraction time. Using spectral analysis, Power Spectral Density (PSD) is calculated by calculating the Fourier Transform (FT) of the autocorrelation function of sEMG signal. Mean (MnPF) and median (MdPF) power

frequencies are calculated from the PSD of the sEMG signal to observe the frequency shift [91]. These frequency variables are defined as follows.

Median power frequency (MdPF) represents the division of power spectrum in two regions with equal integrated power, shown in equation 2-3. Whereas, mean power frequency (MnPF) represents the average frequency value and is calculated as the sum of the product of power spectrum and the frequency divided by the sum of power spectrum [92], as shown in equation 2-4.

$$\sum_{i=1}^{MDF} P_i = \sum_{MDF}^{M} P_i = \frac{1}{2}\sum_{i}^{M} P_i \quad \ldots\ldots\ldots \quad (2\text{-}3)$$

$$MNF = \sum_{i}^{M} P_i f_i \Big/ \sum_{i}^{M} P_i \quad \ldots\ldots\ldots \quad (2\text{-}4)$$

P_i represents the EMG power spectrum at frequency bin 'i', M represents the total number of power spectrum and f_i represents the frequency of spectrum at frequency bin 'i'.

For assessing muscle fatigue under dynamic contractions, MdPF use is recommended over MnPF. It is due to its lower sensitivity to random noise in the high-frequency band of EMG power spectrum and higher affect by muscle fatigue [93]. Furthermore, as running involves a cyclic dynamic contraction, various researchers have proposed the use of time-dependent analysis of MnPF and MdPF [92, 94]. This helps in monitoring muscle activation dynamics at different time intervals during fatigue protocol. Therefore, time-dependent mean (TdMnPF) and median frequency (TDMdPF) were calculated by using the sliding window timing technique to determine the change in frequency. This research used TDMdPF instead of TDMnPF because the median frequency was found to be less affected by high-frequency noise within the sEMG signal and is a reliable measure of muscle fatigue [91]. Some other classic and modern techniques like wavelet analysis, Dimitrov fatigue index, fractal analysis, entropy, recurrence quantification analysis, linear and non-linear techniques have been proposed and their suitability to fatigue detection is application dependent. Such techniques are not covered in this review. The details on these modern techniques can be found in a review study by Miriam et al. [95, 96] for further understanding.

Combined Analysis of sEMG spectrum and Amplitude

The sEMG electrical activity (amplitude) and spectral frequency are both affected by force and fatigue. Their combined analysis can help to understand whether changes in sEMG are fatigue-

induced or force-related [87]. The literature distinguishes four paradigms to understand the dynamic changes in time and frequency domain variables [87, 97].

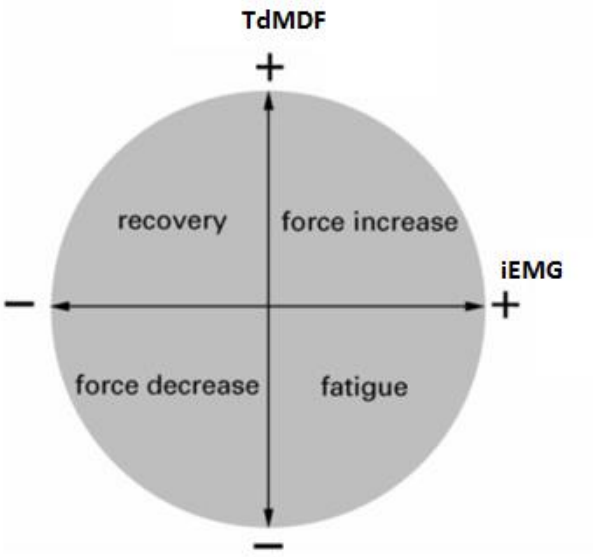

Figure 2-7: Schematic representation of the EMG Spectrum and Amplitude: jointly analysis of the sEMG amplitude (iEMG) and time-dependent median frequency (TDMdPF) to distinguish between various EMG-change causations. [97]

Considering the four cases, reported by Luttmann et al. [97], if the iEMG amplitude increases and TDMdPF shifts towards the right, probably the muscle force increase is due to recruitment of fast twitch muscle fibers and higher electrical activity in the working muscle. The decrease in iEMG and TDMdPF is probably due to reduced cortical drive and metabolic changes in the working muscles. On the other hand, increase in iEMG and decrease in TDMdPF is likely due to muscle fatigue (reflect due to changes in metabolic product and insufficient cellular adaptation for the required intensity). The decrease in iEMG and increase in TDMdPF is associated with the muscle fatigue recovery phase. However, it is evidently reported that the use of sEMG signal for interpreting CNS muscle control strategies requires advanced signal processing and detection techniques at the single MU level [98]. Though dependencies of the spectral variables on force and fatigue still need further attention [98], above four cases will be used to reach a reasonable conclusion.

Interaction of sEMG signal with physiological system

During fatiguing contractions, biochemical and physiological changed are directly related with properties of the sEMG signal [87]. Running at AT produces significant metabolic stress and the amount of lactate accumulation within the skeletal muscle is dependent upon the rate of metabolic removal. After a certain level of fatigue or at the onset of fatigue, the blood flow gets restricted due to intramuscular pressure and makes the muscle ischemic. This ischemic condition changes the muscle pH [75] which further changes the muscle fiber conduction

velocity (MFCV) and triggers the myoelectric manifestations of muscle fatigue [99, 100]. Lowering the MFCV is one of the causes of signal power spectrum shift toward lower frequencies which increases the sEMG signal amplitude because of the low-pass filtering effect of the tissue [101]. Myoelectric manifestations of muscle fatigue cannot solely be attributed to decrease in MFCV. Other associated factors are the rate of depolarization and repolarization of the sarcolemma [102], muscle fiber composition [103], time synchronization in the activity of motor unit, muscle temperature and muscle fiber recruitment strategy [104-106].

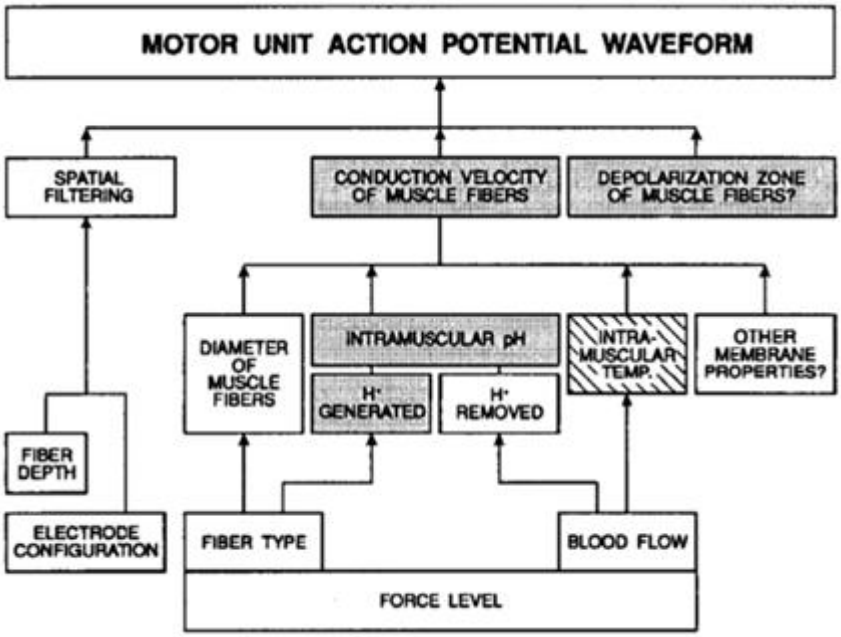

Figure 2-8: Factors which affect the shape of the motor unit action potential. Shaded boxes indicate factors that are modified as a function of time whereas white boxes indicate factors influenced by the type of contraction. Adopted and modified from De Luca et al. [*107*].

SPF kinetics are critical in understanding biochemical and physiological changes in skeletal muscle during the muscle-fatiguing process. Formation of the BLa has also been viewed as a potential contributor to frequency shift [108] and its myoelectric manifestations of muscle fatigue are presented [99, 109]. Effects of all the intrinsic and extrinsic factors affecting EMG signal are shown in Figure 2-8.

Training status of the individual does also affect the SPF kinetics because of higher mitochondrial density, which delays the metabolic alterations in trained individuals than in untrained individuals. Gamet et al. [110] have reported four varied patterns to understand SPF kinetics in dynamic fatiguing contractions among individuals during an incremental exercise protocol. These patterns are a continuous increase, a continuous decrease, an increase followed by a decrease, a decrease followed by an increase. The increase in SPF was due to increase in fast-twitch muscle fiber recruitment and muscle temperature outstripped the accumulation of

metabolic by-products. Whereas a decrease in SPF was due to metabolic changes within the muscles [110]. It can be concluded from above explanations that the overall balance between MU activity, local metabolites, muscle temperature, task nature, exercise intensity and duration of exercise determine SPF trend. It is quite difficult to establish a general fatigue paradigm for a given task due to a variety of conflicts in vivo and in-vitro research conducted on human and animals. Therefore, this study aimed to investigate its own pattern of lower extremity muscle fatigue along with BLa buildup process during endurance protocols.

2.1.4 Biological Marker of Fatigue

A biomarker is a measurable substance that indicates the biological measure of fatigue during exercise. Biomarkers of peripheral and central fatigue are used to detect abnormalities in the muscle contractile machinery, causing muscle fatigue. These biomarkers may have an association with perceived exertion and exercise performance impairments. The detail on these biomarkers is discussed below.

2.1.4.1 Biological Indicator of Peripheral Fatigue

Selection of the biomarker of peripheral muscle fatigue is based on the mechanism of fatigue related to ATP metabolism, acidosis, or oxidative metabolism [111]. During anaerobic metabolism or glycolysis, inadequate oxygen supply increases intracellular acidosis, due to lactic acid and H^+ accumulation, which in result reduces muscle pH [25] and decreases muscle force. The elevated serum lactate levels reflects the combined contribution of aerobic metabolism and anaerobic glycolysis to meet ATP demand [111]. In addition, when phosphate (PCr) metabolic source contribute to meet ATP demand, lactate production further increases [71] and may cause the lactate acidosis. Having such observation in literature, the increase in serum lactate can be linked with metabolic demand, exercise intensity and metabolic stress during exercise. Serum lactate can also be used to determine the onset of blood lactate accumulation [112] in relation to exercise intensity and duration. The onset of blood lactate accumulation was further correlated with muscle deoxygenation [113] that results in muscle oxidative stress and muscle fatigue. There has been a debate in the literature, suggesting that there is no single mechanism but multiple mechanisms to cause acidosis. Serum lactate was considered critical to be monitored as it reflects the ongoing metabolic state of the working muscles. Serum lactate was found practically viable to be measured and has a significant relationship with the rating of perceived exertion (RPE) [114].

Table 2-1: Biomarkers of muscle fatigue based on pathways [*111*]

Biomarker	Source
ATP metabolism biomarkers	
Lactate	Serum
Ammonia	Serum
Oxipurines	Serum

2.1.4.2 Biological Indicator of central fatigue

Central fatigue is associated with the reduced central drive to the working muscle. It is very likely that changes in motivational level and increased RPE at the same absolute workload may have a profound effect on the cortical drive to reduce endurance performance [61, 115]. It is also elicited that central fatigue is sensitive to low brain oxygen [20]. Brain oxygen is calculated by the product of arterial oxygen content (CaO_2) and cerebral blood flow (CBF). However, low brain oxygen in submaximal, long duration whole body exercise effect remained unknown on central command [20]. Figure 2-11 shows the effect of oxygen transport and interlinked fatigue mechanisms.

It has also been discussed that sensory afferent feedback, stemming in locomotory muscle, to CNS is a key determinant of conscious/subconscious regulator of the cortical drive. A study, by Ishii et. al [116], has stated that blood lactate concentration and muscle blood flow, which reflect muscle metabolism, convey load intensity information to the sensorimotor cortex during muscle fatigue at the submaximal activity. This recommends a strong link between peripheral and central fatigue. The inhibitory neural feedback, rate of peripheral fatigue development and sensitivity to arterial oxygen content has a certain relationship with the central mechanism of fatigue [81]. Therefore, peripheral fatigue variable (blood lactate) with upper confined limit and different arterial oxygen content may represent the existence of central fatigue [20, 81, 82] and account for the reduction in exercise performance.

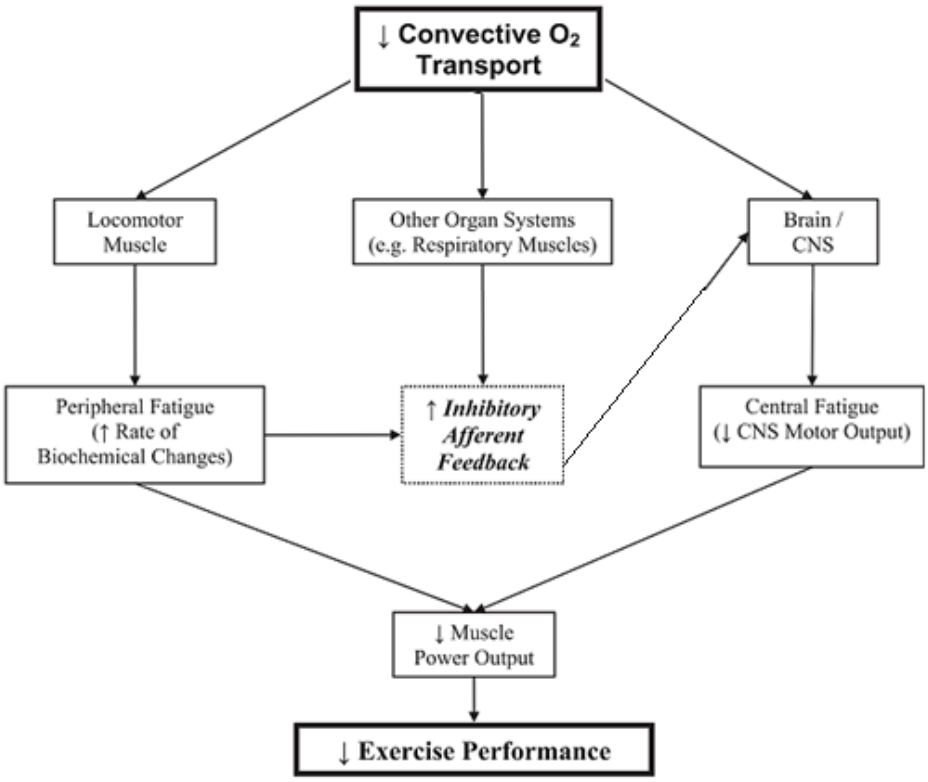

Figure 2-9: Connective oxygen transport and fatigue-related mechanisms influencing exercise performance [*20*]

2.1.5 Rating of Perceived Exertion

The perception of effort or discomfort, experienced during exercise, is known as a rating of perceived exertion (RPE) and its relationship to fatigue has and still being reviewed and estimated based on different training protocols, gender, and demographics. Several scales have been developed to quantify exertion in the literature [117]. Regarding the use of RPE, currently, two viewpoints exist in the literature. Most recent argument suggest that RPE works independently of afferent feedback from skeletal muscle, heart and lungs muscles [118]. This suggests that perception of effort is centrally generated by corollary discharge from the motor to sensory areas of the cerebral cortex [118]. It is somehow convincing that increased corollary discharge from the motor at same exercising workload with locomotor muscle fatigue is perceived as increasing effort [118]. However, when evaluated for the cardiac function, the experiment did not support a relationship between HR and RPE [119] whereas respiratory muscles reflected the sense of respiratory effort [120]. The second viewpoint believes that RPE involves the integration of multiple afferent signals from a variety of perceptual cues that allows exercise performance to be precisely regulated to accomplish the task within the biomechanical and metabolic limits of the body [117]. These perceptual cues can originate from within the muscle or joints or central factors (RR, HR) [55]. This view was valid until

neurobiological mechanism and the discovery of muscle receptor function was not clearly understood and lead to the conclusion that these receptors were responsible for sensation related to muscle contractions [121].

Considering this viewpoint and reported findings, the perception of effort does appear to have an associated effect rather than causative effect with RPE [119]. Following Table 2-2 represents the individual weight of each sensation in relation to perceived effort.

Table 2-2: Subjective symptoms of prolonged work [55]

Perceived Effort	Subjective Symptoms		
	Local or Muscular	General	Cardiovascular
Low Intensity	Muscle aches		
Moderate Intensity	Muscle fatigue, leg itching, heavy	Feeling tired, Perspiring	Dyspnea, Breathlessness
High Intensity	Muscle pain, Cramps, Leg shaky, Tremor	Perspiring feeling of pain, Task aversion	Difficulty with breathing, Heart pounding, Chest pain

Literature has examined the sensory cues in association with perceived exertion [117, 122]. These sensory cues are categorized into central and locomotory cues for perceived exertion. Central parameters linked to perceived exertion include heart rate (HR), ventilatory minute volume (V_E), respiratory rate (RR) and oxygen consumption ($\dot{V}O2$) [55, 122]. Every individual parameter has a certain correlation with RPE. RPE-OMNI reported a correlation of 0.81- 0.95 ($P<0.01$) between RPE, HR and $\dot{V}O2$ responses on a bicycle ergometer [123] and correlation of 0.67- 0.88 ($p<0.05$) during walking/ running exercise [124]. Whereas peripheral parameters associated with RPE include serum lactate and proprioceptive responses [122]. BLa is considered to have a high correlation with RPE at higher exercise intensities and is believed to be a valid indicator of exercise intensity [114, 125]. Cortisol response has been also reported to be significantly linked with low and high intensity work along with RPE [126]. Therefore, RPE can be considered as a valid and reliable tool [126].

RPE-OMNI scale [124] will be used as a valid tool in this research to quantify muscular (RPE_M), cardiorespiratory (RPE_C) and overall body feel (RPE_O) as a subjective measure of fatigue.

2.2 Physiological Response to Fatigue

The human body responds through a series of integrated functional changes in musculoskeletal and physiological systems when challenged with any physical task. The musculoskeletal system through synchronous activation of agonist and antagonist muscles from central cortical drive provide the movement. Whereas physiological system (i.e. cardiovascular and respiratory

system) helps in providing the ability to sustain that movement over an extended period of time through metabolic adjustments [127]. Many physiologists (Hill 1927, Dill 1938, Basset & Howley 1997) in past have used the cardiovascular model to explain fatigue during prolonged submaximal exercise. They have consequently evoked changes in cardiovascular function to improve endurance performance [127]. In the current state of fatigue art, it has been clear that only cardiovascular system is not solely responsible for limiting prolonged submaximal exercise under fatiguing scenario when blood flow and oxygen supply is adequate. Therefore, integrated model approach including neuromuscular, biochemical, cardiorespiratory and biomechanical aspects are needed to be evaluated for fatigue evaluation in real time.

2.2.1 Cardio-Respiratory Response

The primary function of the cardio-respiratory system is to provide oxygen (O_2), to get rid of carbon dioxide (CO_2) & metabolic waste products, maintain body temperature, acid-base balance and meet the energy demand of skeletal working muscles [128]. As muscle activity increases above a certain workload, the cardio-respiratory system lacks in providing oxygen demand to the working muscles. It triggers anaerobic metabolism in parallel with aerobic metabolism to meet the energy demand. Thereafter, metabolic accumulations start disrupting homeostasis and hence fatigue development process starts [20, 21, 127]. Reduced arterial oxygen starts affecting the central command unit in regulating peripheral fatigue [20, 82] and cardio-respiratory stress increases.

To measure cardio-respiratory response and to reflect on metabolic system, metabolic cart analyzers have been developed by many biomedical companies like COSMED and Medical Graphics Corporation that can be synchronized with POLAR heart rate strap sensor. This synchronized system provides the measurement for ventilation volume (V_E), oxygen consumption ($\dot{V}O_2$), CO_2 exhale (VCO_2), respiratory rate (RR), heart rate (HR), respiratory exchange volume (RER), CO_2 end-tidal pressure ($PETCO_2$). All these measures provide the understanding of physiological response and determination of ventilatory threshold. This technology provides the reliable and gold standard measure of a cardiorespiratory system that will also be used in this research. Metabolic accumulation will be monitored through serum lactate sample collection using the pricking device and will be analyzed in lactate analyzer. The normal site for blood sample collection is ear lobe, arterial blood through vein and finger pricking method. In this research, a blood sample will be collected through finger due to mobility issues.

2.2.2 Determinants of Anaerobic Threshold & Physiological Stress

The anaerobic threshold (AT) is defined as the highest constant workload that leads to an equilibrium between lactate production and lactate elimination [129]. This is important to the recreational and endurance athlete/runners to enhance cardio-respiratory fitness in recreational sports and plan training programs [130]. Currently, HR, RR, RER, VE/V̇O2, VE/VCO_2, $PETCO_2$ and blood lactate (BLa) have been used in literature to identifying anaerobic thresholds [43, 111-113, 128, 130]. The most direct and accurate method among these has been BLa measurement [112].

HR monitors (HRMs) have been widely used to monitor planned intensities during training sessions, estimation of V̇O2 and energy expenditure [131]. They are also popular with endurance sports and guideline over the heart rate intensity zones [132], have also been made available for better planning of training regimes. The factors which affect heart rate are likely day to day variability, hydration status, environmental factors and altitude [131] which restrict its predictive accuracy. Furthermore, fatigue is also found to cause the cardiovascular drift, it has a potential to be considered as part of influential factors to change HR from its optimal value [133, 134].

During prolonged exercise, cardiorespiratory adjustments in response to fatigue development, the relation between the rise in HR, BLa and RPE can help to have a better understanding on the physiological strain and to identify the fatigue influence. This will help to evaluate the significance of these factors with fatigue development and to evaluate endurance performance. There is also need to study the interaction between HR, $\%HR_{max}$, RPE, and BLa to determine close predictors of physiological strain that could be used in current HRMs.

2.2.3 Determinants of Physiological Response

Few pieces of evidence from the literature suggest that effect of central command on the cardiovascular response is closely related to the perceived effort of the exercise intensity and perceived exertion during the exercise [135, 136]. Studies involving partial or full neuromuscular blockade have reported greater cardiovascular response, resulting from a higher level of central command as per individual perceived effort [135-137]. The cardiovascular response is also further mediated by III and IV sensory afferent feedback from functional skeletal muscle [138]. These findings suggest that an individual's perceived exertion along with sensory feedback from muscle contribute towards establishing the magnitude of cardiovascular response. However, few more studies showed that muscle feedback was not only the requisite component to change central command response as the increase in muscle unit recruitment or force production were coupled with increased perceived exertion. It was

found that changes in perceived effort, even without changes in afferent feedback can modify cardiovascular response [139, 140]. The sense of effort elevated cardiovascular response, yet reductions in sense of effort did not decrease cardiovascular response. This lack of cardiovascular change, in response to a decreased sense of effort, serves to confirm the importance of afferent input from the exercising skeletal muscle in establishing the magnitude of cardiovascular response, required to sustain a given metabolic demand [139].

RPE has been a physiologically valid tool for prescribing exercise intensity when the intent is to detect lactate threshold and blood lactate concentration during exercise [141]. Few studies exist over lactate concentration regulated by RPE [114] as a non-invasive method. Similarly, RPE will be used in relation to physiological changes to determine the physiological fatigue in this research.

2.3 Running Biomechanics and Fatigue

Biomechanical analysis of endurance performance is critical to monitor adverse effects of running on the musculoskeletal system. Running biomechanics represent the coordinated outcome of integrated central control, the biochemical status of the working muscles and physiological status of the supporting organs [142]. The runner's full body acts as a chain of kinematic events to produce locomotion. Foot segment serves as a basic link between the ambulatory surface and remainder of this chain of kinematic events. The function of the foot includes adaptation to uneven terrain, proprioception for proper position, balance and leverage for propulsion [143]. Whereas the remainder chain in the lower and upper extremity coordinated in a balanced way to provide locomotory support.

Running requires support from the whole-body segments [30], various studies have shown the importance of upper and lower body running mechanics in improving the running form and efficiency. As running injuries are considered as the critical factor to define the importance of evaluating running mechanics in lower and upper body mechanics, Blair, S.N., et. al. [10] and van Gent et. al. [6] have evaluated the rate of injuries for the foot, ankle, knee, hip, back, shoulder and elbow. They reported that lower extremity was at the higher risk of developing running injuries, especially the knee. The most likely reasons for the development of such injuries have been running stress, training frequency, and fatigue [6, 8, 9, 144], as shown in Figure 2-10. As fatigue is believed to affect proprioception, movement coordination and reaction time of the working muscles [38, 145, 146], it is a matter of interest that how fatigue changes the interaction of the body with ground and affect the spatiotemporal gait parameters and gait mechanics. It has also been reported that the effect of the fatigue of gait parameters appear to be dependent on the fatigued muscles [38]. Therefore, neuromuscular activity in the

lower extremity skeletal muscles was examined in this research to evaluate muscle fatigue and its interaction with joint mechanics and injury development. The literature showed lower extremity injury rate ranged from 19.4% to 79.3% [6] with higher prevalence in the knee. Therefore, the landing mechanics at the MS phase of running gait cycle were analyzed in relation with neuromuscular fatigue [144, 147].

It is the matter of interest that how the fatigue changes the landing behavior and running mechanics during the stance phase of running gait cycle. Also, how runner's kinematic asymmetries are addressed or corrected to understand its interaction with injury development. Improper alignment of the lumbar spine and compensatory movement of muscles around the bones and joints in lower extremity due to fatigue will also change the impact transfer dynamics from lower body to upper body and may increase the probable risk of injuries [8, 9, 41, 144, 148]. Therefore, understanding and quantification of running gait parameters for the knee, hip, and ankle during the braking phase of stance (early to mid-stance) are critical in running gait cycle. This is important in understanding performance, biomechanical fatigue status, limb stiffness control and its interaction with injury development. The relationship of landing mechanics with injury development is critical during fatiguing contractions because poor mechanics will either increase the muscle load or the landing force on the body. These both conditions of fatigue will increase stress which may become excessive for the runner and cause injury, based on the body capacity and amount of running.

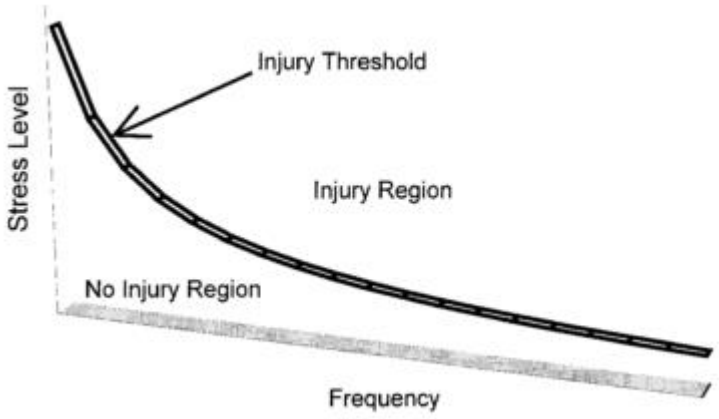

Figure 2-10: Fatigue curve showing the theoretical relationship between training stress and frequency with the injury threshold curve to represent the balance [*144*]

2.3.1 Running Gait Parameters

Gait cycle, a basic unit of measurement in gait analysis, is described as a series of movements of lower extremity between initial foot contact with the surface followed by re-contact with the surface of the same foot [59]. The gait cycle is divided into two phases, stance and swing phase.

Stance phase represents the duration of foot in contact with the ground and it ends when the foot is no longer in contact with the ground. While swing phase represents the flight duration of foot starting from toe-off to in contact with the ground of the same foot [59, 149]. While float represents both feet off the ground during running. Figure 2-11 represents phases of running gait cycle with toe-off and in-contact events with the ground.

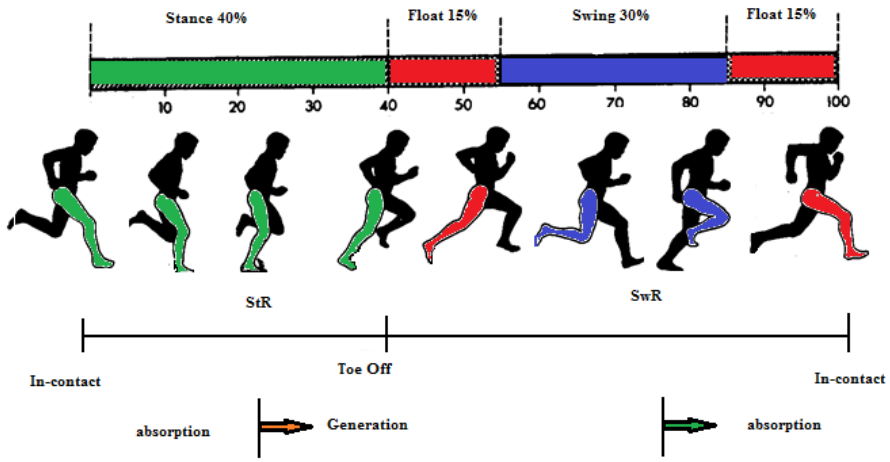

Figure 2-11: Running gait cycle: StR, stance phase reversal; SwR, swing phase reversal; Generation, from StR through toe-off to SwR; absorption, from SwR through in-contact to StR, adapted from [*149*]

During submaximal running, characteristics of the gait cycle change with speed. Centre of gravity shifts in a sinusoidal curve in space, lower extremity joints increase their range of motion and require more flexibility and eccentric muscle strength [149] and simultaneously cadence, stride length and step length changes. During the steady state running, studies on Center of Mass (COM) have shown that body mass center position travels downward and its forward speed decreases during early to the mid-stance phase (braking phase) of stance cycle [150]. Running kinematics changes during early to mid-stance phase (braking phase of stance) [150, 151]. Ground reaction force (GRF), loading rate and tibia impact acceleration also increase in the linear fashion [152]. During mid to late stance of stance phase, body mass center moves upward and its forward speed increases [150]. Running kinematics changes again following the mid to late stance [151].

During the early part of stance phase, quadriceps group of muscles contributes majorly to support braking acceleration and to stabilize the knee joint [150]. Leg stiffness control changes to have an efficient energy absorption and to produce optimal propulsion [153]. All of these factors do affect the running economy [45, 143], known as the determinant of endurance performance.

Various studies on endurance runners have reported the influence of these biomechanical factors on RE and hence performance [34, 154, 155]. Studies have also reported the association

between the kinematic profile of the hip, knee, ankle and pronation angles at braking phase of stance (early to mid-stance) of running gait cycle with running injuries [6, 37, 144, 147]. Fatigue is also known to place the knee joint at greater risk for joint pathology and injury potential for studies quadricep group of muscle [156]. Therefore, it is important to look at these variables during the braking phase in conjunction with fatigue development.

Different fatigued protocols at different speeds in literature have reported significant changes in running parameters, like STR [37, 43, 148], SL [148], contact time, loading rate (BW/s) [42], GRF [31, 42, 144], I_T [9, 37, 41, 144], knee flexion at IC [37], knee flexion at MS [45], total plantar flexion [45], knee extension [37] and COM oscillation [150]. Alteration in the biomechanical parameters can also either improve or deteriorate the running performance as well. As most the studies include an elite class of runners, evaluation of the active recreational active runners is important to broaden the perspective of real-time fatigue monitoring, improve running mechanics, optimize intensity training and reduce the probability of running injuries in a large population. This research will help to fill that gap by determining the biomechanical performance predictors in the recreational class of runners and how they are interlinked with RE and fatigue, considering their inter-individual body fitness differences.

2.3.2 Limb Dominancy, Bilateral Asymmetry, and Fatigue

Bilateral KA understanding during running is important for preventing loading stresses, side to side kinematic adjustments and in resolving unilateral pathology. KA has also been identified as a risk factor as it may expose bone to higher loading stresses [37] on one side of the lower extremity. KA also rejects the hypothetical assumption of considering lower limb symmetry in order to address gait interpretations [157]. This acceptance of asymmetry due to limb dominance is not only important for clinicians, coaches, and investigators but also important for researchers to understand its effect on biomechanics and to know the relation with fatigue. Biomechanical research studies have reported kinematic and kinetic asymmetries in runners [158-162]. They have tested a variety of parameters, like leg stiffness, contact time, step length, flight time, joint kinematics, ground reaction force, vertical loading rates and tibia impact acceleration. Tibia impact acceleration has a significant correlation with vertical ground reaction force [163], localized muscle fatigue [164] and overall body fatigue development [37, 41]. Therefore, this study considered tibia impact acceleration for KA evaluation.

In our knowledge, no study has evaluated kinetics asymmetry (KA) and its interaction with muscular rated perceived exertion (RPE_M), blood lactate (BLa) and overall rated perceived exertion (RPE_O) at individuals' critical speed during a non-continuous and continuous fatigue protocol. Fatigue alters running mechanics in as little as 15 minutes of running [41]. It was

hypothesized that, if dominant and non-dominant leg behaves differently during non-continuous and continuous speed protocol, the dominant and non-dominant leg will fatigue at a different rate and KA will be different. It was also hypothesized that KA may be linked with metabolic stress (BLa) and/or RPEo. It may give a better explanation about the understanding of its existence against fatigue and could be used as a predictor of fatigue.

2.3.3 Neuromuscular Control and Fatigue

Muscle activity during walking and running are well documented in the literature [149, 165, 166]. In general, during running, muscles were more active in anticipation to landing on the ground and were consistent with DeVita's contention [167]. Events surrounding IC were more important than toe-off (TO) as runners experienced relatively large external forces and moments. Following IC, the ankle and knee flexion went into coordination to absorb the vertical landing forces on the body, which at distance running speed was 2 to 3 times of bodyweight. To counterbalance such landing force, central nervous system increased neuromuscular activation level of the lower extremity to absorb the impact.

Muscle activation pattern along with joint kinematics during the running gait cycle is shown in Figure 2-12. Quadricep muscles were activated following late swing to prepare the leg for ground contact, shock absorption, patellar and knee stabilization. All major driving and stabilizing leg muscles remain active to absorb the impact, known as the landing or braking phase of running gait cycle. Tibialis Anterior (TA) remained active in the first phase of stance to provide control in lowering the foot to the ground and during stance phase to allow ground contact with the hind foot. Only rectus femoris (RF) muscle proceeded activation during the early swing, probably to restrain the posterior movement of the tibia with knee flexion due to its biarticular nature. Hamstring and hip flexor muscles extend the hip in the second half of swing and the first half of stance. Hamstring helps to decelerate the momentum of the tibia as knee extends before in contact with the ground. Hamstring and gastro-soleus both have important eccentric and concentric function while hip extensor probably functions concentrically only [149].

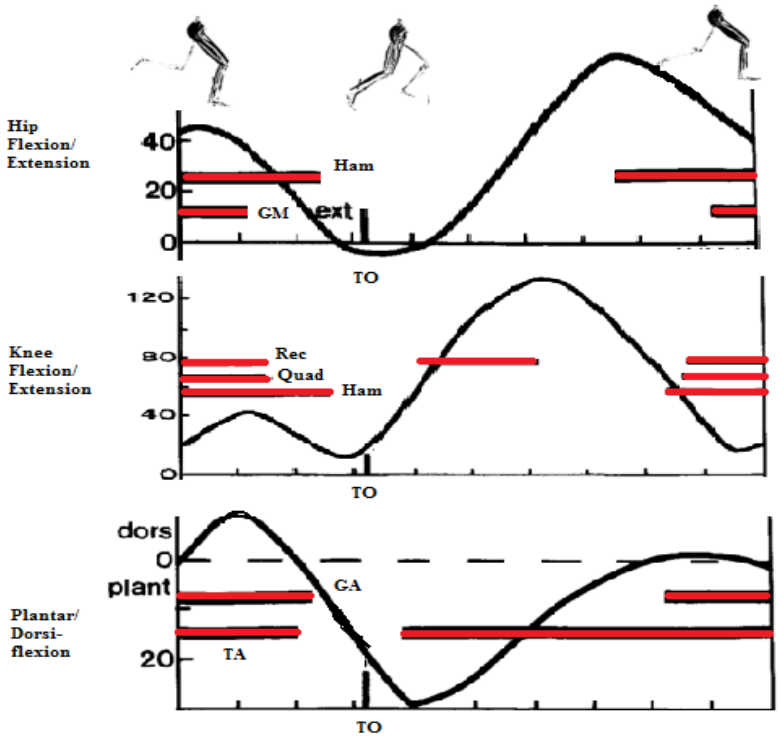

Figure 2-12: Muscle activation pattern synchronized with joint kinematics over the gait cycle, adapted from [149, 165]

During absorption phase (early part of stance phase), quadriceps group had the largest contribution to braking (i.e., backward acceleration of the mass center) and support. From mid-stance to toe-off, the soleus and gastrocnemius muscles play the greatest contribution in propulsion and in accelerating the body center of mass [150]. For progressive speeds, an increase in muscle activity and force production has been observed in quadriceps, hamstring and gastrosoleus group of muscle [44, 168].

During a prolonged activity like endurance running, impairments in muscle activation profile affect muscle performance and result in biomechanical adaptations, higher ground reaction forces, and impacts as reported in these studies [9, 30, 44, 156]. The closed-loop interaction of neuromuscular impairments with physiological, kinematic and metabolic alterations under intense exercise protocol is shown in Figure 2-13. More specific and analytical explanations against fatigue development in lower extremity group of stabilizing and driving muscles are needed for a recreational class of runners. This is required to understand the limitations during the performance and to explain neuromuscular alterations due to fatigue and its interaction with kinematic, metabolic and physiological adjustments. A closed-loop neuromuscular study in relation with biomechanical adjustments, physiological strain, metabolic stress and perceived exertion is conducted in this research. This will help to identify the muscles which are

susceptible to earlier fatigue in lower extremity during endurance run. This will also help to understand its interaction with biomechanical adaptations and metabolic accumulations.

Furthermore, there are very little to no study to evaluate the underlying pattern of muscle activity during continuous and non-continuous fatiguing protocol for the recreational class of runner. They may differ from high-end athlete due to higher muscle oxidative capacities, muscle mass and muscle composition, intracellular restitution and glycogen energy reserve. There is a need to investigate how individual muscle experiences fatigue under the different fatiguing protocols at the same endurance pace in recreational male runners. According to our knowledge, there is no study that has shown similar comparison under two different fatiguing protocols (continuous and non-continuous).

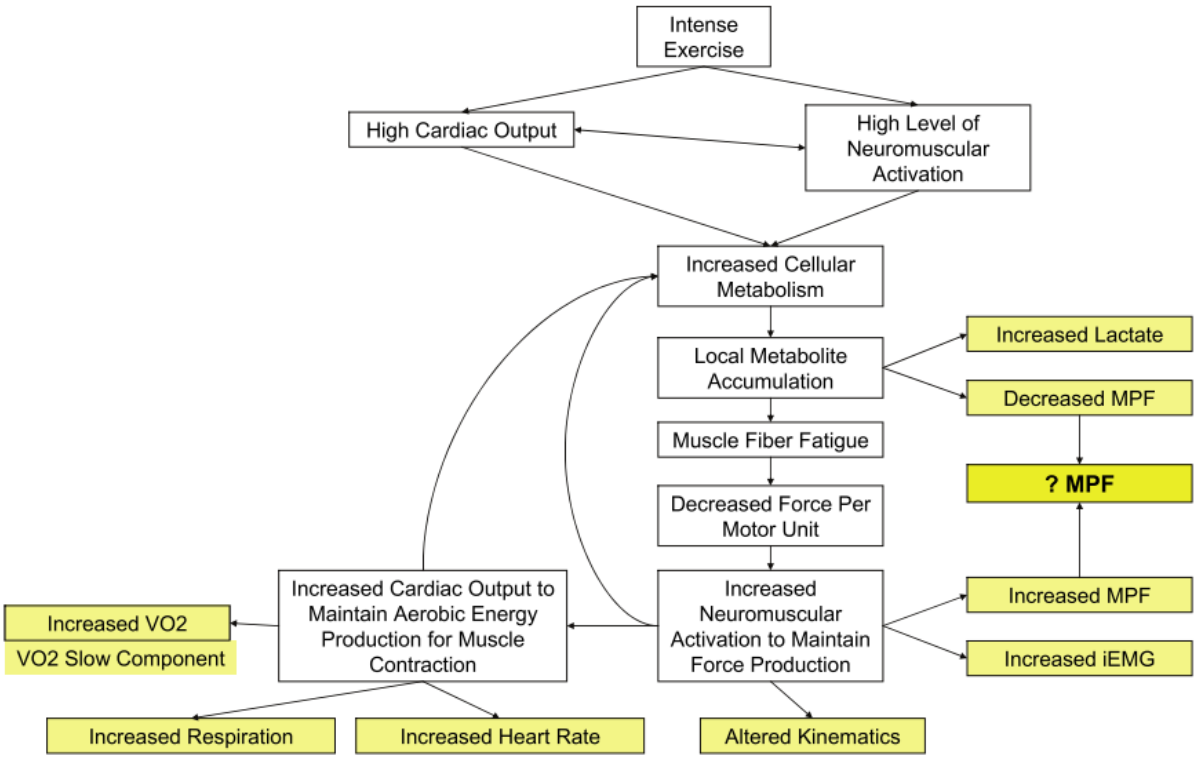

Figure 2-13: Neuromuscular fatigue effect on multiple factors related to metabolic stress and running performance [*30*]

2.3.4 Foot Mechanics and Fatigue

The foot is the basic kinematic link which interacts with the ground. Joint mechanics in the lower extremity are dictated by the foot mechanics, particularly ankle and foot [143]. Pronation and supination of the foot and ankle joint causes restricted motion in the entire kinetic chain [143] as shown in Table 2-6.

Table 2-3: Effect of pronation and supination up kinetic chain [*143*]

	Pronation			Supination		
	Sagittal	Frontal	Transverse	Sagittal	Frontal	Transverse
Lumbosacral	Extension	Lat flexion same side	Protraction	Extension	Lat flexion opp side	Retraction
Pelvis	Anterior rotation	Translation and elevation, same side	Forward rot same side	Anterior rotation	Translation opp side; depression same side	Rear rot same side
Hip	Flexion	Adduction	Internal rotation	Extension	Abduction	External rotation
Knee	Flexion	Abduction	Internal rotation	Extension	Adduction	External rotation
Ankle	PF-DF		Internal rotation	DF-PF		External rotation
STJ	PF	Eversion	Adduction	DF	Inversion	Abduction
MTJ	DF	Inversion	Abduction	PF	Eversion	Adduction

Abbreviations: DF, dorsiflexion; Lat, lateral; MTJ, midtalar joint; Opp, opposite; PF, plantarflexion; rot, rotation; STJ, subtalar joint.

In early stance phase of running gait, energy absorption is a key function of the lower extremity. Factors contributing to proper impact absorption are joint motion, eccentric muscle contraction and articular cartilage compression [169]. As forward progression occurs following heel contact, subtalar joint (STJ) pronates within first 20% of stance phase to allow solid contact with ground followed by hindfoot eversion and tibial internal rotation [143]. The tibialis anterior contracts concentrically to stabilize the ankle and to accelerate tibia over the fixed foot. At the same time, to provide stability to ankle, gastrocnemius-soleus contracts eccentrically to control tibial forward progression [143]. Along with ankle dorsiflexion, knee and hip flexion help to dissipate impact force at heel contact [151]. Rectus femoris contracts eccentrically to control the height of COM and to resist excess knee flexion and hamstring remains active throughout the stance phase as body progress forward on the fixed limb [143]. Active muscle control is important over this phase to absorb the impact, avoid overpronation/supination and to generate enough power for propulsion phase.

Fatigue does affect foot posture and foot dynamics over the endurance run [170]. Some studies have reported its significant correlation with ground reaction force (GRF) [42, 54, 171], plantar pressure [172] and foot pronation [173, 174]. There are also many reported findings on runner's overuse injuries and foot biomechanics [8, 144, 173]. Therefore, this study has considered evaluating the loading foot mechanics through experienced tibia impacts, ankle dorsiflexion and maximum foot pronation at MS phase of running gait cycle. Furthermore, no study has evaluated the activation difference between gastromedialis (GM) and gastrolateralis (GL) muscle with fatigue progression to understand its effect on foot pronation, following MS to TO

activation phase. This research aimed to evaluate the activation differences between GM and GL during running gait cycle to understand its interaction with overpronation/supination.

2.4 Existing Non-invasive Technology for Assessing Fatigue

Fatigue is attributed to both central and peripheral factors [70]. These factors can be estimated using a combination of voluntary and electrically stimulated force measures, 31-phosphorus Magnetic Resonance Spectroscopy (^{31}P MRS), Transcranial Magnetic Stimulation (TMS), twitch interpolation, and EMG recordings [70, 85-87, 109]. Technological instruments, like ^{31}P MRS, twitch interpolation and TMS, are good in measuring peripheral and central factors of fatigue but they have a limitation to be used in real-time fatigue assessment while running. Therefore, these technologies will not be discussed further in this literature here.

A review study, done by Al-Mulla et al. [67], have summarized the existing non-invasive technologies to detect/predict muscle fatigue using autonomous systems. One of those autonomous systems is 'sEMG' which measures the electrical potential of the muscle. Several signal modalities like time domain methods (sEMG amplitude, zero crossing rate), frequency domain methods (Fourier transform), joint analysis of the EMG spectrum and amplitude (time-frequency and time-domain methods, time-varying autoregressive approach) and fractal analysis and recurrence quantification can be applied as per the biomechanical application [87]. As this research involves the dynamic repeated contraction at constant endurance pace, 'joint analysis of the EMG spectrum and amplitude' signal modality was implemented to determine time-dependent changes in iEMG and median frequency (TDMdPF). The selection of 'sEMG' was most appropriate to this research due to its practical viability in assessing real-time fatigue and to be implemented in wearable devices that could be used in running scenarios.

The other autonomous systems, discussed in review study by Al-Mulla et al. [67], include the use of Mechanomyography (MMG), Near-infrared Spectroscopy (NIRS), and rating of perceived exertion (RPE) scale. MMG has contributed greatly towards developing an understanding of muscle activity in isometric and isotonic contractions and peripheral and central fatigue [67, 175, 176]. However, Al-Zahrani et al. [177] have cautioned against using MMG for assessing muscle fatigue in dynamic contractions using traditional parameters (Root Mean Square (RMS) and iEMG). NIRS contribute significantly in understanding oxidative metabolism in muscles [178] and needs further studies to understand fatigue. The applicability of NIRS is also limited to static contraction. The RPE scale which is used to monitor perceived effort and exertion will be used in this research due to its wide use in research [124]. It is also used by sports coaches and athletes to control exercise intensity in training and competition [124, 179].

2.5 Key Findings of Literature, Research Gaps, and Methodology

The recreationally active runners exist in masses in the real world and have a higher probability of developing running injuries due to lack of knowledge on running stress and fatigue. As fatigue regulates the exercise response [115] and is considered critical in developing lower extremity injury [9, 10, 172], it is a matter of interest to understand and analyze its manifestation on the physiological and biomechanical system during endurance running. Variety of studies on endurance performance have reported changes in physiological and biomechanical variables [34, 45, 154]. The interaction between the neuromuscular fatigue, the physiological system [82, 180] and the central governor system [181] make the implications complicated to understand in relation with metabolic accumulations, and running mechanics adjustments. Furthermore, the compensation in the running pattern was also argued to be the attempt of the runner to improve running economy and enhance performance at the later stage of the race [171, 182]. Therefore, considering such rationale between localized muscle fatigue in lower extremity skeletal muscles and changes in kinematics, kinetics, kinetics asymmetry, and leg stiffness control properties, there are very limited to no studies [37, 41, 164] evaluating lower extremity neuromuscular fatigue in runners in an integrated fashion along with physiological and running mechanics response during recreational endurance running.

Identifying muscle impairment, causing performance decrement, is subject to the limitation of available technologies (nerve stimulation [183], TMG [84], TMS [184]). Surface EMG (sEMG) provided the flexibility to monitor fatigue in real time for the selected lower extremity muscles (RF, VL, BF, ST, GM, GL, TA). To our knowledge, it is the first study which focused on studying the neuromuscular fatigue of all major locomotory and stability group of muscle in the lower extremity in comparative fashion (continuous vs. non-continuous) for recreational active runners. The outcome will help to understand the lower extremity locomotory & stabilizing muscle's endurance dynamic contraction capability, force fatigability relation against sustained endurance time and individual muscle fatigue profile during both protocols. Individual muscle fatigue correlation with biomechanical adaptations over fatigue run to exhaustion will help to identify the core muscles causing biomechanical changes and hence musculoskeletal stress in the recreational class of runners.

For identifying the endurance fatigue protocol difference, this study examined the physiological difference between the non-continuous and continuous protocol for recreational active runners. A study, done by Penteado et al. [49] on trained runners and triathletes, has reported that runner's TTE was ~2 times higher during the non-continuous test in comparison with the continuous test. However, the physiological evidence was not reported to explain such

difference in performance. To understand the physiological difference and to test the TTE for recreational active runners, this study evaluated their physiological response under laboratory conditions during the non-continuous and continuous test. Effect of 1-min rest was also examined on runner's endurance time and physiological and biomechanical response. Furthermore, studying the differences in physiological and biomechanical changes during continuous and non-continuous endurance protocol and fatigue influence on bilateral kinetic asymmetry (KA) in this research were novel to help researchers, sports scientists and coaches understand the protocol dependent changes in exercise performance and its determinants in the recreational class of runner. Up to our knowledge, such observed findings were novel for the recreational class of runner.

This research also wanted to evaluate the significance of other physiological markers in relation with RPE to determine BLa, non-invasively, during endurance running. For trained runners, RPE has shown the valid response for predicting BLa in progressive speed run [185], however contradictory evidence do exist over the use of RPE rise against BLa rise during intermittent running [50]. RPE is also known to prescribe the running intensity with blood lactate of 2.5 $mmol.l^{-1}$ and 4.0 $mmol.l^{-1}$ for endurance runners [114]. Knowing all these aspects of RPE for trained runners, this research examined the use of RPE to predict BLa for recreational active runners under the studied endurance protocols (continuous and non-continuous). Furthermore, it evaluated the use of $\%HR_{max}$ (as a physiological marker) to predict BLa in recreational active runners non-invasively. This will help recreational active runners in monitoring their metabolic stress during endurance training session using existing heart rate monitors.

Fatigue has been evidently reported to change the physiological and biomechanical response during endurance running [49, 127, 186] and many significant fatigue predictors are reported for trained endurance runners. However, there is a dearth of knowledge on recreational active runners. Therefore, this research conducted continuous endurance test on recreational active runners and determined the significant physiological and biomechanical fatigue predictors. The significant predictors were modeled to develop a regression model which could predict subjective fatigue measure (RPE). This model was first of its kind, due to integrative nature of fatigue evaluation on the biomechanical and physiological system.

CHAPTER 3. EXPERIMENTAL DESIGN, METHODOLOGY & PROCEDURE

This chapter includes the detail on participant's recruitment, experimental design methodology, and procedures for conducting this research. Endurance training protocol will be discussed in detail in the order of testing. Methodology for data analysis will be explained in the last section of this chapter.

3.1 Experimental design

Experimental design strategy along with subject selection criteria, instrumentation and testing procedures are discussed in detail in the following section of this chapter.

3.1.1 Ethical Approval

Before conduct of experimental research, ethical approval was sought through Institutional Review Board (IRB) Nanyang Technological University. All procedures regarding subject selection criteria, study design, experimental procedures, equipment safety measures and fatiguing protocol were evaluated by the IRB for approval of the study.

3.1.2 Participants Recruitment

The study was advertised within NTU's sports facilities, sports recreational center and leisure places. Following the advertisement, a total of 30 male participants (NTU/NIE students) volunteered to participate in this research study. After health history and activity questionnaire screening, only 22 recreational active runners qualified for the study. A "written consent agreement" as per the guidelines of "Institutional Review Board, NTU" was signed by these qualified participants. Maximum aerobic power ($\dot{V}O_{2max}$) was determined for all these shortlisted individuals. 5 participants failed to pass the criteria of aerobic power ($\dot{V}O_{2max}$ > 50 ml. $kg^{-1}.min^{-1}$) whereas 17 recreational male runners were successfully recruited to participate in the study.

3.1.2.1 Inclusion criteria

Only male runners were selected in this study due to the physiological difference in performance between male and female distance runners [51, 52, 187]. Participants were asked to fill up the "health history questionnaire" and "activity questionnaire", attached in the appendix section. Following criteria were strictly followed to recruit the participants.

- ✓ $\dot{V}O2$ max > 50 ml. $kg^{-1}.min^{-1}$
- ✓ 18-25 body mass index (BMI) range
- ✓ In between 18 to 35 years of age
- ✓ no heart disease record previously
- ✓ no airways/lungs disease (asthma, etc.) record previously

- ✓ No muscle/ bone fracture record for lower body
- ✓ No spinal cord injuries
- ✓ No Blood Diseases
- ✓ Performing normal training routines for at least last three months
- ✓ No neurological or metabolic disease
- ✓ No allergy to adhesives used for data collection
- ✓ No emotional or mental disorder or anxiety at higher stress levels of exercise
- ✓ No lower extremity muscle or bone injury

Participants were evaluated against the provided data in the questionnaires and qualified individuals were selected for the study and were introduced about the equipment and procedures within the laboratory. Participants failing the above criteria were denied participating in this study.

3.1.3 Sample size determination

Research studies, conducted on neuromuscular fatigue by evaluating the mean/ median power frequency changes of the lower body locomotory and stabilizing muscles (RF, VL, etc...) [30, 156] recommend the conservative estimate of sample size. The mean decrease in MnPF (9.3 Hz) and standard deviation of MnPF (10.9 Hz) using a power of 0.9 and alpha 0.05 were used to calculate sample size (n). The neuromuscular data using two-sided tailed test yielded 16 participants.

Similarly, kinematic changes, while running for 30 minutes above an AT speed, a study done by Mizrahi [37] has revealed that stride rate (STR) decreased from 1.46±0.05 to 1.39±0.03 per second, knee flexion from 13.6±6.3 to 8.1±3.0 degree and tibia impact acceleration from 6.9±2.9 to 11.1±4.2 g. Using alpha = 0.05 and power = 0.9 for two-sided test, this kinematic data yielded sample size n=6, n=14 and n=11 respectively.

Therefore, a sample of 17 (n = 17) was selected in this study to provide sufficient power to reveal a significant difference in the non-fatigued and fatigued state for this study.

3.1.4 Instrumentation for Experiment Methodology

Laboratory instrumentation included digital physician scale, body mass composition analysis (InBody720), metabolic cart (Parvo Medics' TrueOne® 2400), POLAR chest strap heart rate sensor (POLAR Inc.), blood lactate analyzer (YSI 2900), RPE-OMNI 10-point scale, a Trigno Wireless IM sensor, Trigno wireless EMG system (DELSYS), two digital video cameras (CASIO EX100 HS) and h/p/cosmos (WOODWAY) Treadmill. For data processing, the software includes Microsoft Excel (Microsoft Corporation), MATLAB, EMGworks (DELSYS), Kinovea, OriginPro and SPSS 20.

3.1.4.1 Anthropometric Measurements and Body Composition Analysis

Participant's height (cm) was measured using digital physician scale followed by "InBody 720" body composition analyzer. Participants were asked to remove their socks, wear light clothing, remove gadgets (electronic/metallic) from the pocket before stepping onto the footpad. Participants were instructed to stand on the footpads as per the shape of electrodes guide. Following the inbuilt weight measurement setup, a new entry of the participant was created and information about the height, gender and age were given. After successful registration on the analyzer, a proper posture was adopted by putting the thumb on the top and four fingers on the bottom of the handgrip, straightened elbows, space between the armpits and body. Body composition was measured using multi-frequency-bioelectrical impedance analysis technique and values were recorded for body fat mass, skeletal muscle mass, body mass index (BMI), percent body fat (% body fat) and total weight. These measurements were used as descriptive variables for the selected group of participants about their inter-individual body differences.

3.1.4.2 TrueOne® 2400 Metabolic System and POLAR Heart Rate Sensor

TrueOne® 2400 metabolic system along with POLAR chest strap heart rate sensor was used to monitor cardiopulmonary data (using breath by breath analysis) and heart rate data, using 5 breath averaging algorithm. The metabolic cart was first calibrated using two-step calibration process (the gas calibration and the flowmeter calibration). The gas calibration requires a 4-liter high-efficiency mixing chamber, which was calibrated by releasing the gas from E-cylinder into the mixing chamber. The gas mixture for this cylinder was 16% O_2 and 4.05% CO_2 and calibration was accepted if the detected error from the mixing chamber sensor was less than ±1%. The flow meter calibration process used a 3-liter syringe to simulate a breathing flow of exhaled gasses from the participants. Total 5 strokes were recorded by the system with increasing velocity to determine the volume of exhaled gasses into the system. Flow meter calibration was accepted if the detected error was within ±1%. The main purpose for doing calibration was to measure O_2 and CO_2 and compare it with the known values to negate the error and to check air flow measurement and composition through known air volume.

During the testing trial, mouthpiece along with the headgear and tubing, nose clip, and POLAR chest strap are shown in Figure 3-1, were securely placed onto the participant to monitor cardiopulmonary data during the running trial.

Figure 3- 1: Headgear set and POLAR heart chest strap sensor

3.1.4.3 Trigno™ Wireless EMG System

Surface electromyography (sEMG) data was recorded using Trigno™ Wireless EMG system to monitor underlying muscle activity. Trigno™ Wireless EMG consisted of seven 'Trigno™ sensors' (EMG and 3-axis accelerometer (±9g), the sampling rate of 1926 Hz and 148.1 Hz respectively) and two Trigno™ IM sensor (EMG and IM (±16g), sampling rate 1926 Hz and 148.1 Hz respectively). EMGworks® acquisition software was used to capture the data and EMGworks® analysis software was used for post analysis of the capture EMG and IM data.

3.1.4.4 Digital Video Camera System

Once dominant leg was identified, passive markers (1-4) were placed in sagittal plane at the center of the outer side of thigh, knee joint, ankle joint and metatarsophalangeal joint and on frontal place, two pairs of passive markers (5&6, 7&8), at the heel and in the longitudinal direction of achille tendon, were attached to measure hip, knee, ankle angles and foot pronation respectively during the MS phase of running gait cycle, shown in Figure 3-2(A). Two CASIO EX100 HS digital cameras (240 Hz sampling rate) were placed perpendicular to sagittal plane to capture side video and frontal plane to capture the rear view of a runner, shown in Figure 3-2(B). Later, the videos were transported to "Kinovea" software for digitization.

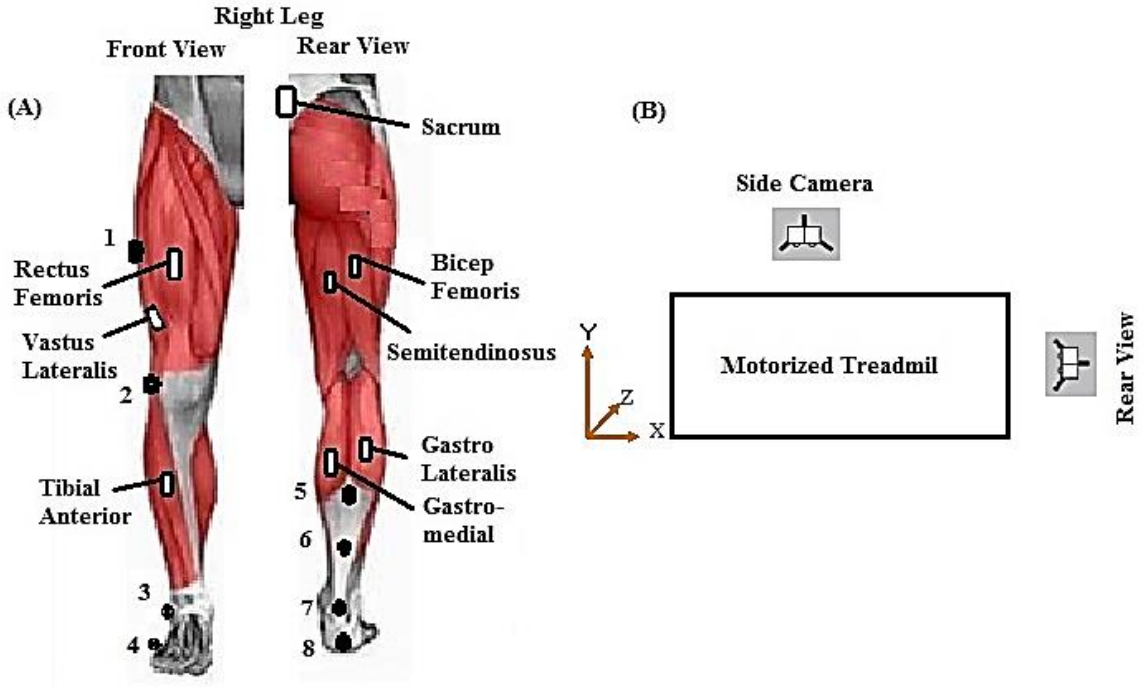

Figure 3-2: Front and Rear view of the right leg (dominant leg) in the lower extremity. (●) represent the location of the passive markers and (□) location of the Trigno wireless sensors for muscles of interest in lower extremity, courtesy: the musculoskeletal system

3.1.4.5 H/P/COSMOS (WOODWAY) treadmill

The H/P/COSMOS (WOODWAY) motorized treadmill was used to simulate designed running protocols in this research study under controlled laboratory conditions.

3.1.4.6 YSI 2900 Biochemistry Analyzer

YSI 2900 biochemistry sample analyzer was used as gold standard bio-instrument due to its known high accuracy and rapid results. Blood sample size of 50ul was collected in the 100 ul tube using the finger pricking device. Sample aspiration of only 25 microliters was used by the YSI 2900 analyzer to measure BLa in the body in relation to running intensity and fatigue.

3.1.4.7 RPE-OMNI Scale

RPE-OMNI scale [124], attached in the appendix section, was used in this study to quantify RPE for the chest (RPE_C), legs (RPE_M) and overall body feel (RPE_O). Participants were instructed to self-evaluate their exertion feelings while looking at the pictorial representation of RPE-OMNI scale during the non-continuous and continuous test and describe the RPE using the hand gestures for each body segment. After the detailed description, RPE_C, RPE_M, RPE_O data was collected during the last one minute of each active stage during the non-continuous test and after every 2 minutes during the continuous test to track and monitor perceived exertion.

3.1.4.8 Hardware and Data Synchronization Technique

H/P/COSMOS treadmill was programmed through the TrueOne® 2400 metabolic system software to control the speed, duration and gradient autonomously. Whereas for kinematic data and neuromuscular activity (EMG) data, digital videos for the side and rare view and sEMG data for RF, VL, ST, BF, GM, GL and TA and acceleration data for the shank segment were manually recorded using the time stamping method through the digital video camera and Trigno™ Wireless EMG system respectively. All the data synchronization was done manually due to lack of support of laboratory resources and integration compatibility between different measurement systems.

3.1.4.9 Participant's Dominant Leg

The dominance in the lower extremity is critical to being examined, due to biased motor control strategies, developed over time, for a specific task [188]. Therefore, for dominance evaluation in runners, three manipulative tasks were conducted. The dominant leg was selected based on the higher probability of leg preference among these three tasks, stated below.

a. Back push-off test

Participants were asked to stand straight with balanced space between both legs. To determine the dominant leg, a back-push force was applied as a disturbance. The stabilizing leg was considered as a dominant leg.

b. Step on the chair

The participant was asked to stand straight in front of the chair. Once the climb instruction was given, participants were required to step onto the chair. The knee that goes first to climb the chair was considered as a dominant one.

c. Kick the soccer ball

The participant was asked to stand straight in front of the soccer ball. Once the kick instruction was given, participants were required to kick the soccer ball. The leg that goes first to kick the ball was considered as a dominant one

3.2 2D Biomechanical Gait Model

Running biomechanics play a key role in injury development [189]. Evaluating the complex kinematic abnormalities to injury development requires a high end 3D motion capture system with the instrumented treadmill. However, several studies on 2D video kinematic analysis have shown its reliability in comparison with the 3D systems in evaluating kinematic variables during dynamic tasks in the frontal and sagittal plane [190-192]. Therefore, this research

included the use of 2D video analysis to meet the practical endurance conditions and to track the kinematic changes during the fatiguing run.

The adopted 2D biomechanical model [189, 193] was constructed by placing 4 spherical retroreflective markers of about 2 cm in diameter and 4 spherical retroreflective markers of about 1.2 cm in diameter each, placed over four anatomical locations (R thigh, R knee, R ankle, R-MT joint) and four shank and foot segment (R heel 1, R heel 2, R achille 1, R achille 2) on the dominant leg respectively. Placement of the marker, shown in Figure 3-3, uniquely defines the position of each body segment on lower extremity in the 2D plane of motion.

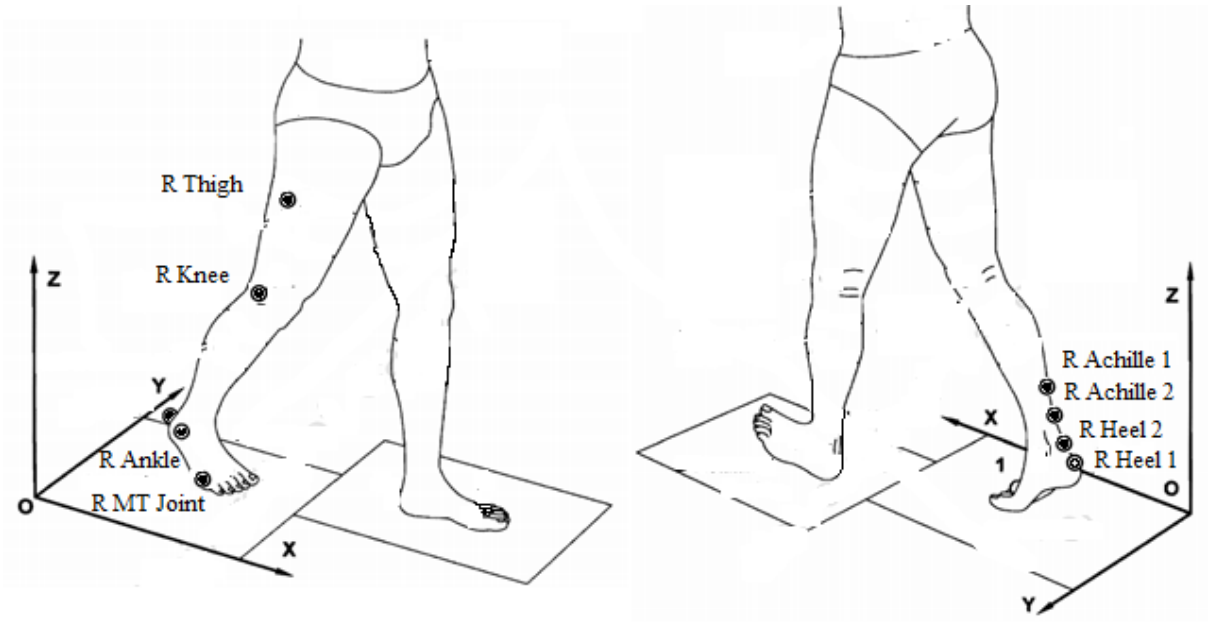

Figure 3-3: Passive marker placement on the dominant side of the leg for kinematic motion analysis of running gait, adopted and modified from [*194*]

Links for the lower extremity segments were created by connecting 'R knee' marker with 'R thigh' in the direction of X1 to form thigh segment, 'R ankle' marker with 'R knee' in the direction of X2 to form tibia segment and 'R-MT joint' marker with 'R ankle' in the direction of X3 to form foot segment. For thighs, the X1Z1 plane is formed by the hip joint, the thigh marker and the knee marker and Y1 axis was at the right angle to the X1Z1 plane as seen in Figure 3-4 (A). For calves, the X2Z2 plane was formed by the knee joint, the calf marker, and the ankle joint and Y2 axis was at right angles to the X2Z2 plane as seen in Figure 3-4 (A). Similarly, for feet, the X3Y3 plane was formed by the ankle joint, the heel marker, and the toe position and Z3 axis was at right angles to the X3Y3 plane and points to the person's left as per right-hand rule are shown in Figure 3-4 (A). In summary, the hip angle was defined as an angle between X_1 and global axis X around Z_1, the knee angle was defined as an angle between

X_1 and X_2 around Z_2 and the ankle angle was defined as an angle between X_2 and X_3 around Z_3, shown in Figure 3-4(B).

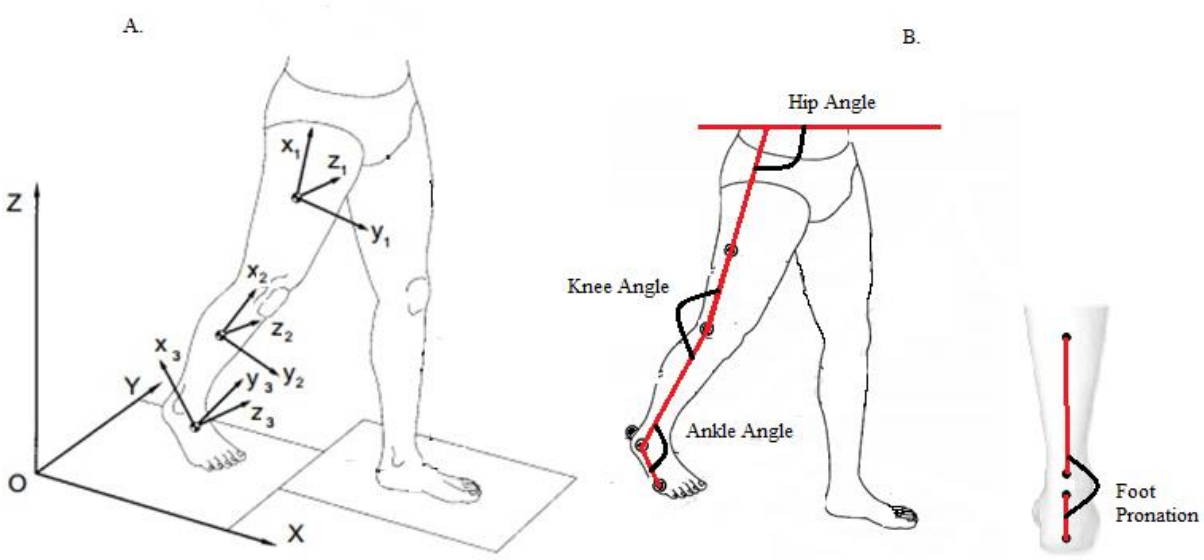

Figure 3-4: knee joint understanding for flexion/extension, abduction/adduction and internal/external rotation on right side and associated frame of reference for the segments on left side [*194*]

Measuring foot pronation is quite challenging in the 2D plane as it involves the complex movement of the foot, measuring its component known as heel eversion/inversion can provide its linkage with foot pronation and injury development [195, 196]. Furthermore, heel inversion/eversion do interact with medial arch support [197] and causes the distal joint of the foot from the ankle to move either inward or outward during foot progression. Its measurement in MS phase has been linked with foot supination and foot pronation. Foot pronation, shown in Figure 3-4(B), was defined as an angle between Y3 and X2 around X3 and was determined as a relative angle between links, formed by connecting the two heel markers and two achille tendon markers.

3.3 Methodology

Experiment methodology and related information are discussed in detail in the following section.

3.3.1 Participants

For this study, 17 healthy male recreational active runners (age 22.94±1.48 years, BMI 22.16±1.92, $\dot{V}O_{2max}$ 57.63±5.46 $ml.kg^{-1}.min^{-1}$, HR_{max} 190.47±7.89 $beats.min^{-1}$, % body fat 13.01±3.31) participated in data collection. Inclusion criteria was strictly followed.

3.3.2 Experiment Design

To avoid undue fatigue before tests, participants were instructed to restrain from exercise (gym or running workouts) for the last 36 hours before the test. Participants were also required to fill up **"How Do You Feel"** form, before the start of the test, to know about recovery status, emotional drive, physical exertion and mental stress. Furthermore, no intake of food was allowed before at least 4 hours of the test and participants were instructed to remain hydrated by consuming water.

Participants were explained thoroughly about the testing equipment, safety-related procedures, RPE-OMNI scale, blood sample collection methodology and emergency control over the treadmill to respond in case of an emergency. Tests were conducted under laboratory controlled conditions at the same hours of the day to avoid any circadian variation on oxygen kinetics [198]. Participants were instructed to wear same footwear and attire to avoid external factors affecting running performance and economy [199]. Before the start of each test, resting blood lactate level (<1.0 $mmol.l^{-1}$) was tested to ensure lactate value was returned to its baseline [200]. A warm-up session of 5-10 minutes at 8-8.5 KPH on the WOODWAY treadmill was conducted as a part of the testing session to regulate the body temperature and to have a stable physiological response to the running pace, selected in the test session.

For physiological monitoring, Parvo Medics TrueOne 2400 and YSI 2900 biochemistry analyzer were configured to monitor cardiorespiratory and lactate response as discussed in each protocol. For kinematic analysis, two digital video cameras were mounted on the sagittal and frontal plane. For neuromuscular performance, Trigno wireless EMG sensor and IM sensors were attached to the anatomical segments of interest. The detail about these system's configuration and settings have been discussed thoroughly in above section (instrumentation).

3.3.3 Fatigue Protocol

The study included three test sessions with a recovery period of 5-7 days in-between. Session 1 was administered to determine critical speed (CS), maximum cardiac capacity (HR_{max}) and maximum aerobic capacity ($\dot{V}O_{2max}$). For endurance fatigue evaluation, Session 2 with non-continuous protocol was devised to track BLa response during endurance running and to evaluate the effect of recovery on endurance performance and fatigue. Session 3 was designed to study continuous endurance performance to identify correlates of fatigue in physiological and biomechanical system and to develop a real-time fatigue prediction model.

The detailed procedure of each protocol is discussed below. The study hypotheses, for session 2 and session 3, are discussed in chapter 4 and 5, respectively.

Session 1: Progressive Speed Run to Exhaustion Protocol

A progressive submaximal treadmill run to exhaustion ($\dot{V}O2_{submax}$) test, shown in Table 3-1, was conducted on H/P/COSMOS WOODWAY motorized treadmill. 1% gradient was selected to equate the energetic cost of treadmill and outdoor running [201] whereas 4-minute duration was considered as an optimal duration to elicit high physiological load in relation to selected running pace [50]. Blood samples were collected from finger during resting intervals after every active stage run to determine CS. The individual CS was later used to simulate endurance pace [47, 48].

Table 3-1: Submaximal Treadmill speed run to exhaustion during session 1.

Stage	Speed (KPH)	Gradient (%)	Active Duration (min)	Rest (min)
1	10	1	4	1
2	11	1	4	1
3	12	1	4	1
…	…	…	…	…
N	Increment 1kph every next stage till exhaustion	1	4	1

After completion of $\dot{V}O_{2submax}$ test with 30 minutes rest, Astrand-modified $\dot{V}O_{2max}$ test (starting from 10KPH with 1% gradient and followed by 1KPH increment every next minute till treadmill speed of 15KPH and then speed was kept constant and gradient was increased by 2% every next minute till maximal exhaustion) [202] was conducted to determine the $\dot{V}O_{2max}$ and HR_{max} through the use cardio-respiratory system. The maximal effort was verified by either plateau in $\dot{V}O_2$, respiratory exchange ratio (RER) >1.1 or heart rate in the range of 95% of maximal heart rate (HR_{max} = 220-age) [203].

Session 2: Non-continuous constant speed test to exhaustion

After initial preparation of the equipment setup, a warmup session for 5-10 minutes at 8-8.5 KPH was conducted. A non-continuous constant critical speed run to exhaustion protocol, having work to rest ratio of 4:1 min with constant CS, was conducted to stress the physiological, biomechanical and perceptual response till volitional exhaustion (RPE=10), as shown in Table 3-2. 4-min stage duration was considered good enough to elicit high physiological load [49, 50]. 1-min rest in-between stages were subject to provide an imbalance in intracellular restitution and maintenance of O_2 kinetics and to replicate MLSS conditions [204].

Table 3-2: Non-continuous constant speed protocol run to exhaustion protocol

Stage	Speed	Intermittent stage (min)	Resting stage (sec)	Stopping Criteria
1	CS	4	1	---
2	CS	4	1	---
---	---	----	---	----
N	CS			Till exhaustion (RPE =10)

Session 3: Continuous constant speed test to exhaustion

After initial preparation of the equipment setup, a warmup session for 5-10 minutes at 8-8.5 KPH was conducted. A continuous critical speed run to exhaustion protocol, starting with constant individual's CS till exhaustion (RPE=10), shown in Table 3-3.

Table 3-3: Continuous constant speed run to exhaustion protocol.

Speed	Test duration
CS	Till Exhaustion (RPE=10)

3.3.4 Data Acquisition, Signal Conditioning, and Measurands

Data acquisition and signal condition methodology for the cardio-respiratory system, electromyography (EMG) system and video capture system are discussed in detail in the following section. The cardio-respiratory data collection methodology was adopted for all tested sessions whereas for EMG and video recording methodology was adopted for fatigue protocol data only, captured during session 2 & session 3. The parameters of interest were calculated from the experimentally collected data for the physiological, perceptual and biomechanical system.

3.3.4.1 Physiological and Perceptual Measures

During session 1, physiological data of each participant was exported with 15 sec averaging window to determine $\dot{V}O_{2max}$, maximum RER and HR_{max} and blood sample was tested at termination to determine maximum BLa buffer capacity for each participant. The progressive $\dot{V}O_{2submax}$ treadmill run was used to determine participant's CS using the spline curve estimation function between speed and BLa response.

During session 2 and 3, physiological data files were exported with 5 breath averaging algorithm followed by the 1-min averaging algorithm. The physiological variables ($\dot{V}O_2$, HR, RR, RER) were calculate at every 4th minute of each active stage during session 2 and after every minutes following the 3rd minute of continuous run during session 3. The RPE_C, RPE_M

and RPE_O data were also collected in a similar fashion to observe the relation between all these physiological variables and perceived exertion. Blood samples were collected and analyzed at the start, resting intervals during the test and at termination in session 2. Whereas in session 3, blood samples were only collected at 'rest' and at 'termination' during session 3. Furthermore, data for all the physiological variables, calculated during session 2 & 3, RPE and BLa responses were plotted against percentage completion time (% Completion time) to represent the variable adjustment along the course of fatigue run to exhaustion in majority of runners in this study.

During session 2, HR values during the 4th minute of each consecutive stage run (HR_{Ti}) and recovered heart rate during 1- min rest (HR_{Si}) were extracted. Heart rate intensity ($\%HR_{max}$), heart rate recovery (HRR), decrease in %HRR ($\%HRR_{decrease}$) and increase in $\%HR_{max}$ ($\%HR_{increase}$) till termination were computed using equation 3-1, 3-2, 3-3 & 3-4 respectively. Whereas during session 3, HR_{Ti} represents HR value of every consecutive recording interval and HR_{T1} represent the reference HR value at the '4th minute of the run' (optimal HR value). $\%HR_{max}$ and $\%HR_{increase}$ were computed using equation 3-1 and 3-4 respectively. HR_{max} was determined from session 1.

$$\%HR_{max} = HR_{Ti} / HR_{max} \quad \text{.....} \quad (3\text{-}1)$$

$$HRR = HR_{Ti} - HR_{Si} \quad \text{.....} \quad (3\text{-}2)$$

$$\%HRR_{decrease} = (HRR_{Si} - HRR_{S1}) / HR_{max} \; (i>1, subsequent\_stages) \quad \text{.....} \quad (3\text{-}3)$$

$$\%HR_{increase} = (HR_{Ti} - HR_{T1}) / HR_{max} \; (i>1, subsequent\_stages) \quad \text{.....} \quad (3\text{-}4)$$

3.3.4.2 Electromyographic (EMG) Measures in Lower Extremity

For EMG data acquisition, the skin hairs at the muscle of interest were removed to improve adhesion under humid and sweaty conditions. The shaved surface was cleaned with alcohol patched under controlled pressure to get less impedance and better signal strength [205]. After skin cleansing and preparation, 7 Delsys Trigno Wireless EMG sensors, having 1926 Hz sampling rate, were placed on the belly of RF, VL, BF, ST, GM, GL and TA muscles in the direction of muscle fibers (pennation angle, shown in Table 3-4). Location of the muscles of interests is shown in Figure 3-5.

Table 3-4: Muscle of interest and their pennation angle along with functionality during stance and swing phase of gait cycle

Parameter of interest	Muscles susceptible to fatigue	Pennation Angle, α (◦)	Functionality
EMG	Rectus femoris	13.9 [206]	Knee extension, hip flexion
	Vastus Lateralis	18.4 [206]	Knee extension
	Bicep Femoris	11.6 [206]	Hip extension, knee flexion
	Semitendinosus	12.9 [206]	Knee flexion, hip extension
EMG	Tibial Anterior	9.6 [206]	Ankle dorsiflexion
	Lateral Gastrocnemius	12 [206]	Ankle plantar flexion
	Medial Gastrocnemius	9.9 [206]	Ankle plantar flexion
IM & Accelerometer	Tibial Anterior (left and Right)	--	Tibia loading impact
	Sacrum	--	Hip Impact and Hip forward acceleration

After sensor placement, marked in a square shape (□) in Figure 3-2, Trigno wireless hardware acquisition unit was integrated with "EMGworks acquisition software' and sensors were configured as per their anatomical location. Real-time test data during rest was recorded to test signal strength and noise due to interference or bad connection with the skin. Once the connection was tested and reliable reading was found, participants running data was recorded and stored for post analysis of fatigue. In case of system connection loss or total loss of signals from the sensors, the test was re-conducted in the following week to ensure the good collection of data.

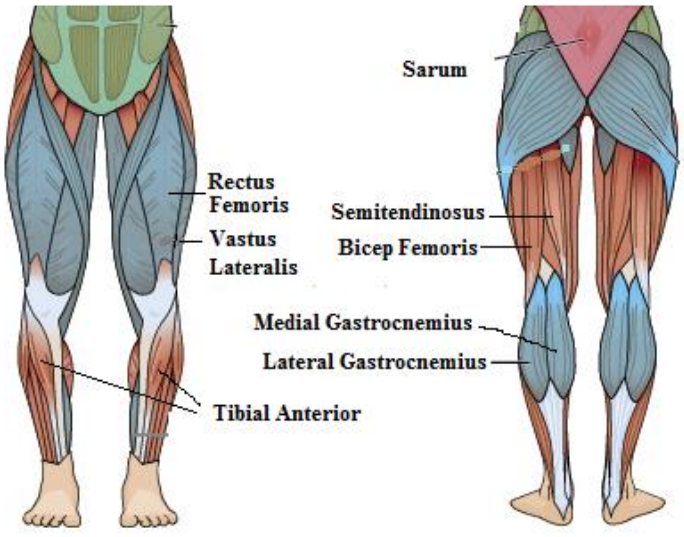

Figure 3-5: Human muscle anatomy representing selected muscle with labels, courtesy: The Muscular System

During session 2, Lower extremity muscle's EMG data were recorded from 3:30 to 3:50 (min: sec) before the completion of each 4-min stage till exhaustion. During session 3, lower extremity muscle's EMG data were recorded after every two minutes for 20 seconds till RPE=8. Once RPE reached 8, data were recorded after every 1 minute for 20 seconds till

volitional exhaustion (RPE=10). Noise reduction and signal processing of sEMG data were done in 'EMGworks Analysis' software using the flowchart methodology, shown in Figure 3-6, to determine TDMdPF and iEMG for the muscles of interests (RF, VL, BF, ST, GM, GL, TA). TDMdPF was determined using median frequency analysis in EMGworks for 5 consecutive running gait cycle. iEMG was determined by conducting the 'cyclic analysis algorithm' in 'EMGWorks' software to determine the average neuromuscular activity over five running gait cycles using IM data as a step identification threshold. The data was resampled at 100Hz to determine the iEMG at a particular stage to track neuromuscular activity level in this research.

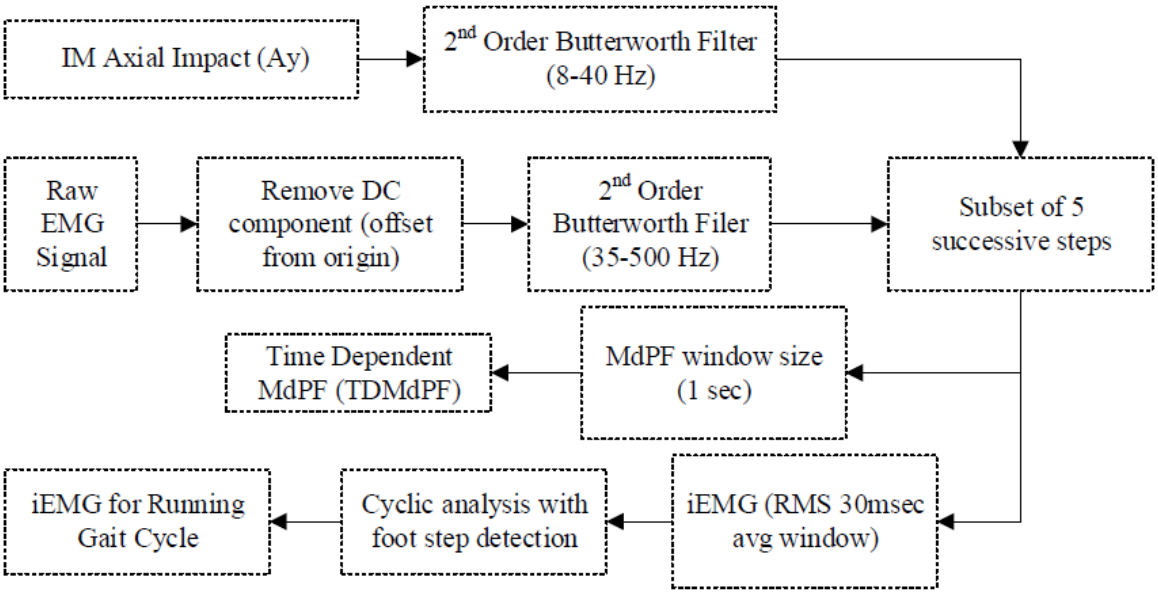

Figure 3-6: Signal processing methodology for the raw EMG signal to determine time-dependent median power frequency (TDMdPF) and integrated EMG (iEMG) for the running gait cycle.

Power index (Pi) was determined to explain the increase or decrease in neuromuscular activity over the running gait cycle in progression with fatigue till exhaustion using equation 3-5. Furthermore, considering median frequency as a gold standard variable to evaluate fatigue [91], fatigue index (Fi) was determined, using equation 3-6 to understand individual muscle kinetics in relation with fatigue. The combined 'Pi' and 'Fi' analysis will help in understanding the underlying muscle fiber recruitment dynamics and muscle activation levels during endurance training, and synergic contribution of agonist and antagonist muscles to support endurance under fatiguing conditions, as explained in fatigue measurement section in chapter 2.

$$\text{Power\_Index}=\left[\left(\text{Amplitude}_{i}/\text{Amplitude}_{1^{st}\text{stage}}\right)-1\right]*100 \quad i=2^{nd}\ \text{stage \& onward} \quad \ldots \qquad (3\text{-}5)$$

$$\text{Fatigue\_Index}=\left(\left(\text{TDMdPF}_{i}/\text{TDMdPF}_{1^{st}\text{stage}}\right)-1\right)*100\,,\ i=2^{nd}\ \text{stage \& onward} \quad \ldots. \qquad (3\text{-}6)$$

3.3.4.3 Inertial Measures in Lower Extremity

After skin preparation and cleansing the surface at both leg's TA muscle belly and sacrum, Two Delsys Trigno IM sensors (±16g, 148 Hz) and one Trigno EMG sensor (±9g, 148 Hz) were placed at the anatomical location as shown in figure 3-2. Trigno wireless hardware acquisition unit was integrated with "EMGworks acquisition software' and IM data was synchronized with EMG data collection system. During session 2 & 3, Lower extremity IM data was recorded in the same fashion as of EMG data. For determining the I_H (impact force in 'g', transferred from the ground to the hip segment during landing phase), ACC_H (propulsion acceleration in term of gravity 'g') and I_T (impact force in 'g', transferred from the foot to the tibia bone) on both legs, IM data files were exported to MATLAB and were analyzed using the flowchart methodology, shown in Figure 3-7.

Power spectral density (PSD) analysis was performed on the tibia and hip acceleration data to determine impact frequency and angular cyclic motion bandwidth for the selected participants in this study. For angular motion, PSD analysis represented first power peak between 2 to 8 Hz for hip and tibia acceleration data. For impacts. PSD reported bandwidth of 8-20 Hz which was found to have a close association with ground impacts. The FFT analysis for tibia impact was found in close association with Martyn et al. [207].

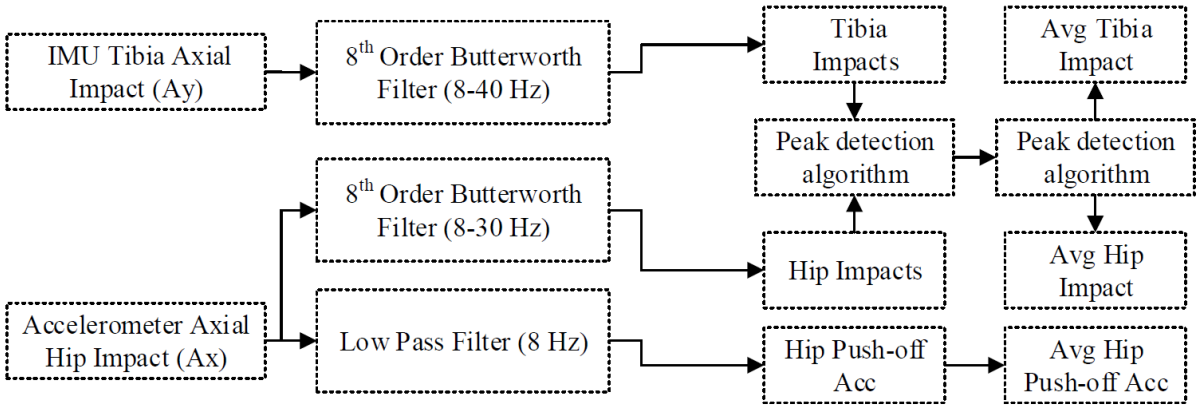

Figure 3-7: Signal processing methodology for the raw hip accelerometer data (Ax in direction of spine) and IM data (Ay in direction of tibia bone) to determine average tibia impact, average hip impact, and average hip push-off acceleration.

Tibia and hip impact data were first filtered using 8th order Butterworth zero-phase filter followed by peak detection and averaging algorithm during session 2 and 3. For hip push-off acceleration, low pass filter (8 Hz cut-off frequency) was implemented to determine the acceleration profile, followed by peak detection algorithm to determine maximum hip push-off acceleration. All these algorithms were programmed in MATLAB to measure I_T, I_H and ACC_H.

Bilateral Asymmetry and Kinematic Evaluation within Lower Extremity

For evaluating bilateral kinetic asymmetry, I_T was selected due to its close association and significant correlation with ground reaction force (GRF) and peak plantar pressure (PPP) during running [163] and vertical jumping [208]. Following the proposed signal processing methodology in Figure 3-7, average peak tibia impact on the dominant side (I_{DT}), average peak tibia impact on the non-dominant side (I_{NDT}), average peak hip impact through the dominant side (I_{DH}), average peak hip impact through the non-dominant side (I_{NDH}), average hip impact (I_H), average peak hip push-off acceleration following the dominant leg (ACC_{DH}), average peak hip push-off acceleration following the non-dominant leg (ACC_{NDH}) and average hip push-off acceleration (ACC_H) were determined for each recording during the session 2 & 3. KA for the tibia impact (KA_{Ti}), hip impact (KA_{Hi}) and hip push-off acceleration (KA_{Ha}) were determined following equation 3-7, 3-8 and 3-9 respectively. For determining the impact attenuation capability of the dominant and non-dominant side and to understand the changes in stiffness behavior in the dominant and non-dominant leg with fatigue progression, equation 3-10, and equation 3-11 were used. For STR, step count was multiplied with three to determine stride rate per minute, shown in equation 3-12.

$$KA_{Ti} = \left[\left(I_{DT} - I_{NDT} \right) / \left(I_{DT} + I_{NDT} \right) * 100 \right] \quad \text{.....} \quad (3\text{-}7)$$

$$KA_{Hi} = \left[\left(I_{DH} - I_{NDH} \right) / \left(I_{DH} + I_{NDH} \right) * 100 \right] \quad \text{.....} \quad (3\text{-}8)$$

$$KA_{Ha} = \left[\left(Acc_{DH} - Acc_{NDH} \right) / \left(Acc_{DH} + Acc_{NDH} \right) * 100 \right] \cdots \quad (3\text{-}9)$$

$$\mathrm{DL}_{\text{Attenuation}} = \left[1 - (I_{DH} / I_{DT}) \right] * 100 \quad \text{.....} \quad (3\text{-}10)$$

$$\mathrm{NDL}_{\text{Attenuation}} = \left[1 - (I_{NDH} / I_{NDT}) \right] * 100 \quad \text{.....} \quad (3\text{-}11)$$

$$\mathrm{STR} = \left[3 * (\text{stride count for 20sec}) \right] \quad \text{.....} \quad (3\text{-}12)$$

3.3.5 2D Video Processing for Kinematic Measures

For kinematic assessment of movement in dynamic tasks, high-speed 3D motion analysis is considered as the gold standard. However due to financial constraints and testing conditions, its practical use is limited in real time outdoor conditions and alternatively, 2D video kinematic analysis has been proposed due to ease of use and reduced cost for movement analysis. Several studies have conducted its reliability on different kinematic variables during dynamic tasks in the frontal plane [190, 191] and sagittal plane [192] and have shown a good correlation between 2D and 3D motion analysis. Therefore, this research included the use of 2D video analysis to

meet the practical endurance conditions and to track the kinematic changes during the fatiguing run.

A 2D biomechanical model in this research was constructed by placing the passive marker on the dominant leg, shown in the Figure, 3-3. During session 2, video data was recorded from 3:30 to 3:50 (min: sec) before the completion of each 4-min stage till exhaustion. During session 3, video data was recorded after every two minutes for 20 seconds till RPE=8. Once RPE reached 8, video data was recorded after every 1 minute for 20 seconds till volitional exhaustion (RPE=10). Following that, video data was imported into 'Kinovea' software. Kinematic profile for the hip, knee, ankle and foot pronation angles during the MS phase of running gait cycle was identified to be evaluated due to its interaction with running injuries development [144, 147]. Furthermore, fatigue is also known to interact with neuromuscular activity in the lower extremity [156] that may change the kinematic profile of these joints, changes in the kinematic behavior of hip, knee and ankle joint and foot pronation were evaluated over the course of fatigue run during session 2 and session 3. During each recording, kinematic data for the hip, knee, ankle and foot pronation was evaluated at MS for 5 successive strides as per the recommendation of Heiderscheit et. al. [209]. The kinematic data over 5 successive strides were averaged to reduce the possibility of human error, stride variability and to track the cumulative effect of fatigue on these selected kinematic variables.

CHAPTER 4. FATIGUE MANIFESTATIONS DURING A NON-CONTINUOUS ENDURANCE TRAINING PROTOCOL

Blood lactate is an important parameter that interacts with peripheral and central fatigue mechanisms [111, 116, 181]. Due to existing technological limitations on real-time measurement of BLa during continuous running, this study is designed with a 1-min resting interval to track BLa at the same critical speed (CS), as of the continuous study (shown in Chapter 5). This study evaluates individual's time to exhaustion (TTE), physiological response to fatigue, kinematic changes in lower extremity with fatigue and neuromuscular response to fatigue. It also tested the assumption that running at CS during non-continuous test induces MLSS or not. The MLSS represents the metabolic relation with endurance performance [47, 210-212]. This chapter also investigates the relationship between the rise in RPE and BLa in recreational active runners, as contradictory evidence exists between the rise of RPE and BLa during the intermittent protocol in trained runners [50].

4.1 Study Background and Hypotheses

Metabolic relationship with endurance training is critical to determine the endurance stress as the majority of the endurance-trained runners have been tested to achieve the MLSS conditions during endurance events [210-213]. During the non-continuous endurance study in this Chapter, it is hypothesized that 1-min rest during intermittent stage with CS will result in MLSS response to replicate continuous endurance metabolic response. Fatigue manifestations are examined on the physiological system ($\dot{V}O_2$, RER, HR, HRR, $\%HR_{max}$, RR and BLa), perceptual exertion (RPE_C, RPE_M and RPE_O), running mechanics (hip flexion, knee flexion, ankle flexion, foot pronation, I_T, I_H, ACC_H and bilateral KA) and lower extremity muscles (RF, VL, BF, ST, GM, GL and TA) during the con-continuous test. For the physiological strain, it is hypothesized that physiological ques will adjust with progression in fatigue. For neuromuscular fatigue, it is hypothesized that TDMdPF and iEMG of the lower extremity muscles in the dominant leg may increase or decrease from the non-fatigue state to the fatigue state. It is also hypothesized that neuromuscular fatigue among selected group of muscles may be linked with the changes in running mechanics. To evaluate bilateral Kinetic Asymmetry (KA) in lower extremity, it is hypothesized that fatigue may influence KA during landing and propulsion phase of running gait cycle.

During the intermittent protocol, increase in RPE in well-trained runners is not associated with an increase in BLa [50]. Therefore, for recreational male runners, this study examines the associative relationship between RPE and BLa and hypotheses that there may be a better

cardio-respiratory surrogate to estimate metabolic stress in recreational active runners than RPE.

4.2 Methods

4.2.1 Participants

Demographics of the male recreational active runners are shown in chapter 3.

4.2.2 Non-Continuous Fatigue Protocol and Variables of Interest

After 5-7 days of recovery from the 1st session and following all the detailed preparation procedures regarding the participants and equipment, a non-continuous critical speed run to exhaustion test was conducted (previously presented in chapter 3). Physiological data, perceived exertion data (RPE_C, RPE_M and RPE_O), manually triggered sEMG, IM data, and video data was recorded and analyzed, as explained in Chapter 3. Fatigue manifestations on physiological variables ($\dot{V}O_2$, HR, HRR, $\%HR_{max}$, $\%HR_{increase}$, $\%HRR_{decrease}$. RR, RER and BLa), perceptual response (RPE_C, RPE_M, RPE_O), kinematic variables (hip, knee & ankle angles, pronation angle, tibia impact (I_T), dominant tibia impact (I_{DT}), non-dominant tibia impact (I_{NDT}), hip impact (I_H), dominant hip impact (I_{DH}), non-dominant hip impact (I_{NDH}), hip acceleration (ACC_H), hip acceleration at dominant leg toe-off (ACC_{DH}), hip acceleration at non-dominant leg toe-off (ACC_{NDH}), tibia impact kinetic asymmetry (KA_{Ti}), hip impact kinetic asymmetry (KA_{Hi}), hip acceleration kinematic asymmetry (KA_{Ha}), stride rate (STR)) and neuromuscular variables (iEMG, TDMdPF, Fatigue_index (Fi), Power_index (Pi)) were computed, as explained in data acquisition, signal conditioning and measurement section in Chapter 3.

4.2.2.1 Statistical Analysis

Data for all the physiological variables ($\dot{V}O_2$, HR, HRR, $\%HR_{increase}$, $\%HRR_{decrease}$. RER and BLa), perceptual response (RPE_C, RPE_M, RPE_O), kinematic variables (hip, knee and ankle angle, pronation angle, I_{DT}, I_{NDT}, I_H, ACC_H and STR) and electromyographic variables ('Pi' and 'Fi') was plotted against individual's percentage completion time (%TTE). It provides a generalized response against simulated fatigue through the non-continuous test.

Participants' processed data for all the physiological and kinematic variables were classified into three groups: non-fatigue (captured at the '1st stage'), the onset of fatigue (interpolated at 'AT' point) and fatigued ('End' stage). To identify the significant difference between the means of these three groups, known as within-subjects factors, "Repeated measure ANOVA" (RM ANOVA) with a significance level of 95%, was used.

To study the relationship between different physiological, biomechanical and perceptual variables, "Kendal tau_b" correlation with a significance level of 95% was determined. All the

physiological and kinematic variables' data was re-arranged using the criteria of the '% completion time' from smallest to largest. To determine physiological and biomechanical variables' significance in estimating metabolic stress, RPE_C, RPE_M, and RPE_O, multilinear regression analysis was performed. The assumption of collinearity was checked by observing that none of the independent variables have correlations greater than 0.7. Independent variables having multicollinearity problem were dropped from the study. The assumption of independence of residuals was assessed by the "Durbin-Watson" statistics. All statistical analyses were carried out using "IBM SPSS Statistics for Windows, Version 20.0. Armonk, NY: IBM Corp".

4.3 Results

Participants' $\dot{V}O_{2max}$, HR_{max} and CS, obtained from session 1, were 57.45±5.35 ($ml.kg^{-1}.min^{-1}$), 191±8 ($beats.min^{-1}$) and 3.64±0.417 ($m.sec^{-1}$), respectively. "Kendalls' tau_b" showed a significant negative correlation (tb=-0.307, p=0.045) between %body fat and CS.

On average, all participants completed 9 stages. TTE during the non-continuous test was 37.88±9.81 mins. The selected CS resulted in stressing physiological system towards AT point (onset of fatigue) at 41.25±24.08 % of completion time.

4.3.1 Fatigue Manifestations on Physiological Measures

Table 4-1 shows data in the form of mean ± standard deviation. One-way RM ANOVA showed significant effect of fatigue on $\dot{V}O_2$, HR, RR, $\%HR_{max}$, RER, HRR, RPE and BLa. Fatigue elicited statistically significant change in $\dot{V}O2$ ($F(2,32) = 50.56$, $p<0.0005$), HR ($F(2,32) = 115.74$, $p<0.0005$), $\%HR_{max}$ ($F(1.458,23.331) = 114.95$, $p<0.0005$), HRR ($F(2,32) = 31.057$, $p<0.0005$), RR ($F(2,32) = 36.85$, $p<0.0005$), RER ($F(2,32) = 8.579$, $p<0.002$), RPE_C ($F(2,32) = 78.059$, $p<0.0005$), RPE_M ($F(2,32) = 94.55$, $p<0.0005$), RPE_O ($F(1.438,23.001) = 86.107$, $p<0.0005$) and BLa ($F(1.368,21.886) = 67.669$, $p<0.0005$). Post hoc analysis with "Bonferroni adjustment" only reported non-significant changes in RER between 'AT' and 'End' stage, however, all the physiological variables were statistically significant between '1st stage', 'AT' and 'End' stage. Calculations presented in Greenhouse et. al. [214] were used to correct the one-way RM ANOVA where assumption of sphericity was violated for the analysis of results. "Kendall's tau-b" coefficients showed a strong correlation of BLa (0.581, p=0.0001) and HRR (-0.41, p=0.0001) with $\%HR_{max}$. $\%HR_{max}$ was found to have a same strong correlation with overall fatigue (tb=0.591, p=0.0001) as of BLa (0.583, p=0001). Furthermore, HRR has been reported to be linked with aerobic fitness and changes in performance parameters [215], the negative correlation of HRR with $\%HR_{max}$ does also reveal a better understanding of

physiological strain and fatigue. Therefore, in this research, $\%HR_{max}$ is considered as a strong correlate of BLa, physiological strain and RPE_O.

Table 4-1: Descriptive statistics (mean±SD) of physiological variables at 1st stage, anaerobic threshold (AT) and at termination stage (End) during the non-continuous constant speed fatigue protocol.

	Physiological Variables		
	1st Stage	**AT**	**End**
$\dot{V}O_2$ (ml.kg^{-1}.min^{-1})	45.26±4.96	47.04±5.04 [a]	48.19±5.023 [b,c]
HR (beats.min^{-1})	159.54±7.98	171.3±7.3[a]	179.04±7.82 [b,c]
$\%HR_{max}$	83.79±3.13	89.97±2.6 [a]	94.00±1.76 [b,c]
RR (breath.min^{-1})	42.8±8.45	48.49±7.9 [a]	58.05±8.13 [b,c]
RER	0.992±0.043	0.98±0.037 [a]	0.966±0.037 [c]
HRR (beats.min^{-1})	46.29±10.76	40.16±9.3 [a]	28.68±9.38 [b,c]
RPE_C	2.53±1.18	5.58±2.43 [a]	9.47±1.07 [b,c]
RPE_M	2.59±1.06	5.3±2.17 [a]	9.41±1.06 [b,c]
RPE_O	2.65±1.11	5.40±2.3 [a]	9.47±0.78 [b,c]
BLa (mmol. l^{-1})	3.19±0.47	4±0.03 [a]	5.48±0.95 [b,c]

[a] significant difference ($p<0.05$) from the non-fatigue state (1st stage) to the onset of fatigue state (AT).
[b] significant difference ($p<0.05$) from the onset of fatigue state (AT) to fatigued state (End).
[c] significant difference ($p<0.05$) from the non-fatigue state (1st stage) to fatigued state (End).

4.3.2 Fatigue Manifestation on Kinematic Measures

Data are presented as a mean ± standard deviation, as shown in Table 4-2. One-way RM ANOVA has shown a significant effect of fatigue on the ankle. Fatigue elicited statistically significant change in ankle angle ($F(1.339, 21.427) = 5.561$, $p<0.025$) and stride rate ($F(1.381, 22.128) = 4.553$, $p<0.034$). Post-hoc analysis with "Bonferroni adjustment" showed a significant change in ankle angle and STR as shown in Table 4-2. Calculations presented in Greenhouse et. al. [214] were used to correct the one-way RM ANOVA where the assumption of sphericity was violated.

Table 4-2: Descriptive statistics (mean±SD) for kinematic variables at 1st stage, anaerobic threshold (AT) and at termination stage (End) during the non-continuous constant speed fatigue protocol.

	Kinematic Variables		
	1st Stage	**AT**	**End**
Hip (º)	73.99±3.99	73.5±3.6	73.17±3.74
Knee (º)	137.49±4.85	136.99±4.49	137.14±5.2
Ankle (º)	96.56±3.83	96.83±3.54	98.2±3.53 [b]
Pronation (º)	16.59±3.74	17.27±4.05	17.49±4.54
I_{DT} (g)	7.32±1.41	7.34±1.65	7.63±1.64
I_{NDT} (g)	7.1±1.55	7.08±1.49	7.52±1.29
ACC_H (g)	1.42±0.414	1.43±0.43	1.43±0.41
I_H (g)	2.306±0.94	2.41±1.09	2.45±0.92
STR (steps.min^{-1})	173.5±10.51	170.76±10.53 [a]	170.82±8.38

[a] significant difference ($p<0.05$) from the non-fatigue state (1st stage) to the onset of fatigue state (AT).

[b] significant difference ($p<0.05$) from the onset of fatigue state (AT) to fatigued state (End).

[c] significant difference ($p<0.05$) from the non-fatigue state (1st stage) to fatigued state (End).

4.3.3 Influence of Kinematic Variables on Oxygen Cost

A hierarchical multiple regression was run to determine if the addition of joint angles in the lower extremity and then adding landing behavior (I_{DT}, I_{NDT}, ACC_H, I_H) and stride rate (STR) do influence in predicting oxygen cost ($\dot{V}O_2$) of running.

Table 4-3: Hierarchical multiple regression predicting running economy ($\dot{V}O_2$) from kinematic factors, one by one to determine significant predictors of oxygen cost of running.

$\dot{V}O_2$								
	Model 1		Model 2		Model 3		Model 4	
Variables	B	Beta	B	Beta	B	Beta	B	Beta
Constant	128.17*		109.32*		117.36*		131.31*	
Knee Angle (º)	-0.495*	-0.454	-0.431*	-0.395	-0.471*	-0.432	-0.506*	-0.464
Ankle Angle (º)	-0.133	-0.101	-0.114	-0.086	-0.161	-0.121	-0.116	-0.088
Pronation (º)	-0.028	-0.023	-0.082	-0.068	-0.031	-0.025	-0.092	-0.076
I_{DT} (g)			1.336*	0.434	1.273*	0.413	1.534*	0.498
I_{NDT} (g)			-0.098	-0.032	-0.364	-0.118	-0.524	-0.170
ACC_H (g)					2.064*	0.175	2.522*	0.214
I_H					0.270	0.057	-0.080	-0.017
STR (steps.min^{-1})							-0.075	-0.147
R^2	0.201		0.369		0.394		0.403	
F	12.88*		17.78*		13.91*		12.57*	
ΔR^2	0.201		0.168		0.024		0.009	
ΔF	12.88*		20.29*		3.029*		2.32	

Noted N=158, *p<0.05, B=unstandardized coefficients, Beta= standardized coefficients, I_{DT}= dominant leg tibia impact, I_{NDT}= non-dominant leg tibia impact, ACC_H= hip push-off acceleration, I_H=hip impact, STR= stride rate.

Prior to fitting the multilinear regression, multicollinearity was checked by inspecting the correlation coefficients and tolerance/VIF values. Hip and Knee angles were found to have a correlation greater than 0.7 and the hip angle was not significantly correlated with perceived exertion, therefore, it was dropped from the study. There was the independence of residuals, as assessed by a "Durbin-Watson statistic" of 1.852. A basic regression model was analyzed first with joint angles (Model 1) followed by the addition of I_{DT} and I_{NDT} (Model 2), ACC_H and I_H (Model 3) and STR (Model 4). All these models were statistically significant. Statistical significance of each variable is shown in Table 4-3. The results show that the hip angle, knee angle, I_{DT} and hip push-off acceleration (ACC_H) are the only statistically significant variables that were related to the disruption in running economy in Model 4 of Table 4-3.

The observed trends of the significant variables, affecting running economy, are shown in Figure 4-1. The black line represented the linear trend of the observed variable against $\dot{V}O_2$ and dotted blue line represented the 95% confidence interval. Increase in I_{DT} and ACC_H and decrease in knee angle were significantly linked with higher oxygen cost of running and hence the poor running economy. Whereas ankle angle, foot pronation, I_{NDT}, I_H and STR were not statistically affecting the running economy, observed in this study. The descriptive statistics for all the significant variables are shown in Figure 4-1.

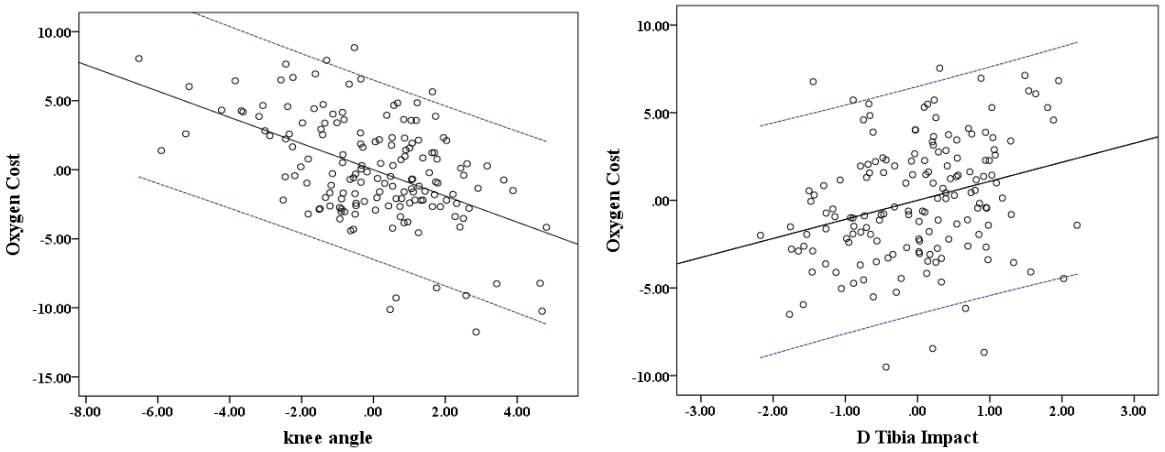

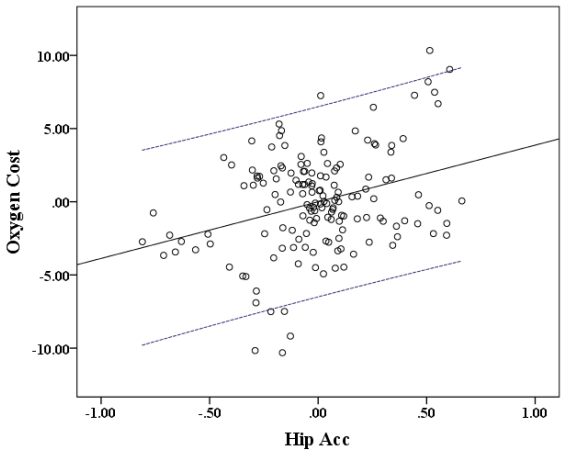

Descriptive Statistics		
	Mean	SD
Oxygen Cost (ml/kg/min)	46.59	4.46
Knee Angle (˚)	137.63	4.09
I_{DT} (g)	7.29	1.45
ACC_H (g)	1.38	.38

Figure 4-1: Partial Regression plot represents the interaction between kinematic variables (knee angle, I_{DT}, and ACC_H,) and oxygen cost of running. The black line represents the linear trend line whereas dotted double blue line represents the 95% confidence interval range values. Descriptive statistics for significant variables are shown in the table with mean and SD.

4.3.4 Biomechanical and Physiological Predictors of Fatigue

A hierarchical multiple regression was run to consider the possible causal effect of physiological and biomechanical variables on the dependent variables (BLa, RPEc, RPE_M and RPE_O one by one). Multicollinearity problem was identified for the hip and knee angle as correlation coefficient was greater than 0.7. Therefore, the hip angle was dropped from the study. For predicting continuous variables (BLa, RPE_C, RPE_M and RPE_O one by one), independence of residuals was observed using "Durbin-Watson statistics" (1.716, 1.579, 1.675, 1.489, respectively). "Durbin-Watson statistics" were observed to be greater than 1% significance points of tabulated lowed bound (dl=1.459) and hence inconclusive autocorrelation to ensure the valid use of multiple linear regression in this research.

Model 'M1' and 'M2', shown in Table 4-4, represent the significance of predicting variables in the physiological and biomechanical system. The coefficients and statistical significance of the predictors are shown in Table 4-4. Statistical significance of the physiological model 'M1' for 'BLa' was F (5, 152) = 41.67, $p < .0001$, $R^2 = .578$, however, when kinematic predictors were added into the model 'M2', the coefficient of determination improved by 17.3% ($R^2 = .678$), as shown in Table 4-4. Statistical significance of the physiological model 'M1' for dependent variable RPE_C was F (5, 152) = 44.83, $p < .0001$, $R^2 = .596$, however when kinematic predictors were added into the model 'M2', the coefficient of determination was improved by 30.8% ($R^2 = 0.76$), as shown in Table 4-4. Statistical significance of the physiological model 'M1' for RPE_M was F (5, 152) = 46.70, $p < .0001$, $R^2 = .606$, however when kinematic predictors were added the coefficient of determination was improved by 28.38% ($R^2 = 0.777$). Similarly, statistical significance of the physiological model 'M1' for RPE_O was F (5, 152) =

74.14, $p < .0001$, $R^2 = .709$. When kinematic predictors were added in model 'M2', the coefficient of prediction was improved by 16.36% ($R^2 = 0.81$).

Table 4-4: Hierarchical multiple regression predicting BLa, RPE_C, RPE_M, and RPE_O from physiological and biomechanical factors. The significance of each variable and model along with significance is shown below.

Hierarchical Multilinear Regression Analysis								
	uSC: BLa		uSC: RPE_C		uSC: RPE_M		uSC: RPE_O	
Variables	M 1	M 2	M 1	M 2	M 1	M 2	M 1	M 2
(Constant)	-16.19*	-15.13*	-25.44*	-30.16*	-28.74*	-48.75*	-30.08*	-65.59*
$\dot{V}O_2$	.004	-0.017	0.105*	0.045	0.146*	0.089*	0.113*	0.113*
RR	.007	0.007	0.078*	0.083*	0.043*	0.004	0.065*	0.055*
RER	4.21*	3.948	-7.03	-6.04	-4.06	-1.235	-5.78	-0.218
HRR	-.01	-0.008	-0.02	-0.03*	-0.041*	-0.077*	-0.034*	-0.07*
$\%HR_{max}$	.18*	0.193*	0.338*	0.336*	0.347*	0.355*	0.383*	0.34*
Knee Angle (º)		-0.047*		-0.09*		-0.059		0.05
Ankle Angle (º)		0.053*		0.263*		0.296*		0.232*
Pronation Angle (º)		0.022		0.014		0.022		0.056
I_{DT} (g)		-0.007		0.116		0.366*		0.144
I_{NDT} (g)		0.013		0.599*		0.179		0.319*
I_H (g)		0.198*		-0.13		0.301*		0.403*
ACC_H (g)		-0.164		-0.823*		0.310		-1.284*
STR (Steps/min)		-0.003		-0.061*		-0.021		0.017
R^2	0.578	0.678	0.596	0.76	0.606	0.777	0.709	0.81
F	41.67*	23.32*	44.83*	39.30*	46.70*	38.68*	74.14*	52.46*
ΔR^2	0.578	0.100	0.596	0.184	0.606	0.172	0.709	0.116
ΔF	41.67*	5.58*	44.83*	15.08*	46.70*	13.88*	74.14*	12.02*

Noted N=158, uSC = Un-Standardized Coefficients, *$p<0.05$

4.3.5 Bilateral Kinetic Asymmetry & Fatigue

Bilateral asymmetry related data are presented as a mean ± standard deviation, as shown in Table 4-5. Bilateral KA was computed based on tibia impacts, hip impacts, and hip push-off acceleration. Results have shown that participants experienced relatively higher impacts on hip through the non-dominant leg than the dominant leg. Hip impact asymmetry (KA_{Hi}) was observed opposite to hip push-off acceleration asymmetry (KA_{Ha}) and tibia impacts asymmetry (KA_{Ti}). This observed difference in hip impact asymmetry reflects towards better strength and coordinated muscle control capabilities of musculoskeletal structure in the dominant leg.

Though overall, no effect of fatigue, using one-way RM ANOVA with a significance level of 95%, was observed on bilateral kinetic asymmetry (KA) for a selected group of participants against fatigue. The statistical significance and descriptive measures for all asymmetry related variables are shown in Table 4-5.

Table 4-5: Descriptive statistics (mean±SD) of lower extremity impact and acceleration dynamics on hip and shank segment during push-off and MS phase of running gait cycle. The significance of these variables was tested using paired sample t-test.

	Lower Extremity Asymmetry Analysis		
	1st Stage	**AT**	**End**
ACC_{DH} **(g)**	1.441±0.458	1.444±0.469	1.437±0.435
ACC_{NDH} **(g)**	1.399±0.384	1.41±0.404	1.43±0.395
KA_{Ha} **(%)**	0.844±6.048	0.585±5.039	-0.151±5.98
I_{DH} **(g)**	2.320±1.019	2.378±1.177	2.431±1.081
I_{NDH} **(g)**	2.295±0.915	2.446±1.048	2.464±0.842
KA_{Hi} **(%)**	-0.218±8.697	-1.902±8.996	-1.532±10.488
I_{DT} **(g)**	7.324±1.414	7.338±1.65	7.633±1.643
I_{NDT} **(g)**	7.096±1.547	7.077±1.489	7.52±1.293
KA_{Ti}**(%)**	1.766±10.212	1.672±10.46	0.371±10.244

[a] significant difference ($p<0.05$) from the non-fatigue state (1st stage) to the onset of fatigue state (AT).
[b] significant difference ($p<0.05$) from the onset of fatigue state (AT) to fatigued state (End).
[c] significant difference ($p<0.05$) from the non-fatigue state (1st stage) to fatigued state (End).

4.3.6 Electromyographic Fatigue in Lower Extremity

Two participants generalized iEMG data for five consecutive running gait cycles has been presented in this section to observe neuromuscular activation difference in response to fatigue stages (‘1st stage’, ‘AT’ and ‘End’ stage) during endurance running. The neuromuscular iEMG data for the above two participants against fatigue stages is shown in Figure 4-2, where ‘A’ represents participant ‘1’ and ‘B’ represents participant ‘2’. Total generalized data of the neuromuscular activity (iEMG and TDMdPF) in term of power index ‘Pi’ and fatigue index ‘Fi’ for all 17 recreational active runners is shown in Figure 4-3 and Figure 4-4.

Most recreational active runners were observed to have decreased iEMG during different phases of running gait cycle. During the weight acceptance phase of running gait cycle, the main contributing muscles were RF, VL, GM, and GL. With fatiguing contractions over consecutive stages, agonist muscles (RF, VL) were observed to decrease neuromuscular activation level during stance and swing phase of running gait cycle whereas antagonist muscle (BF) was observed to have increased activity level. The coordination between agonist and antagonist muscles were to absorb the impact and to provide relevant knee and hip stability support. At the shank segment, the changes in neuromuscular activation level of GM and GL muscles and reduced tibialis anterior activity were observed during different phases of running gait cycle with fatigue progression, as shown in Figure, 4-2 (A, B).

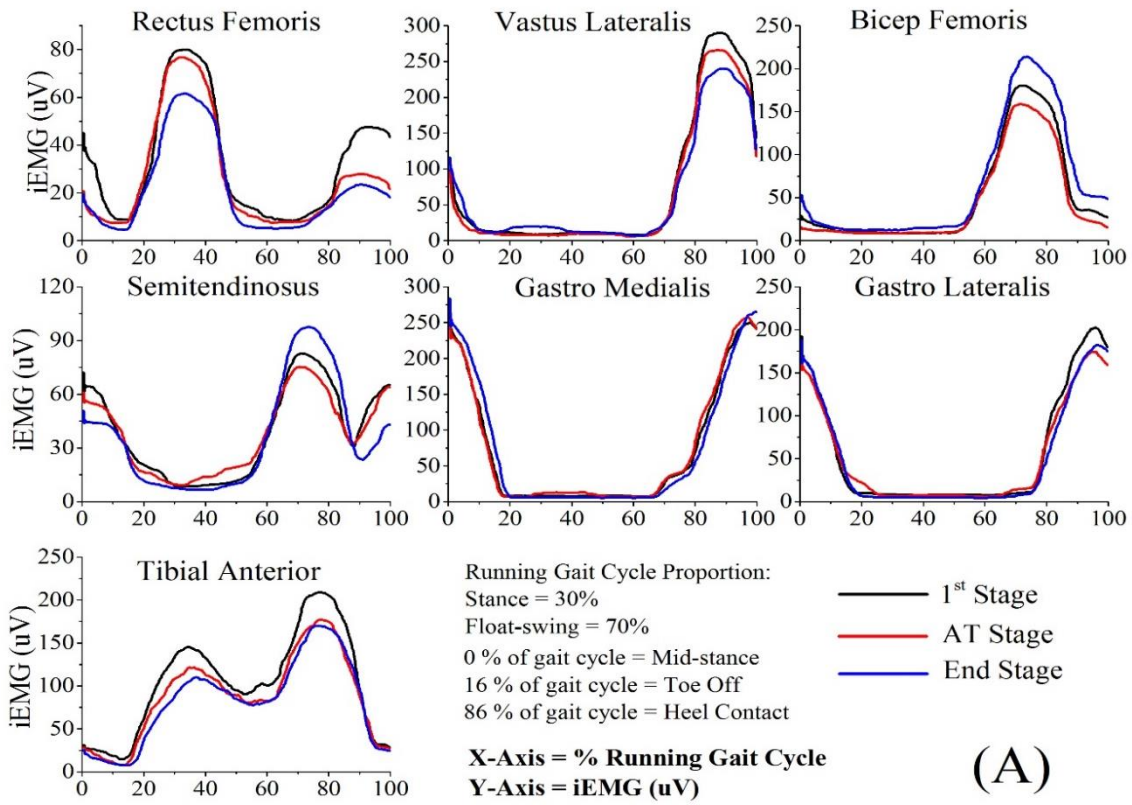

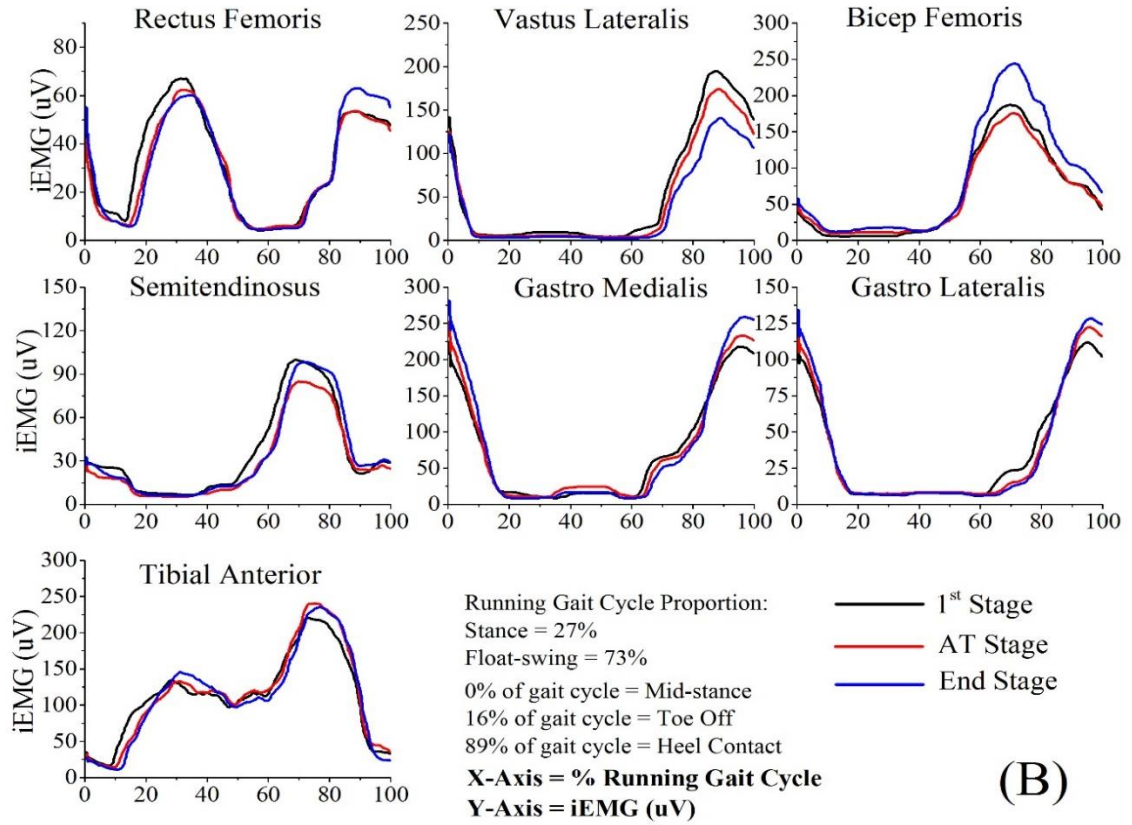

Figure 4-2: Comparison of muscle activation profile of the lower extremity muscles against fatigue (1st stage, AT and End) for participant 'A' (running at anaerobic threshold speed of 4.31 m/sec with toe-off of 16% of the running gait cycle) and for participant 'B' (running at 4.5 m/sec with toe-off 16% of the running gait cycle).

Results of the neuromuscular fatigue (TDMdPF) reported a significant Kendal tau-b correlation between pronation and fatigue status of GM (tb=0.164, p=0.007) and GL (tb=0.223, p=0.0001) muscle, ankle angle had a negative correlation with TA (tb=-0.159, p=0.005) muscle, hip angle had negative correlation with BF (tb=-0.167, p=0.022) and ST (tb=-0.245, p=0.0001) and knee angle had negative correlation with ST (tb=-0.271, p=0.0001).

4.3.6.1 Power Index Dynamics with Fatigue Progression

The power index represents the cumulative increase or decrease in neuromuscular activity over the running gait cycle during different fatiguing contractions, determined using equation 3-5. Figure 4-3 represents the overall normalized response of the iEMG for RF, VL, BF, ST, GM, GL and TA muscles during running gait cycle in reference to the relevant iEMG level at the "1st stage" of that muscle for all studied participants.

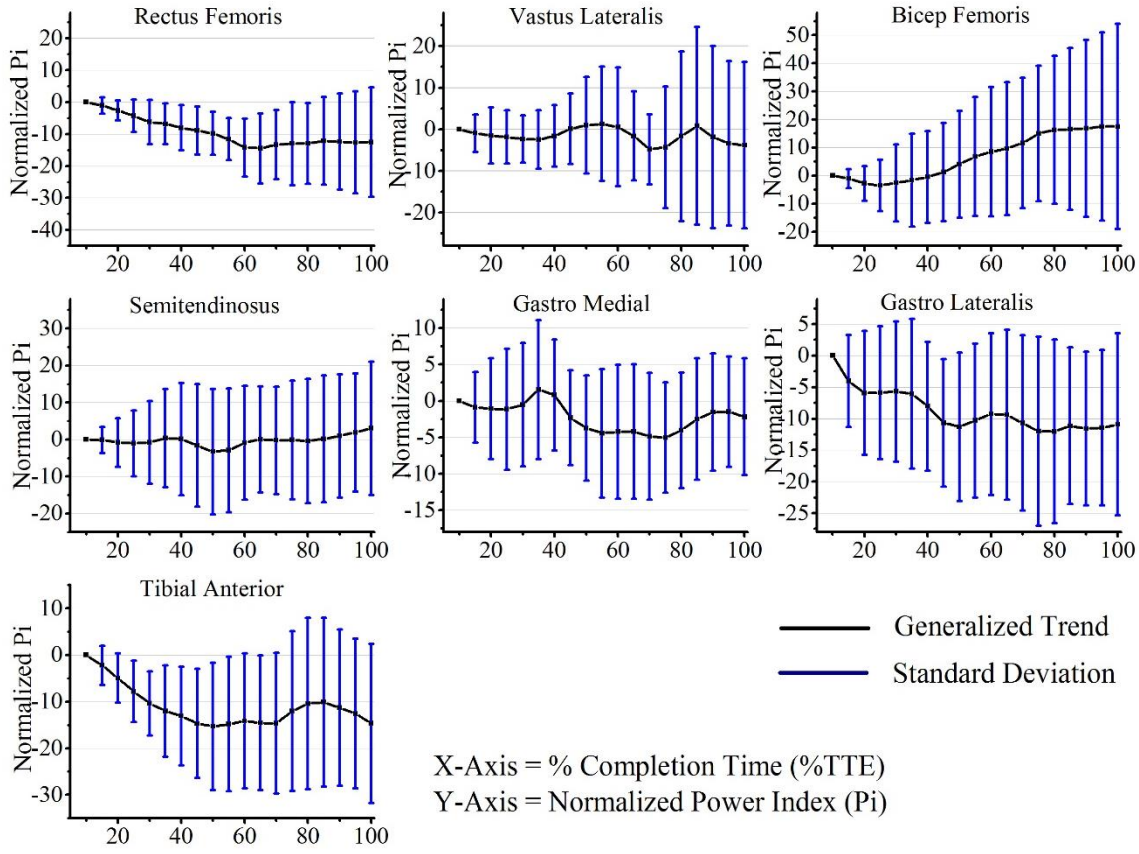

Figure 4-3: Normalized power index (mean±SD) for the captured iEMG over the running gait cycle during consecutive stages in comparison with a 1st stage to determine the degree of variability of EMG activation levels from non-fatigue state to fatigue state.

To evaluate the 'Pi' of each muscle relationship with RPE_M, "Kendall tau_b" correlation was run with 95% significance. "Kendall tau_b" showed a significant correlation of RF (tb=-0.359, p<0.0001), VL (tb=-0.116, p=0.013), BF (tb=0.379, p<0.0001), ST (tb=0.133, p=0.002), GM

(tb=-0.09, p=0.039), GL (tb=-0.103, p=0.011), and TA (tb=-0.183, p<0.0001). All the muscles' power profile was significantly correlated with muscular perceived exertion. Similarly, the variance in BLa (metabolic stress) was significantly correlated with the activation dynamics of RF (tb = -0.336, p<0.0001), BF (tb= 0.158, p=0.001), GL (tb= -0.103, p=0.008) and TA (tb = -0.254, p<0.0001) whereas non-significant effect was observed by VL, ST and GM.

4.3.6.2 Fatigue Index Dynamics with Fatigue Progression

The Fatigue index represents the relative change in median power frequency over the running gait cycles during different fatiguing contractions, determined using equation 3-6. Figure 4-4 represents the overall normalized response of the TDMdPF for RF, VL, BF, ST, GM, GL and TA muscles with the development of fatigue.

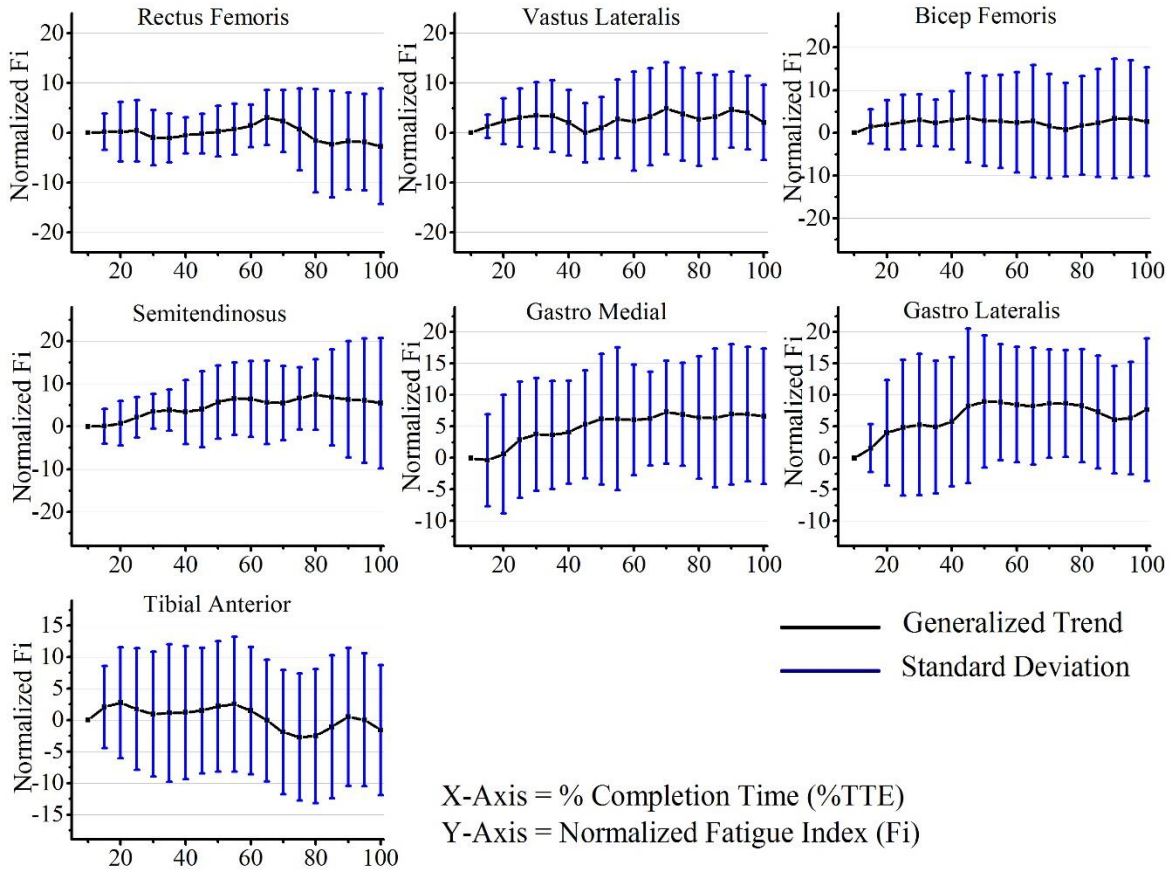

Figure 4-4: Normalized fatigue index (mean±SD) of the captured EMG data over the running gait cycle during consecutive stages in comparison with a 1st stage to determine the degree of variability of time-dependent median power frequency (TD-MdPF) from non-fatigue state to fatigue state.

"Kendall's tau-b" correlation was run to determine the relationship between "Fi' of each muscle with RPE_M. There was a significant correlation of BF (tb=-0.113, p=0.028), ST (tb= 0.169, p<0.0001), GM (tb=0.245, p<0.0001), GL (tb= 0.155, p=0.005), and TA (tb=-0.143, p=0.001) with lower extremity muscular fatigue perception (RPE_M). Similarly, the variance in BLa

(metabolic stress) was significantly correlated with the fatigue dynamics of VL (tb = 0.095, p=0.034), ST (tb= 0.286, p<0.0001), GM (tb= 0.227, p<0.0001) and TA (tb = -0.147, p<0.0001) whereas non-significant effect was observed by the changes in RF, BF, and GL.

4.4 Discussion

The non-continuous protocol was designed at the critical speed (CS) (also known as endurance pace) to examine BLa response during endurance training. The 1-min rest was selected due to its limited impact on recovery from the running stress and fatigue [204]. As 1-min rest may provide partial balance between intracellular restitution and maintenance of high $\dot{V}O_2$ on-kinetics [204], this chapter examined its effect on the physiological and biomechanical response in relation to the rise in BLa and perceived exertion (RPE_O). This chapter also seeks to determine the non-invasive cardio-respiratory surrogate of BLa to estimate metabolic stress in recreational active runners with a least possible error. Detailed findings of each individual system are discussed below in relation to progression of fatigue.

4.4.1 Physiological Understanding of Fatigue

The chosen methodology of running at the critical speed (CS) with 1-min rest interval resulted in sufficient cardiorespiratory stress. A significant effect of fatigue was observed on all physiological and perceptual variables ($\dot{V}O_2$, HR, $\%HR_{max}$, HRR, RR, RER, RPE and BLa) at termination in comparison with the '1st stage' and 'AT', as shown in Table 4-1. Endurance time (TTE) for each participant was observed to be different. The likely reason for such difference in TTE among participants includes the selection of personalized critical speed, exercise intensity induced metabolic response, personalized difference in energy contribution models, training history, aerobic fitness, intracellular restitution dynamics, and energy recovery dynamics [216-219].

On average, every participant ran for 9 stages during the non-continuous test, as observed in this study. Participants reached 'AT' by the 12th minute. 'BLa' concentration at the 12th minute was 3.95±0.65 mmol.l^{-1} and at the termination was 5.48±0.95 mmol.l^{-1}. The 'BLa' response at the termination, in this study, shows close proximation to the criterion of 1 mmol.l^{-1} [220] to achieve MLSS at 4 mmol.l^{-1}. Only 5 participants among 17 recreational active runners showed lactate increase higher than 2 mmol.l^{-1} and it can be considered that these participants were running at a very close pace to MLSS [221].

The physiological ($\dot{V}O_2$, HR, HRR, $\%HR_{increase}$, $\%HRR_{decrease}$, RER and BLa) and perceptual (RPE_C, RPE_M, and RPE_O) responses against development of fatigue during the non-continuous study are shown in Figure 4-5. The physiological and perceptual data was generalized against percentage completion time (%TTE). Participants reached 'AT' at 41.24±24.1% of the

completion time with 89.97±2.59% of HR_{max} and 81.58±3.14% of $\dot{V}O_{2max}$. An increase in $\%HR_{max}$ and decrease in HRR were observed, most likely due to the rise in intramuscular pressure, muscular strain and metabolic stress [133, 134]. HRR has been used as a tool to maintain balance in training load and recovery in well trained athletes [215] and it also has potential to determine training-induced fatigue due to significant correlation with RPE_O (tb=-0.381, p<0.0001). Heart rate intensity also showed a significant correlation with RPE_O (tb=0.597, p<0.0001). The increase in heart rate intensity ($\%HR_{increase}$) and decrease in HRR ($HRR_{decrease}$) offer potential to examine exercise-induced stress, an imbalance in training load and recovery and to determine fatigue during intermittent training [222]. $\%HR_{max}$ also showed a strong correlation with BLa (0.583, p=0001) and has potential to be used in real-time applications to determine the rise in the physiological strain, BLa and running stress [222].

An increase in $\dot{V}O_2$ and decrease in RER has also been observed for most of the participants. Only 5 participants showed an increase in RER over the course of fatigue run. Such difference in observed trend is most likely due to the differences in substrate utilization in relation to the intensity-induced response, individua's muscle oxidative capacity and aerobic fitness, altered pattern of muscle fiber recruitment, energy kinetics to the working muscles and/or oxidative stress [71, 216, 218].

RPE_O, as a measure of running stress in relation with time to exhaustion, shows that the individuals reached 'AT' at 5±2.2 (40±23.8 % of completion time). The observed variation (SD = 2.2) in RPE_O at 'AT' is most likely due to the individual's metabolic response to CS. Participants, whose BLa rose faster towards 'AT' in response to exposed running time, reported RPE less than 5. Whereas, those participants whose BLa delayed towards 'AT' against exposed running time, reported RPE higher than 5. This gives rise to the tendency of under or overestimating the associated BLa while running at the same CS and using RPE as an intensity prescription. It is also possible that BLa may not be the only factor towards increased perceived exertion [50, 122]. Literature has reported that fatigue involves the integrative neural processes which might be causing an increase in perceived exertion [14, 16]. A study on self-paced interval training for trained runners has shown the absence of an associative relation between BLa and the rise in RPE [50]. However, this study on recreational active runners has shown the association between BLa and RPE_O due to the linearity of the relationship between the observed responses, as shown in Figure 4-5. This association does not solely reveal the causative effect of the rise in BLa on RPE_O during interval training exercise for recreational active runners.

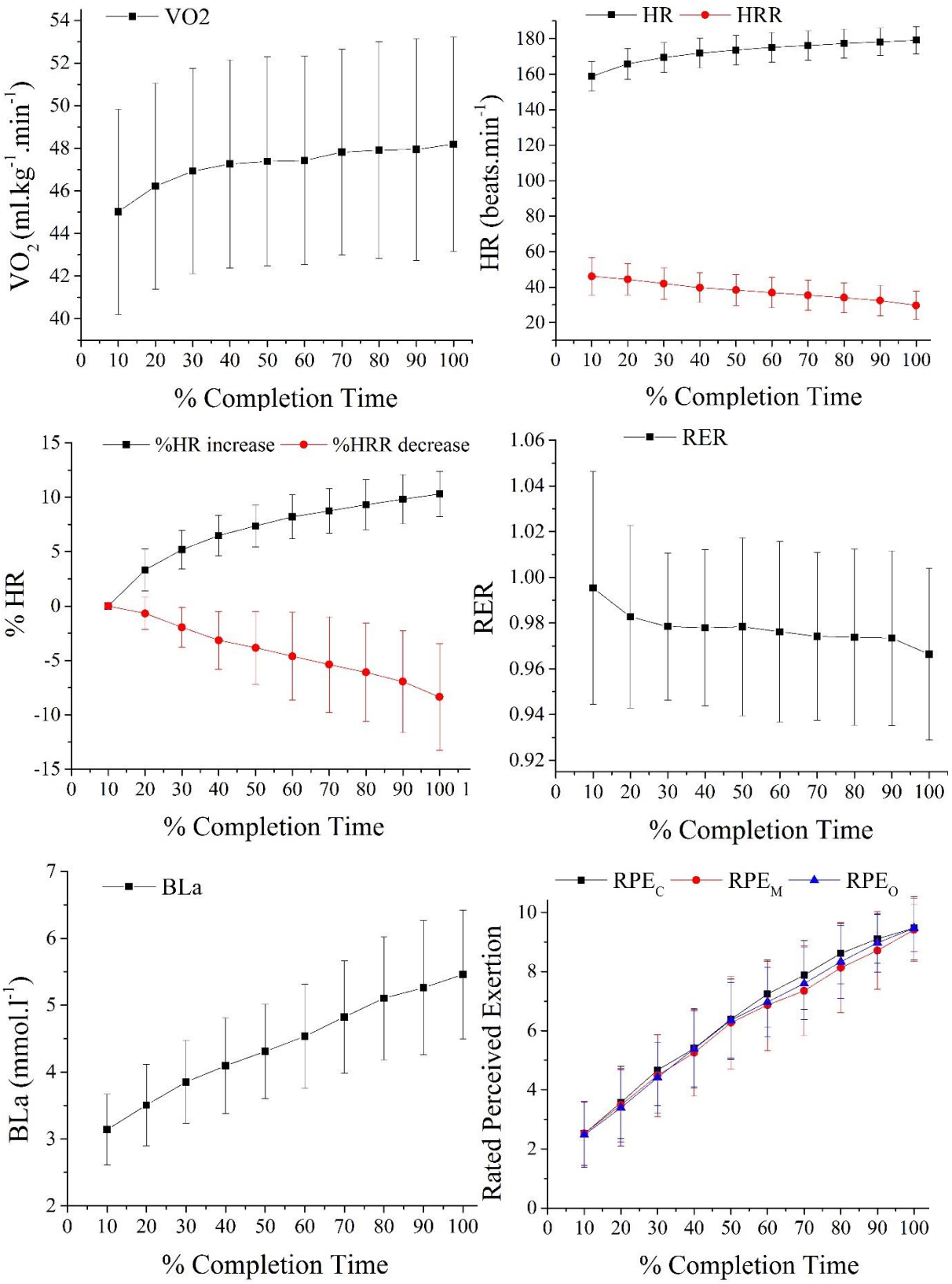

Figure 4-5: Physiological system responses (mean±SD) for V̇O2, HR, HRR, %HR, $\%HR_{increase}$, $\%HRR_{decrease}$, RER, BLa and RPE against % completion time from non-fatigue state to fatigue state.

While observing the perceived exertion for RPE_C, RPE_M, and RPE_O, shown in Figure 4-5, RPE_C, after almost 50% of completion time, was found to be slightly dominant than RPE_M.

Such observation is likely due to 1-min rest between running stages that might have helped in recovering muscle fiber and resulting in less sensory afferent feedback to the central region of the brain, which determines the perception of exertion through localized feedback mechanisms [181, 223].

4.4.2 Biomechanical Understanding of Fatigue

During endurance training, runners are prone to developing running injuries. To reduce running injuries, alteration in running form has been suggested by various researchers in the literature [144, 147, 173, 224]. The most simple and practical alteration is the changed in stride rate. Stride rate helps to have better control on landing forces [144], the rate of pronation [144, 173], the center of mass vertical excursion [224], shock attenuation [224], energy absorption at the hip, knee and ankle joints [209, 224]. However, when individuals start getting fatigued, they tend to reduce the stride rate (STR), which increases the vertical excursion of the center of mass, ground impacts and reduces impact attenuation by decreasing knee flexion and ankle plantarflexion [37].

Fatigue manifestation on running mechanics, in this Chapter, resulted in a significant change in ankle plantarflexion and stride rate when evaluated through the discrete measures at the 1st stage, AT and End stage, as shown in Table 4-2. When all cumulative kinematic variables (averaged trends shown in Figure 4-6) were analyzed to explain variance in perceived exertion (RPE_O), the ankle angle, I_{NDT}, I_H and ACC_H were found to be significantly linked with increasing perceived exertion. The STR was not identified to be significantly linked with RPE_O. This was most likely due to motorized treadmill running, as runners tends to lack control on stride pattern adjustments as compared to overground running [225].

In the literature, an increased STR reduces the magnitude of several key biomechanical factors associated with running injuries [224]. In present study, personalized differences in stride patterns were observed. Six runners among selected participants were either found to have increased STR by 3-5% or did not shift from their optimal value over the course of the fatigue run. Majority of participants were found to reduce the STR by 2-6%. Such personalized observation represented the differences in adaptation to running form in response to fatigue development. Participants with increasing STR showed decrease in tibia impact, hip impact and hip push-off acceleration and vice versa. Most likely reason for such observation is better coordination between lower extremity muscles during ‘MS’ and ‘TO’ phase of running gait cycle. The overall average STR trend, as shown in Figure 4-6, did not show the significant variation, most likely because of the differences in participant’s STR patterns, observed during

progression in fatigue till termination. However, STR was found to be significantly linked with chest fatigue (RPE_C), identified through the multilinear regression analysis.

The observed adjustments in studied kinematic variables were an indication of the fatigue as per runner's exertion status [40, 226]. The cumulative trend in studied recreational active runners showed a decrease in STR with exposed running time. Tibia impact was higher on the dominant leg in the lower extremity. Foot pronation were found to increase with fatigue progression. Among joint angles, a decrease in hip and knee angle and an increase in ankle angle and pronation angle was observed. Among joint angles, only ankle angle showed statistical significance in response to fatigue. The observed overall trend of all these kinematic variables are shown in Figure 4-6.

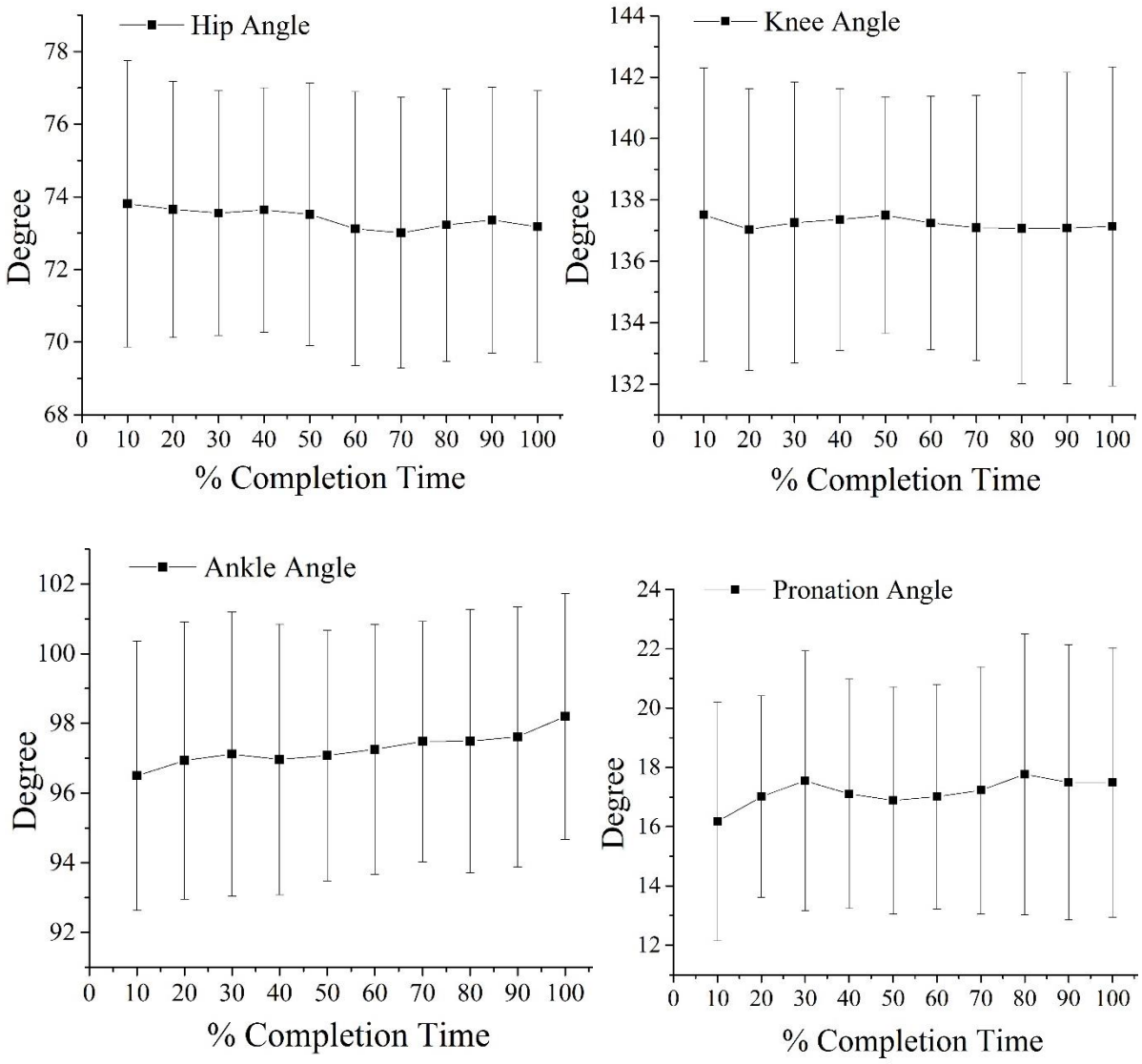

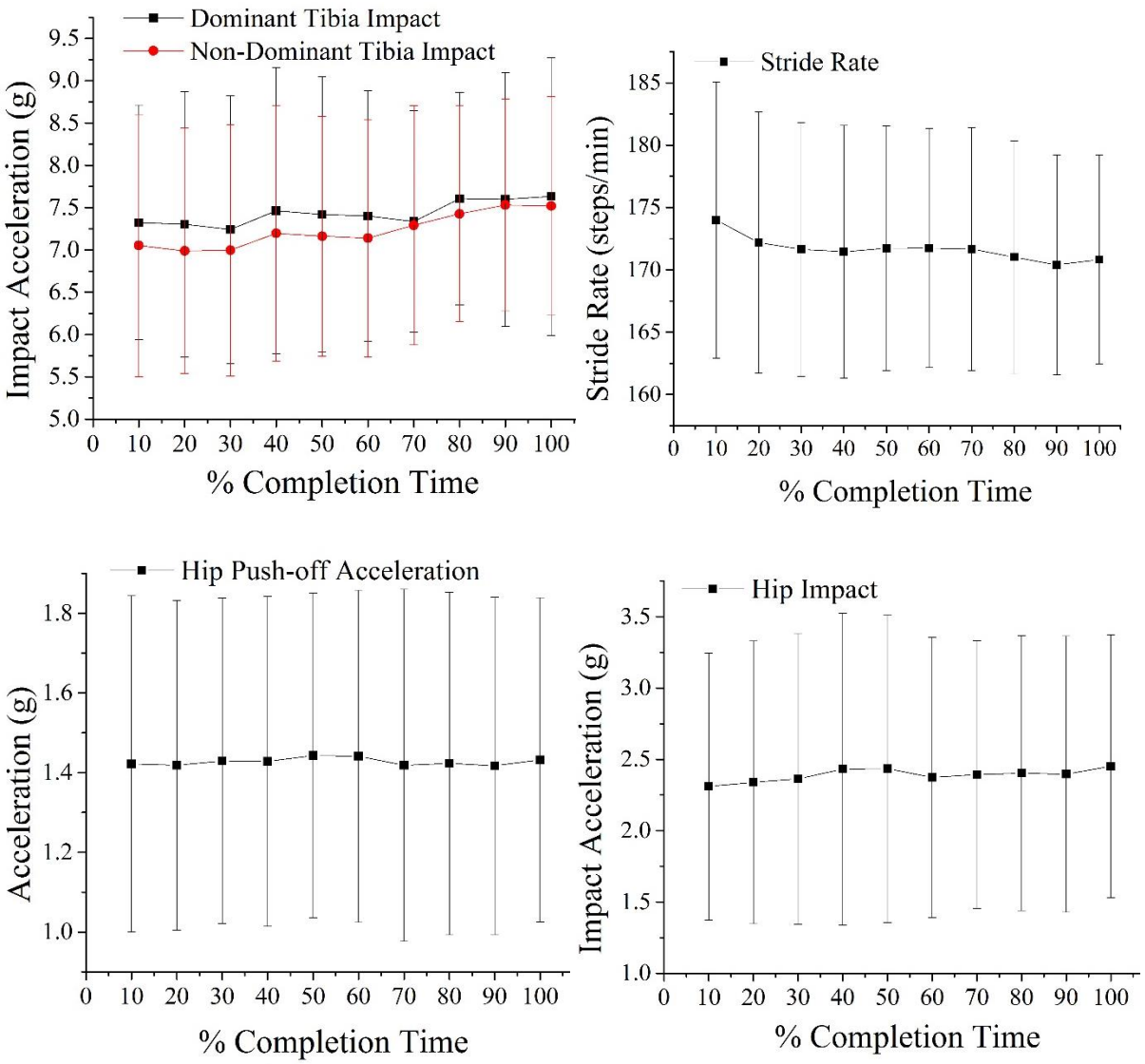

Figure 4-6: kinematic variable (mean±SD) responses for hip, knee, ankle and pronation angle at MS phase of running gait cycle, dominant and non-dominant tibia impact on the lower extremity, stride rate, hip impact and hip push-off acceleration against % completion time from non-fatigue state to fatigue state.

Laterality and its effect on running biomechanics during running gait cycle is a subject of interest in biomechanics literature [157, 160, 162, 227, 228]. Due to laterality, runners resort to a less stable and less coordinated gait. It also limits the ability to further increase stride rate at a certain speed [227]. Fatigue is also known to affect the stride rate. There is a possibility that laterality act as a limiting factor to influence the stride rate. Therefore, laterality was examined in this research to determine the influence of fatigue on the dominant and non-dominant leg during braking and propulsion phase of running gait cycle. Sadeghi et al. [229] have reported that propulsion is related to predominant muscle power generation and impact absorption is related to support and control function of the predominant leg. The results of the present study showed that, during fatiguing contraction, tibia impact was high on the dominant

side. Whereas impacts transferred from the non-dominant leg to the hip segment were higher. The non-dominant leg was identified to lack the capability of impact shock attenuation in comparison to the dominant leg. It again supports the argument that the dominant side has better strength and coordination while running from non-fatigue to fatigue state. However, no significant effect of fatigue was observed on limb laterality, examined through kinetic asymmetry, shown in table 4-5.

For understanding fatigue influence on $\dot{V}O_2$ during endurance running, researchers have reported various significant environmental, physiological and biomechanical factors [41, 43, 45, 53, 155, 171, 230] Environmental factors were kept constant under controlled environmental conditions in the laboratory setup. Physiological factors were very individualistic, based on individual training history, aerobic capacity, muscle fiber composition [231] and metabolic response to speed [53]. To understand the influence of biomechanical factors on running economy, several relationships have been reported in the literature. The most frequently analyzed relationship has been between stride length and/or stride frequency and RE [34, 230, 231]. It has also ben argued that no single variable or small subset of variables can explain differences in oxygen cost of running [154], as it is the weighted sum of the influences of many variables. Other studies on trained endurance runners have shown some existence of influence on running economy by kinematic measures (vertical oscillation of the center of mass, stride frequency, stride length, internal knee, ankle angles at foot strike) [34]. For recreational active runners in this study, multiple regression analysis revealed the significant influence of knee angle, I_{DT} and ACC_H on running economy (decrease in $\dot{V}O_2$) whereas no significant effect of ankle angle, pronation, I_{NDT}, I_H and STR on $\dot{V}O_2$. The stride rate (STR) was not significantly linked with $\dot{V}O_2$, most likely due to 1-min rest that might have helped in recovering the neuromuscular fatigue in the lower extremity and reduced control on STR during treadmill running.

4.4.2.1 Neuromuscular Fatigue & Running Mechanics

Changes in electromyographic activity in the musculoskeletal structure at critical speed is at the heart of changing running mechanics and running economy [34, 171]. The adjustments in the neuromuscular activity are basically because of force fatigability relation of the working muscle, physiological status and sense of effort of the working muscles [19, 109].

During prolonged running, changes in the endurance profile of the lower extremity skeletal muscles are caused by recruitment of different types of muscle fibers (I/IIA/IIB). The effect of these groups of muscle fibers on oxygen uptake has also been analyzed in the literature [231, 232]. Slow twitch fibers were identified to not significantly affect running economy, whereas,

fast twitch fibers were observed to have a significant effect [232]. Furthermore, a study on endurance-trained runners has reported the effect of the electromyographic activity of the rectus femoris and semitendinosus muscles on running economy [34].

In this chapter, finding of lower extremity muscles' power dynamics over the running gait cycle in response to fatigue showed an average decrease in 'Pi' for RF, VL, GM, GL and TA muscles. BF muscle was observed to increase and ST did not register any change in 'Pi', as shown in Figure 4-3. The decrease in neuromuscular activity is likely due to the reduced cortical drive, reduced firing rate, reduced action potential and/or fatiguing status of muscle's fast twitch fibers [87, 233] at termination stage in comparison with the 1st stage. During the weight acceptance phase of running gait cycle, the relative decrease in quadriceps group of muscles (RF, VL) and increase in hamstring muscle (BF, ST) were observed to compensate and stabilize the knee and hip joint, as shown in Figure 4-2 and Figure 4-3. Considering the 'TDMdPF' of the quadriceps and hamstring group of muscles, the hip angle had a significant correlation with BF (tb=-0.167, p=0.022) and ST (tb=-0.245, p=0.0001). However, the knee angle had a significant correlation with ST (tb=-0.271, p=0.0001).

For the calf and the shank, the neuromuscular activity changes with fatigue progression. Relative difference in iEMG of GM and GL muscles at 'MS' and 'TO' phase of running gait cycle were observed. Such observations during heel off at externally rotated and internally rotated feet position has also been studied by Riemann et al. [234]. Their study supports the notion that altering foot position during heel-off will prompt varying degrees of MG and LG activation. Some participants reported a decrease in foot pronation and majority reported an increase in foot pronation during this study. "Kendall's tau_b" showed a significant correlation between pronation and fatigue status of GM (tb=0.164, p=0.007) and GL (tb=0.223, p=0.0001) muscles. The observed differences in correlation strength and the relative difference in activation between GM and GL muscles may be linked with foot pronation, though it needs further studies for concrete evidence.

TA muscle was found to be active throughout the running gait cycle. However, reduced TA activity was observed before initial contact, MS, and swing phase of running gait cycle, during the progression of fatigue in this study. Ankle angle was also found to have a negative correlation with TA (tb=-0.159, p=0.005), which shows that reduced TA activity due to fatigue increases the ankle angle at MS, hence reducing the impact energy absorption during landing at the ankle joint. Such mechanics helps in increasing the impact transfer from feet to the upper segments of the body, as observed in this study (increase in I_{DT} and I_H with fatigue).

4.5 Conclusion

The results in this chapter establish a link of CS with MLSS for the recreational active runners. The selected CS, with 1-min rest, stressed the physiological and biomechanical system significantly and alterations in the physiological and biomechanical system were observed. During the physiological analysis, interestingly, a decrease in RER and increase in $\dot{V}O_2$ were observed with fatigue progression. $\%HR_{max}$ was found to be the potential surrogate for estimating metabolic stress, non-invasively, and was found to have a strong correlation with BLa and RPE_O. Neuromuscular analysis of the lower extremity muscles revealed that the 'iEMG' of the RF, VL, BF, ST, GM, GL and TA muscles, and "TDMdPF" of BF, ST, GM, GL, and TA muscles were linked with muscular fatigue (RPE_M). Significant kinematic predictors of fatigue included ankle angle, non-dominant tibia impact (I_{NDT}), hip impact (I_H) and hip push-off acceleration (ACC_H) whereas physiological predictors of fatigue included $\dot{V}O_2$, RR, HRR and $\%HR_{max}$. Bilateral kinetic asymmetry (KA) was found to be non-significant in relation to fatigue. However, limb dominance was observed due to higher tibia impact and higher hip push-off acceleration from the predominant leg.

CHAPTER 5. FATIGUE MANIFESTATIONS DURING A CONTINUOUS ENDURANCE TRAINING PROTOCOL

To investigate fatigue manifestations on the physiological and biomechanical system, a continuous constant critical speed protocol, previously discussed in chapter 3, was used. This chapter also presented that case that whether running at critical speed on the continuous basis will result in MLSS, known as endurance stress, or not. Cumulative analysis strategy, as presented in this chapter, is devised to analyze endurance performance, determine endurance time, identify significant physiological and kinematic fatigue predictors, examine neuromuscular fatigue in the lower extremity, investigate the relationship between neuromuscular fatigue, running mechanics and running economy with the development of fatigue. RPE was used as a gold standard measure of fatigue and $\%HR_{max}$, identified as a non-invasive surrogate for determining BLa in Chapter 4, was validated based on its significant correlation with perceived exertion in this chapter.

5.1 Study Background and Hypotheses

Critical speed (CS) has been investigated, in literature, to show the similarity with the maximal lactate steady state intensity during cycling [235] and running [210, 212]. The pioneering study [236] had suggested that the CS is an intensity which could be maintained for a very long time. However, subsequent studies on continuous exercise at this intensity, have shown a systematic increase in BLa concentration and times to exhaustion range between 20—40 min [237, 238]. From this point of view, CS can be characterized as the boundary between steady state (below) and non-steady state (above) intensity domain [239, 240]. Because of its practicality, the critical speed test has become widely accepted as an index of endurance-specific performance for trained endurance runners [241]. However, for recreational active runners in this study, critical speed was hypothesized to achieve same metabolic relation (MLSS) with endurance performance as of endurance runners.

For evaluating endurance fatigue during continuous running in this chapter, fatigue manifestations are being studied on physiological system ($\dot{V}O_2$, RER, HR, %HR, $\%HR_{max}$, RR and BLa), perceptual exertion (RPE_C, RPE_M and RPE_O), running mechanics (hip flexion, knee flexion, ankle flexion, foot pronation, I_T, I_H, ACC_H and bilateral KA) and electromyographic activity in RF, VL, BF, ST, GM, GL and TA muscles. Relationship between neuromuscular fatigue in the lower extremity, running economy and running mechanics are also examined to understand the changes in endurance performance. To determine the key biomechanical and physiological factors, it is hypothesized that the subjective perception of fatigue should

increase with runner's physiological strain and runner's kinematic adjustments. To determine major locomotory and stability muscles (susceptible to fatigue) in lower extremity, this study hypotheses that TDMdPF and iEMG of the lower extremity muscles in the dominant leg should increase or decrease with the change from non-fatigue state to the fatigue state. It is also hypothesized that relative change in neuromuscular activity (among selected group of muscles) may be linked with the changes in running economy and running mechanics, during progression of fatigue. To evaluate bilateral KA in lower extremity, it is hypothesized that impact asymmetry will be similar, resulting in consideration of tibia impact (I_T) during landing and hip push-off acceleration (ACC_H).

5.2 Methods

5.2.1 Participants

Demographics for the male recreational runner are shown in Chapter 3.

5.2.2 Continuous Fatigue Protocol and Variables of Interest

After 5-7 days of recovery from the 2nd session and following all the detailed preparation procedures regarding the participants and equipment, a continuous critical speed run to exhaustion test was conducted, discussed in Chapter 3. Cardio-respiratory data, BLa data, perceived exertion data (RPE_C, RPE_M, and RPE_O), manually triggered EMG and IM data, and video data were recorded and analyzed (as explained in Chapter 3). After data collection, the effect of fatigue on physiological variables ($\dot{V}O_2$, HR, $\%HR_{max}$, $\%HR_{increase}$, RR, RER and BLa), perceptual response (RPE_C, RPE_M, RPE_O), kinematic variables (hip, knee and ankle angle, pronation angle, I_T, I_{DT}, I_{NDT}, I_H, I_{DH}, I_{NDH}, ACC_H, ACC_{DH}, ACC_{NDH}, KA_{Ti}, KA_{Hi}, KA_{Ha}, STR) and neuromuscular variables (iEMG, TDMdPF, Fatigue_index, Power_index) was computed. For further details, please refer to the data acquisition, signal conditioning and measurands section in Chapter 3.

5.2.2.1 Statistical Analysis

Data for all the physiological variables ($\dot{V}O_2$, HR, RR, $\%HR_{increase}$, and RER), perceptual response (RPE_C, RPE_M, RPE_O), kinematic variables (hip, knee and ankle angle, pronation angle, I_{DT}, I_{NDT}, I_H, ACC_H and STR) and electromyographic variables ('Pi' and 'Fi') was plotted against individual's percentage completion time (%TTE). It provides a generalized response against simulated fatigue through the continuous test.

Participant's processed data for all the physiological and kinematic variables were classified into three groups: non-fatigue (captured at the 4th minute of the continuous test), the onset of fatigue (AT, identified through $\%HR_{max}$ during the non-continuous test) and fatigued (End, termination at RPE = 10). To identify the significant difference between the means of these

three groups, known as within-subjects factors, "Repeated measure ANOVA" (RM ANOVA) with a significance level of 95%, was used.

To identify the significance of $\%HR_{max,}$ as a non-invasive surrogate for regulating the running stress, "Kendal tau_b" correlation with a significance level of 95% has been used to finds its association with RPE_O. "Kendall's tau_b" correlation was studied to determine the relationship between different physiological, biomechanical and perceptual variables. All the physiological and kinematic variables data was re-arranged using the criteria of the '% completion time' from smallest to largest for all participants. To determine physiological and biomechanical variables' significance in estimating RPE_C, RPE_M, and RPE_O, multilinear regression analysis was performed. The assumption of collinearity was checked by observing that none of the independent variables have correlations greater than 0.7. Independent variables, having multicollinearity problem were dropped from the study. The assumption of independence of residuals was assessed by the "Durbin-Watson" statistics. All statistical analyses were carried out using "IBM SPSS Statistics for Windows, Version 20.0. Armonk, NY: IBM Corp".

5.3 Results

Average TTE for all the participants during this study was 23.94±9.75 mins. Individual's CS resulted in stressing physiological system towards 'AT' at 53.51±21.7% of the individual's percentage of completion time and maximum BLa concentration was 6.77±1.48 $mmol.l^{-1}$ at the termination of the test.

5.3.1 Fatigue Manifestation on Physiological Measures

Table 5-1 shows data as mean ± standard deviation. "One-way RM ANOVA" with 95% significance showed significant effect of fatigue on $\dot{V}O_2$, HR, RR, RER, $\%HR_{max}$, $\%HR_{increase}$, $RPE_{C,}$ RPE_M, and RPE_O. Fatigue elicited significant change in $\dot{V}O2$ ($F(2,32) = 76.604$, $p<0.0005$), HR ($F(2,32) = 111.698$, $p<0.0005$), RR ($F(2,32) = 77.005$, $p<0.0005$), RER ($F(2,32) = 1.571$, $p=0.080$), $\%HR_{max}$ ($F(2,32) = 115.19$, $p<0.0005$), $\%HR_{increase}$ ($F(2,32) = 114.877$, $p<0.0005$), RPE_C ($F(1.385,22.153) = 96.478$, $p<0.0005$), RPE_M ($F(1.147,23.616) = 121.322$, $p<0.0005$) and RPE_O ($F(1.348,21.563) = 110.258$, $p<0.0005$). Post-hoc analysis with Bonferroni adjustment reported that all the only RER was statistically different with 90% confidence level from 'AT' to 'End' stage, however, all other physiological variables were significant in-between all groups (4^{th} min, AT and End). Greenhouse et. al. [214] calculations were used to correct the "One-way RM ANOVA" where assumption of sphericity was violated for the analysis of results.

Table 5-1: Descriptive statistics (mean±SD) for physiological variables at the 4th minute of the run, anaerobic threshold (AT) and at termination stage (End) during continuous constant speed test to exhaustion protocol.

	Physiological Variables		
	4th Min of Run	**AT**	**End**
$\dot{V}O2$ (ml.kg^{-1}.min^{-1})	45.17±5.79	47.69±5.72 [a]	49.50±5.66 [b, c]
HR (beats.min^{-1})	159.52±7.93	171.30±7.35 [a]	180.78±8.42 [b, c]
RR (breath.min^{-1})	42.00±10.34	48.31±8.46 [a]	58.61±8.39 [b, c]
RER	0.989±0.05	0.986±0.03	0.998±0.04 [d]
RPE_C	2.35±1.22	6.25±2.42 [a]	9.82±0.53 [b, c]
RPE_M	2.18±1.24	5.92±2.35 [a]	9.76±0.56 [b, c]
RPE_O	2.18±1.19	6.14±2.53 [a]	9.94±0.24 [b, c]
$\%HR_{max}$	83.78±3.28	89.97±2.58 [a]	94.91±2.25 [b, c]
$\%HR_{increase}$	0.00±0.00	6.18±3.50 [a]	11.13±2.20 [b, c]

[a] significant difference ($p<0.05$) from the non-fatigue state (1st stage) to the onset of fatigue state (AT).
[b] significant difference ($p<0.05$) from the onset of fatigue state (AT) to fatigued state (End).
[c] significant difference ($p<0.05$) from the non-fatigue state (1st stage) to fatigued state (End).
[d] significant difference ($p<0.05$) from the onset of fatigue state (AT) to fatigued state (End).

"Kendall's tau-b coefficients" reported a strong positive correlation of $\%HR_{max}$ with RPE_C (tb=0.626, p=0.0001), RPE_M (tb=0.651, p=0.0001) and RPE_O (tb=0.654, p=0.0001). $\%HR_{max}$ was found to have same strong correlation with RPE_O (tb=0.591, p=0.0001), as of BLa (tb=0.583, p=0.0001) during session 2, a non-continuous constant speed test. $\%HR_{max}$ also reveals better understanding on physiological strain and fatigue as cardiovascular drift ($\%HR_{increase}$) was found to have strong correlation with $\dot{V}O_2$ (tb=0.113, p=0.036), RR (tb=0.312, p=0.0001), RPE_C (tb=0.612, p=0.0001), RPE_M (tb=0.587, p=0.0001) and RPE_O (tb=0.592, p=0.0001). Therefore, it can be postulated that $\%HR_{max}$ can be used to not only predict the rise in BLa concentration but also is a potential marker to determine physiological strain during continuous endurance performance.

5.3.2 Fatigue Manifestation on Kinematic Measures

Table 5-2 shows the data in the form of mean ± standard deviation. "One-way RM ANOVA" showed significant effect of fatigue on STR ($F(2,32) = 6.587$, $p<0.005$). Post-hoc analysis with Bonferroni adjustment reported that the 'STR' at 'End' was significantly different from 'AT' with 90% confidence level and from '4th min of run' with 95% confidence level.

Table 5-2: Descriptive statistics (mean±SD) for kinematic variables at the 4th minute of the run, anaerobic threshold (AT) and at termination stage (End) during continuous constant speed test to exhaustion.

	Kinematic Variables		
	4th min of run	**AT**	**End**
Hip Angle (°)	73.86±2.99	73.96±3.01	73.67±3.38
Knee Angle (°)	137.06±4.35	137.01±4.71	136.64±5.05
Ankle Angle (°)	95.79±2.97	96.21±2.90	96.89±3.74
Pronation Angle (°)	17.53±3.86	17.75±4.29	18.48±4.44
I_{DT} (g)	7.74±1.67	7.68±1.63	7.80±1.41
I_{NDT} (g)	7.36±1.96	7.61±1.50	7.62±1.37
ACC_H (g)	1.41±0.37	1.41±0.38	1.36±0.35
I_H (g)	2.28±0.92	2.43±1.08	2.49±1.15
STR (steps.min^{-1})	172.41±9.55	171.57±10.76	167.29±7.61 [b,c]

[a] significant difference ($p<0.05$) from the non-fatigue state (1st stage) to the onset of fatigue state (AT).
[b] significant difference ($p<0.10$) from the onset of fatigue state (AT) to fatigued state (End).
[c] significant difference ($p<0.05$) from the non-fatigue state (1st stage) to fatigued state (End).

5.3.3 Influence of Kinematic Variables on Oxygen Cost

A hierarchical multiple regression analysis was used to determine the influence of joint angles (hip, knee and ankle angles and pronation angle), inertial measures (I_{DT}, I_{NDT}, ACC_H, and I_H), and stride rate (STR) on oxygen cost of running, known as running economy. Prior to fitting the multilinear regression, multicollinearity was checked by inspecting the correlation coefficients and tolerance/VIF values. No independent variable was found to have a correlation greater than 0.7 and tolerance values were also greater than 0.1. Hence, no multicollinearity problem was identified. There was the independence of residuals, as assessed by a Durbin-Watson statistics 1.999.

A hierarchical multilinear regression model was analyzed first with joint angles (Model 1) followed by the addition of I_{DT} and I_{NDT} (Model 2), I_H and ACC_H (Model 3) and STR (Model 4). All these models were statistically significant and statistical significance of each variable is shown in Table 5-3. The findings of the study reported that hip angle, knee angle, foot pronation, $I_{DT,}$ and STR were the only statically significant variables that were related to the disruption in $\dot{V}O2$ during continuous constant speed test, shown in Table 5-3.

Table 5-3: Hierarchical multiple regression predicting running economy (V̇O2) from kinematic factors, one by one to determine significant predictors of oxygen cost of running (running economy).

$\dot{V}O_2$								
	Model 1		Model 2		Model 3		Model 4	
Variables	uSC	SC	uSC	SC	uSC	SC	uSC	SC
Constant	155.77*		125.95*		122.52*		91.31*	
Hip Angle (˚)	0.574*	0.330	0.650*	0.373	0.674*	0.387	0.692*	0.398
Knee Angle (˚)	-0.953*	-0.806	-0.918*	-0.777	-0.915*	-0.774	-0.852*	-0.721
Ankle Angle (˚)	-0.222*	-0.138	-0.101	-0.063	-0.09	-0.056	-0.094	-0.058
Pronation (˚)	0.097	0.074	0.115	0.088	0.116	0.089	0.205*	0.157
I_{DT} (g)			0.697*	0.198	0.704*	0.20	0.555*	0.158
I_{NDT} (g)			0.274	0.084	0.280	0.086	0.435	0.133
ACC_H (g)					0.206	0.013	0.149	0.010
I_H (g)					-0.118	-0.024	0.318	0.063
STR (Step.min^{-1})							0.112*	0.183
R^2	0.416		0.474		0.474		0.489	
F	27.57**		22.99**		17.02**		15.92**	
ΔR^2	0.416		0.058		0.000		0.014	
ΔF	27.57**		8.50**		0.013		4.212**	

Noted N=161, *p<0.05, uSC=unstandardized coefficients, SC= standardized coefficients

The observed trends in the data are shown in Figure 5-1, for all the observed kinematic variables against oxygen cost ($\dot{V}O_2$). The black line represents the linear trend of the kinematic variable against $\dot{V}O_2$ and the dotted blue line represents the 95% confidence interval. Increase in hip angle, foot pronation, I_{DT} and STR and decrease in knee angle were significantly linked with higher $\dot{V}O_2$, hence resulting in poor running economy. Whereas, ankle angle, I_{NDT}, I_H and ACC_H were not statistically affecting $\dot{V}O_2$, as observed in this study. The descriptive statistics for all the selected kinematic variables are shown in Figure 5-1.

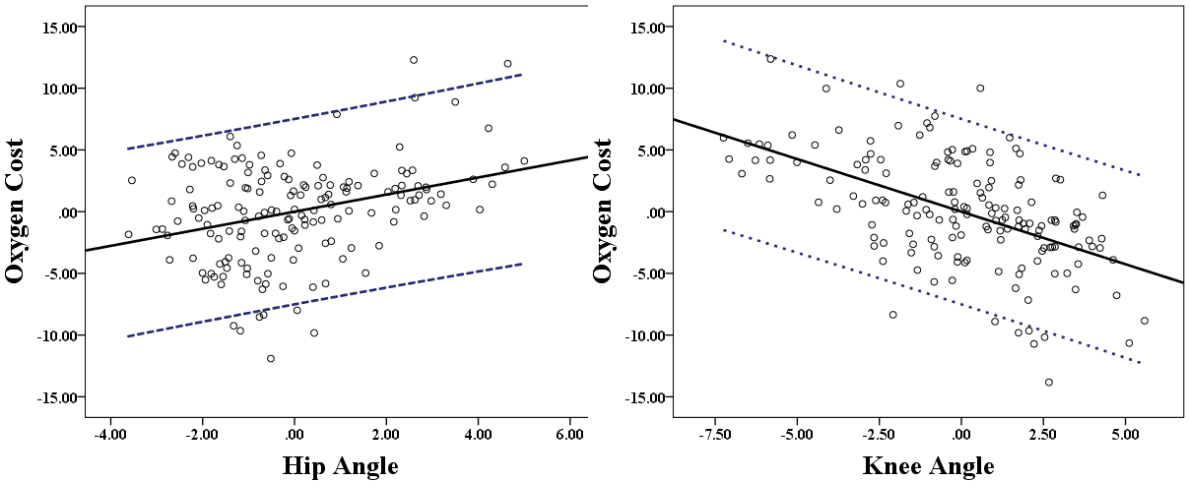

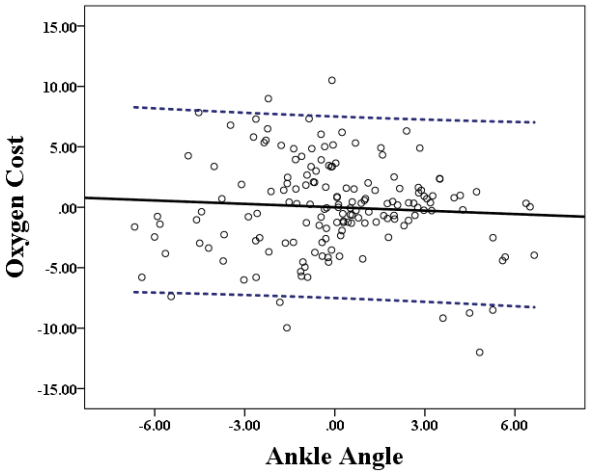
Oxygen Cost
15.00
10.00
5.00
.00
-5.00
-10.00
-15.00
-6.00
-3.00
.00
3.00
6.00
Ankle Angle

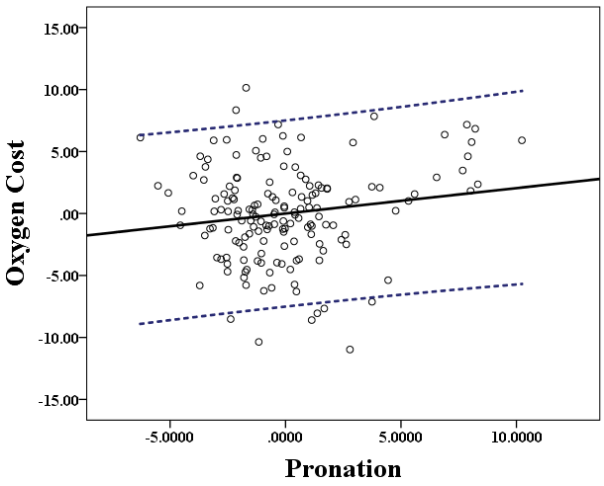
Oxygen Cost
15.00
10.00
5.00
.00
-5.00
-10.00
-15.00
-5.0000
.0000
5.0000
10.0000
Pronation

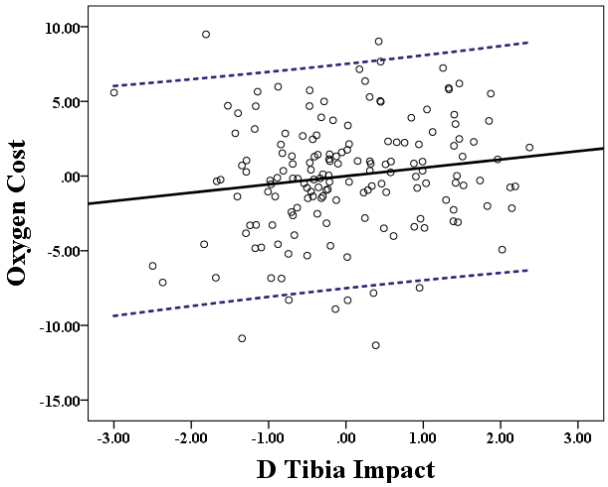
Oxygen Cost
10.00
5.00
.00
-5.00
-10.00
-15.00
-3.00
-2.00
-1.00
.00
1.00
2.00
3.00
D Tibia Impact

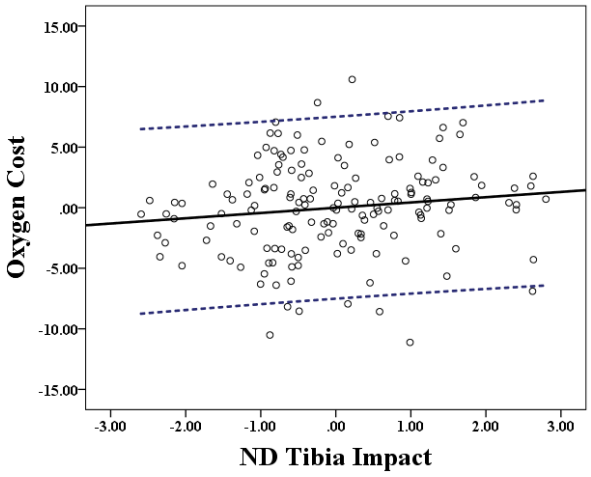
Oxygen Cost
15.00
10.00
5.00
.00
-5.00
-10.00
-15.00
-3.00
-2.00
-1.00
.00
1.00
2.00
3.00
ND Tibia Impact

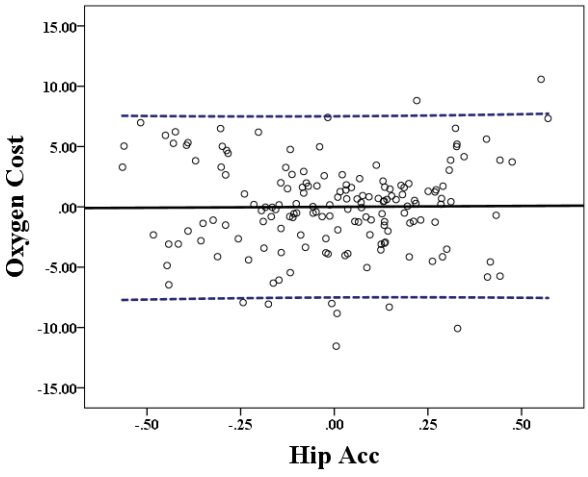
Oxygen Cost
15.00
10.00
5.00
.00
-5.00
-10.00
-15.00
-.50
-.25
.00
.25
.50
Hip Acc

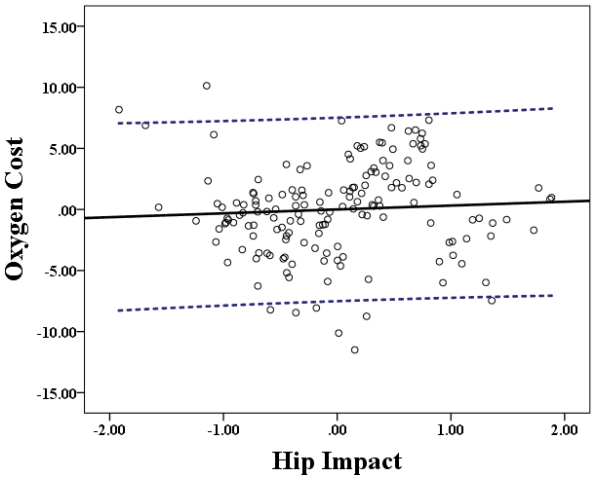
Oxygen Cost
15.00
10.00
5.00
.00
-5.00
-10.00
-15.00
-2.00
-1.00
.00
1.00
2.00
Hip Impact

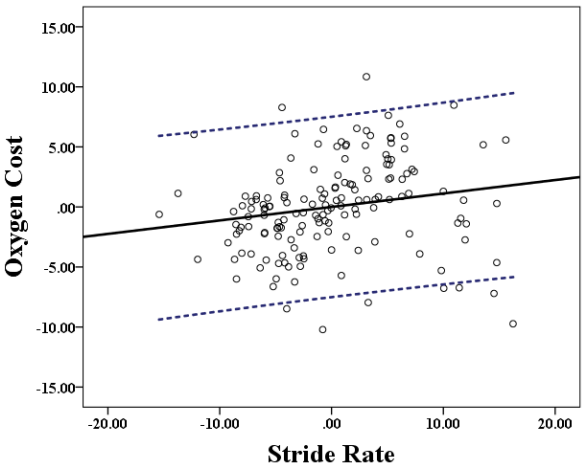

Descriptive Statistics		
	Mean	SD
Oxygen Cost (ml/kg/min)	47.73	5.22
Hip Angle (˚)	74.17	3.00
Knee Angle (˚)	137.29	4.42
Ankle Angle (˚)	96.90	3.25
Pronation Angle (˚)	17.96	4.01
I_{DT} (g)	7.64	1.48
I_{NDT} (g)	7.44	1.60
ACC_H (g)	1.38	0.34
I_H (g)	2.46	1.04
STR (Steps/min)	169.90	8.54

Figure 5-1: Partial Regression plot, representing the interaction between kinematic variables (hip, knee, ankle and pronation angle, D tibia impact, ND tibia impact, hip acceleration and hip impact and stride rate). The black line represents the linear trend line whereas dotted double blue line represents the 95% confidence interval range values. Descriptive statistics for each variable are shown in the table. The mean value represents the center line (zero) at the graph for all the dependent and independent variables.

5.3.4 Biomechanical and Physiological Predictors of Fatigue

A hierarchical multilinear regression was used to determine the influence of several physiological and kinematic variables on fatigue (RPE_C, RPE_M, and RPE_O one by one). Prior to using multiple regression, 'multicollinearity problem in the independent variables' and 'independence of residual' assumptions were tested by observing the correlation between independent variables and 'Durbin_Watson' statistics, respectively. No multicollinearity problem was identified for any independent variable. There was the independence of residuals for dependent variables (RPE_C, RPE_M and RPE_O, tested one by one), as Durbin-Watson statistics were 1.730, 1.637, and 1.587, respectively. Durbin-Watson statistics were observed to be greater than 1% significance points of tabulated lowed bound (dl = 1.463) and hence inconclusive autocorrelation.

Model 'M1' and 'M2', as shown in Table 5-4, represent the physiological model and combined physiological and kinematic model, respectively. The unstandardized coefficient of each predictor and its statistical significance is shown in Table 5-4. Statistical significance of the physiological model 'M1' for RPE_C was F (4, 155) = 96.12, $p < .0001$, $R^2 = 0.713$. When kinematic predictors were added into the model 'M2', the coefficient of determination improved by 7.2% ($R^2 = .765$). Statistical significance of the physiological model 'M1' for RPE_M was F (4, 155) = 135.703, $p < .0001$, $R^2 = .778$. When kinematic predictors were added into the model 'M2', the coefficient of determination improved by 5.4% ($R^2 = 0.820$).

Statistical significance of the physiological model 'M1' for RPE_O was F (4, 155) = 143.439, p < .0001, R^2 = 0.787. When kinematic predictors were added into the model 'M2', the coefficient of determination was improved by 6.1% (R^2 = 0.835).

Table 5-4: Hierarchical multiple regression predicting RPE_C, RPE_M and RPE_O from physiological and biomechanical factors along with the significance of each variable, tested in the continuous test. Model accuracy and significance is shown in term of R_2 and F change.

Hierarchical Multilinear Regression Analysis						
Variables	uSC: RPE_C		uSC: RPE_M		uSC: RPE_O	
	M 1	M 2	M 1	M 2	M 1	M 2
(Constant)	-25.788*	-6.598	-25.448*	-26.592*	-24.749*	-21.979*
$\dot{V}O2$ (ml/kg/min)	0.026	0.039	0.045	0.060	0.048*	0.053
RR (breath/min)	0.045*	0.035	0.056*	0.023	0.062*	0.035
RER	-17.75*	-14.319*	-19.566*	-14.817*	-21.787*	-17.243*
$\%HR_{max}$	0.513*	0.542*	0.512*	0.588*	0.524*	0.577*
Hip Angle (º)		-0.029		-0.009		0.05
Knee Angle (º)		-0.078		-0.063		-0.098*
Ankle Angle (º)		-0.008		0.023		0.017
Pronation Angle (º)		-0.147*		-0.121*		-0.127*
I_{DT} (g)		-0.044		-0.167		-0.078
I_{NDT} (g)		0.122		0.208*		0.171*
ACC_H (g)		-1.579*		-0.920*		-1.307*
I_H (g)		0.122		0.415*		0.321*
STR (Steps/min)		-0.046*		0.009		-0.002
R^2	0.713	0.765	0.778	0.820	0.787	0.835
F	96.12*	36.53*	135.703*	51.218*	143.44*	56.84*
ΔR^2	0.713	0.052	0.778	0.042	0.787	0.048
ΔF	96.12*	3.598*	135.703*	3.814*	143.44*	4.689*

Noted N=158, uSC = Un-Standardized Coefficients, *p<0.05

5.3.5 Bilateral Kinematic Asymmetry & Fatigue

Table 5-5 shows data in the form mean ± standard deviation for bilateral asymmetry, based on tibia impacts, hip impacts, and hip push-off acceleration. Contrary to the non-continuous test, in Chapter 4, participants, in the continuous study, experienced higher impact on the hip through the dominant leg. Bilateral asymmetry for the hip impact (KA_{Hi}) and hip push-off acceleration (KA_{Ha}) remained in favor of the dominant side, most likely due to better control on the dominant side under higher metabolic stress, as experienced in this study.

One-way RM ANOVA did not show any significant effect of fatigue on asymmetric behavior for selected recreational active runners against fatigue during the continuous run. The statistical significance and descriptive measures for all asymmetry analyzing variables and bilateral asymmetries are shown in Table 5-5.

Table 5-5: Descriptive statistics (mean±SD) of lower extremity impact and acceleration dynamics on hip and shank segment during push-off and MS phase of running gait cycle.

	Lower Extremity Asymmetry Analysis		
	4th Minute of Run	**AT**	**End**
ACC_{DH} **(g)**	1.435±0.385	1.426±0.408	1.388±0.371
ACC_{NDH} **(g)**	1.389±0.364	1.389±0.366	1.333±0.337
KA_{Ha} **(%)**	1.556±4.170	1.019±5.674	1.840±6.791
I_{DH} **(g)**	2.317±1.031	2.456±1.123	2.515±1.153
I_{NDH} **(g)**	2.229±0.849	2.405±1.095	2.457±1.197
KA_{Hi} **(%)**	0.485±10.163	0.174±10.101	1.281±9.038
I_{DT} **(g)**	7.741±1.673	7.675±1.625	7.796±1.415
I_{NDT} **(g)**	7.361±1.958	7.606±1.495	7.625±1.373
KA_{Ti}**(%)**	3.029±9.629	0.333±9.726 [a]	1.111±7.065

[a] significant difference ($p<0.05$) from the non-fatigue state (1st stage) to the onset of fatigue state (AT).
[b] significant difference ($p<0.05$) from the onset of fatigue state (AT) to fatigued state (End).
[c] significant difference ($p<0.05$) from the non-fatigue state (1st stage) to fatigued state (End).

5.3.6 Electromyographic Fatigue in Lower Extremity

For the sake of understanding the neuromuscular activity against the development of endurance fatigue, generalized iEMG data of the five consecutive running gait cycles has been shown in Figure 2(A&B). This data was collected from the RF, VL, BF, ST, BM, GL and TA muscles of the dominant leg from two participants (participant 'A' and participants 'B'). The black line represents the iEMG data during running gait cycle at the 4th minute of the run. The red line represents iEMG during running gait cycle at the anaerobic threshold 'AT', and the blue line represents the iEMG during running gait cycle at the 'End' stage. Differences in activation profile, in response to exposed endurance time, represent individual muscle work with fatigue development and coordinated activation control between agonist and antagonist muscles based on the individual muscle physiological status. The generalized trend of the neuromuscular activity (iEMG and TDMdPF) for total 17 participants in term of 'Pi' and 'Fi', is shown in Figure 5-3 and Figure 5-4, respectively, against percentage completion time (%TTE).

Participants were observed to have increased or decreased iEMG levels, during different phases of running gait cycle. The most likely reasons are the recruitment of fast twitch fibers, changes in the firing rate, the fatiguing status of muscle's fast twitch fibers or reduced central drive towards 'End' in comparison with '4th minute of run' and 'AT'. During the landing phase, the major contributing muscles were RF, VL, GM, and GL. All four groups of muscles were observed to have increased iEMG, reading based on their individual contribution toward knee and hip joint stability, during braking and weight acceptance phase of running gait cycle.

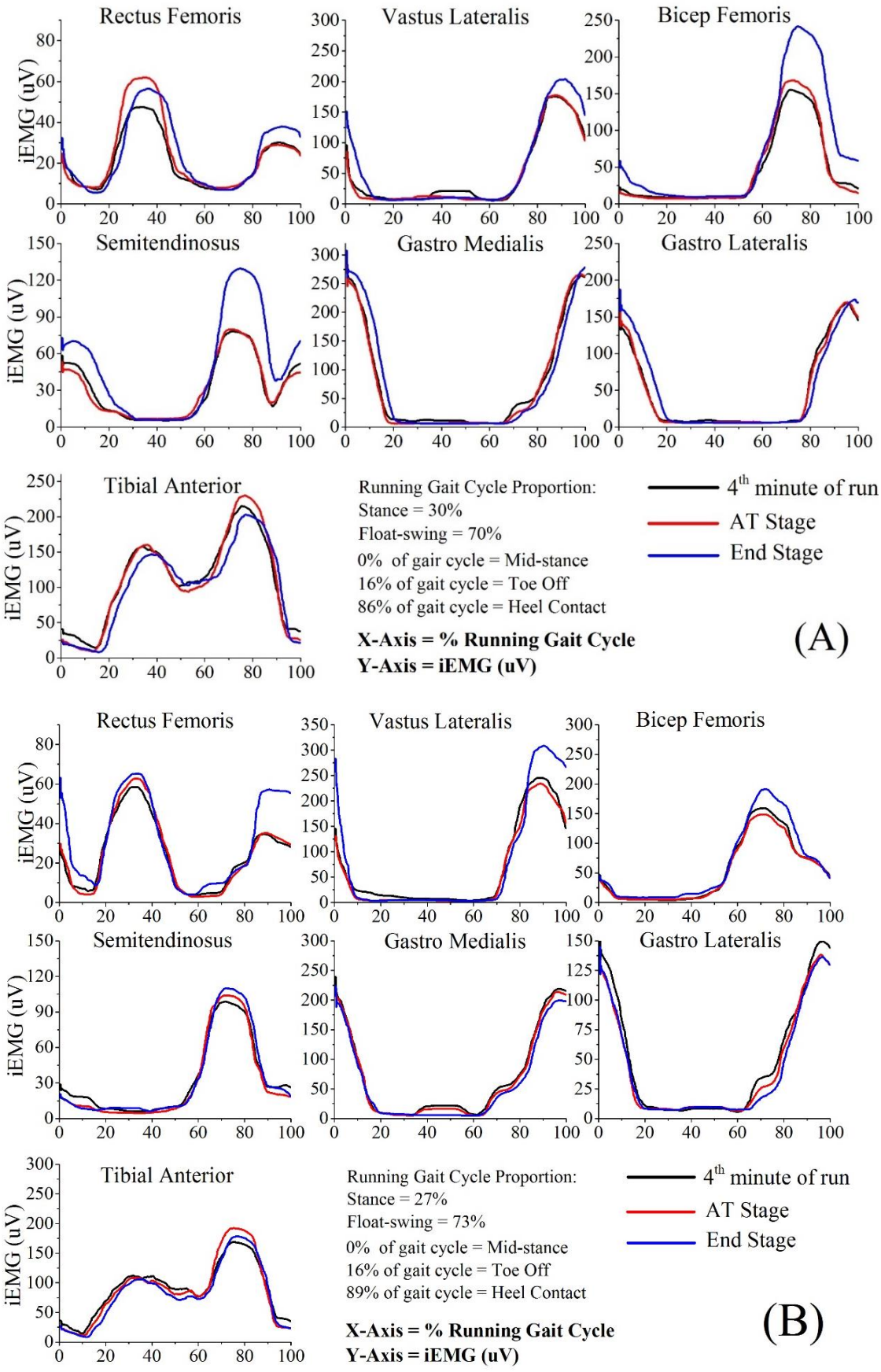

Figure 5-2: Comparison of muscle activation profile of the lower extremity muscles against fatigue (4th minute of run, AT, END) for participant 'A' (CS of 4.31 m/sec with toe-off of 16% the running gait cycle) and for

participant 'B' (CS of 4.5 m/sec with toe-off 16% of the running gait cycle). Black line represents the 1st stage (4th minute of the run), the red line represents the 'AT' and the blue line represents the 'End' stage of continuous constant speed run to exhaustion protocol.

In comparison with the non-continuous test, as discussed in Chapter 4, endurance fatiguing participants were observed to differ in their neuromuscular activation profile, most likely due to fatigue profile in each muscle, physiological status against endurance time, and motor response to fatigue. In participant (A & B), iEMG readings were high at the 'End' stage in comparison with 'AT' and '4th-minute' stage during hip flexion and knee extension phase (quadriceps muscles (RF, VL), as shown in Figure 5-2. Similarly, an increasing trend was observed in the hamstring muscles (BF, ST), as shown in Figure 5-2. At the shank segment, the difference in iEMG of GM and GL muscles and reduced TA activity were observed, with the progression of fatigue. The relative change in GM and GL neuromuscular activity can link with dynamic foot pronation, observed during the stance phase of running gait cycle. However, it requires more validation studies to reach this conclusion. The observed mean difference in foot pronation for all participants was 17.53±3.88 to 18.48±4.44 degree.

Results of the lower extremity neuromuscular fatigue, in this study, showed a significant "Kendal tau-b" correlation between pronation and fatigue status of GL (tb=-0.117, p=0.05). Ankle angle showed a positive correlation with TA (tb=0.237, p=0.0001) muscle. Hip and knee angle did not show a strong correlation with quadriceps and hamstring group of muscle during fatiguing contraction. When data were compared with the non-continuous test, neuromuscular activation levels showed a different fatigue response which gives a clear indication of customized fatigue development, based on protocol selection.

5.3.6.1 Lower Extremity Power Index Dynamics with Fatigue Progression

The generalized trend of the 'Pi' of all 17 participants (normalized against the iEMG at '4th minute of the run') for RF, VL, BF, ST, GM, GL and TA muscles are shown in Figure 5-3. To determine the relationship between 'Pi' of each muscle against muscular perceived exertion, "Kendall's tau_b" correlation has been determined. "Kendall tau_b" showed a significant correlation of GM (tb=-0.124, p=0.006), GL (tb=-0.206, p<0.0001), and TA (tb=-0.144, p=0.001), whereas non-significant correlation was observed by RF, VL, BF and ST. However, during the non-continuous test, 'Pi' for all studied muscles was significantly correlated with muscular fatigue.

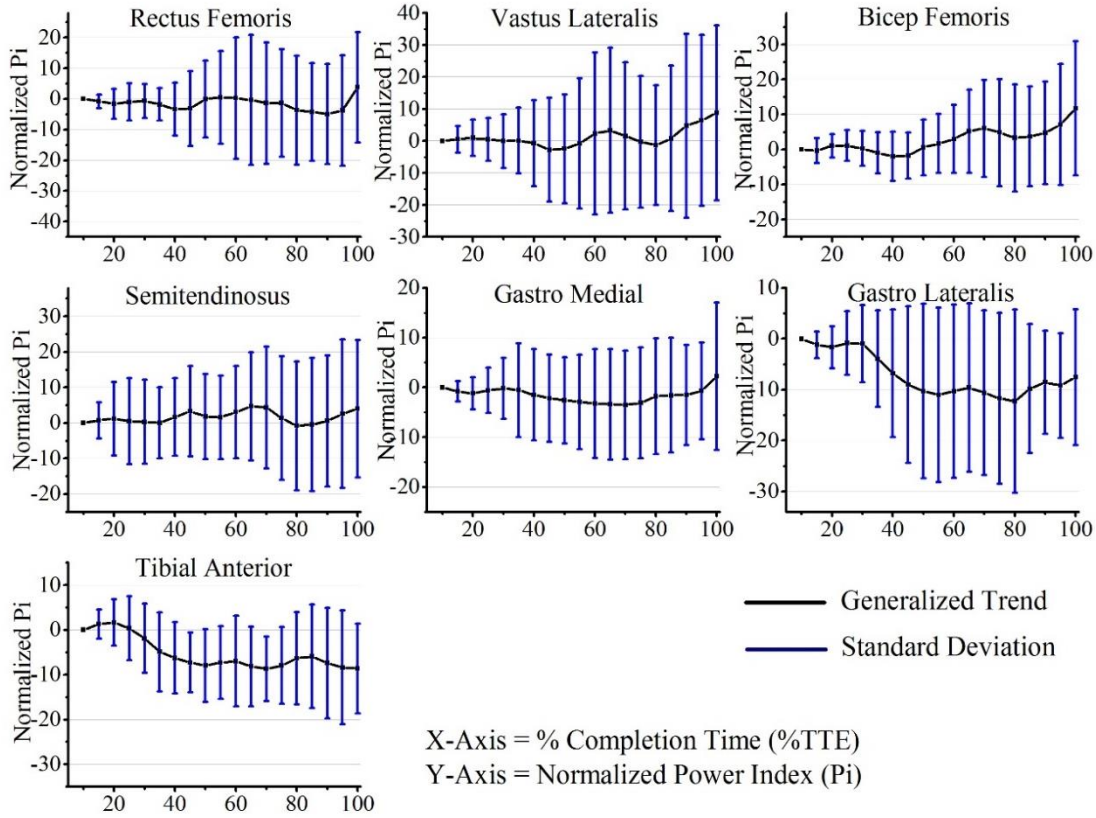

Figure 5-3: Normalized power index (Pi) data for the captured iEMG over the running gait cycle during consecutive stages in comparison with 1st stage '4th minute of run' to determine the degree of variability of EMG activation levels from non-fatigue state to fatigue state.

5.3.6.2 Lower Extremity Fatigue Index Dynamics with Fatigue Progression

The generalized response of the 'Fi" for all 17 participants (normalized against the TDMdPF at the '4th minute of run') for RF, VL, BF, ST, GM, GL and TA muscles are shown in Figure 5-4. To investigate the relationship between 'Fi' of each muscle against muscular perceived exertion, "Kendall's tau_b" correlation has been determined. "Kendall tau_b" showed a significant correlation of RF ($tb=-0.237$, $p<0.0001$), VL ($tb=0.160$, $p<0.0001$), BF ($tb=0.136$, $p=0.004$), GM ($tb=0.191$, $p<0.0001$), GL ($tb=0.096$, $p=0.028$) and TA ($tb=0.105$, $p=0.017$), whereas, non-significant correlation was only observed for ST. However, during the non-continuous test, 'Fi' of BF, ST, GM, GL, and TA were significantly correlated with muscular fatigue.

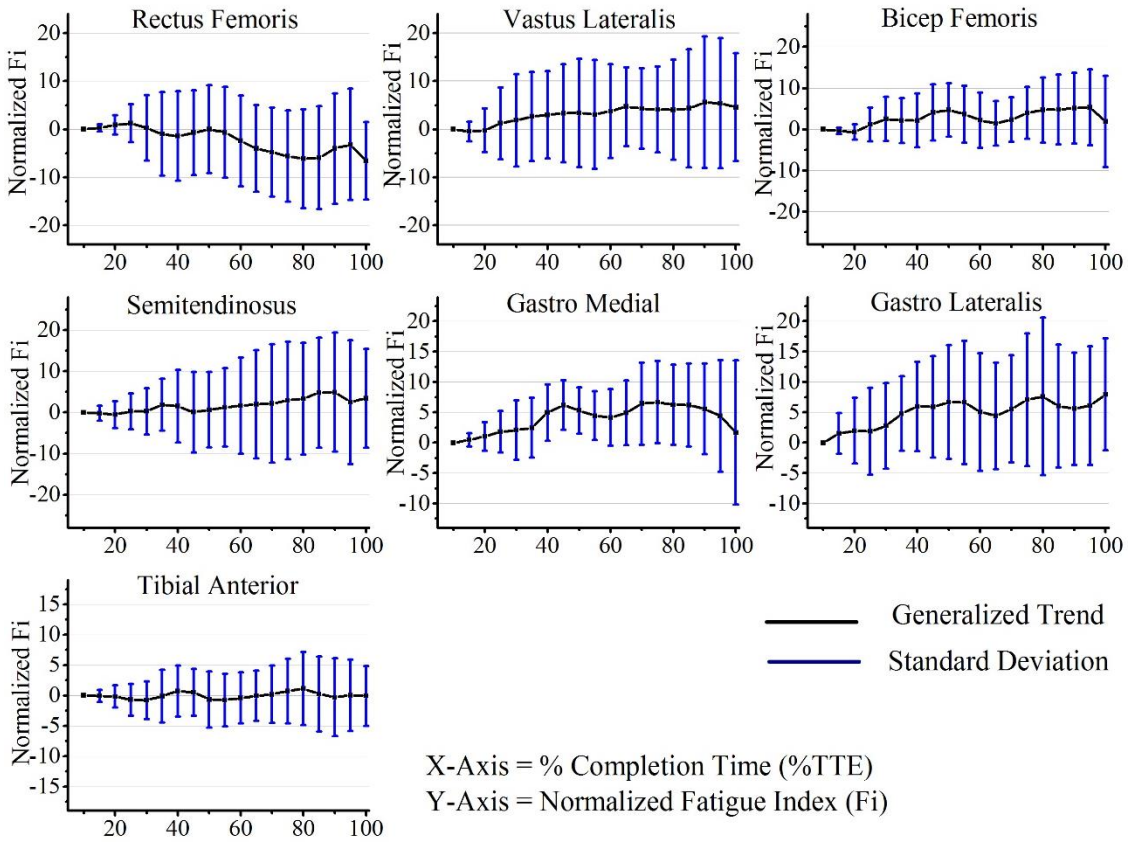

Figure 5-4: Normalized fatigue index (Fi) of the captured EMG data over the running gait cycle during consecutive stages in comparison with 1st stage '4th minute of run' to determine the degree of variability of time-dependent median power frequency (TDMdPF) from non-fatigue state to fatigue state.

5.4 Discussion

Due to existing hyperbolic relationship between work rate and time to exhaustion (TTE) [242], it was important to examine the metabolic relation with endurance performance at CS in this study. Along with that, the aim of this chapter was to study and evaluate the response of the physiological and biomechanical (neuromuscular and running mechanics) system in response to endurance fatigue. Details for each individual system are discussed below, in relation with perceived exertion, to determine physiological and biomechanical determinants of RPE_C, RPE_M and RPE_O. This chapter also discussed the differences in kinematic and neuromuscular response with progression in fatigue during continuous and non-continuous run. Whereas the difference in physiological responses between continuous and non-continuous tests are discussed in the next Chapter 6. The relationship between neuromuscular fatigue and running mechanics has also been studied in the following sections.

5.4.1 Physiological Understanding of Fatigue

Critical speed in this chapter was selected with an assumption to provide an indirect estimation of maximum lactate steady state [243]. However, several studies on continuous running have

shown systematic increase in BLa concentration at CS, due to imbalance in lactate production and removal rate [200], and TTE ranged between 20-40 mins [49, 237]. Critical speed, in this chapter, reported the maximum BLa of 6.77±1.48 mmol.l^{-1} at the termination of the test and TTE was 23.94±9.75 minutes. Only 4 participants among recreational active runners met the criterion of 1 mmol.l^{-1} [220] to determine MLSS. Whereas, 13 participants were found to have increased BLa concentration greater than 2 mmol.l^{-1} from the MLSS. Therefore, it is evident that the selected CS resulted in higher metabolic stress in recreational active runners as compared to endurance metabolic demand of endurance-trained runners [48, 57]. The observed difference in TTE ranged from 11 minutes to 50 minutes with an average TTE of 23.94±9.75 minutes. The most likely reasons for such difference in TTE among participants are customized CS, difference in aerobic capacity, anaerobic fitness level, sorts training history, metabolic tolerance, and participant's motivation [237, 244].

Millet et al. [226] proposed a novel model to explain exhaustion. In that model, RPE represents a buoy inside a water container. The buoy increases or decreases depending on the water fill and flush rate. The filling rate depends on the feedforward and feedback mechanisms together with environmental conditions that contribute to regulate this buoy [226]. In a present study, the environmental factors were maintained constant during the TTE trials, one could suppose that the filling rate was associated with inherent physiological, biochemical, metabolic and sensory feedback mechanisms [14, 122, 127, 223]. These inherent mechanisms, while running till exhaustion, leading the buoy to increase until maximal perceived exertion. Another study also suggested that exercise tolerance is highly limited by the perception of effort, as strong correlation was observed between perceived exertion and TTE at maximal aerobic power [245]. In the present study, perceived exertion (RPE_O) was also found to achieve its maximal limit while running at constant speed and showed a strong correlation with TTE (t_b=0.789, $p<0.0001$). From the observed perceptual response against chest (RPE_C), legs (RPE_M) and overall body (RPE_O), as shown in Figure 5-5, RPE_C was found to be slightly dominant than RPE_M and RPE_O. The most likely reason is the physiological stress, which goes underline while meeting the metabolic demand during continuous running.

The physiological cues ($\dot{V}O_2$, HR, RR, $\%HR_{max}$, $\%HR_{increase}$) of 'perception of effort' were found statistically significant at terminal stage 'End' in comparison with the '4th minute of run' and 'AT' stage. The statistical significance of the physiological and perceptual measures is shown in Table 5-1.

On average, participants reached 'AT' at 53.51±21.68% of TTE and $\%HR_{max}$ was 89.97±2.59%. Following fatigue progression from the non-fatigue state (4th minute of the run),

decrease in running economy (increase in $\dot{V}O_2$ and increase in RER) and increase in $\%HR_{max}$ were observed in present study, The most likely reasons for such observations are peripheral muscular strain, metabolic demand and changing pattern of muscle fiber recruitment [246, 247]. The increase in $\dot{V}O_2$ and HR against sustained time has also been observed while cycling at the critical power [237]. Slow component rise in $\dot{V}O_2$ has showed significant correlation to determine TTE whereas HR had a reservation due to HR-drift (because of the environmental factors and HR variability among participants). In this study, $\%HR_{max}$ was used to suppress error due to HR-drift, caused by inter-individual variability and environmental factors were controlled under the laboratory setup. TTE was found to be significantly correlated with $\dot{V}O_2$ (t_b=0.188, $p<0.001$), $\%HR_{max}$ (t_b=0.656, $p<0.0001$), RER (t_b=0.111, $p=0.039$), and RR (t_b=0.423, $p<0.0001$). The observed correlation of TTE with $\dot{V}O_2$, $\%HR_{max}$, RER, and RR also support the notion that CS did not result in steady state response in recreational active runners. When these physiological variables were tested to explain the variance in perceived exertion, RPE_O was significantly affected by $\dot{V}O_2$, RR, RER and $\%HR_{max}$. Whereas RPE_C and REP_M did not show any significant variance due to $\dot{V}O_2$. The trends (mean±SD(s)) for all these physiological and perceptual variables are shown in Figure 5-5.

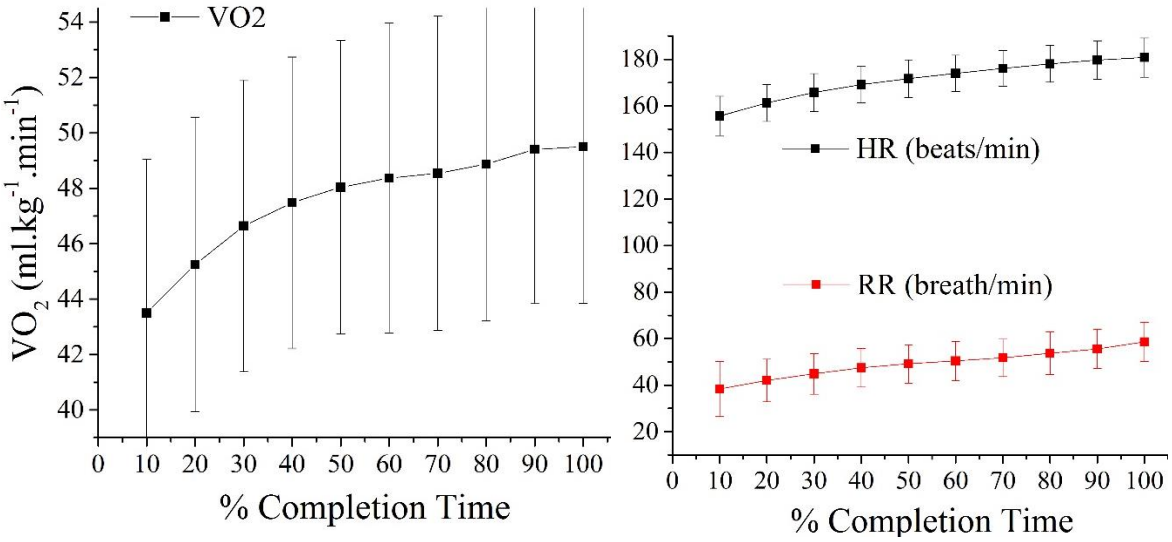

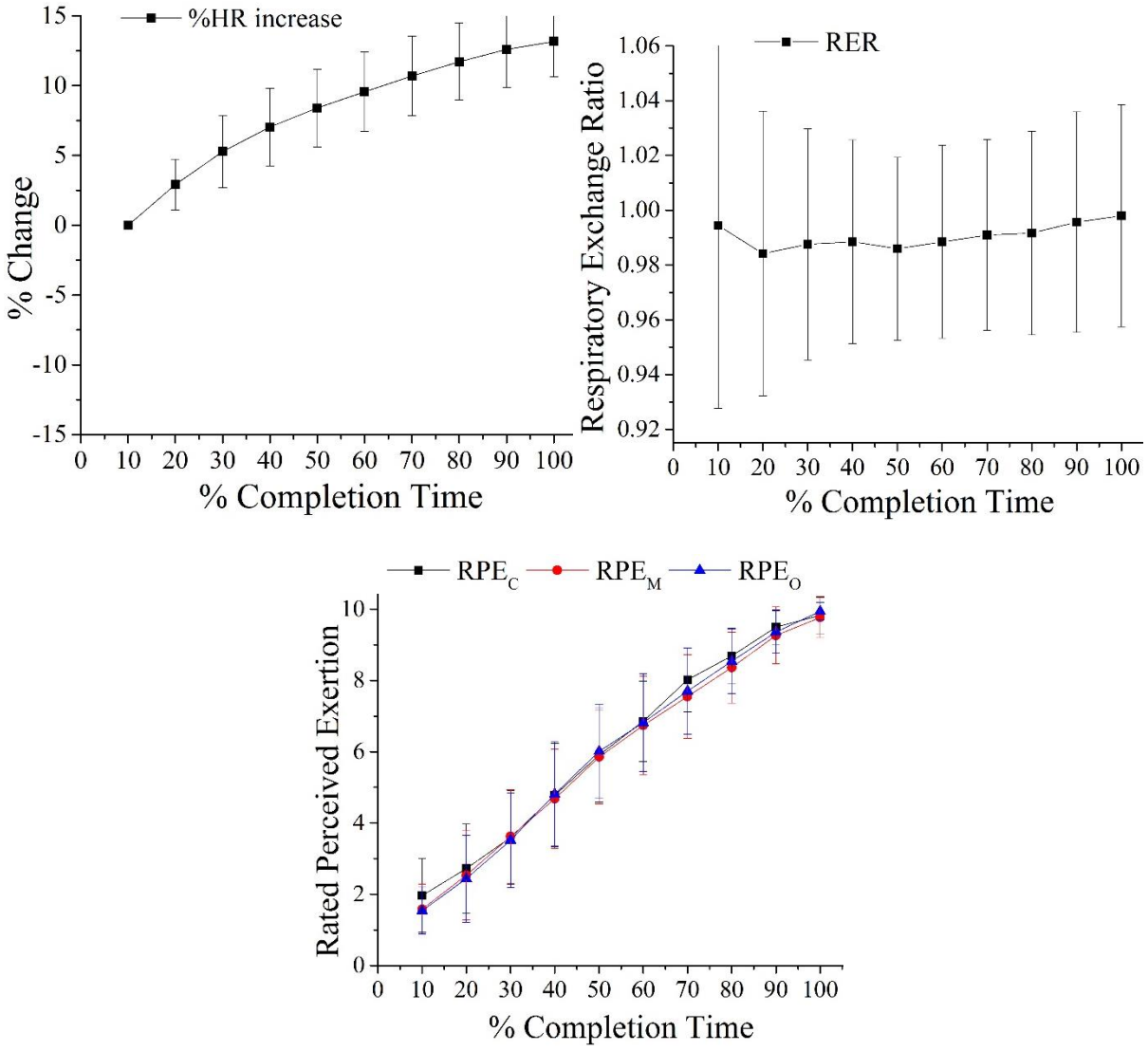

Figure 5-5: Physiological system responses (mean±SD) for $\dot{V}O_2$, HR, RR, $\%HR_{max}$, %HRincrease, RER and RPE_C, RPE_M, and RPE_O against % completion time from non-fatigue state to fatigued state during continuous speed fatigue protocol.

5.4.2 Biomechanical Understanding of Fatigue

Fatigue manifestations on the biomechanical system are important to be studied to examine its relationship with running injuries development. Several factors associated with running injuries and their relationship with the endurance fatigue is discussed in Chapter 4.

In this chapter, endurance fatigue resulted in significant decrease in STR at termination stage in comparison with the '4th minute of run' and "AT' stage, when evaluated through discrete measures. The remaining other variables were not statistically significant, as shown in Table 5-2. Whereas during the non-continuous run, ankle plantarflexion at the mid-stance was also found to be statistically significant in addition to STR. The most likely reason is the fatiguing status of the TA muscles, as increase in ankle angle was linked with decrease in TDMdPF of TA muscle. "Kendal tau_b" also reported a negative significant correlation with ankle angle

during the non-continuous test. The 'Pi' and 'Fi' of the TA muscle was also found to be negatively correlated with the muscular fatigue (RPE_M) during the non-continuous test. This shows that the most likely reason is the reduced firing rate, reduced MFCV, reduced action potential and/or fatiguing status of the fast twitch muscle fibers [232, 248].

The increase in perceived exertion (endurance fatigue) was significantly during continuous running was significantly explained by the variance in knee angle, pronation angle, I_{NDT}, ACC_H and I_H, as identified by the multilinear regression analysis. However, during the non-continuous running, the knee angle did not show any significance whereas the ankle plantarflexion was found significant predictor. The most likely reason is the difference in neuromuscular activity in the lower extremity muscle, recruitment of fast twitch fiber in the TA muscle and fatiguing status of the RF muscle in the lower extremity during continuous running. The average trend for all the studied kinematic variable during continuous run to exhaustion are shown in Figure 5-6.

Interesting, during both continuous and non-continuous running tests, the STR was found to be non-significant in relation with perceived exertion. However, different participants in the present study showed different pattern of STR variations. Twelve participants were found to have reduced STR by 2 - 9%, two participants reported an increase in STR by 2 - 6% and three runners did not shift from their optimal STR over the course of the fatigue run. A study on stride parameter has also shown different changes in stride characteristics among participants [148]. Participants with increasing STR were observed to have decreased tibia impact, most likely to have better control on landing during fatiguing contractions [144, 173]. The fatigue was a deteriorating factor in adjusting the control behavior of the runner, as tibia impact was found to be increasing with time to exhaustion [41]. Overall averaging revealed that selected participants were found to decrease STR and the overall tibia impact (I_T) was found to be higher on the dominant side than the non-dominant side. The non-significant effect of STR could be a result of the motorized treadmill running vs over-ground running [225]. The observed adjustments in kinematic factors (shown in Figure 5-6) over different segments of the lower extremity were an indication of the adoptive motorized control strategies or neuromuscular fatigue, as per runner's exertion status.

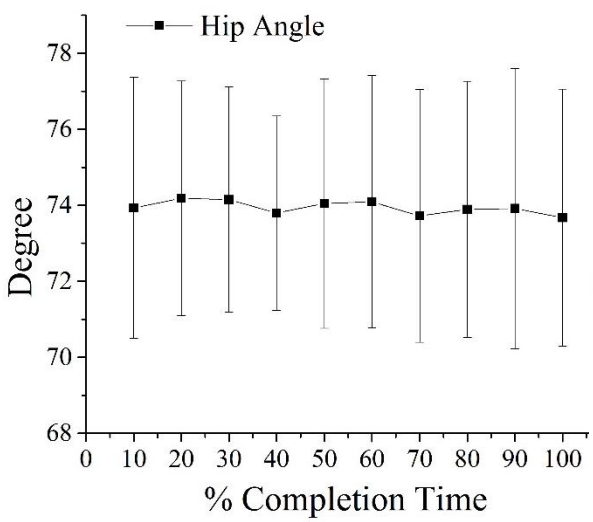
Hip Angle
Degree
% Completion Time

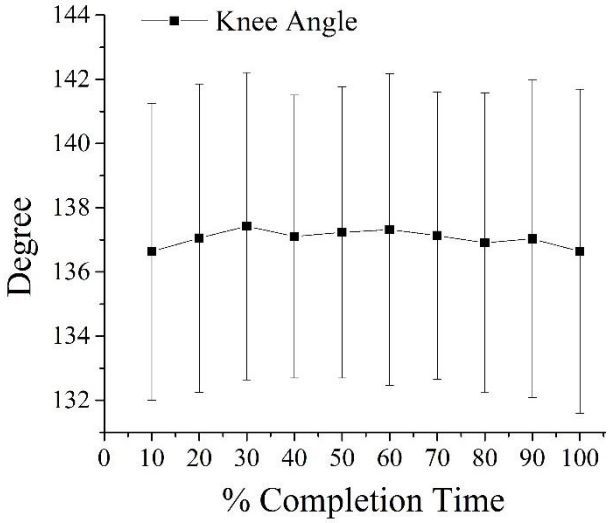
Knee Angle
Degree
% Completion Time

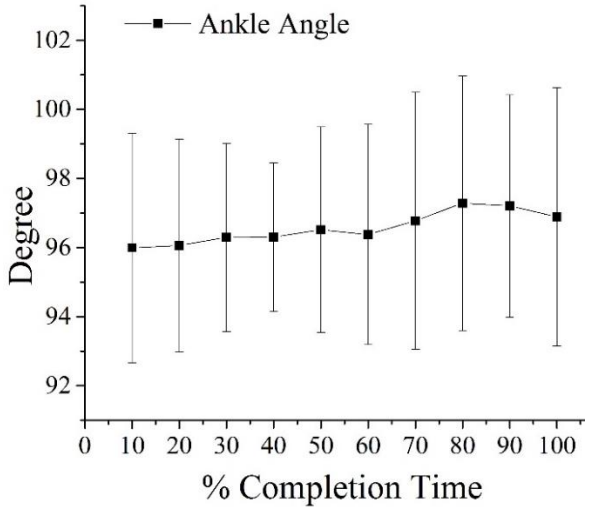
Ankle Angle
Degree
% Completion Time

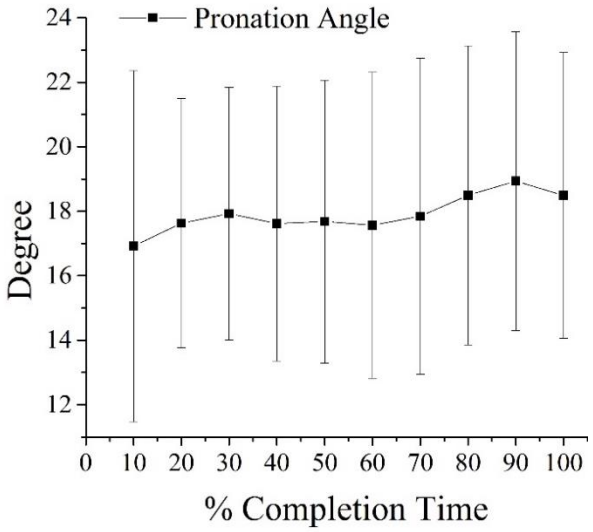
Pronation Angle
Degree
% Completion Time

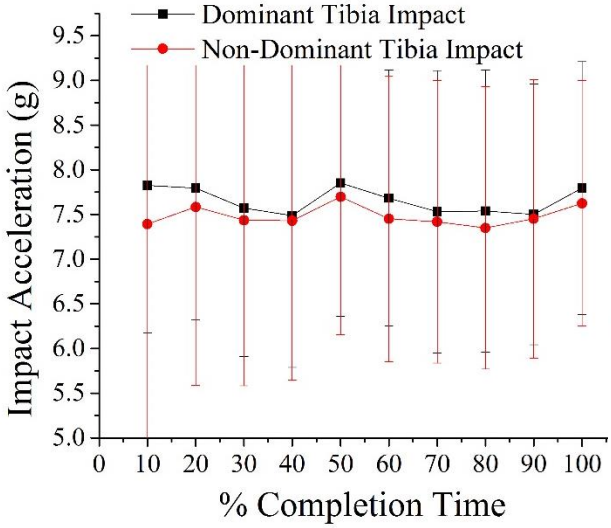
Dominant Tibia Impact
Non-Dominant Tibia Impact
Impact Acceleration (g)
% Completion Time

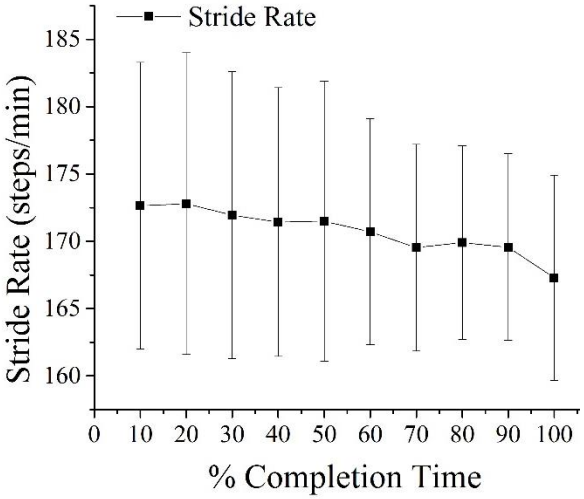
Stride Rate
Stride Rate (steps/min)
% Completion Time

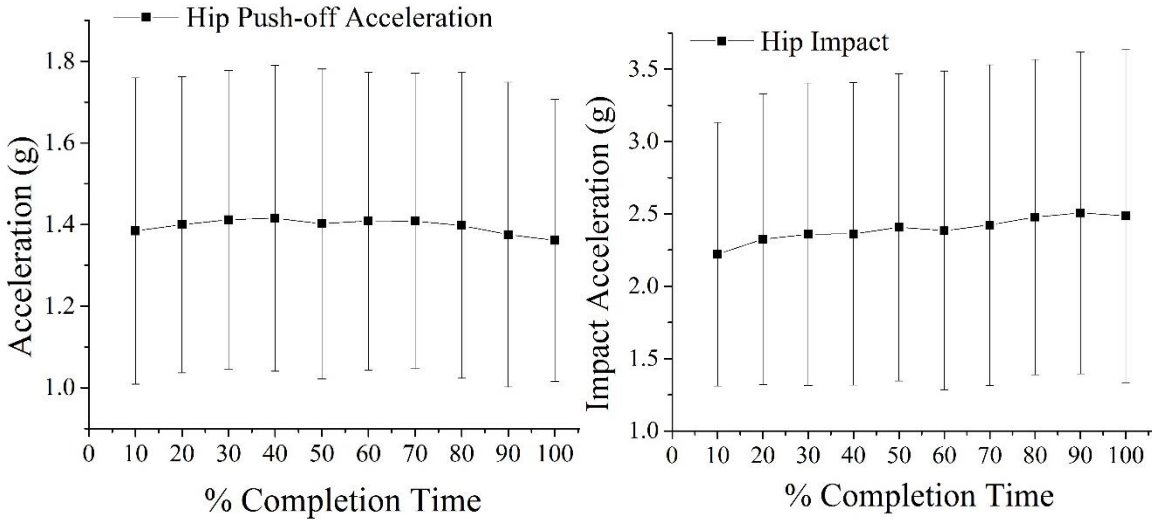

Figure 5-6: kinematic variable responses (mean±SD) for hip, knee, ankle, and pronation angle at MS phase of running gait cycle, dominant and non-dominant tibia impact on the lower extremity, stride rate, hip impact and hip push-off acceleration against % completion time from non-fatigue state to fatigue state.

Similarly, when I_H and ACC_H were analyzed for the selected group of participants, an increase in STR from the optimal response was linked to a decrease in ACC_H and a decrease in I_H, as observed by Schubert et. al. [224]. This observation replicated the control behavior of the lower extremity. Fatigue was observed to influence the strategy of adaptive changes and participants were found to experience higher I_T. Furthermore, on average, participants were observed to increase the hip impact and reduce the hip push-off acceleration, following the onset of fatigue (53.51±21.68 % of completion time) to fatigue state (100% of completion time), as shown in Figure 5-6. Similar findings on the knee flexion, tibia impact, hip impact and hip acceleration were also by other fatigue evaluation on running kinematic studies [37, 41, 202].

Limb laterality, is known to effect running gait symmetries in runner's biomechanics [157], was evaluated to examine fatigue in the lower extremity in this study. Kinematic asymmetry was determined as discussed in Chapter 4. The results showed that fatigue did not influence the kinematic behavior of the predominant limb. The non-dominant leg was identified to lack the capability of impact shock attenuation in comparison to the dominant leg, as higher impacts were experienced on the hip segment through the non-dominant side at the start of the test till 65% of the completion time. With the progression of fatigue, impact attenuation from the non-dominant side also got improved, likely because of the active neural control strategy to cater fatigue. However, this needs further study to prove this notion that impact attenuation in the non-dominant side got improved due to better neuromuscular control.

To get insight into the influence of running mechanics on running economy, several studies have been reported in the literature [34, 43, 45, 154, 249]. The most talked about parameter is

the stride length/ stride frequency and its influence on RE [34, 230]. In the present study, STR was significantly linked with increase in oxygen cost of running and hence, decreased running economy, as shown in Figure 5-1. However, during non-continuous test, STR was not found to significantly affect the oxygen cost of running. The most likely reason is the recovery of fast twitch muscle fibers during 1-min resting intervals as recruitment of fast twitch muscle fibers was linked with increase in slow component rise in oxygen cost [35]. The other factors which influence the oxygen cost during continuous running in present study were hip angle, knee angle, pronation angle, I_{DT} and STR. However, the non-continues running only reported significant effect of knee angle, I_{DT}, and I_H.

5.4.2.1 Neuromuscular Fatigue & Running Mechanics

Neuromuscular activity is at the heart of changing running mechanics [40, 156, 172]. A study, by Murdock et. al. [156], has reported changes in quadriceps muscle activation patterns, following fatigue protocol, which resulted in reduced external knee flexion and torque generation. Another study, by Roger et. al. [172], has reported that reduced neuromuscular activity in gastrocnemius medial, gastrocnemius lateralis, and soleus muscle was linked with the risk of stress fractures of the metatarsals under fatiguing conditions. A study on the elite runners has shown the earliest sign of fatigue in bi-articular hip-mobilizing muscles (RF and BF) when studied neuromuscular fatigue in all major lower extremity muscles during progressive treadmill speed test [33]. Similarly, changes in running economy have also been evident by the increase in electromyographic activity in the rectus femoris and semitendinosus muscle in endurance runners [34].

Neuromuscular activation generalized data for ‘Pi’, in this chapter, showed that GL and TA muscle’s iEMG values were observed to decrease, RF, ST, and GM muscles almost remained stable, VL and BF were observed to increase (as shown in Figure 5-3). The decrease in neuromuscular activity is likely because of the fatiguing status of muscle’s fast twitch fibers or physiological status of the working muscles or reduced firing rate or activation potential towards termination stage [101, 232]. Considering the TDMdPF dynamics in the quadriceps and hamstring group of muscles, hip angle and knee angle did not show any strong correlation in these group of muscles. However, during the weight acceptance phase of running gait cycle (as shown in Figure 5-2), participant A & B experienced a relative increase in iEMG for quadriceps group of muscles (RF, VL), whereas, hamstring muscle (BF, ST) was observed to compensate and stabilize the knee and hip joint. For the calf and shank, the neuromuscular activity changed with fatigue progression and might link with foot position during gait cycle. A study by Riemann et al. [234] has showed the relative differences in GM and GL during heel

off at externally rotated and internally rotated feet position. Hence, it is can be said that varying difference in neuromuscular activation may change the associated joint mechanics. Results of the present study showed significant correlation between pronation and fatigue status of GL muscle (tb=-0.117, p=0.05) and non-significant correlation with GM muscle during the continuous running. The ankle angle was linked with TA (tb=0.237, p=0.0001) whereas knee and hip angle did not show any significant correlation with the fatiguing status of the lower extremity muscles.

For examining the lower extremity relative power 'Pi', the present study identified significant correlation of muscular fatigue with 'Pi' of GM (tb=-0.124, p=0.006), GL (tb=-0.206, p<0.0001), and TA (tb=-0.144, p=0.001) muscles. Whereas, this study showed significant correlation of muscular fatigue with 'Fi' of RF (tb=-0.237, p<0.0001), VL (tb=0.160, p<0.0001), BF (tb=0.136, p=0.004), GM (tb=0.191, p<0.0001), GL (tb=0.096, p=0.028) and TA (tb=0.105, p=0.017). Whereas, during the non-continuous test, most of the lower extremity muscles were significantly correlated with muscular fatigue, shown in Chapter 4.

5.5 Conclusion

The results in this chapter establish that the CS resulted in higher BLa concentration than the required metabolic relation (MLSS) during endurance running. The selected CS significantly stressed the physiological and biomechanical system and adjustments in the physiological and biomechanical system were observed. Interestingly, increasing trend in RER at the CS was observed and $\dot{V}O_2$ was found to increase with fatigue progression, which explains the deterioration in running economy. The decrease in running economy was found to be linked with increase in hip angle, pronation angle, I_{DT}, and STR and a decrease in knee angle. Neuromuscular analysis of the lower extremity muscles revealed that 'Pi' of the GM, GL and TA muscles and 'Fi' of RF, VL, BF, GM, GL, and GL muscles were significantly linked with muscular fatigue (RPE_M). Furthermore, significant kinematic predictors of overall body fatigue included knee angle, pronation angle, I_{NDT}, I_H and ACC_H, whereas physiological predictors of fatigue included RER, and $\%HR_{max}$. No significant effects of fatigue were observed on bilateral KA. This KA was not recommended to be used as a significant factor towards prediction of fatigue. $\%HR_{max}$, a non-invasive surrogate of metabolic stress, identified in Chapter 4, was also found to be strongly linked with RPE_C, RPE_M and RPE_O during the continuous test. It is recommended that $\%HR_{max}$ has the potential to be used to monitor endurance intensity and BLa non-invasively as a replacement of RPE.

CHAPTER 6. PHYSIOLOGICAL DIFFERENCES BETWEEN A NON-CONTINUOUS & A CONTINUOUS ENDURANCE TRAINING PROTOCOL

The purpose of this chapter is to investigate the physiological difference between the non-continuous and continuous endurance training protocols. To examine protocol (continuous Vs. non-continuous) dependent changes, this study analyzed that how 1-min rest led a difference in time to exhaustion (TTE), metabolic stress (BLa) at termination, cardiorespiratory stress at termination and perceptual fatigue at termination over different body segments. This chapter also discussed a viewpoint that whether running at 'AT' (known as CS) reflects more towards physiological fatigue or muscular fatigue , as contradiction between lactate (La) and muscle fatigue [250] and 'BLa' kinetics with O_2 transport system [20]. The relationship between anaerobic fitness ($\%\dot{V}O_{2max}$), $\dot{V}O_{2max}$, systematic oxygen reserve ($\Delta\dot{V}O_2 = \dot{V}O_{2max} - \dot{V}O_{2CS}$), individual's CS, TTE and maximum BLa concentration are also studied in this Chapter. To study relative change between BLa and RPE, this chapter shows how accurately the RPE can be used to predict the 'AT' in recreational active runners. Furthermore, this Chapter also discusses the use of RPE and $\%HR_{max}$ in predicting BLa in recreational male runners.

6.1 Study Background and Hypotheses

The tested non-continuous and continuous endurance training protocols have been discussed in Chapter 3 and their corresponding physiological measures were discussed in Chapter 4 and 5. This study analyzed the physiological difference between both protocols in comparative fashion against fatigue. To the best of our knowledge, no study has investigated physiological response and metabolic stress in comparative fashion for recreational active runners at selected endurance speed (CS). Considering the reported findings of one similar study on trained runners and triathletes [49], this study hypothesis that 1-min rest during a non-continuous test might result in a difference in fatigue manifestations on the physiological system, as compared to the continuous test. The second hypothesis is that running at critical speed will stress more on the physiological system or muscular system. The third hypothesis is that the differences in TTE may be linked with physiological difference among both protocols.

In literature, CS and $\dot{V}O_{2max}$ are believed to be endurance performance predictors in endurance runners [56, 57]. To understand endurance performance in recreational active runners, it is important to study how TTE is related to CS, $\Delta\dot{V}O_2$, $\%\dot{V}O_{2max}$ and how, running at CS influences the perceptual fatigue at different body segments (RPE_C, RPE_M and RPE_O). The effects (if any) of RPE_C and/or RPE_M, while running at constant CS during continuous and non-continuous protocols, on the rise of BLa are not evident from the current literature. Recent

studies have shown contradicting evidence over the lactate production and muscle fatigue [250, 251]. It has also been reported that lactate production in response to endurance exercise and fatigue are more strongly linked with the body's energy supply systems [217] and convective oxygen transport system [20]. Considering such complexity, this study categorized RPE_C, RPE_M and RPE_O during both protocols and tested the hypothesis that rise in lactate will be strongly linked with RPE_O, rather than individual's exertion feeling about chest (RPE_C) or legs (RPE_M). Furthermore, this study discusses the validation of RPE as a non-invasive predictor of AT in recreational active runners. It proposes an alternative non-invasive parameter to determine AT in the recreational male of runners, studied in this research.

6.2 Methods

6.2.1 Variables of Interests

From endurance performance analysis (discussed in Chapter 4 and 5), participant's CS, $\dot{V}O_2$, $\Delta\dot{V}O_2$, HR, $\%HR_{max}$, RR, RER, BLa, TTE and RPE_O were collected for 'AT' and 'End' stages of the same participants in both the studies. To study the effect of RPE_C, RPE_M and RPE_O on physiological and endurance measures, three classes have been defined using the criteria of high reported value among RPE_C, RPE_M and RPE_O at 'End' stage. Physiological and endurance data has been grouped and averaged to determine the mean and standard deviation.

6.2.2 Data Processing and Statistical Analysis

Collected physiological ($\dot{V}O_2$, HR, RR, RER and $\%HR_{max}$) and perceptual (RPE_O) data for all participants were plotted against percentage completion time (% TTE) to represent the variable adjustment with fatigue progression till termination of the test. To summarize the "Kendal tau_b" correlation results in physiological system (discussed in Chapters 4 & 5), this chapter examined the relationship between BLa, $\%HR_{max}$, RPE_O and physiological variables for both the protocols. Paired sample t-test with a significance level of 95% was used to determine the significant change in physiological, perceptual and endurance variables between the non-continuous and continuous test. To determine the effect of each prevalent perceptual factor among RPE_C, RPE_M and RPE_O on physiological and endurance measures, three classes were defined among runners. One factor RM ANOVA with significance level of 95% was used to determine the effect of the perceptual fatigue (RPE_C, RPE_M and RPE_O) on physiological and endurance measures within both protocols. Regression analysis has been performed to determine BLa using RPE_O and $\%HR_{max}$. All statistical analyses were carried out using "IBM SPSS Statistics for Windows, Version 20.0. Armonk, NY: IBM Corp" and "Origin (OriginLab, Northampton, MA)".

6.3 Results

Average TTE for the non-continues test is 37.88±9.81 minutes and for the continuous test is 23.94±9.75 minutes (discussed in Chapter 4 and 5 respectively). Participants experienced relatively higher metabolic stress (6.77±1.48 mmol.l^{-1}) in the continuous test than in non-continuous test (5.48±0.95 mmol.l^{-1}). Statistics (mean ± SD) for the physiological variables (HR, RR, $\dot{V}O_2$, etc…), RPE, blood lactate at 'AT' and 'End', for the non-continuous & continuous tests are summarized in Table 6-1 & 6-2.

Table 6-1: Individual and mean ± SD values for time to exhaustion (TTE), heart rate (HR), respiratory rate (RR), respiratory exchange ratio (RER) and overall perceived exertion (RPE_O) during a non-continuous critical speed run to exhaustion.

Participants	Non-Continuous (4:1) Protocol													
	TTE	$\dot{V}O_2$		HR		$\%HR_{max}$		RR		RER		RPE_O		BLa
		AT	End	AT	End	AT	End	AT	End	AT	End	AT	End	End
1	36	45.07	46.38	174	182	87.97	91.95	55	73	0.95	0.93	6	9	4.55
2	24	56.07	57.51	177	183	91.74	94.60	58	59	0.99	0.97	8	10	5.25
3	44	51.53	53.06	179	181	88.86	90.14	45	52	0.96	0.96	7	8	4.36
4	36	46.73	46.73	167	167	92.45	92.45	57	57	0.97	0.97	8	8	3.9
5	44	39.86	40.63	178	193	88.59	95.95	39	43	0.99	0.95	4	10	5.77
6	52	46.19	45.29	171	175	93.60	95.86	49	57	0.97	0.94	4	10	5.11
7	24	54.51	56.31	163	176	88.29	95.00	57	56	1.05	1.02	6	9	6.24
8	28	54.72	54.67	179	186	92.72	96.13	58	74	1.01	0.99	7	10	6.47
9	36	45.12	46.27	173	188	86.18	93.76	39	56	0.93	0.89	3	10	6.09
10	52	45.27	47.47	175	179	93.50	95.68	45	55	0.95	1.00	8	10	6.3
11	36	50.92	52.50	166	173	90.34	93.82	43	53	0.91	0.93	7	10	6.13
12	48	45.55	46.65	180	184	91.28	93.23	43	47	0.93	0.91	5	9	4.51
13	20	49.00	50.13	164	168	90.85	92.78	55	62	1.02	1.00	8	10	5.08
14	36	40.40	42.84	171	180	87.68	92.45	57	65	1.01	1.02	4	10	6.77
15	48	45.23	46.84	176	189	89.69	96.60	34	57	1.00	0.99	2	10	7.08
16	36	42.69	42.77	166	172	91.35	94.38	51	66	0.97	0.96	3	8	4.49
17	44	40.79	43.14	152	168	84.41	93.28	39	56	1.01	0.99	1	10	5.1
mean	37.88	47.04	48.19	171.31	179.04	89.97	94.00	48.49	58.05	0.98	0.97	5.39	9.47	5.48
SD	9.81	5.04	5.02	7.33	7.82	2.59	1.76	7.91	8.13	0.04	0.04	2.25	0.80	0.95
Paired t-test	*		*								*		*	*

TTE: time to exhaustion (min), $\dot{V}O_2$: oxygen cost of running (ml.kg^{-1}.min^{-1}), HR: Heart Rate (min^{-1}), $\%HR_{max}$: heart rate working intensity, AT: at anaerobic threshold, End: at termination, RR: respiratory rate (min^{-1}), RER: respiratory exchange ratio, RPE_O: overall rated perceived exertion, BLa: blood lactate concentration (mmol.l^{-1}).
* Significant at the 0.05 level (2-tailed). * Significant at the 0.05 level (2-tailed).

Table 6-2: Individual and mean ± SD values for time to exhaustion (TTE), heart rate (HR), respiratory rate (RR), respiratory exchange ratio (RER) and overall perceived exertion (RPE_O) and blood lactate (BLa) during a continuous critical speed run to exhaustion.

Participants	Continuous Protocol													
	TTE	$\dot{V}O_2$		HR		$\%HR_{max}$		RR		RER		RPE_O		BLa
		AT	End	AT	End	AT	End	AT	End	AT	End	AT	End	End
1	33	48.32	48.40	174	184	88.02	92.89	56	74	1.00	0.97	6	10	5.78
2	15	57.82	58.87	177	185	91.75	95.81	50	58	0.99	1.00	6	10	7.66
3	50	52.25	53.52	179	187	88.87	93.16	49	61	0.97	0.97	8	10	5.79
4	25	46.95	46.73	167	168	92.38	92.65	45	50	0.99	0.99	7	9	5.13
5	20	38.86	41.93	178	192	88.59	95.30	31	43	0.99	0.97	6	10	7.43
6	26	43.30	45.14	171	180	93.59	98.36	48	55	0.97	0.99	7	10	9.05
7	12	55.79	59.66	163	176	88.29	95.30	56	58	1.03	1.07	5	10	9.07
8	11	56.70	57.78	179	186	92.70	96.37	65	71	0.99	1.00	9	10	7.57
9	19	46.17	48.13	173	191	86.19	94.84	41	56	1.02	1.02	2	10	7.31
10	31	45.05	47.66	175	181	93.48	96.60	48	56	0.99	1.02	8	10	6.6
11	27	51.64	51.84	166	167	90.30	90.81	45	57	0.91	0.92	10	10	3.87
12	30	45.35	44.70	180	183	91.29	92.78	46	49	0.93	0.94	9	10	5.05
13	14	50.84	55.16	164	178	90.86	98.18	51	64	1.01	1.05	7	10	6.85
14	27	41.37	46.58	171	189	87.66	97.16	60	69	1.00	1.02	3	10	7.4
15	31	45.20	48.08	176	189	89.69	96.53	35	51	0.95	0.98	3	10	8.59
16	18	45.38	45.63	166	167	91.35	91.59	54	67	0.99	0.99	7	10	5.19
17	18	39.70	41.73	152	171	84.40	95.20	42	57	1.04	1.06	2	10	6.71
mean	23.94	47.69	49.50	171.30	180.78	89.97	94.91	48.31	58.61	0.99	1.00	6.14	9.94	6.77
SD	9.75	5.72	5.66	7.35	8.42	2.58	2.25	8.46	8.39	0.03	0.04	2.53	0.24	1.48
Paired t-test	*		*								*		*	*

TTE: time to exhaustion (min), $\dot{V}O_2$: oxygen cost of running ($ml.kg^{-1}.min^{-1}$), HR: Heart Rate (min^{-1}), $\%HR_{max}$: heart rate working intensity, AT: at anaerobic threshold, End: at termination, RR: respiratory rate (min^{-1}), RER: respiratory exchange ratio, RPE_O: overall rated perceived exertion, BLa: Blood lactate concentration ($mmol.l^{-1}$).
* Significant at the 0.05 level (2-tailed). * Significant at the 0.05 level (2-tailed).

Paired sample t-test between 'End' stage of the continuous test and 'End' stage of the non-continuous elicited a statistically significant effect of fatigue, through mean increase in $\dot{V}O_2$ of 1.131 (95% CI, 0.335 to 2.294), RER of 0.0315 (95% CI, 0.0139 to 0.0492), BLa of 1.285 (95% CI, 0.627 to 1.943) and mean decrease in TTE of 13.94 (95% CI, -18.33 to -9.54). No significant variation was found between 'AT' of the continuous test and 'AT' of the non-continuous test.

Table 6-3: Correlation of physiological variables with RPE and heart rate working intensity (%HR_{max}) using Kendall's tau_b correlation with 95% significance level.

Kendall's tau_b Correlation			$\dot{V}O_2$	HR	RR	RER	RPE_O	BLa
Non-continuous Protocol	RPE_O	Correlation Coefficient	.236**	.434**	.358**	-.053	1.000	.583**
		Sig. (2-tailed)	.000	.000	.000	.347		.000
	$\%HR_{max}$	Correlation Coefficient	.094	0.478**	.229**	-.028	.591**	.581**
		Sig. (2-tailed)	.078	0.000	.000	.607	.000	.000
Continuous Protocol	RPE_O	Correlation Coefficient	.266**	.488**	.401**	.029	1.000	--
		Sig. (2-tailed)	.000	.000	.000	.605		--
	$\%HR_{max}$	Correlation Coefficient	.148**	0.530**	.353**	.220**	.654**	--
		Sig. (2-tailed)	.006	0.000	.000	.000	.000	--

** Correlation is significant at the 0.01 level (2-tailed). * Correlation is significant at the 0.05 level (2-tailed).

A Kendal tau-b correlation showed a significant correlation of RPE_O and $\%HR_{max}$ with $\dot{V}O_2$, HR, RR and BLa. $\%HR_{max}$ has been found to have a stronger correlation with BLa during the non-continuous test and has been found to have a stronger correlation with RPE_O in both the tests, as shown in Table 6-3. Model fitting (linear for RPE_O and exponential for $\%HR_{max}$) analysis of variance (ANOVA) reveals that during non-continuous test, BLa concentrations were found to be more responsive to the change in $\%HR_{max}$ (R value = 0.764) than RPE_O (R value = 0.742) and residual root mean square error for predicting BLa was also smaller (0.685, 0.71 respectively).

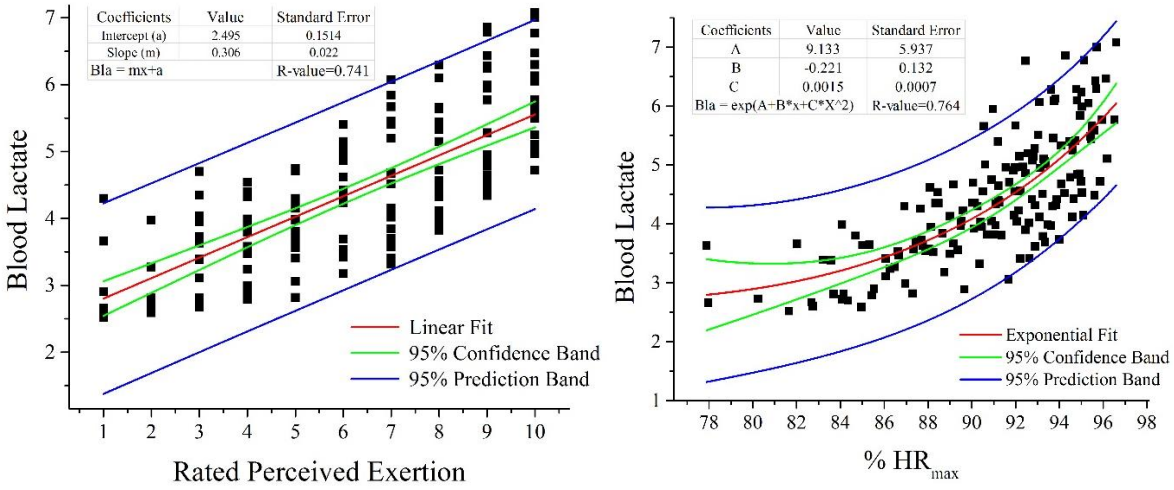

Figure 6-1: Linear (on left) and exponential (on right) model fit curve for predicting blood lactate concentration based on RPE and $\%HR_{max}$. The red line represents the fitted curve whereas two green lines show 95% confidence band and blues lines represent 95% prediction band.

Considering prediction variables from session 2, mean±SD at termination stage during session 3 was found to be higher for RPE (1.23±1.46) than $\%HR_{max}$ (1.36±1.00), due to a reduction in standard deviation range. The best fit underlying function for the lactate prediction using RPE_O and $\%HR_{max}$ with 95% confidence band and prediction band are shown in Figure 6-1.

Prediction range for the $\%HR_{max}$ using stated exponential function shown in Figure 6-1 (right side) is applicable and limited to 73-100% HR_{max}.

Considering the perceptual responses (RPE_C, RPE_M, and RPE_O) to categorize chest, muscular and overall stress during the non-continuous and continuous test, we have performed the following analysis. During the non-continuous test, the stopping factor was RPE_C for 6 participants, RPE_O for 6 participants and RPE_M for 5 participants. RPE_C stopping factor experienced relatively higher metabolic stress (5.48±1.20 $mmol.l^{-1}$) and less endurance time (33.33±10.01 mins) than RPE_M (less metabolic stress (4.73±0.35 $mmol.l^{-1}$) and higher endurance time (44.80±5.93 mins)). For the continuous test, the stopping factor was RPE_C for 4 participants, RPE_O for 12 participants and RPE_M for 1 participant. Statistics for the relatively higher stress levels causing termination of the test are summarized in Table 6-4. The data are presented as a mean ± standard deviation, while N represents the number of participants, classified based on stopping factors against RPE_C, RPE_M, and RPE_O.

Table 6-4: Mean±SD statistics for termination stage blood lactate (BLa), $\dot{V}O_{2max}$, oxygen reserve ($\Delta\dot{V}O_2$), time to exhaustion (TTE), critical speed and individual's anaerobic fitness against RPE_C, RPE_O and RPE_M.

Stopping Factor	Variable	Summary for Session 2		Summary for Session 3	
RPE_C (Chest)	BLa ($mmol.l^{-1}$)	5.48±1.20	6	6.17±1.64	4
	$\dot{V}O_{2max}$ (ml/kg/min)	56.76±3.78		55.19±2.26	
	$\Delta\dot{V}O_2$ (ml/kg/min)	10.81±2.05		11.87±2.16	
	TTE (minute)	33.33±10.01		26.75±6.75	
	Critical Speed (m/s)	3.67±0.42		3.57±0.16	
	An. Fitness ($\%\dot{V}O_{2max}$)	80.86±3.94		78.57±3.31	
RPE_O (Overall)	BLa ($mmol.l^{-1}$)	6.12±0.54	6	6.90±1.46	12
	$\dot{V}O_{2max}$ (ml/kg/min)	59.23±6.65		57.69±5.80	
	$\Delta\dot{V}O_2$ (ml/kg/min)	12.44±1.94		12.61±2.61	
	TTE (minute)	36.67±10.25		24.08±10.24	
	Critical Speed (m/s)	3.76±0.54		3.60±0.44	
	An. Fitness ($\%\dot{V}O_{2max}$)	78.64±4.82		77.98±4.74	
RPE_M (Muscular)	BLa ($mmol.l^{-1}$)	4.73±0.35	5	7.57±0.00	1
	$\dot{V}O_{2max}$ (ml/kg/min)	56.40±6.62		64.95±0.00	
	$\Delta\dot{V}O_2$ (ml/kg/min)	13.92±2.97		10.29±0.00	
	TTE (minute)	44.80±5.93		11.00±0.00	
	Critical Speed (m/s)	3.45±0.21		4.28±0.00	
	An. Fitness ($\%\dot{V}O_{2max}$)	75.46±3.22		84.16±0.00	

For session 2, one-factor ANOVA between these stopping factors revealed a significant change for BLa ($p=0.041$), $\Delta\dot{V}O_2$ ($p=0.045$), $\%\dot{V}O_{2max}$ ($p=0.047$) and TTE ($p=0.05$). For session 3, no statistically significant variation has been found between these groups. One-factor ANOVA reported that one-minute resting interval, during session 2, resulted in different metabolic stress

levels for physiological and muscular fatigue and BLa was strongly linked with chest fatigue than muscular fatigue. No significant change was reported in session 3. To measure the association between $\%\dot{V}O_{2max}$, $\Delta\dot{V}O_2$ and TTE in sessions 2 & 3, "Kendall's Tau_b" reported a statistically significant negative correlation (τb=-0.806, p=0.0001) between $\Delta\dot{V}O_2$ and $\%\dot{V}O_{2max}$, positive correlation (τb=0.408, p=0.030) between $\Delta\dot{V}O_2$ and non-continuous TTE, positive correlation (τb=0.558, p=0.002) between $\Delta\dot{V}O_2$ and continuous TTE, negative correlation (τb=-0.503, p=0.008) between $\%\dot{V}O_{2max}$ and non-continuous TTE, negative correlation (τb=-0.528, p=0.004) between $\%\dot{V}O_{2max}$ and continuous TTE, positive correlation (τb=0.35, p=0.05) between $\%\dot{V}O_{2max}$ and CS.

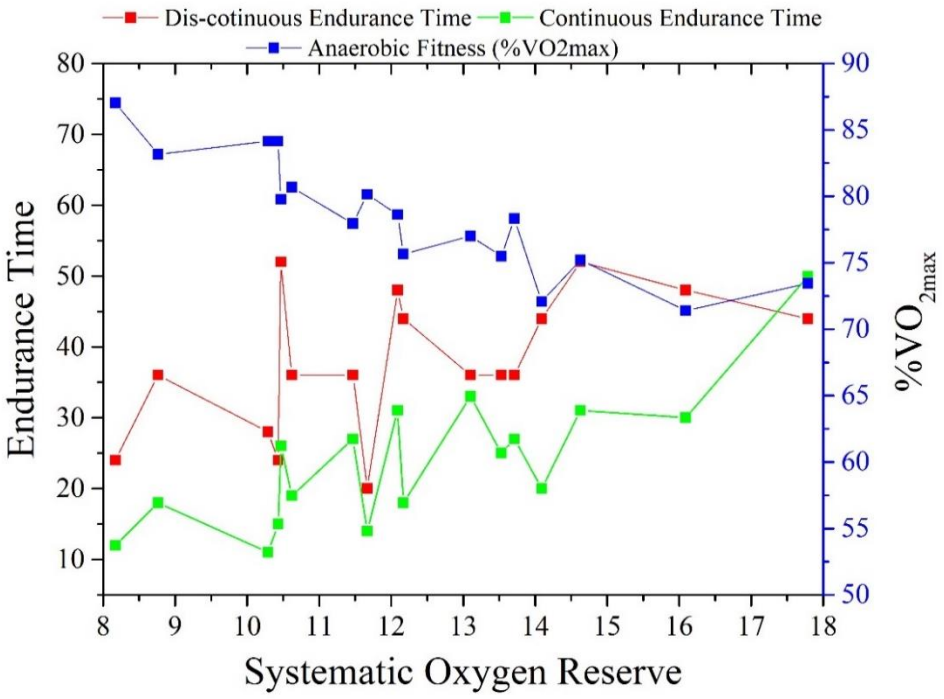

Figure 6-2: Systematic oxygen reserve ($\Delta\dot{V}O2$) relationship with endurance time and anaerobic fitness ($\%\dot{V}O2$ max) at critical speed run to exhaustion

The personalized CS, $\%\dot{V}O_{2max}$, $\dot{V}O_{2max}$ and $\Delta\dot{V}O_2$ of each participant resulted in different TTE for both non-continuous and continuous training protocols, as shown in Figure 6-2. However, increase in $\Delta\dot{V}O_2$ at the individual's CS and lower $\%\dot{V}O_{2max}$ has been found to be linked with higher TTE, which suggests that, $\Delta\dot{V}O_2$ along with $\dot{V}O_{2max}$ can be used to predict endurance performance rather than just using $\dot{V}O_{2max}$ [252].

6.4 Discussion

The main purpose of this chapter is to examine the protocol (continuous Vs. non-continuous) dependent fatigue manifestations on recreational runner's physiological response. The 1-min rest during the non-continuous test was introduced to partially restore the balance between

intracellular restitution and maintenance of O_2 kinetics and to simulate lactate steady state conditions [49, 204]. Both protocols showed sufficient cardiorespiratory stress on the physiological system such that significant effect was found on $\dot{V}O_2$, HR, $\%HR_{max}$, RR and RPE between onset of fatigue 'AT' and fatigued 'End' stage, as shown in Chapter 4 & 5.

Comparison of the non-continuous and continuous protocol showed a significant effect of fatigue on $\dot{V}O_2$, RER, BLa, TTE and RPE_O, as shown in Table 6-1 and 6-2. The overall trends of these variables are shown in Figure 6-3 for both tests. The participants were more physiologically stressed, running economy was poor, BLa was higher and RPE_O was also higher during the continuous test, in comparison to the non-continuous test. Reduced TTE was observed during continuous running. Participants were also observed to significantly stress themselves above MLSS condition [49, 212, 240], which might have exacerbated the fatigue manifestations.

The observed increase in TTE during non-continuous running (~1.6 times as compared to continuous TTE) suggests that CS intermittent running protocol is better suited to match the metabolic demand of endurance performance. It also exposes working muscles at same metabolic demand, as of endurance stress [48], for a long duration during endurance training. The observed changes in TTE in recreational active runners were also found to be in close concordance with the distance runners and triathlete (~2 times of continuous TTE), studied by Pendeato et. al. [49]. The physiological reasons for observed changes in TTE are most likely due to decreasing RER and better lactate clearance due to 1-min rest. Resting intervals might have also increased lipid metabolism (fatty acid mobilization and oxidation), recover the muscle glycogen through the altered pattern of muscle fiber recruitment and hence better TTE [219]. The observed TTE differences in studied recreational active runners and trained endurance runners by Pendeato et. al. [49] are most likely due to the aerobic fitness, the metabolic relationship with CS, muscle fiber composition in the lower extremity, and training history [216, 218]. However, future study is needed to find the valid reason for such probable change in TTE by studying the inherent physiological systems.

The trend (mean±SD(s)) for the physiological and perceptual variables ($\dot{V}O_2$, HR, RR, RER, $\%HR_{max}$ and RPE_O) during the non-continuous and the continuous running protocols are shown in Figure 6-3.

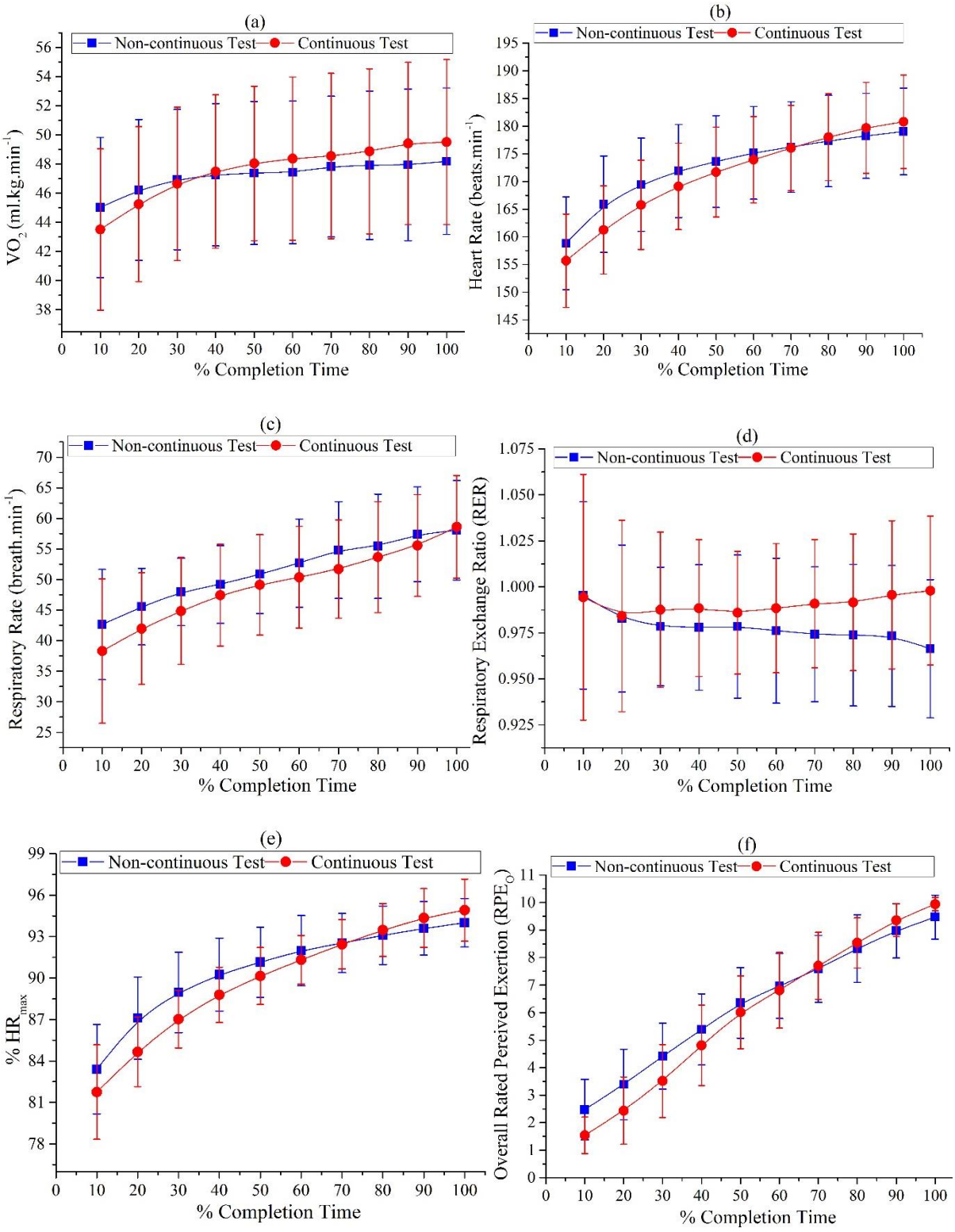

Figure 6-3: Difference in physiological response (mean±SD) of V̇O2 (a), HR (b), RR (c), RER (d), %HR_{max} (e) and overall perceived exertion (f) against % completion time during non-continuous and continuous test. All values are represented as mean±SD (s) at every 10% of completion time.

Overall perceived exertion (RPE_O) (a measure of running intensity relative to sustained time) shows that the individuals reached at the 'AT' at 5±2.2 (40±23.8 % of completion time) during the non-continuous test and at 6±2.5 (52.7±21.35 % of completion time) during the continuous test. The differences in reported RPE_O among individuals was due to BLa response. Individuals, whose BLa rose faster towards AT in response to sustained time at CS, reported their RPE_O to be less than 5 during the non-continuous test and less than 6 during the continuous test. Similarly, for those individuals whose BLa response delayed towards AT against sustained time, the RPE_O was higher than the mean value for both tests. It gives rise to the tendency of under or over-estimating the associated metabolic stress with RPE 5 during the non-continuous test and RPE 6 during the continuous test. The variation in reported RPE_O at 'AT' for both tests are shown in Figure 6-4. A plethora of evidence exists regarding the relationship between RPE_O and BLa (summarized in [122]. The validity of using RPE_O as a remote parameter to determine AT is somewhat controversial. However, the reported RPE_O relationship with BLa rise confirms the findings reported in the existing body of literature [253].

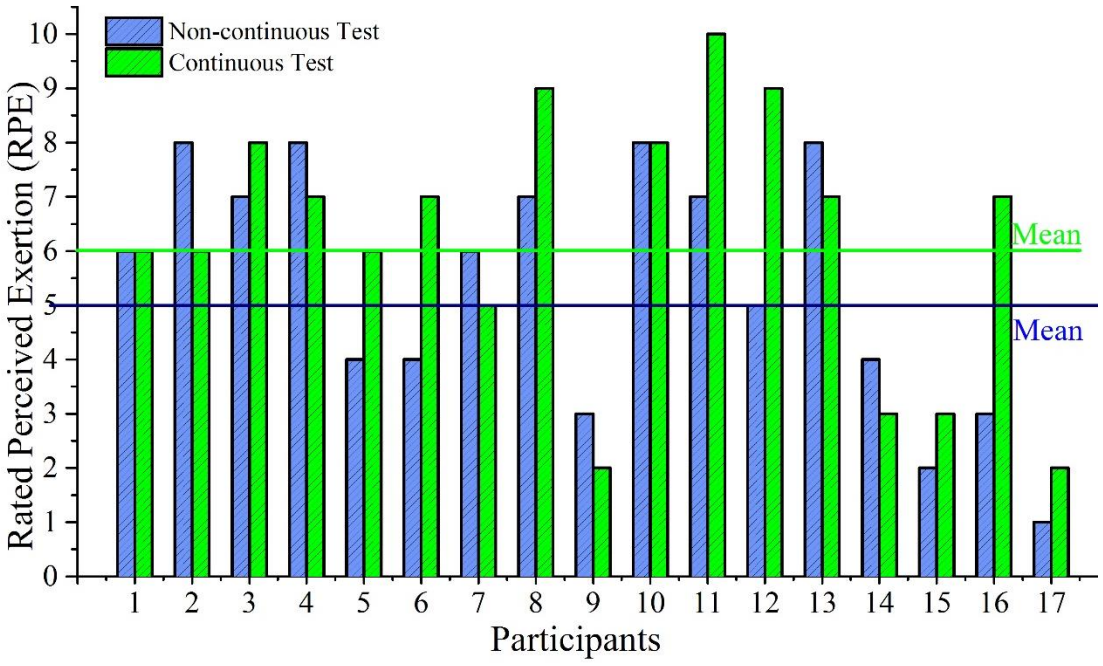

Figure 6-4: Overall rated perceived exertion at anaerobic threshold (AT) during non-continuous and continuous constant speed test.

Regarding the perceptual fatigue of the body segments (chest, legs or overall) and the rise in BLa, there is a need to evaluate whether BLa rise is more strongly linked with RPE_C, RPE_M or RPE_O. New studies are showing a contradicting viewpoint over the lactate production and muscle fatigue [250, 251]. It has also been reported that lactate production in response to

endurance exercise and fatigue has strong linkage with the body's energy supply systems [217] and convective oxygen transport system [20]. Considering the controversy and analyzing the perceptual fatigue on different body segments, findings in this study showed that the BLa is significantly linked with RPE_C as compared to RPE_M. RPE_O showed the most significant relationship with BLa as opposed to PRE_M and PRE_C. It means that the BLa production depends on both the physiological state of the muscle and supporting physiological system.

As per our knowledge, only one study [49] has partially addressed similar questions but their selected sample was limited to trained runners & triathletes and the study was conducted outside laboratory without physiological data evidence. However, this research study is focused on recreational active male runners and seeks to explain the research questions posed with physiological data evidence. This research study is prone to some limitation as will be discussed in Chapter 8.

6.5 Conclusion

The results in this chapter establish that increase in $\Delta\dot{V}O_2$ along with $\dot{V}O_{2max}$ are linked with better TTE. CS was found to be associated with MLSS during non-continuous running (due to 1-min rest). However, continuous running showed a significant increase in BLa above MLSS. TTE during the non-continuous test was almost 1.6 times higher than the continuous test, believed to be due to better running economy (decreasing RER), lower metabolic stress and RPE_O. BLa rise at CS during the non-continuous run was strongly linked with overall perceived exertion (RPE_O) in comparison with RPE_C or RPE_M. Continuous fatiguing protocol significantly increased the $\dot{V}O_2$, RER, BLa and RPE_O and decreased the RER in comparison with the non-continuous test. RPE_O was found to be changing linearly with the rise in BLa and could be used to determine BLa concentration during continuous endurance running. $\%HR_{max}$ was shown to have almost similar correlation strength but less prediction error than RPE_O. Therefore, $\%HR_{max}$ may be considered as a proxy to RPE_O to estimate metabolic stress in recreational active runners.

CHAPTER 7. REAL-TIME FATIGUE PREDICTION MODEL

This chapter presents a regression model approach to model fatigue in runners using significant physiological and biomechanical predictors that were determined in Chapter 5. The data used for developing regression model was the same which was used for studying fatigue manifestation on the physiological and biomechanical system. The predictors, used in this regression model were extracted from the continuous study, presented in Chapter 5, with a condition of practical measurability (practically measurable and robust) in the existing state of the art wearable technology. Furthermore, a normalized optimized model has also been proposed, with fewer predictors and good accuracy in this chapter, to suit the practical running scenario for runners with different gait variations due to different body sizes. Lastly, a wearable system approach, attached in appendix section, has also been presented to practically incorporate prediction model in the real world.

7.1 An Interconnected Approach to Model Fatigue

Fatigue, during endurance exercise, is the combination of the sensation of tiredness and associated decrement in muscle performance to produce force/power [14]. Research into fatigue-induced decrement in performance is explained by different theories (physiological, cognitive, biomechanical, etc.) and several models have been developed explaining fatigue response that inevitably occurs during prolonged exercise. Some of these models are cardiovascular/anaerobic model, energy depletion model, neuromuscular fatigue model, biomechanical model, psychological model and central governor model [14]. None of these models can explain fatigue solely as fatigue is an integral part of these models.

A complex system model has been introduced by Lambert [15], St Clair Gibson and Noakes [181] and Abbiss [14] where skeletal muscle fatigue was manipulated by the interaction of numerous physiological systems through underlying neural integration processes. The output of this neural integrative process depends on the feedback of the linear fatigue models (biomechanical, neuromuscular, cardiovascular, anaerobic, and central governor model). The output of these models is intensity dependent. For example, during maximal aerobic activity, performance is largely limited by the insufficient supply of O_2 to the working muscle by the cardiovascular system. Whereas, during submaximal aerobic activity, it may be because of the neurological alterations causing a reduction in central drive or energy depletion or muscle fiber composition and fatiguing status of muscles' active and resting fibers or muscle trauma that result in performance degradation or altered running mechanics. [14]

Considering fatigue as an unconscious perception of received afferent feedback, the interconnected linear fatigue models, shown in Figure 7-1, send signals to the Central Nervous System (CNS), and CNS analyzes them and responds to protect organism (skeletal muscle, heart, lungs, etc.) from death or injury by reducing the body performance to cope with body capability at identified fatigue or exhaustion level. Based on this invasive systematic complexity, this research adopted a methodology to not interfere with the ongoing self-regulatory behavior of the CNS and focused on the measurable fatigue metrics in the physiological and biomechanical system, along with the perception of effort.

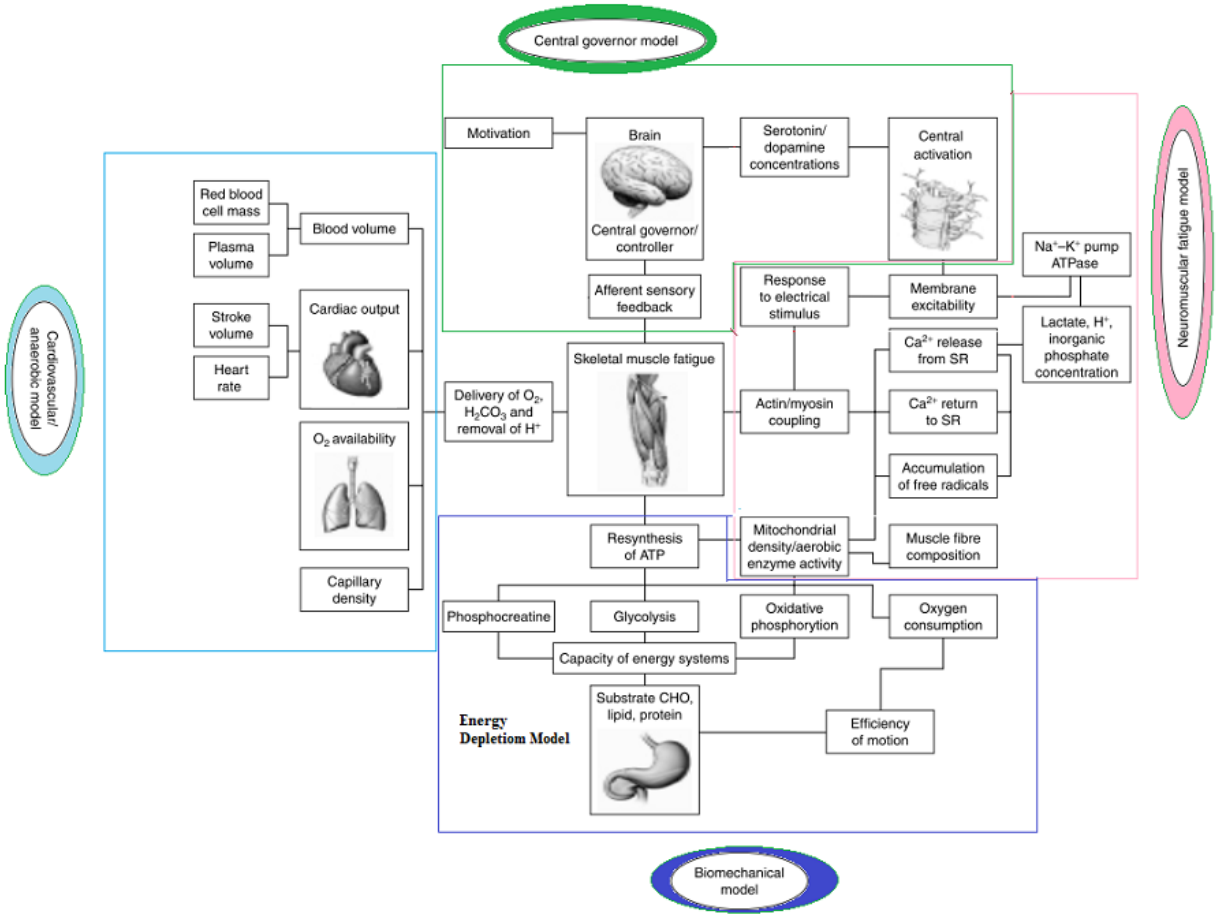

Figure 7-1: Interaction of fatigue development model for endurance runners, adopted and modified from Abbiss et al. [*14*]

7.2 Parameters of Interests to Model Fatigue

Research findings in literature have reported that endurance runner's fatigue can be identified through physiological adjustments [37, 43, 222, 254], biomechanical changes [37, 39, 43, 44, 148, 154, 156, 255] and perception of effort [114, 141, 256] during fatigue transition stage till termination. Similarly, this study has shown changes in significant fatigue predictors (previously summarized in Chapter 5 for the continuous test) during 'transition to fatigue' state, as shown in Figure 7-2. Energy cost of running at CS was also increased with fatigue

development due to change in biomechanical parameters [43] and perception of effort [179], as reported in Chapter 4 and 5. The reported findings in literature are in line with the results obtained through the methodology used in this chapter. Below are briefly described some of the parameters used in our study.

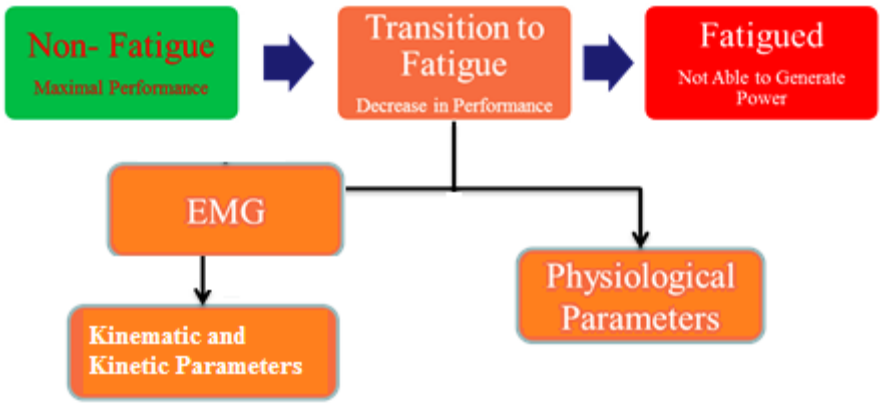

Figure 7-2: Parameters of interest in transition to fatigue stage

Lower Extremity Kinematic and Kinetic Parameters

Selected parameters (knee angle, pronation angle, I_{NDT}, I_H, and ACC_H), were identified to be significantly linked with RPE_O during the continuous test, discussed in Chapter 5. However, knee angle was not significant when linked with RPE_M.

Physiological Parameters

Statistically significant physiological parameters against RPE_O include $\%HR_{max}$ and RER, as described in the result section of Chapter 5. Regression analysis revealed that $\dot{V}O_2$, RR, RER and $\%HR_{max}$ were strongly linked with RPE_C to determine chest fatigue whereas the effect of $\dot{V}O_2$ and RR was not that significant when analyzed against overall perceived exertion (RPE_O). RER was dropped from the study due to the wearable discomfort in practical training scenario. The summary for the physiological predictors against RPE_C and RPE_O are shown in Table 5-4.

7.3 Statistical Analysis

Multilinear regression analysis with a significance level of 95% was performed using significant predictors ($\%HR_{max}$, knee angle, pronation angle, I_{NDT}, I_H and ACC_H) to develop regression prediction model. A developed regression model was subject to deal with inter-individual differences in body anthropometric measurements, force fatigability relationship against different muscle composition in the lower extremity, and adopted motor control strategies with fatiguing contractions during running. To further optimize the model and to find the significance of each predictor, data was normalized against '4^{th} minute of the run' for knee

angle, pronation angle, I_{NDT}, I_H, and ACC_H. Multilinear regression model on normalized data was performed to determine the significance of each selected predictor in this study and after significant normalized predictor, the normalized optimal model was developed.

7.4 Results and Discussion

Multilinear regression model result and model significance is reported below for the generalized and normalized data against selected variables.

7.4.1 Multilinear Regression Fatigue Model

For the observed linear relationship, identified for physiological ($\%HR_{max}$) and explanatory kinematic (knee angle, pronation angle, I_{NDT}, I_H, and ACC_H) variables with response variable (RPE_O), model fitting was performed by fitting a linear equation to the observed data for the selected group of participants.

The regression equation for the selected 6 explanatory physiological and biomechanical variables are defined in equation 7-1, where values β_0, β_1, β_2, β_3, β_4, β_5 and β_6 estimate the coefficient values for the selected predictors, estimating the regression line.

$$RPE_O = \begin{pmatrix} \beta_0 + \beta_1 * (\%HR_{\max}) + \beta_2 * (knee) + \\ \beta_3 * (pronation) + \beta_4 * (I_{NDT}) \\ + \beta_5 * (ACC_H) + \beta_6 * (I_H) \end{pmatrix} + \varepsilon \qquad \ldots\ldots\ (7\text{-}1)$$

In equation 7-1, the first part within brackets describes the regressors and the coefficients to calculate the response variable (RPE_O), while, ε represents the notion of model deviation. As the observed values for RPE_O vary about their mean response, a multiple regression model includes the residual term for this variation, known as 'ε'. Considering the regression model as best fit and residual (output = best fit + residual), the "best fit" term represents the first part of the equation and "residual" term represents the deviations of the observed values *y* from their means values. The response can also be considered as normally distributed with mean 0 and variance σ. The measure for the mean square error is given by the following equation 7-2:

$$S^2 = \left(\sum e_i^2\right) \Big/ n - p - 1 \qquad \ldots\ldots\ldots \qquad (7\text{-}2)$$

In equation (7-2), e_i represents the difference between actual and fitted response values whereas n represents number of observations. The value of 'p' represents the number of explanatory variable and S^2 represent mean square error (MSE).

7.4.2 Model Fitting

Prior to fitting the multilinear regression model, Pearson correlation coefficients along with multicollinearity were determined to check whether any of the predictors had unusually high

correlations among the predictors. No multicollinearity problem was identified using the collinearity statistics (VIF and tolerance) and most relationships appeared linear in nature (identified through partial regression plots). There was the independence of residuals, as assessed by "Durbin_Watson statistics" of 1.702. All these significant predictors under physiological and biomechanical domain were used in multiple linear regression model for the overall perceived exertion outcome. The SPSS V20 statistical software was used to run the statistical model.

7.4.3 Model Fitting Results for Predicting Fatigue in Real Time

The model with all six predictors did not present any evidence of non-linear relationships of the predictors with the response variable, based on standardized residual diagnostics and partial regression plots, shown in Figure 7-3. Assumptions of normality and constant variance for the residual errors were justified. There was also no outlier identified with SD>3.

To determine the goodness of fit, the coefficient of determination (R^2) was determined to explain the proportion of variance in the dependent variable using physiological and biomechanical independent variables. Interestingly physiological variable, $\%HR_{max}$ was individually able to explain 67.5% of the variance in dependent variable (RPE_O) and model statistical significance, shown in Table 7-2, was $F(1, 158) = 327.98$, $p < .0001$, $R^2 = 0.675$. When biomechanical variables were added into the fatigue prediction model, the overall prediction reliability was improved by 15.4% which was found to be significant. The unstandardized coefficients for each predictor and its statistical significance are shown in Table 7-1. After including the kinematic variables into the physiological predictors, the model statistical significance, shown in Table 7-2, was $F(6, 153) = 89.83$, $p < .0001$, $R^2 = 0.779$.

Table 7-1: Regression Model, representing physiological and biomechanical factor coefficients along with its significance. The significance of the model is shown in term of R^2 and F change.

Rated Perceived Exertion Model			Unstandardized Coefficients		Standardized Coefficients	t	Sig.	Model Stats
			B	Std. Error	B			
Physiological Parameter		(Constant)	-42.834	2.741		-15.630	.0001	R^2=0.675
		% HR_{max}	.546	.030	.822	18.110	.0001	F=327.98
Physiological and Kinematic Parameters	β_0	(Constant)	-26.367	4.851		-5.435	.0001	R^2=0.779 F=89.83
	β_1	% HR_{max}	.600	.026	.903	22.968	.0001	
	β_2	Knee Angle (˚)	-.138	.030	-.215	-4.588	.0001	
	β_3	Pronation Angle (˚)	-.164	.034	-.230	-4.795	.0001	
	β_4	I_{NDT} (g)	.240	.078	.136	3.093	.002	
	β_5	ACC_H (g)	-2.038	.380	-.244	-5.359	.0001	
	β_6	I_H (g)	.600	.116	.220	5.177	.0001	

Table 7- 2: Analysis of Variance of Regression Model

ANOVA[a]						
Model		Sum of Squares	dof	Mean Square	F	Sig.
1	Regression	860.134	1	860.134	327.979	.000[b]
	Residual	414.360	158	2.623		
	Total	1274.494	159			
2	Regression	992.703	6	165.451	89.832	.000[c]
	Residual	281.790	153	1.842		
	Total	1274.494	159			
a. Dependent Variable: Overall Rated Perceived Exertion (RPE_O)						
b. Predictors: (Constant), % HR max						
c. Predictors: (Constant), % HR max, Knee Angle, Pronation Angle, ND Tibia Impact, Hip Push-off Acc, Hip Impact						

All the included explanatory variables (physiological and kinematic) in the model were found to have a linear relationship with the response variable. The linear effect of each variable on variance in response variable is shown in regression Figure 7-3. Increase in $\%HR_{max}$, $I_{NDT,}$ and I_H whereas a decrease in knee angle, pronation angle and ACC_H were linked with an increase in RPE_O. Considering the individual estimate, residual ranged from -4 to +4. However, when explanatory variables were combined in a single model, residual error decreased significantly. The reported standard error of estimate was 1.357.

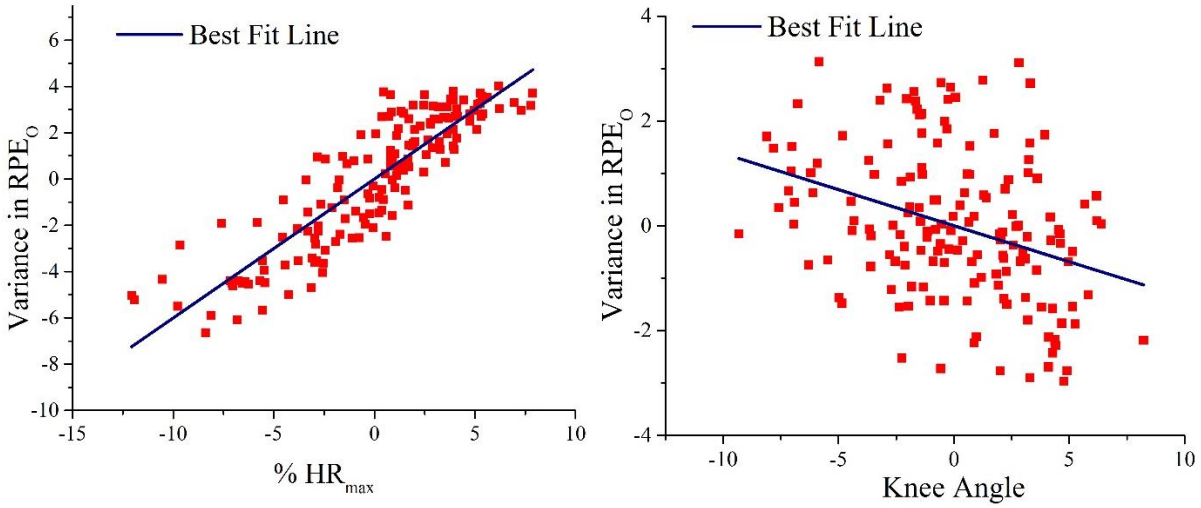

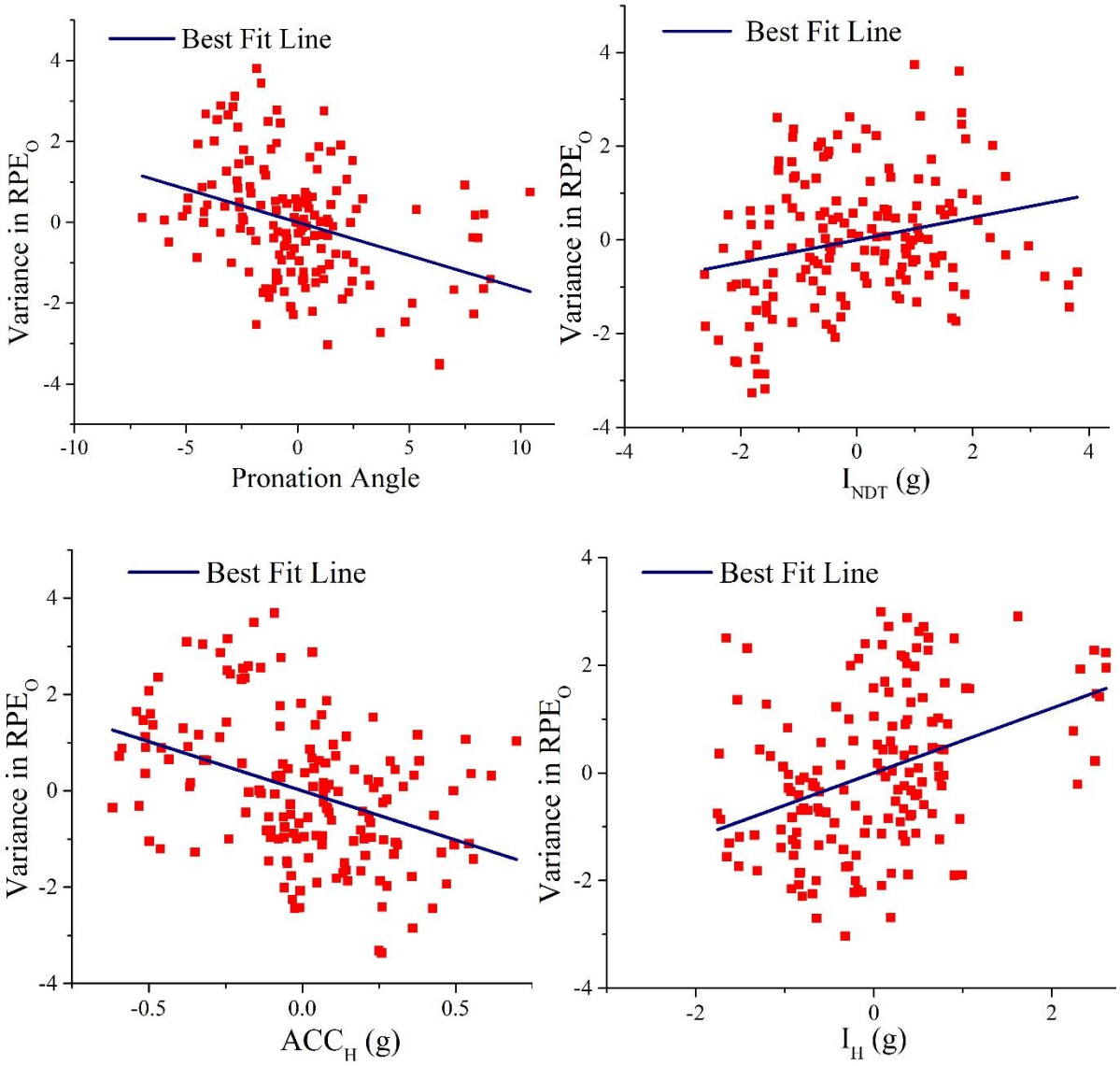

Figure 7-3: Partial regression plot, showing linearity between explanatory variables (%HR_{max}, knee angle (˚), pronation angle (˚), non-dominant tibia impact (I_{NDT}), hip push-off acceleration (ACC_H), hip impact (I_H)) and response variable (RPE_O).

7.4.4 The Modelled Equation

The multilinear regression model for selected parameters of interests, shown in equation 7-1, represent the linear model equation to predict the best-fitted response over the observed response data. The intercept (β_0) is known as the constant in the equation whereas β_1, β_2, β_3, β_4, β_5 and β_6 coefficients are the estimates for %HR_{max}, knee angle, pronation angle, I_{NDT}, ACC_H, and I_H respectively. The values of these coefficients, listed in Table 7-1, were replaced in Eq. 7-1. The final real-time fatigue prediction model is shown in quation 7-3 for recreational active runners. The prediction accuracy results in r-square of 0.779 which explains almost 90% of the variance in response variables, based on significant variables, selectedfrom the continuous run study.

$$RPE_O = \begin{pmatrix} -26.367 + 0.6*(\%HR_{\max}) - 0.138*(knee) - \\ 0.164*(pronation) + 0.24*(I_{NDT}) \\ -2.038*(ACC_H) + 0.60*(I_H) \end{pmatrix} \quad \ldots (7\text{-}3)$$

The prediction error for this model is estimated to be 1.357 which is currently in an acceptable range to identify fatigue in the recreational active class of runners.

7.5 Normalized Optimal Model for Predicting Fatigue

After determining the critical parameters for predicting fatigue, a normalized parameter modeling approach was tested to remove the effect of inter-individual body anthropometric differences and running behavioral shift in runner's kinematics against fatigue. Selected parameters (knee angle, pronation angle, I_{NDT}, $ACC_{H,}$ and I_H) were normalized against the optimal values at the 4th minute of the run during the continuous test (shown in Table 5-2). Differences were accounted to measure the impact of selected parameter with fatigue progression. This approach hypothesized that it might help in determining more common parameters to measure fatigue among all active recreational runner's class, irrespective of their body measurements and behavioral kinematics and kinetics.

The regression model with all six predictors did not present any evidence of non-linear relationships of the predictors with the response variable. Assumptions of normality and constant variance for the residual errors were justified and no outlier identified with SD>3. Interestingly the finding of the regression model reported that normalized values of knee angle, I_{NDT}, and ACC_H did not remain significant to fatigue development, however, $\%HR_{max}$ and normalized pronation angle and I_H were significantly linked with RPE_O. Therefore, the statistics for a more optimized model which include $\%HR_{max}$, normalized pronation angle, and normalized I_H were reported in Table 7-3. Physiological variable, $\%HR_{max}$ was individually able to explain 67.5% of the variance in dependent variable (RPE_O) and model statistical significance, as shown in Table 7-1, was F (1, 158) = 327.98, p < .0001, R^2 = 0.675. When normalized pronation angle and normalized hip impact were added into the fatigue prediction model, the overall prediction reliability was improved by 14.07% which was found to be significant. The unstandardized coefficients for each predictor and its statistical significance are shown in Table 7-3. The normalized RPE_O model ANOVA significance was F (3, 156) = 173.86, p < .0001, R^2 = 0.770.

Table 7-3: Regression Model, representing physiological and normalized biomechanical factor coefficients along with its significance. The significance of the Normalized RPE_O model is shown in term of R^2 and F change.

Normalized RPE_O Model			Unstandardized Coefficients		Standardized Coefficients	t	Sig.	Model Stats
			B	Std. Error	B			
Physiological and Kinematic Parameters	β_0	(Constant)	-46.466	2.385		-19.481	.0001	R^2=0.770 F=173.86
	β_1	% HR_{max}	.583	.026	.877	22.221	.0001	
	β_3	Normalized Pronation (˚)	-.205	.040	-.202	-5.124	.0001	
	β_6	Normalized I_H (g)	2.186	.343	.245	6.375	.0001	

The multilinear regression equation for the normalized RPE_O model is shown in equation 7-4, optimized from equation 7-1 due to non-significance of knee angle, I_{NDT}, and ACC_H coefficients.

$$RPE_O = \begin{pmatrix} \beta_0 + \beta_1 * (\%HR_{max}) + \beta_3 * (Normalized\_pronation) \\ +\beta_6 * (Normalized\_I_H) \end{pmatrix} \quad \ldots\ldots \quad (7\text{-}4)$$

Replacing the coefficient value of β_0, β_1, β_3, and β_6 from Table 7-3 into equation (7-4) gives the final modeled fatigue prediction equation for recreational active runner.

$$RPE_O = \begin{pmatrix} -46.466 + 0.583 * (\%HR_{max}) - 0.205 * (Normalized\_pronation) \\ +2.186 * (Normalized\_I_H) \end{pmatrix} \ldots (7\text{-}5)$$

The prediction error for this model is estimated to be 1.371 which is currently in an acceptable range.

7.6 Model Fitting Results

The model accuracy for the observation data of 17 recreational active runners from continuous test, a comparative plot was drawn for the 'regression fatigue model" and "normalized fatigue model". Equations 7-3 represents generalized regression model and equation 7-5 representing the normalized optimal model for predicting fatigue (RPE_O). The plot shown in Figure 7-4 shows the degree of closeness of optimized normalized model with regression fatigue model. Both models showed an accuracy of about 87% to predict fatigue in real time and their prediction estimated error has also been very close to the original observation data (estimated the error of 1.357 for regression model and 1.371 for normalized fatigue model).

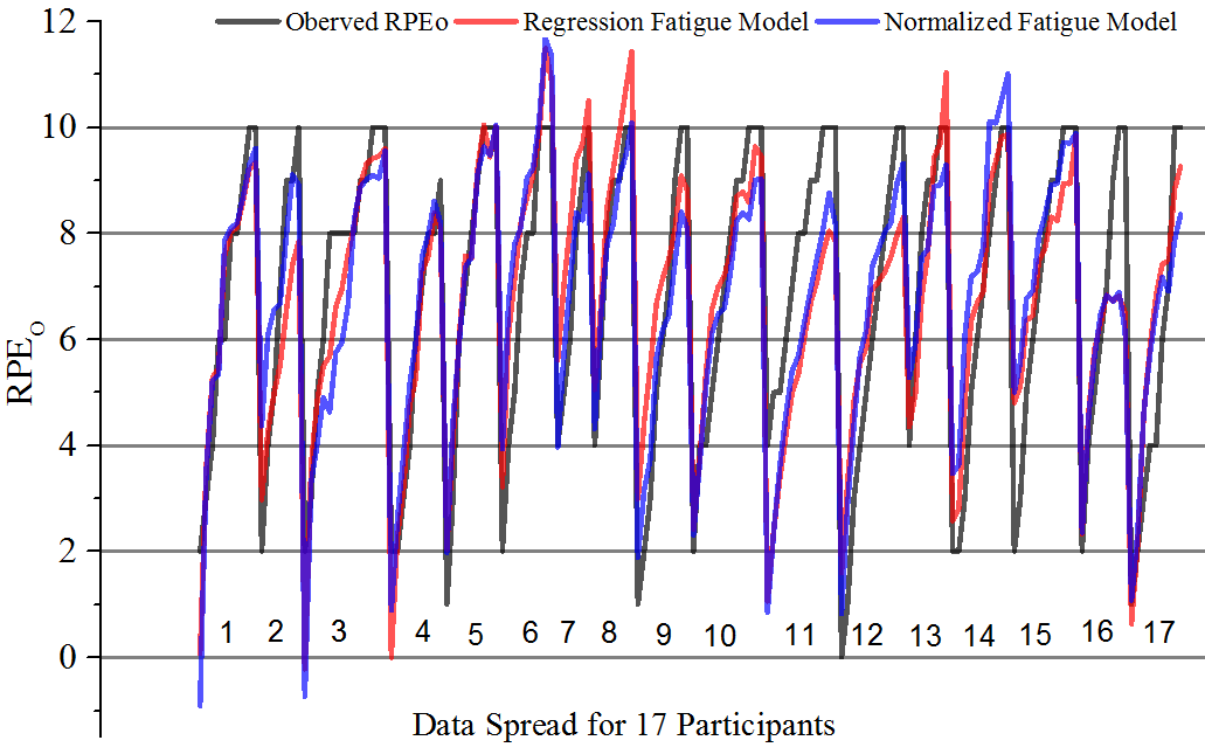

Figure 7-4: Model fitting accuracy. the black line represents the observed data, the red line represents the regression fatigue model that includes all critical variables and the blue line represents the normalized fatigue model that has optimal normalized parameters.

7.7 Fatigue Model Extended Use in Wearable Technology

The proposed fatigue model had the potential to be incorporated into wearable technology by incorporating the measurable senses for the significant physiological and biomechanical variables. A Kinesiological endurance training system (KETS), explained in appendix section, incorporated the significant parameters into its computational model to determine the level of metabolic stress, physiological strain, lower extremity fatigue and overall fatigue during exercise. Such proposed architecture would ultimately help in monitoring metabolic stress and fatigue.

7.8 Conclusion

The proposed regression fatigue model explained 88.3% of the variance (R-value=0.8826) in the observed data (RPE_O) with root mean square error of 1.357. Whereas the normalized fatigue model showed an accuracy of 87.7% of the variance (R-value = 0.877) in the observed data (RPE_O) with an estimated error of 1.371 (RMSE=1.371).

In its current form, the model is only applicable to studied group of recreational male runners, having an anaerobic threshold of 89.97% of HR_{max}. The limitations of the study, discussed in chapter 8, may affect the results of the study under repeated measurement conditions. The most likely reasons would be the difference among the participants' demographics, gender, fitness

level, training history and testing conditions. As this research was performed under laboratory conditions, the significant fatigue predictors (used in real-time fatigue model) may differ from the results of this study. Prediction error will also be high for a participant with different demographics and different experimental conditions, using this model.

This research provided a framework for future studies to incorporate such methodology for developing a robust fatigue prediction model with bigger population size, both gender, varied fitness level and realistic endurance conditions.

CHAPTER 8. CONCLUSION, SUMMARY OF KEY FINDINGS, STUDY LIMITATIONS AND FUTURE DIRECTION

8.1 Conclusion

This study successfully investigated the difference in fatigue implications during continuous and non-continuous training regimes in recreational active runners. It covered physiological, running mechanic, neuromuscular, and perceptual aspects of fatigue development during running to exhaustion.

The observed differences in exercise performance during both tests were due to the difference in physiological response and neuromuscular fatigue between both tests. Time to exhaustion (TTE) was higher during the non-continuous test. Cardio-respiratory stress, metabolic stress, and perceptual fatigue were higher, whereas runny economy was poor at the termination of the continuous test in comparison with the non-continuous test. Participants showed changes in iEMG levels during different phases of running gait cycle in both tests against different fatigue levels ('1st stage', 'anaerobic threshold' and 'End'). The neuromuscular fatigue ('Pi' and 'Fi') showed a difference in correlation strength for different muscle in relation to muscular fatigue (RPE=). $\%HR_{max}$ has been observed to have a significant correlation with BLa during the non-continuous run and has shown the potential to estimate BLa during the continuous running in comparison with the RPE_O for the studied recreational active runners.

The findings from this research also establish a base for the future studies to evaluate exercise performance in an integrated and comprehensive manner. A real-time fatigue prediction model was developed by integrating significant kinematic (knee angle, pronation angle, I_{NDT}, ACC_H, I_H) and physiological ($\%HR_{max}$) parameters (identified from the continuous run test in this research). To make the research findings more impactful in real-time, a kinesiological endurance training system (KETS) was proposed, attached in the appendix section. Currently, the practical use of the developed model is limited to the studied runners under the laboratory conditions. However, further studies are needed to confirm the findings using higher sample size, varied demographics, varied fitness levels and both genders of recreational active runners under outdoor conditions. Such approaches will help to make a robust fatigue prediction model with better statistical significance and less estimation error.

8.2 Summary of Key Contributions

The major contribution and originality of this research are summarized as follows.

1. The TTE analysis of the recruited group of recreational active runners established that increase in systematic oxygen reserve ($\Delta\dot{V}O_2$) along with $\dot{V}O_{2max}$ were linked with better fatigue resistance.
2. Selected critical speed (CS) for recreational active runners was observed to be associated with maximum lactate steady state (MLSS) conditions during the non-continuous run. However, the continuous run test showed a significant increase in BLa over MLSS. These findings were reported to be similar to the trained runners and triathletes, studied by Penteado et al. [49].
3. The difference in time to exhaustion (~1.6 times) between the non-continuous and continuous test was due to 1-min rest interval during the non-continuous test. The physiological evidence (significant increase in RER, $\dot{V}O_2$, BLa, and RPE_O during the continuous run in comparison with the non-continuous run) was showed for the first time in this research. A similar study, done by Penteado et al. [49], did not show the physiological evidence for the trained runners and triathletes while comparing the endurance performance between continuous and intermittent stage fatigue protocol.
4. RPE_O has shown greater variation among runners against BLa rise in this study. Contradictory evidence also exists on the rise of RPE_O and BLa rise during intermittent protocol [50]. Whereas in continuous running, RPE_O has been found to be associated with BLa. Considering all these findings, this research proposed the use of $\%HR_{max}$ as a valid non-intrusive and non-interruptive parameter to predict BLa, due to its strong correlation with RPE_O and BLa studied in this research. During the continuous run test, $\%HR_{max}$ has shown lower prediction error than RPE_O in estimating BLa.
5. During the continuous and non-continuous test, 'Pi' and 'Fi' kinetics in the lower extremity muscles revealed that fatigue stressed different muscles in a different fashion. The continuous test revealed that 'Pi' of the GM, GL and TA muscle and 'Fi' of RF, VL, BF, GM, GL and TA muscles have shown significant change against RPE_M. The non-continuous test revealed that 'Pi' of RF, VL, BF, ST, GM, GL and TA muscles and 'Fi' of BF, ST, GM, GL and TA muscles were linked with RPE_M. Both protocols have resulted in significant changes in 'Pi' of GM, GL, TA and 'Fi' of BF, GM, GL anf TA muscles. Considering these findings, it can be said that neuromuscular fatigue dynamics and its interaction with running mechanics are very much protocol dependent. In our knowledge, such findings were also first of its kind in this research study for the recreational active runners.

6. Bilateral KA in lower extremity showed that dominant leg experienced higher I_T and ACC_H in comparison with the non-dominant leg at the CS. However, KA was not found significant with the progression of fatigue and cannot be used as a potential marker to monitor lower extremity fatigue.
7. An integrated methodology has been proposed in this research to understand the fatigue manifestations on cardio-respiratory, neuromuscular, biomechanical, metabolic and perceptual system.
8. Key biomechanical and physiological parameters have been identified through the integrative analysis methodology proposed in this research. A real-time fatigue monitoring and prediction model has been proposed. Model development methodology will provide useful fundamental knowledge to build more reliable and accurate fatigue prediction model under real-time outdoor running conditions.

8.3 Limitations

This study was not without limitations. The studied participants were the active recreational endurance runners. Limitations in term of participants may include motivation, diet, sports training history, active participation in recreational sports and individual fitness to running. However, participant selection criteria were set in place. Individual's metabolic response, energy reserve, energy distribution kinetics against selected critical speed (CS) and anthropometric measurement difference among the runners were not controlled in this study.

Participants were asked to run for volitional exhaustion against progressive treadmill speed to determine maximum aerobic power ($\dot{V}O_{2max}$) and maximum heart rate (HR_{max}). Though the maximal effort criteria were set in palace but participant may not have exerted themselves to their upper limit due to their personal motivation level or previous fatigue status from the $\dot{V}O_{2submax}$ test in this study. Such limitation may have imposed error on determining HR_{max} and calculated $\%HR_{max}$ values may have slight difference from the original value of $\%HR_{max}$.

Each participant's experience on treadmill running, treadmill surface and type of shoe were the other limiting factors that might have influenced fatigue related kinematics, neuromuscular activity and physiological response [199, 257]. However, these factors were controlled to a certain limit by using same treadmill machine for all runners and same running shoes during both tests which they used to wear during daily training. However, the effect of different shoes between participants may be among the factors that could have influenced running mechanics and running economy in this studied group of recreational endurance runners.

To meet the energy cost of outdoor running, 1% gradient of the treadmill was used [201]. There might be differences in the running mechanics due to the difference in treadmill vs. over-

ground running [54] that may change the fatigue response into some other significant biomechanical or physiological factor. And this study was conducted under laboratory controlled condition. Changes in the environmental factors [258] do also significantly contribute towards changing the fatigue manifestations on the physiological and biomechanical system.

Electromyographic analysis of the selected muscles in the lower extremity is another limitation. There are many other muscles crossing each joint in the lower extremity. The net action and fatigue status of these muscles are also responsible for joint angle change [259]. There is a possibility that one muscle may fatigue but the joint angle does not change due to the compensatory action of surrounding agonist or antagonist muscles. It is also possible that muscles of interests do not show sign of fatigue but surrounding unmeasured muscle may fatigue [30]. Having technological and methodological limitations, measurement of each muscle in the lower extremity has been restricted to the dominant and non-dominant side of the lower extremity. Although the studied muscles in this research provided a broader view of fatigue and its interaction with running mechanics, detailed muscles study is needed as all the lower extremity muscles had the potential to control joint movement.

Muscle temperature is another factor, effecting EMG parameters [106]. In this research, muscle temperature was not measured as it was assumed that muscle temperature will not change much due to submaximal running CS. To minimize its effect, a warmup session of 5 to 10 minutes was conducted to reduce temperature fluctuation in muscle and to achieve a steady thermoregulatory state. Following previous research, muscle temperature remained constant during continuous power exercise and did not affect the EMG parameters. However, in this research, the rise in TDMdPF has been observed in some lower extremity muscles, probably due to variation in temperature at CS against exposure time.

Considering the structural limitation of muscle mass and muscle composition, type II muscle fibers are reported nearer to the skin surface than type I fiber. During running, recruitment of fast twitch fiber may decrease the low-pass filtering effect of tissues on the EMG signal [30] and may mask TDMdPF decrease. Such factors limit the interpretation of EMG findings.

Fatigue manifestations on the physiological and biomechanical system are dependent on running intensity, lower extremity neuromuscular response, nature of fatiguing protocol (continuous vs. non-continuous), fitness level and aerobic profile of the selected group of participants. Therefore, findings reported in this research are limited to laboratory setting and to the studied runners ($\dot{V}O_{2max}$ to be 50-60 $ml.kg^{-1}.min^{-1}$, CS to be 3.64±0.417 $m.sec^{-1}$, BMI to be 22.16±1.92, % body fat to be 13.01±3.31%, HR_{max} to be 190.47±7.89 $beats.min^{-1}$, $\%HR_{max}$

at the AT to be 89.97±2.6%, %$\dot{V}O_{2max}$ to be 81.58±3.14% and running frequency to be around 3 times/week for an average of 30-50 minutes).

Technological and methodological limitations of the study include the use of 2D motion analysis system, EMG for the selected group of muscles and cardiorespiratory analysis. As running is the whole-body activity [30], examining the few lower extremity kinematic variables may not solely represent fatigue. 2D video analysis with image digitization software also includes a certain degree of human error. Considering these limitations, due attention was paid during the computation of angles. Five consecutive running gait cycles were considered for kinematic evaluation whereas only three are recommended for such analysis.

Selection of the few muscles in the lower extremity limits the right understanding of the lower extremity neuromuscular fatigue and its interaction with the running mechanics. A detailed study, including all the lower extremity muscle surrounding the joints, might provide a complete picture of joint angle change with neuromuscular fatigue. Therefore, there is a need to study more muscles in the lower extremity to determine the right source of impairment, causing changes in running mechanics during endurance performance.

The cardio-respiratory system included the use of mouthpiece while running. Such discomfort might not only have affected subject motivation but also be a probable source of the increase in mental discomfort, restricted breathing and subject consciousness about the instrumented running. Participants were asked to neglect such feelings while running and do not pay mental attention to it. However, its effect on the collection of data was not monitored and may also be the source of error in the data. The other limitation is the asynchronous data collection of the selected measurement systems which might have slightly influence the synchronous analysis of the results.

Selected critical speed (CS) was observed to overestimate the maximum lactate steady state response (MLSS) during continuous running in this study. During the outdoor endurance testing conditions, selected critical speed along with environmental factors and running surface may change the fatigue manifestation on the physiological and biomechanical system.

8.4 Future Work

This research has provided deeper understanding of the physiological and biomechanical system under different training regimes (continuous vs. non-continuous) with fatigue development. Difference in fatiguing protocol resulted in difference in neuromuscular response during running and hence different fatigue implications on physiological and biomechanical system. The core message to the recreational active runner is to have a mix of the non-continuous and continuous training at the same critical speed. Non-continuous training protocol

helps recreational active runners to expose their body for a longer duration at MLSS to develop fatigue resistance. Whereas, continuous running exposes the body at higher metabolic stress levels and higher cardio-respiratory stress levels to have better cardio-respiratory training related benefits.

To generalize the findings of this research, future studies should focus on larger sample size, varied fitness level across recreational runner's class, both genders and real-time outdoor testing conditions. Future studies should also include the study of metabolic pathways contribution during training, muscle physiology (muscle fiber composition for selected muscles, muscle activation patterns and factors causing changes in TDMdPF), and muscles at both sides of the dominant and non-dominant leg (as muscles may fatigue differently and change the fatigue implications accordingly). Injury development mechanism should also be studied along with fatigue to provide optimized injury prevention program for the recreational class of runners. To have a robust fatigue prediction model for larger recreational runners, machine learning based intelligent models can be introduced. Real-time computational analytical tools can be deployed to help recreational active runners in monitoring training stress and fatigue and to avoid the ill-effects of inefficient training.

References:

1. O'Keefe, J.H., et al. *Potential adverse cardiovascular effects from excessive endurance exercise*. in *Mayo Clinic Proceedings*. 2012. Elsevier.
2. O'Keefe, J.H. and C.J. Lavie, *Run for your life… at a comfortable speed and not too far*. Heart, 2013. **99**(8): p. 516-519.
3. Lee, D.-c., et al., *Running and all-cause mortality risk-Is more better.* Medicine and Science in Sports and Exercise, 2012. **44**: p. 924-924.
4. Wen, C.P., et al., *Minimum amount of physical activity for reduced mortality and extended life expectancy: a prospective cohort study.* The Lancet, 2011. **378**(9798): p. 1244-1253.
5. La Gerche, A., et al., *Exercise-induced right ventricular dysfunction and structural remodelling in endurance athletes.* European heart journal, 2011: p. ehr397.
6. van Gent, B.R., et al., *Incidence and determinants of lower extremity running injuries in long distance runners: a systematic review.* British journal of sports medicine, 2007.
7. van Mechelen, W., *Running injuries.* Sports Medicine, 1992. **14**(5): p. 320-335.
8. Gefen, A., *Biomechanical analysis of fatigue-related foot injury mechanisms in athletes and recruits during intensive marching.* Medical and Biological Engineering and Computing, 2002. **40**(3): p. 302-310.
9. Mizrahi, J., O. Verbitsky, and E. Isakov, *Fatigue-related loading imbalance on the shank in running: a possible factor in stress fractures.* Annals of biomedical engineering, 2000. **28**(4): p. 463-469.
10. Blair, S.N., H.W. Kohl, and N.N. Goodyear, *Rates and risks for running and exercise injuries: studies in three populations.* Research Quarterly for Exercise and Sport, 1987. **58**(3): p. 221-228.
11. Allman, B.L. and C.L. Rice, *Neuromuscular fatigue and aging: central and peripheral factors.* Muscle & nerve, 2002. **25**(6): p. 785-796.
12. Kayser, B., *Exercise starts and ends in the brain.* European journal of applied physiology, 2003. **90**(3-4): p. 411-419.
13. Green, H.J., *Mechanisms of muscle fatigue in intense exercise.* J Sports Sci, 1997. **15**(3): p. 247-56.
14. Abbiss, C.R. and P.B. Laursen, *Models to explain fatigue during prolonged endurance cycling.* Sports medicine, 2005. **35**(10): p. 865-898.
15. Lambert, E.V., A. St Clair Gibson, and T.D. Noakes, *Complex systems model of fatigue: integrative homoeostatic control of peripheral physiological systems during exercise in humans.* Br J Sports Med, 2005. **39**(1): p. 52-62.
16. Noakes, T.D., A. St Clair Gibson, and E.V. Lambert, *From catastrophe to complexity: a novel model of integrative central neural regulation of effort and fatigue during exercise in humans: summary and conclusions.* Br J Sports Med, 2005. **39**(2): p. 120-4.
17. Brooks, G., et al., *Cardiovascular dynamics during exercise.* Exercise Physiology: Human Bioenergetics and its applications. Mountain View, Ca: Mayfield Publishing Company, 2000: p. 317-339.
18. Brooks, G., T. Fahey, and T. White, *Fatigue during muscular exercise.* Exercise Physiology: Human Bioenergetics and Its Applications, 2000: p. 800-822.
19. Enoka, R.M. and D.G. Stuart, *Neurobiology of muscle fatigue.* J Appl Physiol, 1992. **72**(5): p. 1631-1648.
20. Amann, M. and J.A. Calbet, *Convective oxygen transport and fatigue.* J Appl Physiol (1985), 2008. **104**(3): p. 861-70.

21. Romer, L.M., et al., *Effect of acute severe hypoxia on peripheral fatigue and endurance capacity in healthy humans.* Am J Physiol Regul Integr Comp Physiol, 2007. **292**(1): p. R598-606.
22. Romer, L.M., et al., *Effect of exercise-induced arterial hypoxemia on quadriceps muscle fatigue in healthy humans.* American Journal of Physiology-Regulatory, Integrative and Comparative Physiology, 2006. **290**(2): p. R365-R375.
23. Meeusen, R. and B. Roelands, *Central fatigue and neurotransmitters, can thermoregulation be manipulated?* Scand J Med Sci Sports, 2010. **20 Suppl 3**: p. 19-28.
24. McKenna, M.J., *The roles of ionic processes in muscular fatigue during intense exercise.* Sports Medicine, 1992. **13**(2): p. 134-145.
25. Allen, D.G., G.D. Lamb, and H. Westerblad, *Skeletal Muscle Fatigue: Cellular Mechanisms*. Vol. 88. 2008. 287-332.
26. Seburn, K.L., et al., *Effect of manipulation of plasma lactate on integrated EMG during cycling.* Med Sci Sports Exerc, 1992. **24**(8): p. 911-6.
27. Girard, O., et al., *Alteration in neuromuscular function after a 5 km running time trial.* Eur J Appl Physiol, 2012. **112**(6): p. 2323-30.
28. Longpré, H.S., J.R. Potvin, and M.R. Maly, *Biomechanical changes at the knee after lower limb fatigue in healthy young women.* Clinical Biomechanics, 2013. **28**(4): p. 441-447.
29. Gandevia, S., *Spinal and supraspinal factors in human muscle fatigue.* Physiological reviews, 2001. **81**(4): p. 1725-1789.
30. Smoliga, J.M., *Kinematic and electromyographic analysis of the legs, torso, and arms during an exhaustive run*. 2007: ProQuest.
31. Zadpoor, A.A. and A.A. Nikooyan, *The effects of lower-extremity muscle fatigue on the vertical ground reaction force: A meta-analysis.* Proceedings of the Institution of Mechanical Engineers, Part H: Journal of Engineering in Medicine, 2012. **226**(8): p. 579-588.
32. Clansey, A.C., et al., *Effects of fatigue on running mechanics associated with tibial stress fracture risk.* Med Sci Sports Exerc, 2012. **44**(10): p. 1917-23.
33. Hanon, C., C. Thepaut-Mathieu, and H. Vandewalle, *Determination of muscular fatigue in elite runners.* Eur J Appl Physiol, 2005. **94**(1-2): p. 118-25.
34. Tartaruga, M.P., et al., *The relationship between running economy and biomechanical variables in distance runners.* Research quarterly for exercise and sport, 2012. **83**(3): p. 367-375.
35. Saunders, M.J., et al., *Muscle activation and the slow component rise in oxygen uptake during cycling.* Medicine and science in sports and exercise, 2000. **32**(12): p. 2040-2045.
36. Hausswirth, C., et al., *Evolution of electromyographic signal, running economy, and perceived exertion during different prolonged exercises.* International journal of sports medicine, 2000. **21**(06): p. 429-436.
37. Mizrahi, J., et al., *Effect of fatigue on leg kinematics and impact acceleration in long distance running.* Human movement science, 2000. **19**(2): p. 139-151.
38. Barbieri, F.A., et al., *Systematic review of the effects of fatigue on spatiotemporal gait parameters.* Journal of back and musculoskeletal rehabilitation, 2013. **26**(2): p. 125-131.
39. Williams, K.R., R. Snow, and C. Agruss, *Changes in Distance Running Kinematics With Fatigue.* International Journal of Sport Biomechanics, 1991. **7**(2).

40. Hayes, P.R., S.J. Bowen, and E.J. Davies, *The relationships between local muscular endurance and kinematic changes during a run to exhaustion at v VO2max.* The Journal of Strength & Conditioning Research, 2004. **18**(4): p. 898-903.
41. Derrick, T.R., D. Dereu, and S.P. McLean, *Impacts and kinematic adjustments during an exhaustive run.* Medicine and science in sports and exercise, 2002. **34**(6): p. 998-1002.
42. Gerlach, K.E., et al., *Kinetic changes with fatigue and relationship to injury in female runners.* Medicine and science in sports and exercise, 2005. **37**(4): p. 657-663.
43. Candau, R., et al., *Energy cost and running mechanics during a treadmill run to voluntary exhaustion in humans.* European journal of applied physiology and occupational physiology, 1998. **77**(6): p. 479-485.
44. Hanon, C., C. Thépaut-Mathieu, and H. Vandewalle, *Determination of muscular fatigue in elite runners.* European journal of applied physiology, 2005. **94**(1-2): p. 118-125.
45. Yang, C.-I., *Overview of Factors Affecting Running Economy in Distance Running.* 屏東教大體育, 2013(16): p. 239-248.
46. Porcari, J., C. Bryant, and F. Comana, *Exercise physiology*. 2015: FA Davis.
47. Sjödin, B. and I. Jacobs, *Onset of blood lactate accumulation and marathon running performance.* International journal of sports medicine, 1981. **2**(1): p. 23-26.
48. Santos-Concejero, J., et al., *Onset of blood lactate accumulation as a predictor of performance in top athletes.* RETOS. Nuevas Tendencias en Educación Física, Deporte y Recreación, 2013(23): p. 67-69.
49. Penteado, R., et al., *Physiological responses at critical running speed during continuous and intermittent exhaustion tests.* Science & Sports, 2014(0).
50. Seiler, S. and J.E. Sjursen, *Effect of work duration on physiological and rating scale of perceived exertion responses during self-paced interval training.* Scandinavian journal of medicine & science in sports, 2004. **14**(5): p. 318-325.
51. Barnes, K.R., M.R. Mcguigan, and A.E. Kilding, *Lower-body determinants of running economy in male and female distance runners.* The Journal of Strength & Conditioning Research, 2014. **28**(5): p. 1289-1297.
52. Daniels, J. and N. Daniels, *Running economy of elite male and elite female runners.* Medicine and science in sports and exercise, 1992. **24**(4): p. 483-489.
53. Saunders, P.U., et al., *Factors affecting running economy in trained distance runners.* Sports Medicine, 2004. **34**(7): p. 465-485.
54. Garcia-Perez, J.A., et al., *Effect of overground vs treadmill running on plantar pressure: influence of fatigue.* Gait Posture, 2013. **38**(4): p. 929-33.
55. Borg, G., *Perceived exertion: a note on" history" and methods.* Med. Sci. Sports Exerc., 1973. **5**: p. 90-93.
56. Joyner, M.J. and E.F. Coyle, *Endurance exercise performance: the physiology of champions.* J Physiol, 2008. **586**(1): p. 35-44.
57. Ghosh, A.K., *Anaerobic threshold: Its concept and role in endurance sport.* The Malaysian journal of medical sciences: MJMS, 2004. **11**(1): p. 24.
58. Goodall, S., *Central and peripheral determinants of fatigue in acute hypoxia.* School of Sport and Education, 2011.
59. Nicola, T.L. and D.J. Jewison, *The anatomy and biomechanics of running.* Clin Sports Med, 2012. **31**(2): p. 187-201.
60. Enoka, R.M. and J. Duchateau, *Muscle fatigue: what, why and how it influences muscle function.* J Physiol, 2008. **586**(1): p. 11-23.
61. Davis, J.M. and S.P. Bailey, *Possible mechanisms of central nervous system fatigue during exercise.* Medicine and science in sports and exercise, 1997. **29**(1): p. 45-57.

62. Gandevia, S., *Neural control in human muscle fatigue: changes in muscle afferents, moto neurones and moto cortical drive.* Acta physiologica scandinavica, 1998. **162**(3): p. 275-283.
63. Bigland-Ritchie, B., E. Cafarelli, and N. Vøllestad, *Fatigue of submaximal static contractions.* Acta physiologica Scandinavica. Supplementum, 1985. **556**: p. 137-148.
64. Dulhunty, A.F., *Excitation-contraction coupling from the 1950s into the new millennium.* Clin Exp Pharmacol Physiol, 2006. **33**(9): p. 763-72.
65. Herzog, W., *Sliding Filament Theory*, in *Encyclopedia of Neuroscience*. 2009, Springer. p. 3745-3748.
66. Ashley, C.C., I.P. Mulligan, and T.J. Lea, *Ca2+ and activation mechanisms in skeletal muscle.* Quarterly reviews of biophysics, 1991. **24**(01): p. 1-73.
67. Al-Mulla, M.R., F. Sepulveda, and M. Colley, *A review of non-invasive techniques to detect and predict localised muscle fatigue.* Sensors (Basel), 2011. **11**(4): p. 3545-94.
68. Nielsen, O.B. and F.V. de Paoli, *Regulation of Na+-K+ homeostasis and excitability in contracting muscles: implications for fatigue.* Applied Physiology, Nutrition, and Metabolism, 2007. **32**(5): p. 974-984.
69. Fryer, M.W., et al., *Effects of creatine phosphate and P (i) on Ca2+ movements and tension development in rat skinned skeletal muscle fibres.* The Journal of Physiology, 1995. **482**(Pt 1): p. 123-140.
70. Giannesini, B., *Non-invasive investigations of muscular fatigue: metabolic and electromyographic components.* Biochimie, 2003. **85**(9): p. 873-883.
71. Hargreaves, M., *Skeletal muscle metabolism during exercise in humans.* Clinical and Experimental Pharmacology and Physiology, 2000. **27**(3): p. 225-228.
72. Bottinelli, R., et al., *Force-velocity properties of human skeletal muscle fibres: myosin heavy chain isoform and temperature dependence.* The Journal of physiology, 1996. **495**(Pt 2): p. 573-586.
73. Kyrolainen, H., et al., *Interrelationships between muscle structure, muscle strength, and running economy.* Medicine and science in sports and exercise, 2003. **35**(1): p. 45-49.
74. Conley, K.E., W.F. Kemper, and G.J. Crowther, *Limits to sustainable muscle performance: interaction between glycolysis and oxidative phosphorylation.* Journal of Experimental Biology, 2001. **204**(18): p. 3189-3194.
75. Robergs, R.A., F. Ghiasvand, and D. Parker, *Biochemistry of exercise-induced metabolic acidosis.* American Journal of Physiology-Regulatory, Integrative and Comparative Physiology, 2004. **287**(3): p. R502-R516.
76. Taylor, D., et al., *Energetics of human muscle: Exercise-induced ATP depletion.* Magnetic Resonance in Medicine, 1986. **3**(1): p. 44-54.
77. Taylor, J.L., G. Todd, and S.C. Gandevia, *Evidence for a supraspinal contribution to human muscle fatigue.* Clinical and Experimental Pharmacology and Physiology, 2006. **33**(4): p. 400-405.
78. Enoka, R.M., *Mechanisms of muscle fatigue: central factors and task dependency.* Journal of Electromyography and Kinesiology, 1995. **5**(3): p. 141-149.
79. Gandevia, S.C., *Fatigue: neural and muscular mechanisms.* Vol. 384. 1995: Springer.
80. Todd, G., J.L. Taylor, and S.C. Gandevia, *Measurement of voluntary activation of fresh and fatigued human muscles using transcranial magnetic stimulation.* J Physiol, 2003. **551**(Pt 2): p. 661-71.
81. Amann, M. and J.A. Dempsey, *Locomotor muscle fatigue modifies central motor drive in healthy humans and imposes a limitation to exercise performance.* J Physiol, 2008. **586**(1): p. 161-73.

82. Amann, M., et al., *Arterial oxygenation influences central motor output and exercise performance via effects on peripheral locomotor muscle fatigue in humans.* The Journal of physiology, 2006. **575**(3): p. 937-952.
83. Noakes, T. and A.S.C. Gibson, *Logical limitations to the "catastrophe" models of fatigue during exercise in humans.* British Journal of Sports Medicine, 2004. **38**(5): p. 648-649.
84. Garcia-Manso, J.M., et al., *Assessment of muscle fatigue after an ultra-endurance triathlon using tensiomyography (TMG).* J Sports Sci, 2011. **29**(6): p. 619-25.
85. Jones, D.A., *Changes in the force-velocity relationship of fatigued muscle: implications for power production and possible causes.* J Physiol, 2010. **588**(Pt 16): p. 2977-86.
86. Taylor, J.L. and S.C. Gandevia, *Transcranial magnetic stimulation and human muscle fatigue.* Muscle & nerve, 2001. **24**(1): p. 18-29.
87. Cifrek, M., et al., *Surface EMG based muscle fatigue evaluation in biomechanics.* Clin Biomech (Bristol, Avon), 2009. **24**(4): p. 327-40.
88. Reaz, M., M. Hussain, and F. Mohd-Yasin, *Techniques of EMG signal analysis: detection, processing, classification and applications.* Biological procedures online, 2006. **8**(1): p. 11-35.
89. PETROFSKY, J.S., et al., *Evaluation of the amplitude and frequency components of the surface EMG as an index of muscle fatigue.* Ergonomics, 1982. **25**(3): p. 213-223.
90. Oskoei, M.A., H. Hu, and J.Q. Gan. *Manifestation of fatigue in myoelectric signals of dynamic contractions produced during playing PC games*. in *2008 30th Annual International Conference of the IEEE Engineering in Medicine and Biology Society*. 2008. IEEE.
91. Phinyomark, A., et al., *The usefulness of mean and median frequencies in electromyography analysis*. 2012: INTECH Open Access Publisher.
92. Thongpanja, S., et al., *A feasibility study of fatigue and muscle contraction indices based on EMG time-dependent spectral analysis.* Procedia Engineering, 2012. **32**: p. 239-245.
93. Stulen, F.B. and C.J. De Luca, *Frequency parameters of the myoelectric signal as a measure of muscle conduction velocity.* IEEE Transactions on Biomedical Engineering, 1981(7): p. 515-523.
94. Bonato, P., et al., *Time-frequency parameters of the surface myoelectric signal for assessing muscle fatigue during cyclic dynamic contractions.* IEEE Transactions on Biomedical Engineering, 2001. **48**(7): p. 745-753.
95. Gonzalez-Izal, M., et al., *Electromyographic models to assess muscle fatigue.* J Electromyogr Kinesiol, 2012. **22**(4): p. 501-12.
96. Gonzalez-Izal, M., et al., *EMG spectral indices and muscle power fatigue during dynamic contractions.* J Electromyogr Kinesiol, 2010. **20**(2): p. 233-40.
97. Luttmann, A., M. Jäger, and W. Laurig, *Electromyographical indication of muscular fatigue in occupational field studies.* International Journal of Industrial Ergonomics, 2000. **25**(6): p. 645-660.
98. Farina, D., M. Fosci, and R. Merletti, *Motor unit recruitment strategies investigated by surface EMG variables.* Journal of Applied Physiology, 2002. **92**(1): p. 235-247.
99. Merletti, R., M.A. Sabbahi, and C.J. De Luca, *Median frequency of the myoelectric signal.* European journal of applied physiology and occupational physiology, 1984. **52**(3): p. 258-265.
100. Brody, L., et al., *pH-induced effects on median frequency and conduction velocity of the myoelectric signal.* Journal of Applied Physiology, 1991. **71**(5): p. 1878-1885.
101. De Luca, C.J., *Myoelectrical manifestations of localized muscular fatigue in humans.* Critical reviews in biomedical engineering, 1983. **11**(4): p. 251-279.

102. Brody, L., et al., *pH-induced effects on median frequency and conduction velocity of the myoelectric signal.* J Appl Physiol, 1991. **71**(5): p. 1878-1885.
103. Solomonow, M., et al., *Electromyogram power spectra frequencies associated with motor unit recruitment strategies.* J Appl Physiol, 1990. **68**(3): p. 1177-85.
104. Dimitrova, N. and G. Dimitrov, *Interpretation of EMG changes with fatigue: facts, pitfalls, and fallacies.* Journal of Electromyography and Kinesiology, 2003. **13**(1): p. 13-36.
105. KRANZ, H., et al., *Factors determining the frequency content of the electromyogram.* Journal of applied physiology: respiratory, environmental and exercise physiology, 1983. **55**: p. 392-399.
106. Troni, W., M. DeMattei, and V. Contegiacomo, *The effect of temperature on conduction velocity in human muscle fibers.* Journal of Electromyography and Kinesiology, 1991. **1**(4): p. 281-287.
107. De Luca, C.J., *Spectral compression of the EMG signal as an index of muscle fatigue.* Neuromuscular fatigue. Royal Netherlands Academy of Arts and Sciences, Amsterdam, The Netherlands, 1992: p. 44-51.
108. Horita, T. and T. Ishiko, *Relationships between muscle lactate accumulation and surface EMG activities during isokinetic contractions in man.* European journal of applied physiology and occupational physiology, 1987. **56**(1): p. 18-23.
109. De Luca, C.J., *The use of surface electromyography in biomechanics.* Journal of applied biomechanics, 1997. **13**: p. 135-163.
110. Gamet, D., et al., *Surface electromyogram power spectrum in human quadriceps muscle during incremental exercise.* Journal of Applied Physiology, 1993. **74**: p. 2704-2704.
111. Finsterer, J., *Biomarkers of peripheral muscle fatigue during exercise.* BMC musculoskeletal disorders, 2012. **13**(1): p. 218.
112. Yoshida, T., *Effect of exercise duration during incremental exercise on the determination of anaerobic threshold and the onset of blood lactate accumulation.* European journal of applied physiology and occupational physiology, 1984. **53**(3): p. 196-199.
113. Grassi, B., et al., *Blood lactate accumulation and muscle deoxygenation during incremental exercise.* Journal of Applied Physiology, 1999. **87**(1): p. 348-355.
114. Stoudemire, N.M., et al., *The validity of regulating blood lactate concentration during running by ratings of perceived exertion.* Medicine and science in sports and exercise, 1996. **28**(4): p. 490-495.
115. Noakes, T.D., *Fatigue is a Brain-Derived Emotion that Regulates the Exercise Behavior to Ensure the Protection of Whole Body Homeostasis.* Front Physiol, 2012. **3**: p. 82.
116. Ishii, H. and Y. Nishida, *Effect of lactate accumulation during exercise-induced muscle fatigue on the sensorimotor cortex.* Journal of physical therapy science, 2013. **25**(12): p. 1637-1642.
117. Hampson, D.B., et al., *The influence of sensory cues on the perception of exertion during exercise and central regulation of exercise performance.* Sports Medicine, 2001. **31**(13): p. 935-952.
118. Marcora, S., *Perception of effort during exercise is independent of afferent feedback from skeletal muscles, heart, and lungs.* J Appl Physiol (1985), 2009. **106**(6): p. 2060-2.
119. Noble, B.J. and R.J. Robertson, *Perceived exertion*. 1996: Human Kinetics Champaign, IL.

120. Grazzini, M., et al., *Pathophysiology of exercise dyspnea in healthy subjects and in patients with chronic obstructive pulmonary disease (COPD).* Respiratory medicine, 2005. **99**(11): p. 1403-1412.
121. Proske, U., *What is the role of muscle receptors in proprioception?* Muscle Nerve, 2005. **31**(6): p. 780-7.
122. Mihevic, P.M., *Sensory cues for perceived exertion: a review.* Medicine and Science in Sports and Exercise, 1980. **13**(3): p. 150-163.
123. Robertson, R.J., et al., *Validation of the adult OMNI scale of perceived exertion for cycle ergometer exercise.* Medicine & Science in Sports & Exercise, 2004. **36**(1): p. 102-108.
124. Utter, A.C., et al., *Validation of the Adult OMNI Scale of perceived exertion for walking/running exercise.* Medicine and science in sports and exercise, 2004. **36**(10): p. 1776-1780.
125. Irving, B.A., et al., *Comparison of Borg-and OMNI-RPE as markers of the blood lactate response to exercise.* Medicine & Science in Sports & Exercise, 2006. **38**(7): p. 1348-1352.
126. McGuigan, M.R., A.D. Egan, and C. Foster, *Salivary cortisol responses and perceived exertion during high intensity and low intensity bouts of resistance exercise.* Journal of sports science & medicine, 2004. **3**(1): p. 8.
127. Noakes, T., *Physiological models to understand exercise fatigue and the adaptations that predict or enhance athletic performance.* Scandinavian journal of medicine & science in sports, 2000. **10**(3): p. 123-145.
128. Health, U.S.D.o., *Physical activity and health: a report of the Surgeon General*. 1996: DIANE Publishing.
129. Faude, O., W. Kindermann, and T. Meyer, *Lactate threshold concepts.* Sports medicine, 2009. **39**(6): p. 469-490.
130. Carey, D.G., et al., *Respiratory rate is a valid and reliable marker for the anaerobic threshold: implications for measuring change in fitness.* Journal of sports science & medicine, 2005. **4**(4): p. 482.
131. Achten, J. and A.E. Jeukendrup, *Heart rate monitoring.* Sports medicine, 2003. **33**(7): p. 517-538.
132. Benson, R. and D. Connolly, *Heart rate training*. 2011: Human Kinetics.
133. Mognoni, P., et al., *Physiological responses during prolonged exercise at the power output corresponding to the blood lactate threshold.* European journal of applied physiology and occupational physiology, 1990. **60**(4): p. 239-243.
134. Rowell, L.B., *Human cardiovascular adjustments to exercise and thermal stress.* Physiological Reviews, 1974. **54**(1): p. 75-159.
135. Gandevia, S., et al., *Respiratory sensations, cardiovascular control, kinaesthesia and transcranial stimulation during paralysis in humans.* The Journal of physiology, 1993. **470**(1): p. 85-107.
136. Leonard, B., et al., *Partial neuromuscular blockade and cardiovascular responses to static exercise in man.* The Journal of physiology, 1985. **359**(1): p. 365-379.
137. Gallagher, K., et al., *Effects of partial neuromuscular blockade on carotid baroreflex function during exercise in humans.* The Journal of physiology, 2001. **533**(3): p. 861-870.
138. Mitchell, J.H., *Cardiovascular control during exercise: central and reflex neural mechanisms.* The American journal of cardiology, 1985. **55**(10): p. D34-D41.
139. Williamson, J., et al., *Hypnotic manipulation of effort sense during dynamic exercise: cardiovascular responses and brain activation.* Journal of Applied Physiology, 2001. **90**(4): p. 1392-1399.

140. Williamson, J., et al., *Brain activation by central command during actual and imagined handgrip under hypnosis.* Journal of Applied Physiology, 2002. **92**(3): p. 1317-1324.
141. Steed, J., G.A. Gaesser, and A. Weltman, *Rating of perceived exertion and blood lactate concentration during submaximal running.* Medicine & Science in Sports & Exercise, 1994.
142. Rau, G., E. Schulte, and C. Disselhorst-Klug, *From cell to movement: to what answers does EMG really contribute?* Journal of Electromyography and Kinesiology, 2004. **14**(5): p. 611-617.
143. Dugan, S.A. and K.P. Bhat, *Biomechanics and analysis of running gait.* Phys Med Rehabil Clin N Am, 2005. **16**(3): p. 603-21.
144. Hreljac, A., *Impact and Overuse Injuries in Runners.* Medicine & Science in Sports & Exercise, 2004: p. 845-849.
145. Lin, D., et al., *Acute effects of localized muscle fatigue on postural control and patterns of recovery during upright stance: influence of fatigue location and age.* European journal of applied physiology, 2009. **106**(3): p. 425-434.
146. Parijat, P. and T.E. Lockhart, *Effects of quadriceps fatigue on the biomechanics of gait and slip propensity.* Gait & posture, 2008. **28**(4): p. 568-573.
147. Daoud, A.I., et al., *Foot strike and injury rates in endurance runners: a retrospective study.* Med Sci Sports Exerc, 2012. **44**(7): p. 1325-34.
148. Jidovtseff, B., et al. *INFLUENCE OF FATIGUE ON THE STRIDE CHARACTERISTICS DURING AN INTENSE ENDURANCE RUNTEST*. in *Abstract book of 17th ECSS Congress*. 2012.
149. Novacheck, T.F., *The biomechanics of running.* Gait & posture, 1998. **7**(1): p. 77-95.
150. Hamner, S.R., A. Seth, and S.L. Delp, *Muscle contributions to propulsion and support during running.* J Biomech, 2010. **43**(14): p. 2709-16.
151. Mann, R.A., D.E. Baxter, and L.D. Lutter, *Running symposium.* Foot & Ankle International, 1981. **1**(4): p. 190-224.
152. Keller, T., et al., *Relationship between vertical ground reaction force and speed during walking, slow jogging, and running.* Clinical Biomechanics, 1996. **11**(5): p. 253-259.
153. Butler, R.J., H.P. Crowell III, and I.M. Davis, *Lower extremity stiffness: implications for performance and injury.* Clinical Biomechanics, 2003. **18**(6): p. 511-517.
154. Williams, K.R. and P.R. Cavanagh, *Relationship between distance running mechanics, running economy, and performance.* J Appl Physiol, 1987. **63**(3): p. 1236-1245.
155. Di Michele, R., *Relationships between running economy and mechanics in middle-distance runners.* 2008.
156. Murdock, G. and C. Hubley-Kozey, *Effect of a high intensity quadriceps fatigue protocol on knee joint mechanics and muscle activation during gait in young adults.* European Journal of Applied Physiology, 2012. **112**(2): p. 439-449.
157. Sadeghi, H., et al., *Symmetry and limb dominance in able-bodied gait: a review.* Gait & posture, 2000. **12**(1): p. 34-45.
158. Vagenas, G. and B. Hoshizaki, *A multivariable analysis of lower extremity kinematic asymmetry in running.* International Journal of Sport Biomechanics, 1992. **8**(1).
159. Chang, Y. and H. Chiu. *THE IMPACT ACCELERATION ON THE BILATERAL TIBIA DURING TREADMILL RUNNING*. in *ISBS-Conference Proceedings Archive*. 2010.
160. Brown, A.M., R.A. Zifchock, and H.J. Hillstrom, *The effects of limb dominance and fatigue on running biomechanics.* Gait & posture, 2014. **39**(3): p. 915-919.
161. Rumpf, M.C., et al., *Kinetic asymmetries during running in male youth.* Physical Therapy in Sport, 2014. **15**(1): p. 53-57.

162. Pappas, P., G. Paradisis, and G. Vagenas, *Leg and vertical stiffness (a) symmetry between dominant and non-dominant legs in young male runners.* Human movement science, 2015. **40**: p. 273-283.
163. Lee, J., et al., *Correlation Between Treadmill Acceleration, Plantar Pressure, and Ground ieaction Force During Running (P52)*, in *The Engineering of Sport 7*. 2009, Springer. p. 281-290.
164. Flynn, J.M., J.D. Holmes, and D.M. Andrews, *The effect of localized leg muscle fatigue on tibial impact acceleration.* Clinical Biomechanics, 2004. **19**(7): p. 726-732.
165. Mann, R.A. and J. Hagy, *Biomechanics of walking, running, and sprinting.* The American Journal of Sports Medicine, 1980. **8**(5): p. 345-350.
166. Ounpuu, S., *The biomechanics of running: a kinematic and kinetic analysis.* Instructional course lectures, 1989. **39**: p. 305-318.
167. DeVita, P., *The selection of a standard convention for analyzing gait data based on the analysis of relevant biomechanical factors.* Journal of biomechanics, 1994. **27**(4): p. 501-508.
168. Kyrolainen, H., J. Avela, and P.V. Komi, *Changes in muscle activity with increasing running speed.* J Sports Sci, 2005. **23**(10): p. 1101-9.
169. Dickinson, J.A., S.D. Cook, and T.M. Leinhardt, *The measurement of shock waves following heel strike while running.* Journal of biomechanics, 1985. **18**(6): p. 415-422.
170. Cowley, E. and J. Marsden, *The effects of prolonged running on foot posture: a repeated measures study of half marathon runners using the foot posture index and navicular height.* Journal of foot and ankle research, 2013. **6**(1): p. 1-7.
171. LA INEN, H.K., A. Belli, and P.V. Komi, *Biomechanical factors affecting running economy.* 2001.
172. Weist, R., *The Influence of Muscle Fatigue on Electromyogram and Plantar Pressure Patterns as an Explanation for the Incidence of Metatarsal Stress Fractures.* American Journal of Sports Medicine, 2004. **32**(8): p. 1893-1898.
173. Hreljac, A., R.N. Marshall, and P.A. Hume, *Evaluation of lower extremity overuse injury potential in runners.* Medicine and science in sports and exercise, 2000. **32**(9): p. 1635-1641.
174. Holden, J.P. and P.R. Cavanagh, *The free moment of ground reaction in distance running and its changes with pronation.* Journal of biomechanics, 1991. **24**(10): p. 887-897.
175. Barry, D.T., T. Hill, and D. Im, *Muscle fatigue measured with evoked muscle vibrations.* Muscle & nerve, 1992. **15**(3): p. 303-309.
176. Jaskólska, A., et al., *A comparison between mechanomyographic condenser microphone and accelerometer measurements during submaximal isometric, concentric and eccentric contractions.* Journal of Electromyography and Kinesiology, 2007. **17**(3): p. 336-347.
177. Al-Zahrani, E., et al., *Within-day and between-days reliability of quadriceps isometric muscle fatigue using mechanomyography on healthy subjects.* Journal of Electromyography and Kinesiology, 2009. **19**(4): p. 695-703.
178. Ferrari, M., T. Binzoni, and V. Quaresima, *Oxidative metabolism in muscle.* Philosophical Transactions of the Royal Society of London B: Biological Sciences, 1997. **352**(1354): p. 677-683.
179. Eston, R.G., B.L. Davies, and J.G. Williams, *Use of perceived effort ratings to control exercise intensity in young healthy adults.* European journal of applied physiology and occupational physiology, 1987. **56**(2): p. 222-224.
180. Hepple, R.T., *The role of O2 supply in muscle fatigue.* Canadian journal of applied physiology, 2002. **27**(1): p. 56-69.

181. St Clair Gibson, A. and T.D. Noakes, *Evidence for complex system integration and dynamic neural regulation of skeletal muscle recruitment during exercise in humans.* Br J Sports Med, 2004. **38**(6): p. 797-806.
182. Chan-Roper, M., et al., *Kinematic changes during a marathon for fast and slow runners.* Journal of sports science & medicine, 2012. **11**(1): p. 77.
183. Paillard, T., et al., *Electrical stimulation superimposed onto voluntary muscular contraction.* Sports medicine, 2005. **35**(11): p. 951-966.
184. Taylor, J.L. and S.C. Gandevia, *Noninvasive stimulation of the human corticospinal tract.* J Appl Physiol (1985), 2004. **96**(4): p. 1496-503.
185. Belcher, C.P. and C.L. Pemberton, *The use of the blood lactate curve to develop training intensity guidelines for the sports of track and field and cross-country.* International Journal of Exercise Science, 2012. **5**(2): p. 7.
186. Kyröläinen, H., et al., *Effects of marathon running on running economy and kinematics.* European journal of applied physiology, 2000. **82**(4): p. 297-304.
187. Cheuvront, S.N., et al., *Running performance differences between men and women.* Sports Medicine, 2005. **35**(12): p. 1017-1024.
188. Velotta, J., et al., *Relationship between leg dominance tests and type of task.* Methods, 2011. **11**: p. 2.
189. Souza, R.B., *An evidence-based videotaped running biomechanics analysis.* Physical medicine and rehabilitation clinics of North America, 2016. **27**(1): p. 217-236.
190. Herrington, L. and A. Munro, *Drop jump landing knee valgus angle; normative data in a physically active population.* Physical Therapy in Sport, 2010. **11**(2): p. 56-59.
191. Miller, A. and R. Callister, *Reliable lower limb musculoskeletal profiling using easily operated, portable equipment.* Physical Therapy in Sport, 2009. **10**(1): p. 30-37.
192. Norris, B.S. and S.L. Olson, *Concurrent validity and reliability of two-dimensional video analysis of hip and knee joint motion during mechanical lifting.* Physiotherapy theory and practice, 2011. **27**(7): p. 521-530.
193. Quintin. *Quintin Gait Analysis*. 2D Biomechanical Model]. Available from: http://www.quinticsports.com/wp-content/uploads/2016/06/Alpha-Beta-6mph-BF.pdf.
194. Vaughan, C.L., B.L. Davis, and J.C. O'connor, *Dynamics of human gait*. 1992: Human Kinetics Publishers Champaign, Illinois.
195. Barton, C.J., et al., *Foot and ankle characteristics in patellofemoral pain syndrome: a case control and reliability study.* journal of orthopaedic & sports physical therapy, 2010. **40**(5): p. 286-296.
196. O'Rahilly, R. and F. Müller, *Basic human anatomy: a regional study of human structure*. 1983: WB Saunders Company.
197. Nigg, B.M., *The role of impact forces and foot pronation: a new paradigm.* Clinical journal of sport medicine, 2001. **11**(1): p. 2-9.
198. Carter, H., et al., *The effect of interdian and diurnal variation on oxygen uptake kinetics during treadmill running.* Journal of sports sciences, 2002. **20**(11): p. 901-909.
199. Fuller, J.T., et al., *The effect of footwear on running performance and running economy in distance runners.* Sports Medicine, 2015. **45**(3): p. 411-422.
200. van Hall, G., *Lactate kinetics in human tissues at rest and during exercise.* Acta Physiol (Oxf), 2010. **199**(4): p. 499-508.
201. Jones, A.M. and J.H. Doust, *A 1% treadmill grade most accurately reflects the energetic cost of outdoor running.* Journal of sports sciences, 1996. **14**(4): p. 321-327.
202. Ali, M.J., et al. *KNEE AXIAL SHOCK TRANSMISSION FROM TIBIA TO FEMUR DURING CONTINUOUS SPEED RUN TO EXHAUSTION: AN EXPLORATORY STUDY*. in *1st International Conference in Sports Science & Technology*. 2014. Singapore.

203. Howley, E.T., D.R. Bassett, and H.G. Welch, *Criteria for maximal oxygen uptake: review and commentary.* Medicine and science in sports and Exercise, 1995. **27**(9): p. 1292-1301.
204. Seiler, S. and K.J. Hetlelid, *The impact of rest duration on work intensity and RPE during interval training.* Medicine and Science in Sports and Exercise, 2005. **37**(9): p. 1601.
205. Konrad, P., *The abc of emg.* A practical introduction to kinesiological electromyography, 2005. **1**.
206. Ward, S.R., et al., *Are current measurements of lower extremity muscle architecture accurate?* Clin Orthop Relat Res, 2009. **467**(4): p. 1074-82.
207. Shorten, M.R. and D.S. Winslow, *Spectral analysis of impact shock during running.* International Journal of Sport Biomechanics, 1992. **8**: p. 288-288.
208. Elvin, N.G., A.A. Elvin, and S.P. Arnoczky, *Correlation between ground reaction force and tibial acceleration in vertical jumping.* Journal of applied biomechanics, 2007. **23**(3): p. 180.
209. Heiderscheit, B.C., et al., *Effects of step rate manipulation on joint mechanics during running.* Medicine and science in sports and exercise, 2011. **43**(2): p. 296.
210. Fhrenbach, R., et al., *Determination of Endurance Capacity and Prediction of Exercise Intensities for Training and Competition in Marathon Runners.* International journal of sports medicine, 1987. **08**(01): p. 11-18.
211. Nicholson, R.M. and G.G. Sleivert, *Indices of lactate threshold and their relationship with 10-km running velocity.* Medicine and science in sports and exercise, 2001. **33**(2): p. 339-342.
212. Smith, C.G. and A.M. Jones, *The relationship between critical velocity, maximal lactate steady-state velocity and lactate turnpoint velocity in runners.* European journal of applied physiology, 2001. **85**(1-2): p. 19-26.
213. Almarwaey, O.A., A.M. Jones, and K. Tolfrey, *Maximal lactate steady state in trained adolescent runners.* J Sports Sci, 2004. **22**(2): p. 215-25.
214. Greenhouse, S.W. and S. Geisser, *On methods in the analysis of profile data.* Psychometrika, 1959. **24**(2): p. 95-112.
215. Lamberts, R.P., et al., *Heart rate recovery as a guide to monitor fatigue and predict changes in performance parameters.* Scand J Med Sci Sports, 2010. **20**(3): p. 449-57.
216. Brooks, G.A. and J. Mercier, *Balance of carbohydrate and lipid utilization during exercise: the" crossover" concept.* Journal of applied physiology, 1994. **76**(6): p. 2253-2261.
217. Gastin, P.B., *Energy system interaction and relative contribution during maximal exercise.* Sports medicine, 2001. **31**(10): p. 725-741.
218. Horowitz, J.F. and S. Klein, *Lipid metabolism during endurance exercise.* The American journal of clinical nutrition, 2000. **72**(2): p. 558s-563s.
219. Tomlin, D.L. and H.A. Wenger, *The relationship between aerobic fitness and recovery from high intensity intermittent exercise.* Sports Medicine, 2001. **31**(1): p. 1-11.
220. Beneke, R., *Methodological aspects of maximal lactate steady state—implications for performance testing.* European journal of applied physiology, 2003. **89**(1): p. 95-99.
221. de Lucas, R.D., et al., *Is the critical running speed related to the intermittent maximal lactate steady state?* Journal of sports science & medicine, 2012. **11**(1): p. 89.
222. Ali, M.J., Hoon, K.H., Seet, G,, & Balasekaran, G., *Heart Rate Monitors for Predicting Physiological Stress in Runners During Critical Speed Intermittent Stage Protocol*, in *2nd International Conference in Sports Science & Technology, Singapore*. December, 2016: Singapore.

223. Amann, M., *Significance of Group III and IV muscle afferents for the endurance exercising human.* Clin Exp Pharmacol Physiol, 2012. **39**(9): p. 831-5.
224. Schubert, A.G., J. Kempf, and B.C. Heiderscheit, *Influence of Stride Frequency and Length on Running Mechanics A Systematic Review.* Sports Health: A Multidisciplinary Approach, 2013: p. 1941738113508544.
225. Riley, P.O., et al., *A kinematics and kinetic comparison of overground and treadmill running.* Medicine and science in sports and exercise, 2008. **40**(6): p. 1093.
226. Millet, G.Y., *Can Neuromuscular Fatigue Explain Running Strategies and Performance in Ultra-Marathons?* Sports medicine, 2011. **41**(6): p. 489-506.
227. Frayne, D.H., *Kinetic Asymmetries During Submaximal and Maximal Speed Running.* 2014.
228. Carpes, F.P., C.B. Mota, and I.E. Faria, *On the bilateral asymmetry during running and cycling–A review considering leg preference.* Physical Therapy in Sport, 2010. **11**(4): p. 136-142.
229. Sadeghi, H., P. Allard, and M. Duhaime, *Functional gait asymmetry in able-bodied subjects.* Human Movement Science, 1997. **16**(2): p. 243-258.
230. Nummela, A., T. Keränen, and L. Mikkelsson, *Factors related to top running speed and economy.* International journal of sports medicine, 2007. **28**(08): p. 655-661.
231. Williams, K.R. and P.R. Cavanagh, *Relationship between distance running mechanics, running economy, and performance.* Journal of Applied Physiology, 1987. **63**(3): p. 1236-1245.
232. Scheuermann, B.W., J.T. McConnell, and T.J. Barstow, *EMG and oxygen uptake responses during slow and fast ramp exercise in humans.* Experimental physiology, 2002. **87**(1): p. 91-100.
233. Hanon, C., et al., *Electromyogram as an indicator of neuromuscular fatigue during incremental exercise.* European journal of applied physiology and occupational physiology, 1998. **78**(4): p. 315-323.
234. Riemann, B.L., et al., *Medial and lateral gastrocnemius activation differences during heel-raise exercise with three different foot positions.* The Journal of Strength & Conditioning Research, 2011. **25**(3): p. 634-639.
235. Oyono-Enguelle, S., et al., *Blood lactate during constant-load exercise at aerobic and anaerobic thresholds.* European journal of applied physiology and occupational physiology, 1990. **60**(5): p. 321-330.
236. Moritani, T., et al., *Critical power as a measure of physical work capacity and anaerobic threshold.* Ergonomics, 1981. **24**(5): p. 339-350.
237. Brickley, G., J. Doust, and C. Williams, *Physiological responses during exercise to exhaustion at critical power.* European journal of applied physiology, 2002. **88**(1): p. 146-151.
238. Bull, A.J., et al., *Physiological responses at five estimates of critical velocity.* European journal of applied physiology, 2008. **102**(6): p. 711-720.
239. De Lucas, R., et al., *Time to exhaustion at and above critical power in trained cyclists: The relationship between heavy and severe intensity domains.* Science & Sports, 2013. **28**(1): p. e9-e14.
240. Vanhatalo, A., A.M. Jones, and M. Burnley, *Application of critical power in sport.* Int J Sports Physiol Perform, 2011. **6**(1): p. 128-136.
241. Florence, S.-l. and J.P. Weir, *Relationship of critical velocity to marathon running performance.* European journal of applied physiology and occupational physiology, 1997. **75**(3): p. 274-278.

242. Hughson, R., C. Orok, and L. Staudt, *A high velocity treadmill running test to assess endurance running potential.* International journal of sports medicine, 1984. **5**(01): p. 23-25.
243. Wakayoshi, K., et al., *Does critical swimming velocity represent exercise intensity at maximal lactate steady state?* European journal of applied physiology and occupational physiology, 1993. **66**(1): p. 90-95.
244. Crisp, A.H., et al., *Time to Exhaustion at VO2 Max Velocity in Basketball and Soccer Athletes.* Journal of Exercise Physiology Online, 2013. **16**(2).
245. Marcora, S.M. and W. Staiano, *The limit to exercise tolerance in humans: mind over muscle?* European journal of applied physiology, 2010. **109**(4): p. 763-770.
246. Carter, H., et al., *Oxygen uptake kinetics during treadmill running across exercise intensity domains.* European journal of applied physiology, 2002. **86**(4): p. 347-354.
247. Carter, H., et al., *Oxygen uptake kinetics in treadmill running and cycle ergometry: a comparison.* Journal of Applied Physiology, 2000. **89**(3): p. 899-907.
248. Eberstein, A. and B. Beattie, *Simultaneous measurement of muscle conduction velocity and EMG power spectrum changes during fatigue.* Muscle & nerve, 1985. **8**(9): p. 768-773.
249. Hussain, I. and N. Ansari, *Influence of Kinematics Variables on Distance Running during Competition.* International Journal of Sports Science, 2013. **3**(3): p. 63-67.
250. Macedo, D.V., et al., *Is lactate production related to muscular fatigue? A pedagogical proposition using empirical facts.* Advances in physiology education, 2009. **33**(4): p. 302-307.
251. Moxnes, J.F. and Ø. Sandbakk, *The kinetics of lactate production and removal during whole-body exercise.* Theor Biol Med Model, 2012. **9**(7).
252. Muhammad Jafar Ali, G.B., Hoon Kay Hiang, Seet Gerald, *Effects of physiological predictors on endurance performance in recreational runners*, in *The Physiological Society*. 2016: Dublin Ireland.
253. Zamunér, A.R., et al., *Assessment of subjective perceived exertion at the anaerobic threshold with the Borg CR-10 scale.* Journal of sports science & medicine, 2011. **10**(1): p. 130.
254. Penteado, R., et al., *Physiological responses at critical running speed during continuous and intermittent exhaustion tests.* Science & Sports, (0).
255. Ali, M.J., et al. *EFFECT OF FATIGUE ON RUNNING KINETIC ASYMMETRY IN NONCONTINUOUS & CONTINUOUS CONSTANT SPEED PROTOCOL*. in *ISBS-Conference Proceedings Archive*. 2016.
256. Borg, G.A., *Physical performance and perceived exertion*. 1962: Gleerup Lund.
257. García-Pérez, J.A., et al., *Effects of treadmill running and fatigue on impact acceleration in distance running.* Sports Biomechanics, 2014. **13**(3): p. 259-266.
258. El Helou, N., et al., *Impact of environmental parameters on marathon running performance.* PloS one, 2012. **7**(5): p. e37407.
259. Montgomery III, W.H., M. Pink, and J. Perry, *Electromyographic analysis of hip and knee musculature during running.* The American journal of sports medicine, 1994. **22**(2): p. 272-278.

Bibliography

a) Individual Feedback based on Every Stage

Stages	Heart Rate	Blood Lactate	RPE (physiological)	RPE (Muscular)	RPE- Overall
Resting					
1					
2					
3					
4					
5					
6					
7					
8					
9					
10					
11					
12					
13					
14					
15					
16					
17					
18					
19					
20					
21					
22					
23					
24					
25					
26					
27					
28					
29					
30					
31					
32					

b) HEALTH HISTORY QUESTIONNAIRE PHYSICAL EXAMINATION

PERSONAL HEALTH ASSESSMENT: *For the following questions, please check yes if you are presently having a problem or have had a problem in the past. If there is no significant problem, check no. Briefly, explain all yes answers.*

TO BE COMPLETED BY STUDENT:

Drug Usage:	**Yes**	**No**
Alcohol, Smoke	☐	☐
Comments: _____		

Cardiovascular

Heart Palpation	☐	☐
Chest Pain	☐	☐
High Blood Pressure	☐	☐
Irregular Heart Beat	☐	☐
Enlarge Heart	☐	☐

Comments: _____

Respiratory

Asthma	☐	☐
Chest Infection	☐	☐
Smoke Cigrete	☐	☐
Wheezing	☐	☐

Comments: _____

Mental Health

Medication	☐	☐

Hospitalization	**Yes**	**No**
Admitted to hospital ever	☐	☐
Had surgery?	☐	☐

Comments: _____

Blood

Anemia	☐	☐
Abnormal Bleeding	☐	☐

Comments: _____

Bone and Joint

Any Disease of Bone	☐	☐
Joint fracture	☐	☐
Bone fracture	☐	☐

Comments: _____

Neurology

Convulsion	☐	☐
Fainting	☐	☐
Dizziness	☐	☐

Comments: _____

I certify that above information is true to the best of my knowledge.

_____ _____

Participant Name & Signature: **Date:**

c) How Do You Feel?

This inventory contains a number of items designed to reflect how you feel at this particular moment in time (i.e., Right Now). Please circle the number on each item that indicates HOW YOU FEEL RIGHT NOW.

I FEEL:

1. Great

1	2	3	4	5	6	7
Not at All			Moderately			Very Much

2. Awful (very bad, unpleasant)

1	2	3	4	5	6	7
Not at All			Moderately			Very Much

3. Drained (thirst level, low energy)

1	2	3	4	5	6	7
Not at All			Moderately			Very Much

4. Positive

1	2	3	4	5	6	7
Not at All			Moderately			Very Much

5. Crummy (unwell, depressed)

1	2	3	4	5	6	7
Not at All			Moderately			Very Much

6. Exhausted (physical exertion level)

1	2	3	4	5	6	7
Not at All			Moderately			Very Much

7. Strong

1	2	3	4	5	6	7
Not at All			Moderately			Very Much

8. Discouraged

1	2	3	4	5	6	7

Not at All	Moderately	Very Much

9. Fatigued

1	2	3	4	5	6	7
Not at All			Moderately			Very Much

10. Terrific (tough, hard, getting fear)

1	2	3	4	5	6	7
Not at All			Moderately			Very Much

11. Miserable (uncomfortable, unhappy)

1	2	3	4	5	6	7
Not at All			Moderately			Very Much

12. Tired

1	2	3	4	5	6	7
Not at All			Moderately			Very Much

d) PARTICIPANT CONSENT FORM

Please date and sign this page below to indicate that you understand and accept the conditions of this study.

I hereby acknowledge that:

1. My signature is my acknowledgment that I voluntarily agreed to take part in the above research.
2. I have received a copy of this information sheet that explains the research study. I understand its contents and I have been given the opportunity to ask questions and have had any questions answered to my satisfaction.
3. I am aware that I have the right to withdraw consent and to discontinue my participation at any time, without prejudice or penalty.
4. My rights to compensation for personal injury arising out of the negligence of Nanyang Technological University are preserved. I agree and accept that I (or anyone on my behalf) shall not seek or be entitled to any compensation from the said institution, if I sustain any loss or injuries (including fatal injuries) because of my participation (involvement) in this research where such loss or injuries are caused otherwise than by the negligence of the said institution.
5. I will not have any rights to commercial benefits that result from this research.
6. I agree not to share information about any products/prototypes that I may use and which are still in development stage, are considered proprietary, and which are shared with me only for the purpose of this study.
7. I agree to have the video or photographs that identify me to be used in any subsequent publications resulting from the research. (Personal details such as my name or contact details will NOT be used in any publication/presentation resulting from this research).
8. I agree to be re-contacted if multiple interviews are required

_____ _____

Name and Signature (Participant) Date

e) RELATIVE PERCIEVED EXERTION SCALE (CR-10)

OMNI Scale	
0	Extremely Easy
1	
2	Easy
3	
4	Somewhat Easy
5	
6	Somehow Hard
7	
8	Hard
9	
10	Extremely hard

Pictorial representation of OMNI scale used numerical ratings to describe the perceived exertion rating from 0 to 10. The perceived exertion can be seen in the attached Figure related to intensity zone and exertion rating. The pictorial format will be used so that "the exertion meaning of each pictorial descriptor is constant with its verbal descriptor to quantify exertion.

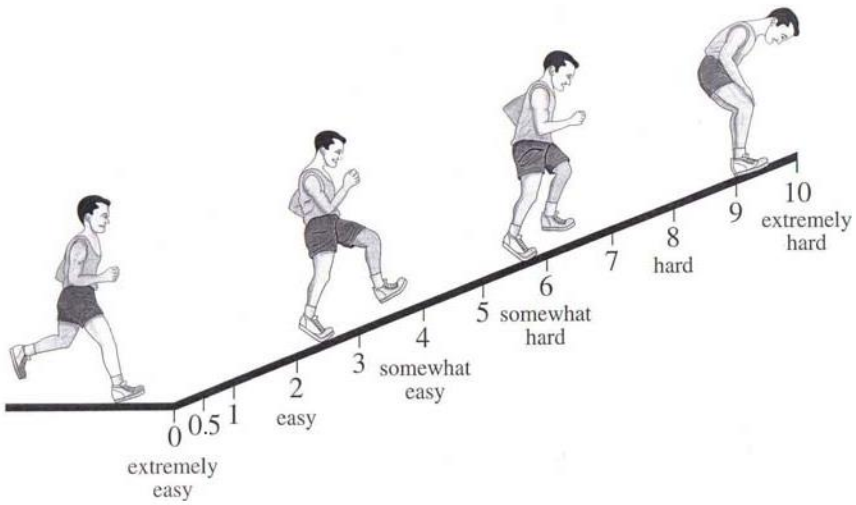

Appendix

PUBLICATIONS

Patent/ Technical Disclosure:

1. Singapore Patent Application No. 10201510435S, NTU Ref: TD/259/15,
   Title: Kinesiological Endurance Training System (KETS)

Journals:

1. Muhammad Jafar Ali, Govindasamay. B., Hoon, K.H, Seet, Gerald., Physiological Differences between a non-continuous and a continuous endurance training protocol in recreational runners and metabolic demand prediction, Physiological Reports, DOI:10.14814/phy2.13546.
2. Ali, M. J., Hoon, K.H, Seet, Gerald, Balasekaran, G., Biomechanical and Physiological Manifestation of Fatigue and Neuromuscular Activity in Runner's Gait during Intermittent Stage Protocol: An Exploratory Study (submitted in Journal of Biomechanics: Confirmation pending)

Conferences:

1. Ali, M. J., Hoon, K.H, Seet, Gerald, Balasekaran, G., & McLaren, J. (2014, 11-12 December 2014). Knee axial shock transmission from tibia to femur during continuous speed run to exhaustion: an exploratory study. 1st International Conference in Sports Science & Technology, Singapore.
2. Muhammad Jafar Ali, Govindasamay. B., Hoon, K.H, Seet, Gerald. (2016). Effects of physiological predictors on endurance performance in recreational runners. Paper presented at The Physiological Society, Dublin Ireland.
3. Muhammad Jafar Ali, Hoon, K.H, Seet, Gerald, Govindasamay Balasekaran. (2016). Effect of fatigue on running kinetic asymmetry in non-continuous & continuous constant speed protocol. 34th International Conference on Bio-mechanics in Sports, Tsukuba Japan
4. Ali, M. J., Hoon, K.H, Seet, Gerald, Balasekaran, G. (2016, 12-13 December 2016). Heart rate monitors for predicting physiological stress in runners during critical speed intermittent stage protocol. 2nd International Conference in Sports Science & Technology, Singapore.
5. Ali, M. J., Hoon, K.H, Seet, Gerald, Balasekaran, G. (2016, 12-13 December 2016). Bilateral impact asymmetry in recreational runners against different speeds and

metabolic stresses. 2nd International Conference in Sports Science & Technology, Singapore.

6. Ali, M. J., Hoon, K.H, Seet, Gerald, Balasekaran, G. (2017, 23-27 July). EMG normalization technique for understanding lower extremity muscle fatigue interaction with joint kinematics in recreational endurance runners. XXVI Congress of the International Society of Biomechanics, Brisbane Australia.
7. Ali, M. J., Hoon, K.H, Seet, Gerald, Balasekaran, G. (2017, 9-10 Dec). Heart Rate Monitors for Monitoring Endurance Stress in Recreational Runners. 231st International Conference on Vehicular, Mobile and Wearable Technology (ICVMWT), Yokohama Japan.

PROJECT TIMELINE

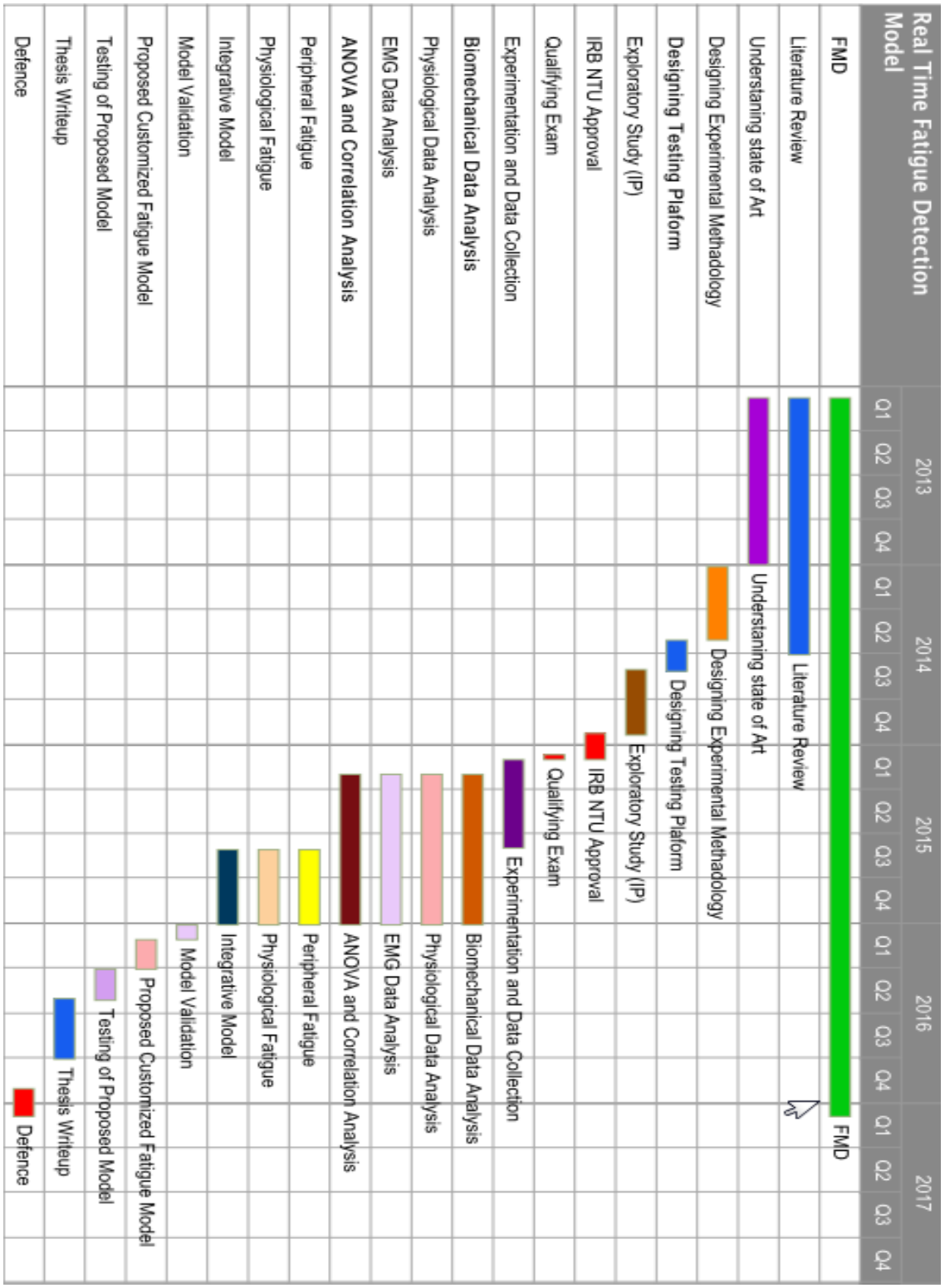

PATENT DOCUMENT

KINESIOLOGICAL ENDURANCE TRAINING SYSTEM

Introduction:

A new concept of a smart coaching system comprising knee braces to monitor knee joint angle, tibia impact loading characteristics and knee joint stability, body posture sensor to monitor upper body posture and axial impact on the spinal cord, transferred through hip from the lower extremity along with cardio-respiratory sensor to measure heart rate (HR) and respiratory rate (RR) in order to track fatigue-related stress on these selected markers. The proposed invention, in this chapter, incorporates several tested and established parameters into its analytical model to determine the level of metabolic stress, cardiorespiratory stress, lower extremity joint stiffness and level of fatigue during exercise. This proposed architecture would ultimately help in reducing the possibility of running injuries, decreasing fatigue-related stress, providing feedback on correcting running form, improving efficiency and running economy with better quality of training and self-awareness capabilities.

Background:

The emphasis on sports industry to analyze performance and lucid presentation of the scientific data has enabled an increasing demand for acquisition and processing of actionable, real-time data from the athletes. Thereby driving strong demand for wearable technology assisted performance analysis and evaluation. By 2016, wearable technology will represent a minimum revenue opportunity of $6 billion, according to World Market for Wearable Technology – A Quantitative Market Assessment – 2012, a new report from IMS Research.

Recent developments in wearable electronics and algorithms from computer science have assisted coaches in all stages of coaching – training sessions, during preparation for a competition, during a competition and in competition debriefing. Real-time performance monitoring systems are particularly useful for their immediate availability of results and analysis during real-time competition and training. With the rapid rate of wireless technology development, it is expected that such systems will become ubiquitous in supporting sports coaches and athletes to monitor performance and to customize training patterns as per individual's strengths.

Considering the existing art of wearable technology, smart coaching has potentially contributed in educating the mass population regarding their personal physical health and fitness. Majority of the available activity trackers and heart rate monitoring devices like POLAR V800 and RCX5, Nike+ smart shoe, Nike+ FUELBAND and PEAR device have potential to monitor

several metrics that were critically being examined to determine training benefits and determining fitness but still these devices lacks the functionality to evaluate measured matrices qualitatively. Existing available smart devices lacks the feedback that could address incorrect running form, lower extremity joint dynamics support, loading stresses, and legs imbalance during real-time performance. There is also need to integrate additional biomechanical and physiological senses to enable more effective training monitoring during prolonged running sports activity. Therefore, this research has aimed to provide meaning understanding on measurable performance and fatigue matrices and to provide actionable feedback to the athlete that could help him to advance his/her performance as per their individual body anthropometric measurements and skeletal functional structure, considering their existing fitness level.

One other major area is to reduce the possibility of the running injuries. The majority of the endurance/recreational/leisure runners frequently face overuse injuries due to muscular activation imbalance during prolonged running. Major causes for such imbalance are the changes in muscle contraction properties with fatigue development [1] and metabolic accumulations that change the force-velocity relationship [2] within driving and stabilizing muscles. Research [3,4] indicates that among lower extremity injuries, hip, knee and ankle and tibia stress fracture are the most probable site of injury due to overuse and repetitive impact coming from the ground during higher stress. This invention is aimed to provide a smart solution to reduce the possibility of these overuse knee injuries by continuously tracking the joint loading conditions along with other lower extremity joint kinematics, spinal impacts, upper body posture, heart rate (HR) and respiratory rate (RR) parameters. This will further extend the scope of training monitoring through continuous tracking of knee joint stability and dynamic support along with training intensity zones and fitness level in order to reduce the possibility of running overuse lower extremity injuries during repetitive motion. This invention will offer a choice of unique, easy-to-use and personalized features to maximize wearable comfort and motivate the individuals during running.

Comparative Analysis of Existing Technologies:

As wearable technology is extending its contribution towards real-time activity monitoring and analysis, sporting technologies have created a variety of products directed at providing feedback on athletic performance related matrices. Currently, these technologies include heart rate monitors, pedometer, and GPS trackers. These devices are mainly designed based on a modular approach for the selected parameters of interest, listed in Table 8-1.

Table 1: Comparison of the existing wearable smart coaching devices

Products	HR	RR	STR	Tibia Impact	Hip Impacts and Push-off Acc.
POLAR V800	✓	✖	✓	✖	✖
BioHarness ™ 3	✓	✓	✖	✖	✖
Nike+ Fuel band	✓	✖	✓	✖	✖
Nike+ smart shoe	✖	✖	✓	✖	✖
PEAR Smart	✓	✖	✓	✖	✖
runScribe Pro	✖	✖	✓	✖	✖

These devices are good in tracking daily activity (active time, steps, heart rate, working intensity zones, etc.…) but lack capability due to the limitation on matrices that are needed to computational data analytics to understand performance, fatigue and injury development. More computationally powered and integrated approaches are the need of time to understand key factors in performance degradation, degradation in running form in real time and probable factors of running injuries development.

KETS Extending the Art of Real-Time Coaching:

KETS solution will acquire and transmit synchronized biomechanical and physiological data (e.g. tibia impact acceleration, braking force, stride parameters, musculoskeletal joint dynamics, joint kinematics, posture, heart rate and respiratory rate) from the athlete with appropriate non-invasive sensors and transducers (S&T) embedded on an exclusively designed wearable medium that is customizable based on specific individual anthropometric measurements. The medium also allows for freedom of movement and comfort, without sacrificing the reliability of the data acquired.

The transmitted data will be then processed and presented in an exclusively designed cognitive-friendly graphical user interface that aims to lucidly present complex analysis in a simple and understandable way to the sports personnel on the wristwatch and mobile application/web interface, after being analyzed through our computational models. The interconnectivity and system approach is shown in Figure 1.

This KETS invention is targeted to extend the state-of-the-art of wearable sports technology as follows:

- KETS is designed using state-of-the-art wearable sensors, integrated into an exclusively designed customizable wearable medium. Computational techniques are incorporated in such a way that they will provide a real-time feedback on running form, leg

asymmetry, and performance detrimental attributes and will also help to reduce possible injuries related to inefficient running biomechanics and muscular stress.

- Exclusively designed cognitive-friendly graphical user control and data presentation interface on the wrist-worn gadget that presents the acquired data and its analysis in a layman-friendly manner to sports personnel. It is not necessary to have a continuous internet connection during exercising for remote monitoring, later data can be transferred to the cloud and computer for maintaining and recording the history of training and performance development.
- Interpretable and understandable data presentation for sports personnel of different sports activities. The initial target is endurance running, sprint running, squat jumping, long jump, cycling, football, and basketball. But in every step of the system development, we are keeping the design general enough so it can be easily reused in other sports disciplines.

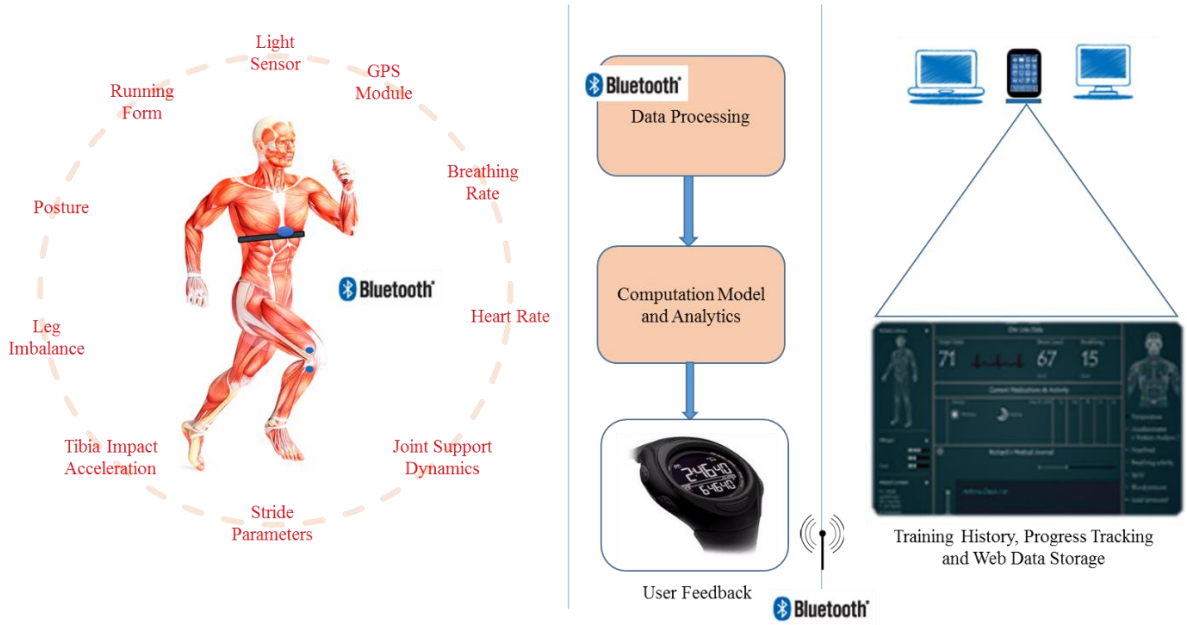

Figure 1: General layout approach of KETS

KETS with its on-field utilization potential, primary data analysis capabilities, and lucid data presentation interface will stand best as per the current need of athletes training and performance monitoring. It include integrated analysis of athlete biomechanics and physiological state acquired and presented during performance training, as shown in general layout structure of Figure 1. KETS can also effectively help to prevent sports-related injuries from overuse or incorrect posture, incorrect landing and gait patterns, legs asymmetry and thus maintaining the athletes' high-performance levels. We see our integrated wearable technology

product being utilized by coaches and sports personnel to optimize and enhance performance along with reducing the risk of injury and fatigue.

Novelty of The Proposed Architecture:

- KETS will be using IMU sensors for the first time to track 3D joint loading condition and joint support characteristics through sophisticated embedded filter along with joint kinematics, solution tested within the exploratory study done under lab conditions [5].
- The optimal integration of cardiorespiratory and biomechanical senses in KETS will generate a unique set of data over which a set of computational principles are performed to analyze sports performance and to detect and quantify fatigue in response to physical exertion during real time scenarios, explained in Chapter 4 & 5.
- In running related sports, KETS feedback can help to delay the onset of fatigue and improve endurance profile by continuously evaluating the running form, loading characteristics, and gait pattern, explained in chapter 4 & 5.
- KETS will help to predict metabolic stress levels for endurance class of runners and perceived exertion along the course of fatigue run without human interruption to performance, explained in chapter 6 & 7.

Technical Description of the Invention:

The proposed invention "KETS", which is a wearable sensing system for monitoring and processing kinematic and physiological data in real time, comprises the following modules.

- Sensing unit to collect kinematic data (Kinematic Unit),
- Sensing unit to collect physiological data (Physiological Unit),
- Communication port to transmit the kinematic data and the physiological data in a wireless manner to a receiving unit (Communication Unit)
- Data processing unit to process the kinematic data and the physiological data in real time based on a predetermined manner, determine user's fatigue level and generate a corresponding feedback data (Data Processing Unit)
- A displaying unit to display the graphic representation of the feedback data. (Display Unit)

Kinematic Unit

In proposed invention, kinematics data sensing unit is designed by integrating 4 inertial measurement units (IMUs). The physiological data sensing unit comprises a wearable elastic chest strap to monitor heart rate, respiratory rate, and upper body posture. In one embodiment, the data processing unit is configured to determine the correlation between the kinematic data and the physiological data. If the correlation is found, the data processing unit is to inform the

user to change the running form. If no correlation is found, the data process unit is to compute the fatigue as a function of physiologic data and kinematic data.

Considering the case of endurance running, wearable knee braces with pocket slot are proposed to be used to place the IMUs at the proximal end of the tibia and the distal end of the femur of both legs for measuring the axial impact coming from the ground and being transferred to the femur through knee joint during the repetitive motion of both legs. Following Figure 2 (on top), represents the placement of IMU sensors for runner and furthermore placement of the sensor can also be customized for individual sports. Once the placement is done, all the sensors will be paired with a data logger, as shown in Figure 2 (on bottom).

In the kinematics data sensing unit, IMUs are being used in integrated fashion to monitor the joint kinematics, in the same fashion as described by Thomas et al. and joint support dynamics during weight acceptance phase of running gait cycle. The initial signal processing of the raw data, coming from accelerometers, is important to remove noise and to improve the signal to noise ratio. Furthermore, a fusion of the accelerometer and magnetometer data helps to determine the orientation and rotation of the IMUs in spatial coordinate space, shown in Figure 3(a).

During the initialization, the accelerometer will be kept stationary and output of the accelerometers will be sampled and averaged to obtain the zero offset voltage or zero acceleration. This offset value will be saved to remove offset and antigravity filter will be used to remove gravity content from the accelerometer. Relative impact filter will be further applied to suppress the high-frequency noise and to determine the peaks within the accelerometer data. Furthermore, acceleration data will be fused together with gyroscope data to determine the quaternion, representing the sensor orientation and magnitude of the acceleration vector. Through rotational transformation, this information will help in determining the relative motion between two IMUs to determine joint kinematics. Considering the case of running, shown in Figure 2 (on top), IMU 1 is attached to the tibia and IMU 2 is attached to the femur bone of the right leg whereas IMU 3 is attached to the tibia and IMU 4 is attached to the femur bone of the left leg. The orientation of IMU will represent the orientation of the limb, to which it is attached as shown in Figure 2 (on top), and rotational transformation will help us to determine knee kinematics. Similarly, joint dynamic support and joint loading characteristics will be determine based on the detected impacts at the tibia and femur and quantified through knee shock attenuation factor, computed through equation 1, 2 and 3.

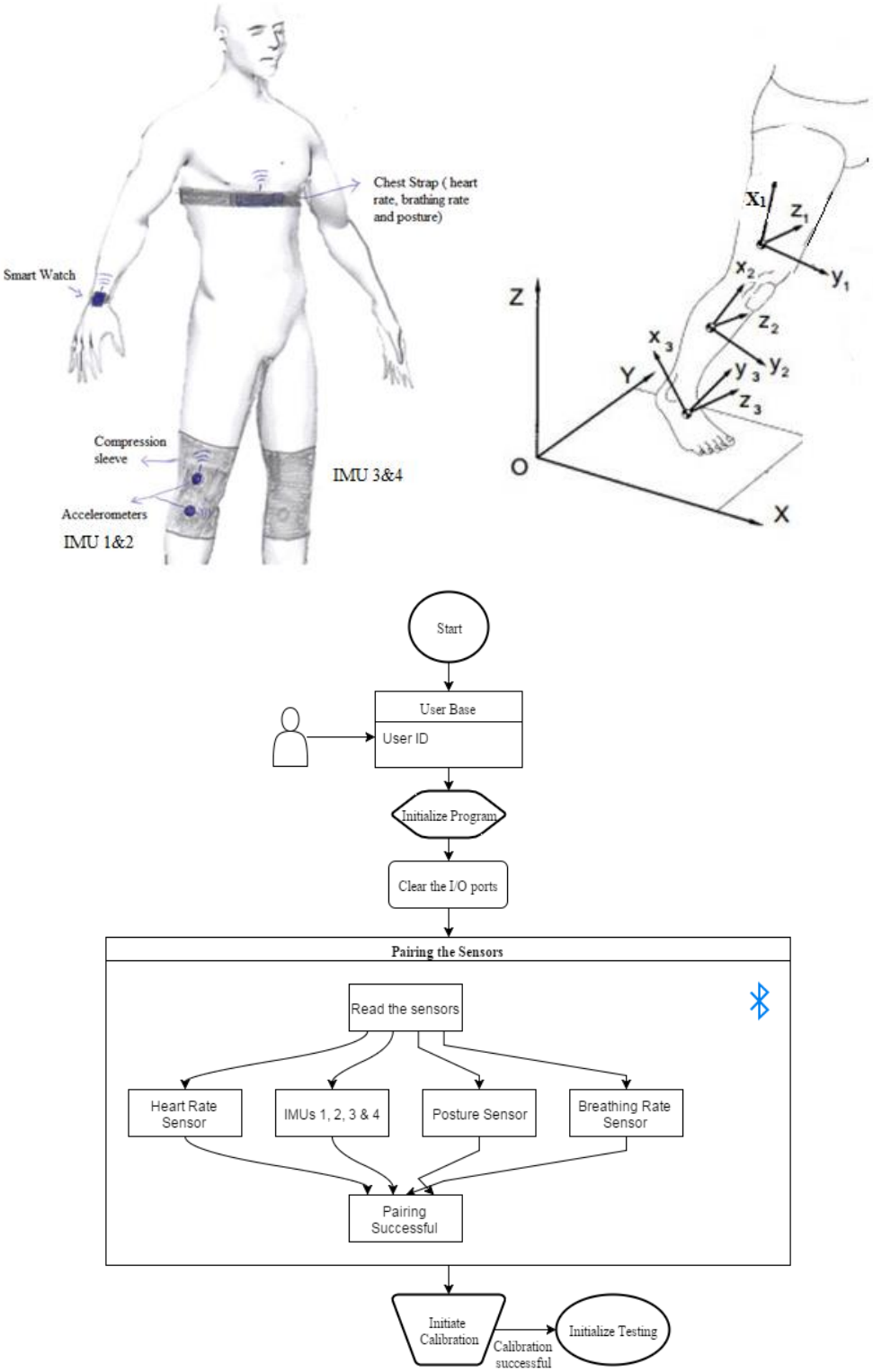

Figure *2*: Sketched diagram representing KETS (on top), b) Flow chart representing system architecture (on bottom)

$$Knee_{axial} = [Acc_{X1} / Acc_{X2}] * 100 \ldots\ldots \quad (1)$$

$$Knee_{Anterior} = [Acc_{Y1} / Acc_{Y2}] * 100 \ldots\ldots \quad (2)$$

$$Knee_{Medial-Lateral} = [Acc_{Z1} / Acc_{Z2}] * 100 \quad \ldots\ldots \quad (3)$$

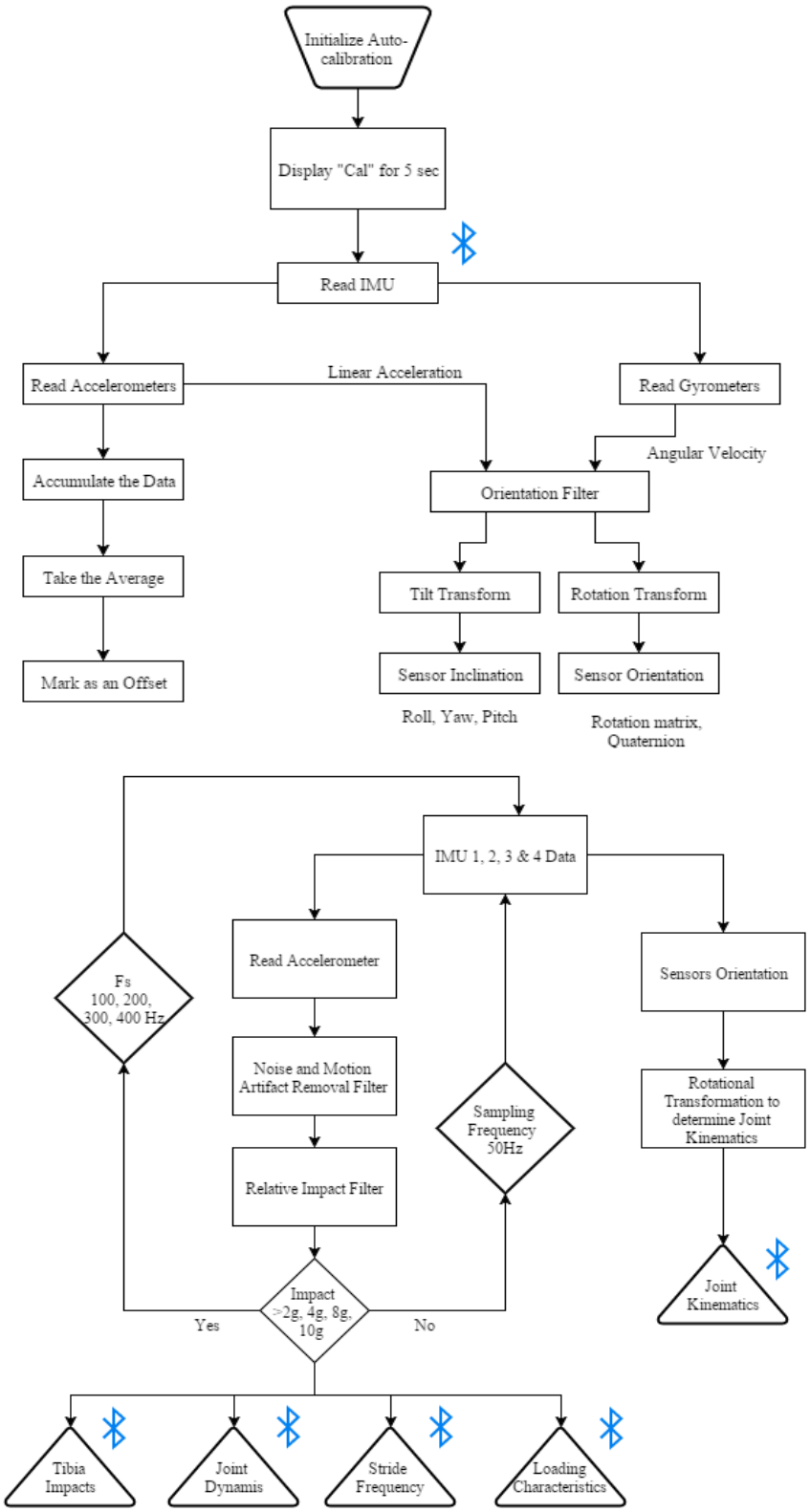

Figure *3*: a) flow chart for sensor offset correction and fusion of data to correctly estimate the sensor orientation (on top), b) Flow chart explaining the signal condition steps to extract biomechanical attributes (tibia impact, joint dynamics, stride frequency, loading characteristics and joint kinematics) (on bottom).

Physiological Unit

For the physiological system, fabric optical heart rate sensor and stretchable breathing rate sensor will be embedded together with IMU sensor to determine cardiorespiratory stress with upper body posture. After initial amplification of the raw signals for the HR and BR sensor, the analogue signal will be digitized using ADC converter and additional filters (notch filter to remove AC component, combination of low and high pass filter/ butter worth filter) will be applied to extract the ECG features, heart rate count, respiratory rate count and respiratory rate interval. For upper body posture, accelerometer, gyroscope, and magnetometer data will be fused together to determine the sensor orientation and inclination in real time. The embedded integrated layout for HR, BR and posture sensor is shown in Figure 4.

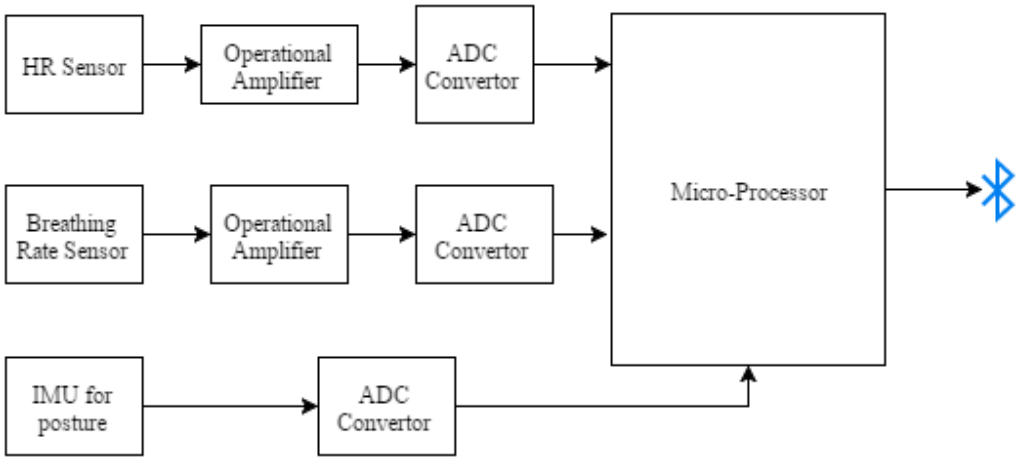

Figure 4: Heart rate sensor, Breathing rate sensor and IMU posture sensor integration layout

Data Processing and Display Unit

This invention further aims to provide a dedicated wrist watch with real-time capabilities of data processing, storage, and biofeedback. GPS module is also integrated to track the outfield trials, outdoor training session, and navigation. Furthermore, the stored data can be transferred to the web cloud and computers/laptops through USB interface, to mobile through Bluetooth wireless synchronization. The integrative layout of the smart data logger is shown in Figure 5.

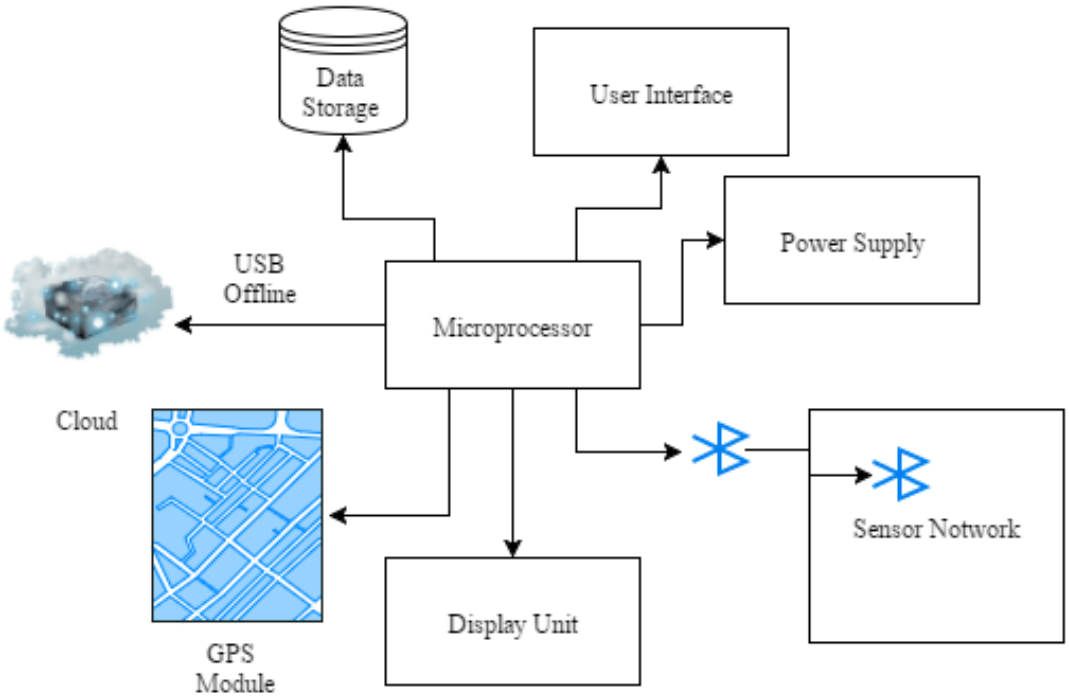

Figure 5: Integrative layout for data acquisition module (dedicated smart wrist watch)

Communication Unit

The complete hardware architecture is shown in Figure 6, explaining about the block circuit diagram for this innovation. This block diagram explains how the individual block of the sensors are connected to the circuit board to communicate with the data logger and server.

All the nodes of IMUs, posture sensor, heart rate monitor, and breathing rate sensor are placed at the body at their appropriate locations to capture the vital signs in real time exercising scenario. After digitization and preprocessing, all the data for the selected sensors are fed to the microprocessor through the Bluetooth communication protocol. Over there, the acquired data is processed through the designed training/coaching algorithm to provide real-time feedback on running performance and running mechanics that may lead to higher chances of running injuries development. The data is also stored in the storage device as well for later data transfer to the cloud.

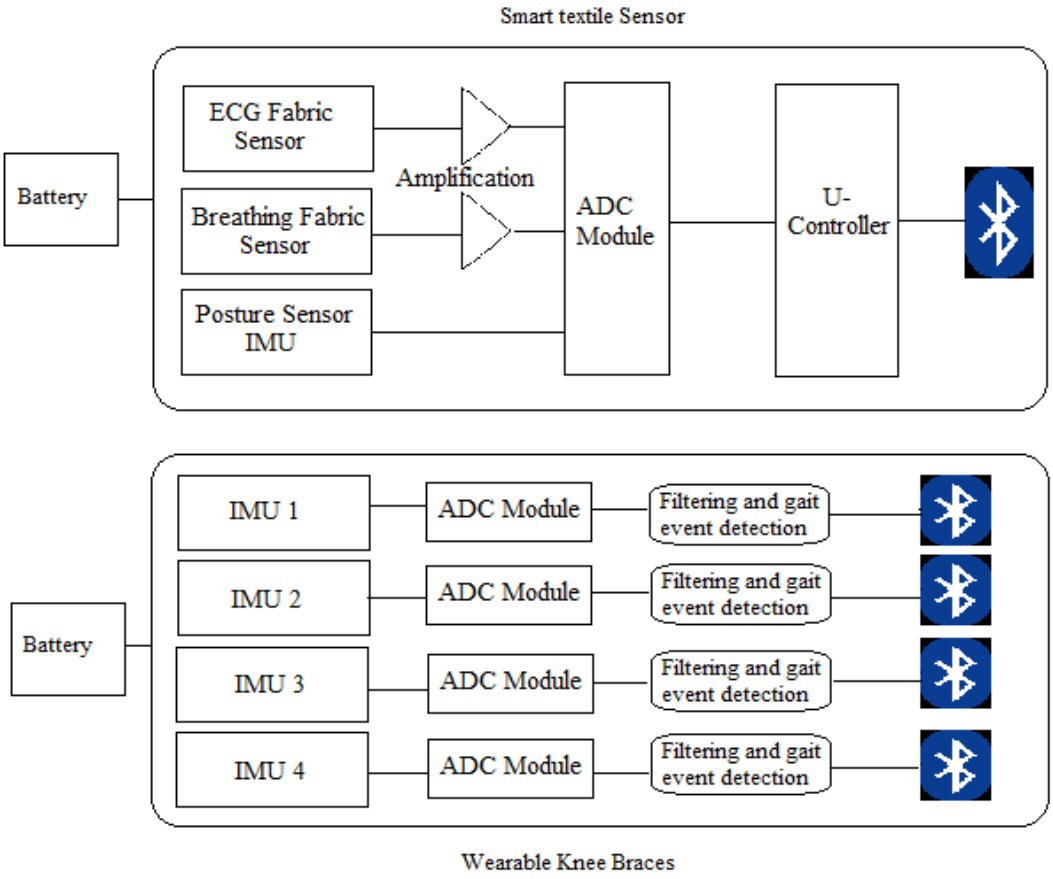

Figure 6: Bluetooth communication network for synchronizing kinematic and physiological unit

Virtual Coaching and Soft Computational Skills of KETS:

The integrative modeling approach in this innovation is not only helping us to monitor measurable metrics (physiological data, gait parameters, biomechanical parameters) but also helping us to further extend the scope of virtual coaching by providing the real-time actionable feedback which can adjust performance to an optimal level and to achieve the training targets. Following flow chart, shown in Figure 7, explains about the understanding of measurable metrics and how they are connected with athlete performance, running form, leg asymmetry, and fatigue prediction. Based on the observed changes in the selected attributes and its significance in relation to time and exercise intensity will help us in understanding the possible shift in that attribute and its impact of running economy, performance and running efficiency.

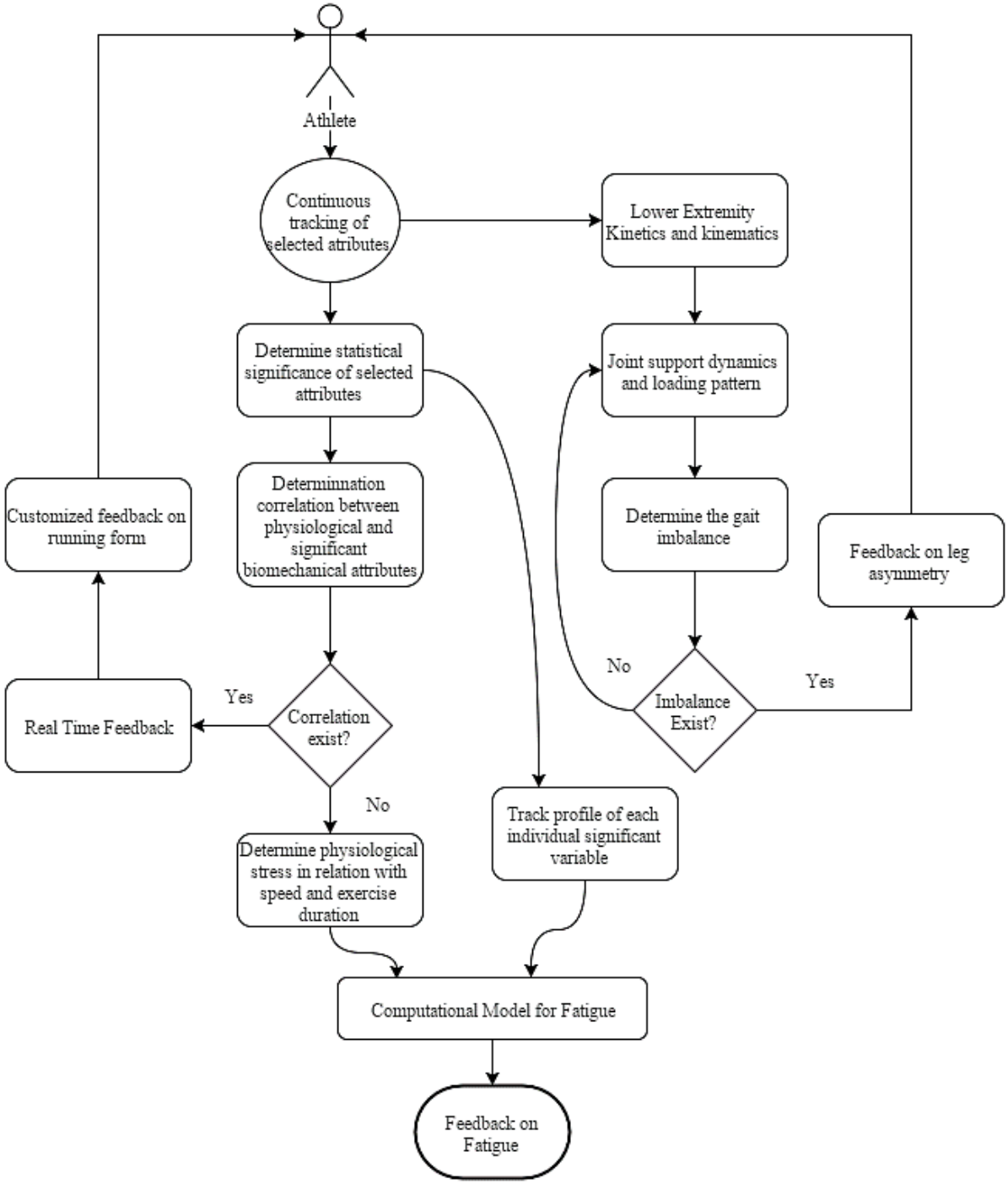

Figure 7: Virtual coaching flowchart explaining the analogy behind the real-time feedback mechanism.

The described flow chart algorithm, considered as the brain of innovation, will help to analyze the running form, loading pattern and associated joint kinematics, gait variations, stride frequency and limb laterality over different speeds and fatigue levels against running duration to understand performance and provide relevant feedback on correcting running form, loading mechanics and limb asymmetry to increase running efficiency, delay the fatiguing process by predicting fatigue levels from the measured matrices. This methodological approach will help

in not only in delaying the onset of fatigue but will also improve endurance profile by continuously evaluating the running form, loading characteristics, and gait pattern.

Outcome of The Proposed KETS Invention:

The optimal integration of biomechanical and cardiorespiratory senses in this invention will generate a unique data set of information through computational principles and more reliable and personalized error free predictive analysis will be carried to determine the exercise intensity, fatigue, lower extremity joint stability, running asymmetry over time during real-time training and performance. Furthermore, this proposed invention will facilitate the following.

- Predictive analysis and intelligent training support for performance enhancement during training without having any limitation of space during training and competition.
- Has potential to be expanded into several other running related applications like activity tracking, performance monitoring and data analysis of several indoor games and outdoor games like basketball, squat jumping, long jump, endurance running, sprint running, soccer, rugby and hockey in order to track the individual fitness and exhaustion level during gaming scenarios.

References:

[1]. Garcia-Manso, J.M., et al., Assessment of muscle fatigue after an ultra-endurance triathlon using tensiomyography (TMG). J Sports Sci, 2011. 29(6): p. 619-25.

[2]. Jones, D.A., Changes in the force-velocity relationship of fatigued muscle: implications for power production and possible causes. J Physiol, 2010. 588(Pt 16): p. 2977-86.

[3]. Daoud, A.I., et al., Foot strike and injury rates in endurance runners: a retrospective study. Med Sci Sports Exerc, 2012. 44(7): p. 1325-34.

[4]. van Gent, B.R., et al., Incidence and determinants of lower extremity running injuries in long distance runners: a systematic review. British journal of sports medicine, 2007.

[5]. Ali, M.J., et al. Knee axial shock transmission from tibia to femur during continuous speed run to exhaustion: an exploratory study. in 1st International Conference in Sports Science & Technology. 2014. Singapore.

[6]. Seel, T., J. Raisch, and T. Schauer, IMU-based joint angle measurement for gait analysis. Sensors, 2014. 14(4): p. 6891-6909.